The effect of maternal obesity/GDM and metformin intervention on maternal, placental and fetal health

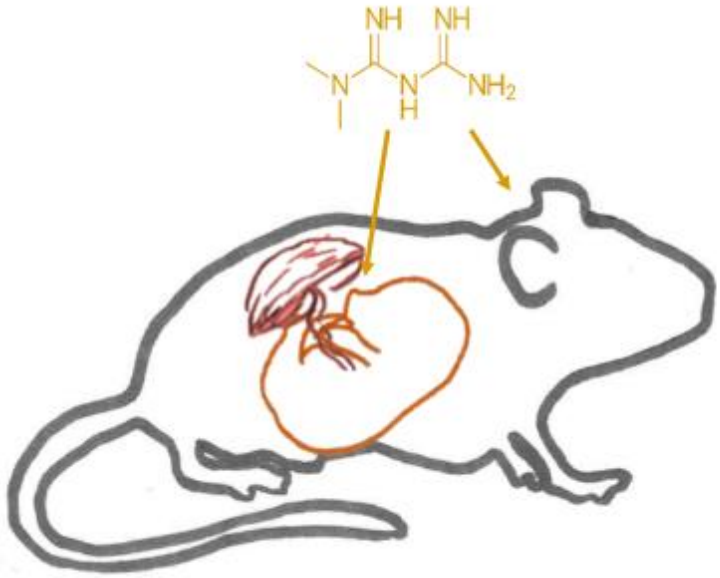

Antonia Sophie Hufnagel

Department of Clinical Biochemistry

Pembroke College

December 2021

This thesis is submitted for the degree of Doctor of Philosophy.

(Butterfly out of immunhistochemically stained mouse placentas and western blotting bands)

Für Papa

Declaration

The work for this thesis has been carried out between October 2018 and December 2021 in the Institute of Metabolic Science at the University of Cambridge. This thesis is the result of my own work and includes nothing which is the outcome of work done in collaboration except as declared in the Preface and specified in the text. I further state that no substantial part of my thesis has already been submitted, or, is being concurrently submitted for any such degree, diploma or other qualification at the University of Cambridge or any other University or similar institution except as declared in the Preface and specified in the text.

It does not exceed the prescribed word limit of 60000 words for the Clinical Medicine and Clinical Veterinary Medicine Degree Committee, this word limit excludes figures, photographs, tables, appendices and bibliography.

21.12.21 *A. Hufnagel*

Date Signed

Summary

In many populations worldwide over 50% of women have a body mass index above 25. Therefore, an increasing number of women enter pregnancy overweight or obese. This increases the risk for pregnancy complications such as Gestational Diabetes Mellitus (GDM). Placental function is often affected in obese and GDM pregnancies, which affects fetal growth and development. Recent years have implicated placental extracellular vesicles (EV) in fetal-maternal communication, with their microRNA (miRNA) content affecting maternal metabolism and potentially the fetus. Overall, it is well-established that obese and glucose-intolerant pregnancies have short- and long-term health consequences for mother and child. Women with GDM are therefore treated to control maternal glycaemia and thereby prevent effects on the fetus caused by excessive glucose exposure. In many countries metformin (an oral glucose-lowering agent) is now the first line pharmacological treatment for GDM as it can control maternal glycaemia and reduce gestational weight gain. However, metformin can cross the placenta and thereby directly affect the fetus.

A few studies in humans and in animal models have reported increased adiposity in offspring exposed to metformin during pregnancy. However, information regarding the immediate actions of metformin on the placenta and fetus is limited. This thesis therefore aimed to assess the impact of metformin treatment of an obese and glucose-intolerant pregnancy in a mouse model on (i) the mother (described in chapter 3), (ii) fetal growth and placental structure (described in chapter 4) and (iii) on the placental lipidome and transcriptome (described in chapter 5). A last aim of this thesis was (iv) the establishment of isolation of placental EVs and characterisation of their miRNA content in an obese and glucose-intolerant pregnancy (described in chapter 6).

In this thesis it is shown (chapter 3) that feeding mice a diet high in sugar and fat prior to and throughout pregnancy increased maternal fat mass and impaired glucose tolerance. Additionally, a preeclampsia-like phenotype with impaired uterine artery compliance and increased serum sFlt levels was induced. All these parameters were improved by treatment of the dams with metformin at clinically relevant doses prior to mating and throughout pregnancy. These findings are consistent with metformin being beneficial for maternal metabolic health, as observed in human studies, including recent data highlighting the potential of metformin to prevent preeclampsia.

Chapter 4 highlights that placentas from obese dams had calcium depositions and a reduced labyrinthine zone. Calcium deposits have been observed previously in pregnancies complicated by GDM and obesity, showing that our model resembles the human situation. The obesity-induced placental pathologies together with the reduced uterine artery supply likely led to the fetal growth restriction observed. Metformin treatment did not rescue any of these obesity-induced changes in the fetus and the placenta. Metformin crossed the placenta and entered the fetal circulation at levels

equivalent to maternal concentrations and was also taken up into fetal tissues. Metformin can therefore exert direct effects on the placenta and/or the fetus that may explain why fetal growth restriction and placental impairments are not rescued by metformin despite the improvement in uterine artery compliance. Reduced body weight in babies exposed to metformin *in utero* has previously been shown in human studies. Metformin did not affect placental AMPK and mTOR signalling as previously reported, but increased apoptosis markers in the male placenta.

As the placenta accumulated substantial levels of metformin and is the key interface between mother and fetus we investigated in chapter 5 effects of metformin on the lipidome and transcriptome by comparing obese untreated and obese metformin-treated placentas. Metformin reduced triglycerides with low carbon numbers and free carnitine. A reduction of carnitine has previously been linked to preterm birth. Additionally, phosphatidylserines (PS) and sphingosine (18:0) were increased in the male placenta and lyso-phosphatidylcholine was reduced in the female placenta upon metformin treatment. A few human studies reported previously increased rates of preterm births in pregnancies exposed to metformin, thereby the reduced carnitine levels together with increased PS levels that could be linked to apoptosis in the male placenta warrant further investigation. Placental transcriptome analysis identified no major changes in mRNA expression upon metformin exposure but highlighted overall sex differences within the placenta that were consistent with increased *in utero* vulnerability of male fetuses to maternal obesity.

Lastly, chapter 6 of this thesis shows the feasibility of extracting placental EVs released from placental explants. In a pilot study EVs and their miRNA cargo from male control placentas were compared to those from male obese placentas. miRNAs previously identified as playing a role in IGF2 signalling, mitochondrial dysfunction and preeclampsia were altered in obese placental EVs. Therefore, further follow-up could identify the role of placental EVs in matching maternal supply and fetal demand via modulating IGF2 signalling and could add evidence for their use as biomarkers to identify impaired placental function and preeclampsia.

Overall, this thesis shows beneficial effects of metformin on maternal metabolic health and adds evidence to the current discussion of metformin as a preeclampsia treatment. However, it also highlights that metformin can have direct effects on the fetus and the placenta, with some evidence that at least some of these effects are sexually dimorphic. The use of metformin in pregnancy is complex and might be good for some women where beneficial effects of metformin in pregnancy might outweigh potential short-and long-term effects on the offspring. However, this might not be the case in other women. Therefore identifying treatment strategies/metformin formulations that retain maternal benefits whilst reducing fetal exposure should be the important goal of future studies.

Publications

Research articles

Hufnagel A*, Fernandez-Twinn D S*, Blackmore H L, Ashmore T, Heaton A R, Jenkins B, Koulman A, Hargreaves I P, Aiken C E, Ozanne, S E. Maternal but not fetoplacental health can be improved by metformin in a murine diet-induced maternal obesity mod*el. J.Physiol.,600 (4), 903-919 (2022)*

Pantaleo L C, Inzani I, Furse S, Loche E, **Hufnagel A**, Ashmore T, Blackmore H L, Jenkins B, Carpenter A A M, Wilczynska A, Bushell M, Koulman A, Fernandez-Twinn D S, Ozanne S E. Maternal diet-induced obesity during pregnancy alters lipid supply to fetus and changes the cardiac tissue lipidome in a sex dependent manner. *Elife, 11:e69078 (2022)*

Jenkins B, **Hufnagel A**, Blackmore H L, Fernandez-Twinn D S, Ozanne S E, Koulman A. A direct comparison between the concentration of metformin and the lipid profile in liver samples following a dietary administered metformin intervention. *(in submission)*

Sandovivi I, Georgopoulou A, **Hufnagel A**, Schiefer S, Santos F, Hoelle K, Lam B, Yeo G, Burlin K, López-Tello J, Reiterer, M, Fowden A, Burton G, Sferuzzi-Perri A, Branco C, Constancia M. Fetus-derived IGF2 matches placental development to fetal demand. *Dev. Cell, 57 (1), 63 – 79.e8 (2022)*

Reviews

Hufnagel A, Dearden L, Fernandez-Twinn D S, Ozanne S E. Programming of cardio metabolic health: the role of maternal and fetal hyperinsulinaemia. *J. Endocrinol., 253(2), R47-R63 (2022).*

Aiken C E M and **Hufnagel A**. 'Sex-specific implications of exposure to an adverse intrauterine environment' in Legato M (ed.) *Principles of Gender-Specific medicine*. Academic Press. *(in revision).*

Sandovici I*, Fernandez-Twinn D S*, **Hufnagel A***, Constancia M, Ozanne S E. Sex-differences in intergenerational inheritance of metabolic traits. *Nat Metab 4, 507–523 (2022).*

Aiken C E M, **Hufnagel A,** Grant I D. The early intrauterine environment and its role in developmental abnormalities. (*under review at Seminars in Cell and Developmental Biology*).

*authors contributed equally

Posters and talks

Posters

17.07.2018 Annual students' symposium from the Institute of Metabolic Science (IMS), Cambridge, UK (best poster prize)

16.07.2019 Annual students' symposium from the Institute of Metabolic Science (IMS), Cambridge, UK

23.10.2019 Developmental Origins of Health and Disease (DOHaD) conference, Melbourne, Australia (together with poster pitch talk)

03.09.2020 Danish Diabetes Academy and Cambridge Metabolic Network conference (DDA-CMN), virtual (together with poster pitch talk)

02.03.2021 Centre for Basic Metabolic Research (CBMR) Metabolism Month conference, virtual

Talks

21.02.2020 Symposium from the Centre of Trophoblast Research, Cambridge, UK

06.05.2021 iPlacenta symposium "Novel perspectives in maternal and fetal health", virtual (second best early career researcher talk prize)

13.05.2021 Symposium from the Centre of Trophoblast Research in Cambridge, virtual

29.07.2021 Internal seminar from the Institute of Metabolic Science in Cambridge, virtual

13.07.2021 Annual students' symposium from the Institute of Metabolic Science (IMS), virtual (best talk prize)

24.11.2021 Away day from the Institute of Metabolic Science for the visit of the science advisory board (SAB), virtual

03.12.2021 External seminar series from the Institute of Metabolic Research in Birmingham, virtual

09.12.2021 Seminar series from the Cambridge Reproduction Strategic Research Initiative (SRI), virtual

Funding

Thanks to the Wellcome Trust for funding my PhD.

Acknowledgments

Most importantly I want to thank my supervisor Sue. Thanks so much for such perfect three PhD years. I am really grateful for all your support and guidance and that I could also develop many own ideas - I have learned so much in these past years. Thanks for all your input when writing this thesis and thanks for understanding personal decisions especially in unprecedented COVID times. Thanks must also go to Denise, for all your help, lovely chats, jams and rhubarb deliveries and long PMs that were never boring. You are probably one of the main reasons why I have decided to come to the Ozanne lab after my rotation as I enjoyed our teamwork during my rotation so much. And I am so glad that I did choose the Ozanne lab, thanks to all of you for creating such a lovely lab atmosphere. Thank you to you, Catherine, for giving me so many opportunities and for helping me to learn R. Thank you, Tom, for being such an honest and good friend in the lab, I will definitely miss your humour. Heather, I loved all our chats and all the fun afternoons with Freddie and Isla. Thanks, Claire for all your help with the mice, for always having a great overview of the mice and for cute Peter videos. Lucas, I am so grateful for all your help with any RNA or bioinformatic work, you are always such a nice and happy helping hand in the lab. Luciana, I am so glad I got to meet you and the kids, it was great having you in the lab. Thanks, Laura K for helping me so much with PMs in the beginning of the cohort and for the great trip to Aberdeen. Lisa, you were not only great as a big help in the lab but also as a mentor when thinking about the next steps after the PhD. Thanks, Laura, I really enjoyed doing the weighing-intensive cohort with you and meeting Florrie and Sophia. Isabella, thanks for all the nice E19 chats but also most importantly all the non-sciency chats. And thanks to Josca and Phoebe for such a wonderful time in Australia. Thanks so much to my fellow PhD students of the programme Phoebe, Emily and Sophie, I still remember our first christmas party at IMS and the marble run. Overall, I really appreciated the lovely students atmosphere in the IMS, especially all the fun public engagement – thanks everyone. Thanks to all my friends in Cambridge who made the past years so wonderful: the wonderful Cambridge Molis (with adoption of Luis), Helena, Jana, my lovely housemate Anjali. And thanks to all my old friends: the good old Jabadabadoo crew, Solveig, Eva, Schlotti, Liya and the Wehrlebauernhof – I am so lucky to have such great friends in all of you!

Final thanks must go to my family. Mama, Papa, Hinni, John and Beppo, I am so grateful for all your support – you are the best family I could ever imagine and incredibly important to me. I dedicate this thesis to you, Papa. Some of your fascination for science must have jumped over to me when I was a baby and lying next to you while you were finishing your thesis.

Finally, I want to thank you, Max, for cooking so much for me in the final write up phase, for letting me work long hours or taking me on long walk when I needed a break. I am so excited to be living with you now and can't wait for all our adventures together in the future – Ich liebe dich, Max.

Table of content

Abbreviations

11β-HSD2	11β-Hydroxysteroids Dehydrogenase type II
AC	Abdominal Circumference
ACOG	American College of Obstetricians and Gynaecologists
ADA	American Diabetes Association
Ago2	Argonaute 2
ALSPAC	Study: Avon Longitudinal Study of Parents And Children
AMPK	AMP Kinase
APGAR	Appearance, Pulse, Grimace, Activity and Respiration
AUC	Area Under the Curve
AWERB	Animal Welfare Ethical Review Body
BCRP	Breast Cancer Resistance Protein
BMI	Body Mass Index
BPA	Bisphenol A
CANDLE	Study: Conditions Affecting Neurocognitive Development and Learning in Early Childhood
CMV	Cytomegalovirus
CO	Cardiac Output
CRL	Crown Rump Length
C-section	Caesarean section
CVD	Cardiovascular Disease
DALI	Study: Vitamin D and lifestyle intervention
DAMPs	Danger-Associated Molecular Patterns
DASH	Diet: Dietary Approach to Stop Hypertension
DHA	Docosahexaenoyl Acid
DOHaD	Developmental Origins of Health and Disease
DPP	Study: Diabetes Prevention Program
E13.5/15.5/18.5	Embryonic day 13.5/15.5/18.5
EDV	End Diastolic Velocity
EFW	Estimated Fetal Weight
ELISA	Enzyme-Linked Immunoassay

EMPOWaR	Study: Efficacy of Metformin in Pregnant Obese Women, a Randomised Controlled Trial
eNOS	endothelial Nitric Oxide Synthase
EPC	Ectoplacental Cone
ESCRT	Endosomal sorting complex required for transport
ETIP	Study: Exercise training and weight gain in obese pregnant women
EV(s)	Extracellular Vesicle(s)
EVT	Extravillous Trophoblasts
ExE	Extraembryonic Ectoderm
FAS	Fetal Alcohol Syndrome
FAT	Fatty Acid Translocase
FATP	Fatty Acid Transport Protein
FFA	Free Fatty Acid
GDF-15	Growth Differentiation Factor 15
GDM	Gestational Diabetes Mellitus
Glp1	Glucagon-like peptide 1
GLUT	Glucose Transporter
GROW	Gestation Related Optimum Weight
GWAS	Genome-Wide Association Studies
GWG	Gestational Weight Gain
H&E	Hematoxylin and Eosin
HAPO	Study: Hyperglycaemia and Adverse Pregnancy Outcomes
HC	Head Circumference
HDL	High Density Lipoprotein
HFD	High-Fat Diet
HIF	Hypoxia-Inducible Factor
HRP	Horseradish Peroxidase
IADPSG	International Association of Diabetes in Pregnancy Study Groups
ICM	Inner Cell Mass
IGF1/2	Insulin-like Growth Factor 1/2
iNOS	Inducible Nitric Oxide Synthase
ipGTT	Intraperitoneal Glucose Tolerance Test

ISEV	International Society for Extracellular Vesicles
IUGR	Intrauterine Growth Restriction
Kcal	Kilocalories
LC-MS	Liquid Chromatography Mass Spectrometry
LDL	Low Density Lipoprotein
LGA	Large for Gestational Age
LIRKO	Liver-specific Insulin Receptor Knock-Out
lncRNA(s)	Long non-coding RNA(s)
LRT	Likelihood Ratio Test
Lyso-PC	Lysophosphatidylcholine
MAP	Mean Arterial Pressure
MC4R	Melanocortin 4 Receptor
MCA	Middle Cerebral Artery
MiG	Study: Metformin in GDM
min	minutes
MiPS	Study: Metformin in Pregnancy Study
miRNA	microRNA
MISEV	Minimal Information for Studies of Extracellular Vesicles
MOP	Study: Metformin in Obese non-diabetic Pregnancies
MSH	Melanocyte-Stimulating Hormones
MVB	Multivesicular Body
NAFLD	Non-Alcoholic fatty Liver Disease
NCD	Non-Communicable Disease
NET	Norepinephrine Transporter
NHP	Non-Human Primate
NICE	The National Institute for Health and Care Excellence
NO	Nitric Oxide
NOD	Non-Obese Diabetic mouse strain
NTA	Nanoparticle Tracking Analysis
OCT	Organic Cation Transporter
OCTN	Organic Cation Transporter Novel

OECD	Organisation for Economic Co-operation and Development
OGTT	Oral Glucose Tolerance Test
padj	adjusted p value
PCA	Principal Component Analysis
PCOS	Polycystic Ovary Syndrome
p-gp	p-glycoprotein
PI	Pulsatility Index
PLAP	Placental Alkaline Phosphatase
POMC	Pro-opiomelanocortin
PPI	Placental Pulsatility Index
PS	Phospatidylserine
PSV	Peak Systolic Velocity
RCT(s)	Randomized Controlled Trial(s)
RI	Resistance Index
RNASeq	RNA Sequencing
SBP	Systolic Blood Pressure
SD	Standard Deviation
SEC	Size-Exclusion Chromatography
SEM	Standard Error of the Mean
SERT	Serotonin Transporter
sFlt	Soluble fms-like tyrosine kinase 1
SGA	Small for Gestational Age
T1D/T2D	Type 1/2 Diabetes
TD-NMR	Time Domain Nuclear Magnetic Resonance
TE	Trophoectoderm
TGC	Trophoblast Giant Cell
THTR2	Thiamine Transporter 2
TNFα	Tumor Necrosis Factor α
TOP	Study: Treatment of Obese Pregnant women
TORCH	Toxoplasma gondii, Other, Rubella virus, human Cytomegalovirus (HCMV), and Herpes simplex virus
TUNEL	Terminal deoxynucleotidyl transferase mediated dUTP nick end labelling

UN	United Nations
UPBEAT	Study: UK pregnancies better eating and activity trial
USPSTF	US Preventive Services Task Force
VEGF	Vascular Endothelial Growth Factor
VLDL	Very Low Density Lipoprotein
VST	Variance Stabilizing Transformation
VTI	Velocity Time Integral
WHO	World Health Organisation

List of Figures

List of Tables

1 Introduction

1.1 Obesity as a critical health burden

1.1.1 Prevalence worldwide

Obesity rates increased dramatically in the past 40 years worldwide reaching pandemic proportions[1]. The steep increase in obesity numbers (Figure 1.1A) and the predicted numbers in 2030 (Figure 1.1B) show that this will continue to be a growing problem for countries all over the world. Many organisations including the World Health Organisation (WHO), United Nations (UN) and World Obesity Federation state that immediate action is needed to reduce the burden of obesity[1,2]. In 2013 multiple organisations officially acknowledged obesity as a disease[1]. It is also recognized that obesity is a relapsing disease with weight loss interventions often not leading to a permanent weight loss[3,4].

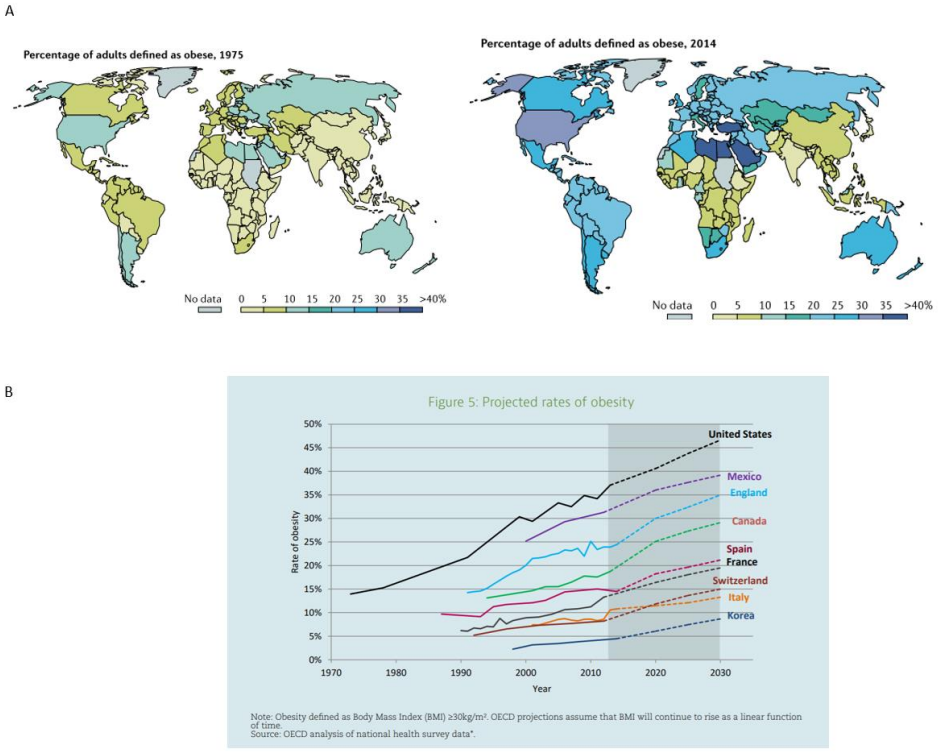

Figure 1.1: Obesity is increasing rapidly worldwide

(A) Percentage of obese adults (BMI 30 kg/m^2) in 1975 and 2014, data from WHO, Global Health Observatory, adapted from Blüher et al. [2], permission for use of figure has been obtained. (B) Projected rates of obesity from 1970 until 2030, data from Organisation for Economic Co-operation and Development (OECD) analysis of national health survey data[5]

The most common way to assess obesity is by body mass index (weight in kg divided by height in metres squared, BMI). The WHO states the following classifications for BMI: BMI <18.5 kg/m^2: underweight, 18.5 – 25 kg/m^2: normal weight, 25 – 30 kg/m^2: overweight, >30 kg/m^2: obese.

Obesity is associated with a reduction in life expectancy of 5-20 years[6]. It is one of the key risk factors

for non-communicable diseases (NCDs) such as cancer or cardiovascular diseases (CVD). NCDs nowadays lead to more than 70% of deaths worldwide[7]. In 2010 the WHO presented its "global action plan for the prevention and control of non-communicable diseases 2013-2020" with a global target to reduce premature mortality from NCDs by 25% and halt the rise in obesity numbers by 2025[8]. This is crucial as obesity is not only a huge health burden for the individual but also for the health care system as obesity increases health care needs and costs drastically[9]. Additionally obesity is an increasing problem in developing countries where health care systems are not well-equipped to deal with the arising comorbidities[10].

1.1.2 Comorbidities

Above a BMI of 25 kg/m^2 every 5 kg/m^2 increase leads to an increase in mortality related to vascular diseases by 40% and related to diabetes by 120%[9]. These observations are based on the BMI but it is increasingly stressed that the BMI does not take the metabolic health of the individual into account, leading to the so-called obesity paradox. The paradox states that a higher BMI does not necessarily correlate with a higher mortality due to CVD as obese individuals can be metabolically healthy. It is well-known that subcutaneous compared to visceral adipose tissue is more benign, therefore assessment of parameters such as insulin resistance, body fat percentage and fat distribution is relevant for a thorough characterisation of metabolic health[11].

Comorbidities are the consequence of altered metabolic factors and induction of a chronic low-grade inflammation in obese individuals[1]. These changes include increased secretion of pro-inflammatory cytokines by adipose tissue and ectopic fat disposition e.g. in the liver. Additionally, obesity is associated with hormonal changes (e.g. higher leptin, adiponectin and insulin levels) and increased levels of circulating cholesterol and free fatty acids. These changes result in obesity being a major risk factor for type 2 diabetes (T2D). The altered metabolic factors also result in a high risk for gallstones, hypertension, stroke and CVD. Additionally, cancer is more frequently observed in obese people, especially in post-menopausal women. Estrogen production by adipose tissue is thought to mediate increased risk of breast and endometrial cancer. Sleep apnoea and osteoarthritis due to the increased fat mass further impact on the life of obese individuals.

Obesity is not only a risk factor for NCDs, studies show that obese people are also more susceptible to infectious diseases and report poorer outcomes[12]. The exact causal relationships and the contribution of obesity-associated comorbidities are yet to be elucidated. The COVID19 pandemic in 2020/2021 made clear that obese patients infected with SARS-CoV-2 are more likely to be admitted to intensive care units and that severe obesity (BMI > 35 kg/m^2) is associated with a dangerous course of the disease[13]. It is also known that abdominal obesity reduced the efficiency of lung ventilation, making the successful care for obese patients with respiratory diseases even more difficult. This highlights that the worldwide pandemic of obesity is conclusively a risk for all kinds of diseases

and a problem for the health care system and wellbeing of the individual. Psychosocial factors worsen the wellbeing even further as obese people encounter stigmatization and social problems. Many experience stigma in health care settings, leading to low adherence to treatment and avoidance of health care by the obese patient[14–16]. Obese individuals are more likely to suffer from depression or anxiety disorders and obese children are more frequently exposed to bullying in school[9].

1.1.3 Obesity in children

Increasing obesity in children is of special concern as obese children are at risk to develop chronic diseases such as T2D early in life, they are more often absent from school and have a lower educational level[9]. Studies show that 90% of children with obesity at age three will still be overweight or obese in adolescence[17]. Therefore, it is concerning that from 1975 to 2016 the prevalence of obesity in boys increased from 0.7% to 5.6% and in girls from 0.9% to 7.8% worldwide. Figure 1.2A shows that large numbers of children aged 2 – 4 years are overweight worldwide. Classifications of obesity in children are age- and sex-specific as the relationship between BMI and fatness during child development highly depends on age and sex. The WHO provides medians from a reference population. Children under 5 are classified as overweight if the BMI is more than 2 standard deviations (SDs) above the median and as obese if more than 3 SDs above the median. In 5 – 19 year olds overweight is already present with a BMI of 1 SD above the median and obese with more than 2 SD above the median[18]. In this age group a steep increase in obesity numbers can be observed across the world (Figure 1.2B). As these children will be the parents for the future generations the problem of obesity is exacerbated leading to more and more babies and children in the future being exposed to obesity *in utero* and early life. As addressed in this thesis, exposure to such an *in utero* environment may establish the roots for developing obesity postnatally (see section 1.3, p.7). To prevent these vicious circles, the causes of obesity need to be well understood (section 1.2, p.4).

It needs to be noted that in children undernutrition is still a problem in many developing countries. In many developing countries obesity and undernutrition coexist especially in children, making this so-called “double burden of malnutrition” a difficult problem to tackle. This further exacerbates comorbidities and the drain on limited health care resources[19].

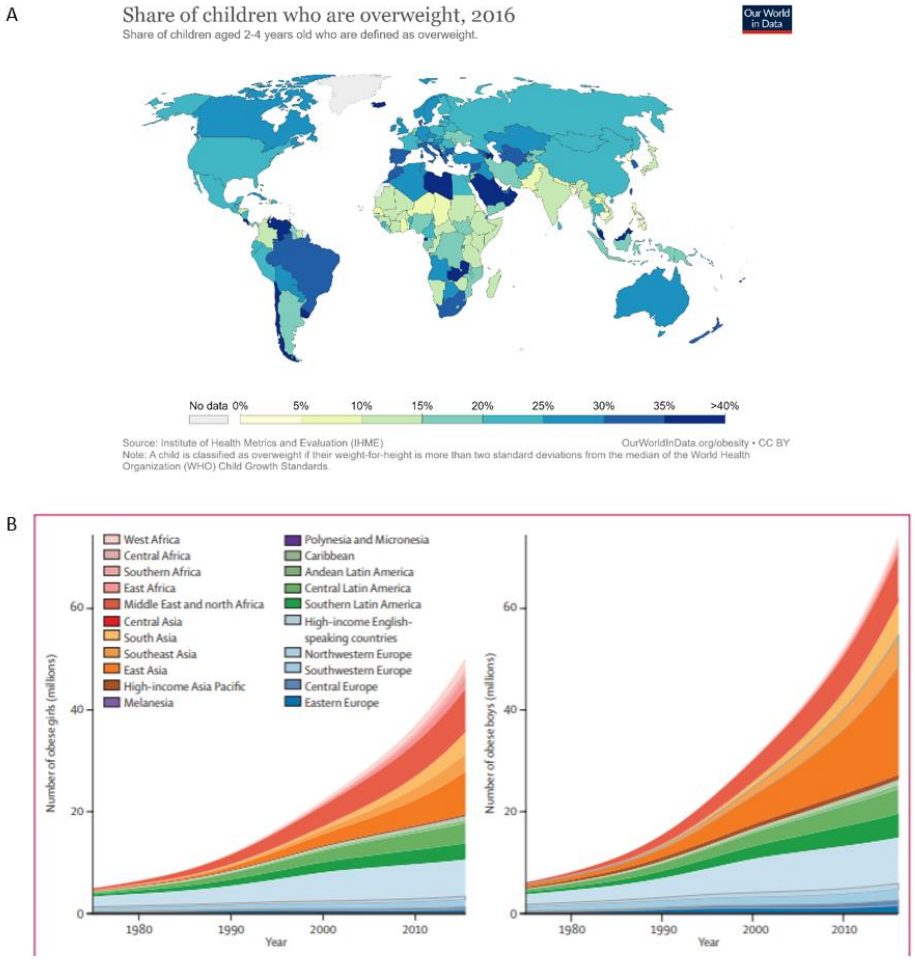

Figure 1.2: Obesity in children is a huge problem worldwide

(A) Percentage of overweight children (BMI > 2 standard deviations from WHO reference population mean) at 2 to 4 years[20], figure used with permission (CC-BY licence). (B) Trajectory of children obesity (BMI > 2 standard deviations from WHO reference population median) from 1975 until 2016[21], figure used with permission (CC-BY licence).

1.2 Causes of obesity

1.2.1 Environment

The steep rise of obesity numbers in the past 40 years is accompanied by an increase in urbanization across the world. Multiple environmental factors, such as sedentary lifestyle and unhealthy energy-rich food, are therefore thought to contribute to the obesity pandemic. The changes are often summarized by the term “westernized lifestyle”. In the 1960s and 70s the food supply in many western countries started to consist of more and more refined carbohydrates and fats[2]. The Food and Agriculture Organization of the UN reported a worldwide increase in the average daily kilocalorie (kcal) intake per person by 487 kcal between 1969 and 2015[22]. In developing countries, a particularly steep increase in the daily calorie intake has been observed. This is mirrored by a very rapid rise in obesity

prevalence in these countries in recent decades. This increase in daily calorie intake is a result of the high-caloric and tasty food with addiction-like effects[23]. This food is easily available and often ultra-processed. It is thereby cheap and ready to eat or very convenient to prepare[24]. These food types are frequently advertised[25]. Children in particular are very susceptible to advertisement and food marketing, often focussing on unhealthy food, snacks and sugary beverages[26].

The past 40 years were not only marked by an increase of unhealthy diet consumption and calorie intake but in addition less energy expenditure. The urbanised lifestyle is characterised by a sedentary lifestyle both at work and in leisure times. This is often referred to as the energy-flipping point with more energy taken in via food than expended[2]. This is a key contributor to obesity.

The local environment such as the density of centres or outdoor opportunities for physical activities, the type of grocery stores close-by, and the characteristics and norms of the neighbourhood are known to influence obesity rates as well. A social experiment moving families from a neighbourhood with high obesity and high poverty rates to a wealthier neighbourhood with a lower obesity rate showed a reduction of extreme obesity prevalence[27]. This supported the hypothesis that high poverty and the neighbourhood both influence obesity occurrence. Additionally, wide income gaps within countries (e.g. High equality in Scandinavian countries and Japan with low obesity rates vs. high inequality in the United Kingdom (UK) or Portugal with high obesity rate) are also thought to contribute to obesity prevalence[2,28].

1.2.2 Genetic factors

Although the current environment in many populations such as the UK favours the development of obesity, not everyone becomes obese in the same obesogenic environment. This is thought to be related, at least in part, to genetic variation shaping the susceptibility to becoming obese. Sometimes the analogy of the pathogenesis of a viral agent is used. The agent in the case of the obesity pandemic is the westernized environment (tasty unhealthy food and little activity) affecting the host who has different susceptibility of getting affected due to genetic variation[1]. The thrifty genotype hypothesis states that genes that favour food collection and fat disposition were beneficial evolutionary in times of famines but in the modern world with high constant abundance of food these become disadvantageous, leading to obesity. Contradictory opinions exist regarding this hypothesis[29], but regardless of its evolutionary origins it is not questioned that obesity has genetic causes.

The hypothalamus in the brain is the key regulator of food intake and energy homeostasis[30]. In the past decades multiple hypothalamic pathways have been identified and genetic variation or loss of function mutations in these pathways have been linked to obesity susceptibility. Three types of genetic causes of obesity need to be distinguished: monogenic, syndromic (obesity associated with other genetically-caused syndromes like Prader-Willi-syndrome) and polygenic causes[31]. In 1997 two children with severe obesity were shown to have congenital leptin-deficiency[32]. Leptin is an adipocyte-

derived circulating hormone that regulates appetite, energy-intake and expenditure via hypothalamic pathways. Individuals with loss of function mutations leading to reduced activity or disrupted signalling via the leptin receptor suffer from severe obesity. This was the first monogenic cause of obesity identified. Similarly mutations in genes for the melanocortin 4 receptor (MC4R) or prohormone convertase 1 lead to obesity by affecting signalling via melanocyte-stimulating hormones (MSH) in pro-opiomelanocortin (POMC)-expressing neurons in the hypothalamus, regulating energy homestasis[30]. Equally impaired development of the neural circuits mentioned above can lead to obesity. This can be seen in the association between obesity and mutations in the transcription factor Sim1, which is involved in the development of the hypothalamus. All these genetic alterations have a very clear effect and clear causal relationship, but they are very rare and explain less than 1% (in the case of leptin deficiency) or 2-5% (e.g. MC4R mutations) of obesity cases[30].

Variants in the genome that occur more frequently (more than 5% of the population) are called common variants. Obesity is thought to be a polygenic disease, being caused by variants in multiple genes which all have a small effect size. This is supported by the fact that genome-wide association studies (GWAS) have identified over 80 different loci where common variants are present that are associated with BMI and body fat distribution[30]. The first ones were variants in the intron of the fat mass and obesity associated gene (FTO) and a downstream region of the MC4R gene. The FTO variant has the largest effects size out of all genetic contributors to obesity susceptibility so far but only explains 0.34% of the inter-individual BMI variation[33]. Overall, even though obesity can be linked to a huge variety of genetic variants these explain only 5% of the BMI variability we observe in populations[30]. There therefore remains a lack of understanding/explanation of what has been described as "missing heritability"[34].

1.2.3 *In utero* environment

Obesity is a complex disease, with interaction between multiple causes and risk factors that are both genetic and environmental in nature. Although our genotype is static, environmental factors can contribute across the life course. The Avon Longitudinal Study of Parents And Children (ALSPAC) was established in the UK 30 years ago and followed more than 8000 children from pregnancy to 7 years of age[35]. It highlighted parental obesity (probably a marker for the genetic susceptibility and the local environment of the child) and high television viewing (low activity levels) as early risk factors for obesity at 7 years of age. In addition, high birth weight and catch-up growth were identified as additional risk factors for childhood obesity. The results demonstrated that the trajectory of growth in the first years of life predicts the obesity risk for the child later in life[36]. This suggested that the early life environment highly influences later obesity risk.

Analysis of the mum-child dyads from the Conditions Affecting Neurocognitive Development and Learning in Early Childhood study (CANDLE) highlighted that children's growth trajectories are

influenced by maternal parameters such as the pre-pregnancy weight and maternal weight gain in pregnancy. This suggested that not only early life but the *in utero* environment is important for a metabolically healthy child[36]. It is well-known that children born to obese mums regardless of genetic factors are more likely to develop obesity, CVD and T2D themselves later in life[37]. Paternal obesity is also thought to influence sperm quality and confer a risk of obesity to the offspring in addition to paternal genetics[38]. Thereby the increasing prevalence of obesity at all ages, specifically in the reproductive age is worrying as many babies are thereby exposed to a detrimental obese environment *in utero.* They are therefore more likely to become obese and expose their children to the same *in utero* environment, creating a vicious intergenerational cycle of obesity. Equally malnourished women[19] deliver babies with low birthweights that frequently show catch-up growth, a major early risk factor for later obesity[39]. Older women are more likely to have children that develop obesity which exacerbates the obesity pandemic further as modern women conceive at older ages[2,40]. Offspring from women exposed to environmental chemicals, infections, stress during pregnancy are also more likely to develop obesity and T2D later in life[41]. This shows that a suboptimal *in utero* environment has direct effects on the fetus, thereby "programming" its long-term health in adulthood with effects already being observed in childhood. This phenomenon of developmental programming is the key component of the field of Developmental Origins of Health and Disease (DOHaD).

1.3 Developmental Origins of Health and Disease (DOHaD)

1.3.1 History

More than 50 years ago multiple studies showed that adverse influences in the first years of a child's life impact their future risk of coronary heart disease in adult life as discussed in[42]. In 1964 Rose et al. in the UK demonstrated a link between infant mortality and death from coronary heart disease, showing that siblings from patients that had coronary heart disease had a doubled rate of infant mortality[43]. The notion that the early life environment plays a crucial role in determining long-term health was further supported by studies from Forsdahl et al. in 1977[44]. They highlighted that Norwegian counties with high infant mortality rates also had high rates of arteriosclerotic heart disease. They thereby suggested a correlation of poor living standards in childhood with heart disease in adult life. This was supported by a study of London civil servants and in a Finish study in 1984 and 1985[45,46].

Subsequently, studies from the epidemiologist David Barker and his colleague Clive Osmond became the basis of the DOHaD field as it is known nowadays[47]. In 1986 they published a study looking at the correlation of mortality rates in 1968 – 1978 with the infant mortality rates from 1921 – 1925 in 112 authorities from England and Wales. Ischaemic heart disease death rates were highly correlated with previous neo- and postnatal mortality[48].

They further confirmed their results by following up 5654 men born between 1911 and 1930 in

Hertfordshire with good records regarding their weight at birth and at one year of age[49]. The results showed that men with the lowest weight at birth and at one year of age had the highest death rate from ischemic heart disease as adults. This suggested that an *in utero* and childhood environment that leads to poor fetal and infant growth has detrimental effects on the long-term cardiovascular health of an individual.

Subsequently, in 1991, Hales and Barker observed, using the same Hertfordshire cohort, that poor fetal and infant growth also resulted in reduced glucose tolerance in these adults[50]. These findings led to the postulation of the thrifty phenotype hypothesis by Barker and Hales in 1992[51]. It proposed that the correlation between a malnourished fetus *in utero* and the development of T2D in adult life resulted from the response of a growing fetus to undernutrition. It proposed that the fetus would adapt to the low-glucose environment, in which a mild insulin resistance is beneficial allowing the limited glucose available to be supplied to the brain for proper development. It also proposed that the fetus would "programme" its metabolism to be thrifty and be very effective at storing fat and taking in increased nutrients whenever they were available. This aids the survival of the fetus short-term in continued conditions of poor postnatal nutrition but has important health consequences later in life if the fetus is born into conditions of adequate or overnutrition.

This shows that in development plasticity exists that ensures adaptation to the maternal conditions the fetus experiences *in utero* to be prepared for the same environment it expects to be born in. But if these adaptive responses do not match the actual experienced environment of the child a mismatch occurs which can lead to detrimental effects. A baby born to a malnourished mum expects low glucose in postnatal life, adapting to be less insulin responsive to supply sufficient glucose amounts to crucial organs rather than insulin-responsive organs. If this child is now exposed to an excessive nutritional environment postnatally, as found frequently in western countries in the last decades, insulin resistance, T2D, obesity or metabolic syndrome are likely to occur. This hypothesis led in 2004 into the postulation of the concept of developmental plasticity and adaptive response by Sultan et al. [52].
All these epidemiological studies and hypotheses (programming, thrifty phenotype hypothesis, developmental plasticity and adaptive response) form the basis of the DOHaD-field.

1.3.2 Evidence for DOHaD

After the initial observations from Barker in England and Wales further studies confirmed his observations in South India and in Finland[53,54]. The Finish cohort followed 3302 men born in Helskini from 1924 – 1933 and showed in 1993 that babies that were thin and light at birth but had an average or above average body mass at seven years of age had a high death rate from coronary heart disease[54]. This led to the notion that this accelerated growth after birth, termed catch-up growth, is detrimental for long-term health. This highlights the complexity of DOHaD and the many contributors shaping a

healthy life *in utero* and in early life.

In addition, Barker et al. showed in 1993 that the timing of undernutrition is an important determinant of the effects[55]. This was confirmed in studies of the Dutch hunger winter due to the occupation by the Germans in World War 2 from 1943 to 1944[56]. Babies that were exposed to famine *in utero* (daily food intake of the mum during a 13-week period below 1000 calories) in late or mid gestation were lighter and smaller than average and had reduced glucose tolerance later in life. If exposure occurred in early gestation the babies were heavier and had an increased coronary heart disease risk later in life, demonstrating the different critical time windows during gestation for different organ systems.

The field of DOHaD started with a huge number of observations from epidemiological association studies and natural catastrophies (such as famines) related to undernutrition in pregnancy resulting in poor fetal and child growth. But the relationship between *in utero* nutrition and growth and cardio-metabolic diseases is nowadays assumed to be U-shaped[57]. Over- and undernutrition both influence long-term offspring health. This is crucial as overnutrition has become highly prevalent in the past years as highlighted in section 1.1.

1.3.3 Programming factors

In recent years the field of DOHaD has evolved beyond the effects of the maternal nutritional status. Exposure to stress, environmental toxins, infections and high-altitude during pregnancy are now also found to influence long-term health of the offspring. Interestingly as the next section demonstrates all these factors affect similar pathways in the developing fetus and child, often leading to cardiovascular and/or metabolic diseases in adult life. It is increasingly shown that all these adverse exposures *in utero* are affecting boys and girls in a different manner, with the male fetus usually being more vulnerable to adverse outcomes[58]. Boys are known to grow faster *in utero* and thereby lack placental reserve functions to adapt to changing environmental cues[59].

Although this thesis focuses on the maternal programming factors, in recent years it has become increasingly evident that the father also contributes to the long-term health of his child. It is known that over- and undernutrition of the dad can lead to epigenetic alterations in the sperm and altered seminal fluid affecting uterine responses influencing implantation and the early embryo environment[60,61]. These effects further translate into adverse long-term cardiometabolic health consequences in the offspring. Full spermatogenesis in humans only takes three months, making it a feasible window to improve paternal health before conceiving, such as diet and exercise interventions to tackle the high prevalence of obesity in men of reproductive age. These have been shown to be successful in animal models[62].

1.4 Environmental cues that lead to fetal programming

1.4.1 Undernutrition

The Dutch hunger winter and other association studies from famines mainly during/in the aftermath of World War II or famines in China, Cambodia or Austria support Barker's findings. The Chinese famine from 1959 to 1961 was the longest and largest famine and offspring exposed to the famine *in utero* had a 2-fold increased risk for hyperglycaemia and showed additionally higher risks for T2D, hypertension, Non-Alcoholic Fatty Liver Disease (NAFLD), obesity, cognitive impairment and metabolic syndrome[63]. The analysis of 325000 Austrian patients under diabetic treatment during 2006/2007 showed clear peaks of an excess diabetes risk in people born in years of three different famines in Austria[64]. Studies in identical twins have helped to demonstrate that the associations of a low birth weight due to an adverse fetal environment or undernutrition with long-term cardiometabolic effects are independent of the genotype[65].

It is important to recognize the adverse outcomes of undernutrition for future generations due to current famines in countries like Somalia or Yemen and the presence of undernutrition in developing countries[66]. As outlined in the previous chapters a mismatch between pre- and postnatal environment is particularly detrimental for the cardiometabolic health of the offspring. Thereby the rapid rise of a westernized lifestyle in developing countries and the type of emergency food sent to countries with acute famines could exacerbate the detrimental effects of *in utero* undernutrition to the long-term health of the offspring[63,66].

In developed countries undernourished pregnancies occur e.g. in teenage mothers. They have an increased risk to deliver babies of low birthweight and neonatal mortality is high. The APGAR score, a score to assess a new-born's health by looking at Appearance, Pulse, Grimace, Activity and Respiration of the baby, is often found to be reduced[67]. A study in the US suggests that this is not attributed to confounding factors such as their socioeconomic or social level, but it is likely to be caused by the unfinished growth of the teenage mum who is therefore competing for nutrients with the fetus. Additionally, her uterine and cervical blood supply is likely to be still immature. Therefore, teenage pregnancies resemble features of an undernourished pregnancy.

Animal studies further support the observations from human studies. Models of maternal/fetal undernutrition exist mainly in rats, but studies in mice and sheep also helped the mechanistic understanding. Undernutrition can be either mimicked by caloric restriction [50% (mild) or 30% (severe) of the daily ad libitum intake] or via restriction of the protein content of the diet to only 5-8% protein content (low protein diet)[68]. A normal chow diet is usually comprised of approximately 15-20 % protein. Both, calorie and protein restriction during pregnancy, lead to growth-restricted fetuses who are more likely to develop hypertension, impaired glucose tolerance and hyperphagia in adulthood[69]. Reproductive health of the offspring is affected as shown by reduced primordial follicle

numbers and follicular health in female offspring from mums fed a low-protein diet during pregnancy[70].

Multiple mechanisms are proposed. Epigenetic alterations in the hypothalamus could explain the hyperphagia seen in the offspring[71] and epigenetic alterations affecting Igf2 signalling in the heart were linked to detrimental myocardial remodelling[72,73]. ~~It was shown that~~ Increased exposure to glucocorticoids may mediate some of the effects of maternal undernutrition to increased hypertension and hyperglycaemia risk later in life[74]. The 11β-hydroxysteroids dehydrogenase type II (11β-HSD2) enzyme in the placenta normally inactivates glucocorticoids to protect the fetus from exposure to high concentrations. Multiple studies suggested a reduced expression of this enzyme in undernutrition models and an increased activation of the maternal hypothalamus pituitary axis increasing maternal glucocorticoid levels further increasing exposure of the fetus to glucocorticoids.

1.4.2 Maternal stress and environmental toxin and hypoxia exposure

High levels of glucocorticoids might also link the detrimental effects of maternal stress exposure to adverse neonatal outcomes. There are multiple studies in women exposed to natural disasters (storms, floods) or distressing life events during pregnancy with the goal to assess the impact on the offspring. Women whose close relatives or partners died during pregnancy experience an increased risk of preterm birth and low birth weight[75,76]. The Ice Storm project which followed up children born to women who conceived shortly after or were pregnant during an ice storm in 1998 in Quebec, Canada showed that their children had an increased obesity risk at 5 years of age[77]. Additionally urinary metabolomic profiles in the offspring in adolescence showed changes in metabolism and protein biosynthesis pathways consistent with an increased risk for metabolic diseases later in life[78]. Effects of maternal stress on neurodevelopment of the offspring have also been demonstrated[79]. Stress during a flood in Queensland and the ice storm in Canada both led to impaired motor development. And maternal stress in general has been associated with mental health problems (such as depression) and schizophrenia in the offspring[79]. Studies of natural disasters pose the difficulty of many confounding factors such as sleep disruption, changed eating as well as general behaviour. Therefore, animal models were helpful in confirming the associations seen in human studies. Pregnant rats that were frequently restrained gave birth to low birthweight offspring which were also hyperglycaemic and had decreased leptin levels[80]. Another rat study reported similar long-term effects on metabolic health but offspring had an increased birthweight[81].

It is well known that smoking and alcohol consumption in pregnancy are detrimental, both leading to reduced fetal growth. Smoking can lead to a reduction of around 250 g in birthweight and quitting smoking at the beginning of pregnancy substantially reduces this harmful effect[82]. Alcohol exposure is well-characterized with high and frequent alcohol exposure in pregnancy leading to fetal alcohol

syndrome (FAS). This syndrome is characterized by pre- and postnatal growth retardation, developmental delay and intellectual impairment in the offspring[83]. FAS cases in the US range from 0.7 to 10 cases per 1000 live births[84]. Equally exposure to environmental toxins such as endocrine disrupting chemicals and heavy metals leads to malformations in the fetus and reduced fetal growth[85].

Troubling cases like prescribing pregnant women thalidomide in the late 1950s to treat morning sickness showed the severe impact of teratogens on fetal development. High fetal mortality was reported and the most characteristic sign of exposed offspring are severely shortened limbs due to impaired limb development[86]. Exposure to pesticides in pregnancy has also been shown to potentially lead to a higher risk of neural tube defects in the fetus and water contaminants (such as nitrates, arsenic and selenium) are linked to a higher risk for spontaneous abortion[87].

With the emerging field of DOHaD long-term risk of exposure to environmental toxins are increasingly being studied. The Generation R study, a cohort in the Netherlands, showed increased risk of obesity in children exposed to smoking *in utero*[88]. This was confirmed in other human studies and a rat experiment that suggested that the ingredient nicotine might be the main driver of the effects[89]. Air pollutants and smoking additionally lead to low oxygen in the mum e.g. via high carbon monoxide concentrations in the maternal blood which affect oxygen delivery to the fetus[90,91]. The reduced oxygen supply impairs fetal growth and development and can also result in an adaption phenomenon called brain sparing. Here the fetus redistributes oxygen to the brain to allow its proper development at the expense of other organs[92]. Thereby hypoxia is also associated with long-term cardiometabolic disease risks.

Evidence suggests that low dose *in utero* exposure to common chemicals in our environment including around 900 endocrine disrupting chemicals present in plastic, air pollution, pesticides or water repellents can impact on long-term health[93]. Exposure to Bisphenol A (BPA), a plastic softener, is present in the urine of 93% of US citizens. Animal and human studies have shown that *in utero* exposure leads to increased weight in the offspring[94]. BPA additionally leads to glucose intolerance in the pregnant mum herself that is retained after delivery. BPA is likely inducing an exacerbated insulin-resistant state in pregnancy, leading to a higher risk of gestational diabetes in the pregnancy which has known consequences for both mother and fetus (see section 1.5, p.14).

Pregnancies at high altitudes above 2500 m are also associated with adverse fetal and, long-term outcomes. These pregnancies are characterised by low birth weight and higher risks for complications such as preeclampsia due to the exposure to a hypoxic environment. It is thought that the maternal cardiovascular system is not able to adapt to pregnancy as sufficiently as under normoxic conditions[95]. The fetus is thereby exposed to inadequately low oxygen levels, leading to hypoxia often in the placenta and the fetus (as described above for smoking and pollution). Hypoxia is a clinically relevant

and frequent stress to which fetuses are exposed. Hypoxia is observed not only in the mentioned circumstances but also in maternal undernutrition, iron deficiency, obesity, GDM and pregnancy complications such as preeclampsia, placental insufficiency or malperfusion[96].

1.4.3 Infections

Infections with viruses, bacteria or parasites during pregnancy can severely affect fetal health often leading to reduced growth, developmental impairments, intrauterine death, preterm birth and/or long-term diseases. The fetus is infected by the mum via so-called vertical transmission. This can be during childbirth or during pregnancy via an ascending infection from the cervix with the pathogens then crossing the fetal membranes[97]. The infection can also occur in the decidua or fetal Hofbauer cells that act as placental reservoirs and replication sites for viruses in the placenta[98]. TORCH (Toxoplasma gondii, Other, Rubella virus, human Cytomegalovirus (HCMV), and Herpes simplex virus) syndrome summarizes infections of the child during pregnancy or childbirth, all resulting in very similar fetal outcomes. The congenital rubella syndrome induced by intrauterine rubella infection is well-described and hence is a pathogen that young women are often immunized against. Its teratogenic effects were first observed in 1941 and it is known to arrest organ development and affect cellular growth[97]. Studies show that intrauterine infection with rubella increases the risk for developing type 1 diabetes in the offspring. As known for other viruses (like enteroviruses, coxsackie B, HCMV and mumps) some of the rubella proteins are similar to pancreatic islet β-cell proteins, thought to cause an autoimmune attack against these β-cells[97]. HCMV infections are highly associated with fetal growth restriction, preeclampsia, still- and preterm birth. It is thought that the high level of placental pro-inflammatory cytokines in addition to cytopathic effects of the virus lead to apoptosis in the placenta, an arrest of placental vascularisation and cytokines diffusing into the fetal brain impairing neurodevelopment. Children with an intrauterine HCMV infection thereby suffer from brain damage[97]. The recent outbreak of SARS-CoV2 and its potential for vertical transmission to the fetus from an infected mum is debated. A study designed in 2012 to look at pregnancy outcomes during a pandemic was quickly reactivated and showed that pregnant women with the same risk factors seen in the general population (mainly obesity and its co-morbitides) were more likely to be infected[99]. Strong evidence of vertical transmission to the fetus has not yet been found. A study looking at the pathology of SARS-CoV2-infected placentae showed no inflammatory pathology in the placentae, but signs of mal-perfusion[100]. More recent studies highlight the increased risk for preterm birth associated with SARS-CoV2 infections in pregnancy[101].

Bacterial infections can also be harmful for the fetus. Very severe effects are seen upon infections with L. monocytogenes. This bacterium is present on raw meat, raw unwashed vegetables and unpasteurized cheese and often leads to spontaneous abortion, intrauterine death and preterm

birth[97]. Studies show that antibiotic treatment is often not sufficient to prevent preterm birth induced by bacterial infections[102,103]. This led to the notion that the induced inflammation rather than the infection itself has the harmful impact on fetal development. Pregnancy is a state of a fine immune balance between defence against pathogens and tolerance of the developing fetus. If this balance is altered, e.g. if the immune system is more active due to inflammatory triggers, this can be detrimental. These triggers don't need to be infections with viruses, bacteria or parasites but can be danger-associated molecular patterns (DAMPs), a so-called sterile inflammation[104]. These DAMPs are released upon cellular stress and death and can be debris, cell free fetal DNA or mitochondrial DNA. These DAMPs can be induced by a myriad of stressors such as hypoxia, vascular dysfunction, obesity or stress in the mother. Thereby inflammation in the placenta and fetal membranes is induced leading to adverse outcomes both in fetal development and later life.

1.4.4 Overnutrition

As detailed above multiple factors are important for healthy fetal development and long-term health. Many of these environmental factors lead to similar effects, such as inflammation, hypoxia, maternal endocrine changes or failure of sufficient pregnancy adaptation. Equally long-term effects repeatedly affect brain and cognitive development, metabolic and cardiac health. As outlined earlier, one environmental factor being highly present in many environments worldwide is overnutrition. The next sections will therefore look at overnutrition in pregnancy, its associated complication gestational diabetes mellitus (GDM), and a detailed analysis of the effects on the mother, fetus, placenta and child.

1.5 The physiology and pathophysiology of pregnancy in human and mice

1.5.1 Maternal adaptations to pregnancy

Maternal physiology changes drastically during mammalian pregnancy to support fetal growth and demand sufficiently. The fetus and the placenta need an appropriate supply of nutrients and oxygen, thereby it is key during pregnancy to increase blood supply to the fetus and enhance nutrient delivery (especially glucose) to the fetus. To accommodate nutrient supply, insulin sensitivity is increased in the first trimester to enhance maternal glucose stores[105]. The increase in insulin sensitivity also increases lipogenesis which together with hyperphagia in pregnancy increases the fat stores during the first two trimesters. Additionally a degree of leptin resistance is physiological in pregnancy, with the placenta producing leptin during pregnancy[105]. A reduction in insulin sensitivity at the end of the second trimester, as a consequence of secretion of placental hormones such as placental lactogen, allows supply of the glucose stores to the fetus. During a healthy pregnancy glucose homeostasis is maintained via β-cell hyperplasia and hypertrophy. The reduced insulin sensitivity causes a breakdown of the fat stores leading to increased lipid supply to the growing fetus[106]. As outlined in the introduction, if β-cell hyperplasia and hypertrophy fail to compensate sufficiently for the insulin

resistance, GDM results[105]. In women with GDM, lipid changes are equally no longer physiological leading to dyslipidemia[107]. In a healthy pregnancy the excess energy is stored in adipose tissue rather than muscle or liver tissue to protect the body from metabolic syndrome. However in GDM, adipocytes have been found to be less differentiated and insulin resistant leading to a non-safe disposal of excess energy stores and potentially gluco- and lipotoxicity in peripheral organs[105]. This phenotype of glucose and fat stores reaching maximum capacity in adipocytes early in pregnancy leading to lipid deposition not in adipocytes later in pregnancy has been observed in mouse and rat pregnancies as well as in humans[108,109].

Pregnancy additionally requires sufficient oxygen supply to the fetus via complex adaptation of the maternal haemodynamic system. The first change in the maternal cardiovascular system is an increase in heart rate, which in human pregnancy occurs at 5 weeks of gestation[110]. Some studies show similar changes in mouse pregnancy, where heart rate was increased to a peak around embryonic day E7 - E9 and then declining to pre-pregnancy levels until birth[111].

In humans spiral arteries are remodelled early in the first trimester, a process that happens in mid-gestation in the mouse[112]. Uterine spiral arteries are small arteries branching off from the uterine artery in the innermost layer of the uterine wall, the endometrium. Spiral artery remodelling in pregnancy involves opening of the spiral arteries into the intervillous space of the placenta. Additionally, endothelial cells are replaced by placental trophoblast cells, so that the remodelled spiral arteries are independent of maternal vasoconstriction, leaving them wide open for sufficient blood supply. The blood supply to the spiral arteries itself is guaranteed by an increase in the uterine artery vessel diameter, reducing vascular resistance[113]. Thereby Doppler measurements of the uterine artery are a good estimate for a healthy pregnancy. With advancing gestation, the common waveform shows an increase of the end diastolic velocity, describing blood velocity at the end of the cardiac cycle. This increase reflects the reduction of vascular resistance in the uterine vessel. The calculation of the pulsatility index (PI = (peak systolic velocity (PSV) - end diastolic velocity (EDV)) / (mean velocity)) and the resistance index (RI = (PSV - EDV) / PSV) thereby allows evaluation of the drop in resistance in the uterine artery. PI and RI are known to decrease across gestation. The reduced vascular resistance is important to avoid hypertension as pregnancy also increases cardiac output (CO=stroke volume x heart rate) by up to 50% of the baseline CO with a peak at 32 weeks of gestation in humans[114]. Additionally the plasma volume is also increased by 50% at 34 weeks of gestation in humans[115]. Therefore, the drop in vascular resistance can avoid the development of hypertension, blood pressure drops at 6 weeks of gestation, stays low during the second trimester and returns to baseline at the end of a healthy pregnancy. In mice (C57Bl/6J) CO increases by around 28 % by embryonic day E9.5 and by E17.5 an increase of 48% in CO can be observed[116]. Comparable to the human situation arterial pressure decreases towards the middle of the mouse pregnancy and plasma volume is increased by 27% by

E17.5 as well. Even slight impairments in the adaption of cardiac output or uterine artery compliance can lead to altered fetal growth, resulting in IUGR[117]. As outlined in the general introduction this can have detrimental effects on long-term offspring health.

A serious condition that can develop if adaptation to pregnancy does not occur appropriately is preeclampsia, characterised by hypertension and proteinuria either early (before 34 weeks of gestation) or late (after 34 weeks) in human pregnancy. Some women also present with an increased concentration of sFlt (soluble fms-like tyrosine kinase 1). This soluble receptor can bind the vascular endothelial growth factor (VEGF) family members VEGF-A and placental growth factor (PLGF) which are both key regulators of angiogenesis and the development of the placental vascular network. By being bound to sFlt they are thought to lead to an angiogenic imbalance, endothelial dysfunction in the mother which can manifest the systemic changes (hypertension) in the mother[118]. Despite its discovery over 200 years ago and a high incidence of up to 10 % of pregnancies worldwide the exact pathogenesis of preeclampsia is very poorly understood[118]. Factors such as maternal smoking, maternal obesity, diabetes, advanced maternal age and genetic factors are known to be associated with increased risk of the condition. One main cause of preeclampsia is thought to be an insufficient remodelling of the spiral arteries (as described above). Thereby the condition is characterised by increased vascular resistance, with a high uterine artery PI and RI and hypertension. A complex interplay of the resulting placental hypoxia and damage of the placenta leading to abnormal secretion of placental hormones is thought to be involved. Additionally recent data highlights that poor cardiovascular health prior to pregnancy contributes to the development as well[117]. This additional risk factor may contribute to increased preeclampsia risk in obese women during pregnancy.

Preeclampsia does not occur spontaneously in mice, unlike humans and some great apes where preeclampsia occurs naturally. This is hypothesized to be due to the human placenta being the most invasive placenta type compared to other species with very high prenatal brain and body growth rates[119]. In mouse models preeclampsia is typically induced by surgical ligation of the uterine artery or through genetic models including inbreeding mice with high blood pressure[118]. However overall haemodynamic changes are similar between mouse and human pregnancies[110].

1.5.2 Fetal health and growth in pregnancy

Appropriate fetal growth, metabolism and physiology are key components of a healthy pregnancy. For accurate fetal growth assessment ultrasound is the main tool in routine obstetric practice. To achieve a good estimate of fetal health and size, dating of the pregnancy is crucial. As recommended by the WHO many countries perform a first ultrasound scan in the first trimester allowing the calculation of gestational age using data from the scan together with the date of the last menstrual period[120]. If this ultrasound is performed before 13 weeks of gestation it is very accurate in predicting the gestational age by measuring the crown rump length (CRL) of the fetus[121]. According to WHO recommendations,

only one ultrasound scan before 24 gestational weeks is required to assess gestational age and detect abnormalities. However, in many countries two ultrasounds are performed, one in the first trimester to assess the age and another one at 18-22 weeks to assess fetal growth and size as outlined for example in the NICE guidelines in the UK. In some countries a third ultrasound scan in the third trimester is offered. On an ultrasound scan abdominal and head circumference (AC and HC) together with the CRL can be assessed. This allows the calculation of the estimated fetal weight (EFW). The international fetal and newborn growth consortium for the 21st century (Intergrowth21) recently assessed the ultrasound measures in healthy, well-nourished women in eight countries to establish international standards[122,123]. These standardized growth centiles allow to assess whether a baby is appropriate for gestational age (AGA), small for gestational age (SGA, below 10th percentile) or large for gestational age (LGA, above the 90th percentile), this is assessed with the birth weight, whereas IUGR is identified by reduced growth of the fetus while in the womb. A recent study assessed the use of these standards at birth in a population of women with T1D, who are at a high risk to deliver LGA babies. This showed that using these standards could successfully identify the LGA babies at birth, which are sometimes missed using other standards due to preterm delivery of the baby. The authors also showed an association of LGA in babies with adverse postnatal complications[124].

The intergrowth centiles do not consider any individual factors such as maternal weight or ethnicity. However it has been suggested that it could be beneficial to customize the centile standards by inputting maternal height, weight, ethnicity and parity and thereby determining the estimated individual growth potential of a fetus[125]. These customized measures are now used to build the Gestation Related Optimum Weight (GROW) centiles developed by Gardosi et al. to monitor fetal growth[126]. These are thought to predict more accurately which fetuses are at risk of abnormal growth and potentially stillbirth[125,126]. However with the current data a causal relationship between reduction of stillbirth and the use of these customized growth assessments can't be drawn with some researchers questioning the objectiveness of the findings from Gardosi et al due to a conflict of interest[127,128]. Regardless of the method all these standards also include centiles for measures of the symphysis-fundal height. As ultrasounds are done during pregnancy only once or at most twice in many countries and as ultrasound is an expensive resource in low-income countries, measurement of the size of the belly (symphysis-fundal height) of a pregnant woman is also used to gain important information about fetal growth[129]. However, it can't detect SGA or LGA fetuses as effectively as ultrasound measures. Thereby pregnancies at high risk e.g. due to hypertension, smoking, maternal age or history of pregnancy with IUGR are usually offered multiple serial ultrasound scans during pregnancy if possible. This intensive monitoring of fetal growth has been shown to detect fetuses at risk[130]. For example, it was found that women at risk of delivering an SGA fetus due to vascular impairments associated with GDM could be detected with additional ultrasounds in late pregnancy[131]. This was especially true for

asymmetric growth that often occurs in the third trimester only. In these circumstances measures such as the blood flow to the placenta and in the middle cerebral artery (MCA) of the fetus become important measures. The middle cerebral artery, part of the circle of Willis in the brain, is a measure for the blood flow in the fetal brain. The cerebroplacental ratio (CPR), the ratio of the PI of the MCA and umbilical artery PI, can show how well the placenta is working. If the placenta is insufficient and the placental resistance therefore high, the diastolic flow in the umbilical artery will be low, resulting in a high umbilical artery PI. This could result in the fetus becoming hypoxic, trying to protect its brain via cerebrovascular dilation, a phenomenon called brain sparing. The PI of the MCA therefore becomes low, resulting in a low CPR value. In the clinic a low CPR value is therefore indicative of a high IUGR risk of the fetus as a low CPR is associated with low fetal growth velocity at the end of pregnancy[132,133]. A summary of the normal growth velocities in a human pregnancy can be found in Figure 4.1A.

In mouse pregnancy fetal weight is well documented throughout gestation as body weight can be directly measured via fetal weighings on each day of gestation. As highlighted in Figure 4.1B and the general introduction, the period of fetal growth is very short in a mouse pregnancy with the mouse fetus growing exponentially at the end of pregnancy. Despite frequent use of the mouse as a model organism in pregnancy research no weight standards exist. Dilworth et al. attempted to provide standards for fetal body weight in their studies and suggested the creation of a repository with fetal weights from a range of different mouse strains[134]. This could help in assessing healthy fetal growth by comparing to the standard weights of wildtypes from a particular strain. However a frequently used measure to assess murine placental and fetal development is the use of the ratio between fetal birth weight and placental weight as a measure of placental efficiency[135].

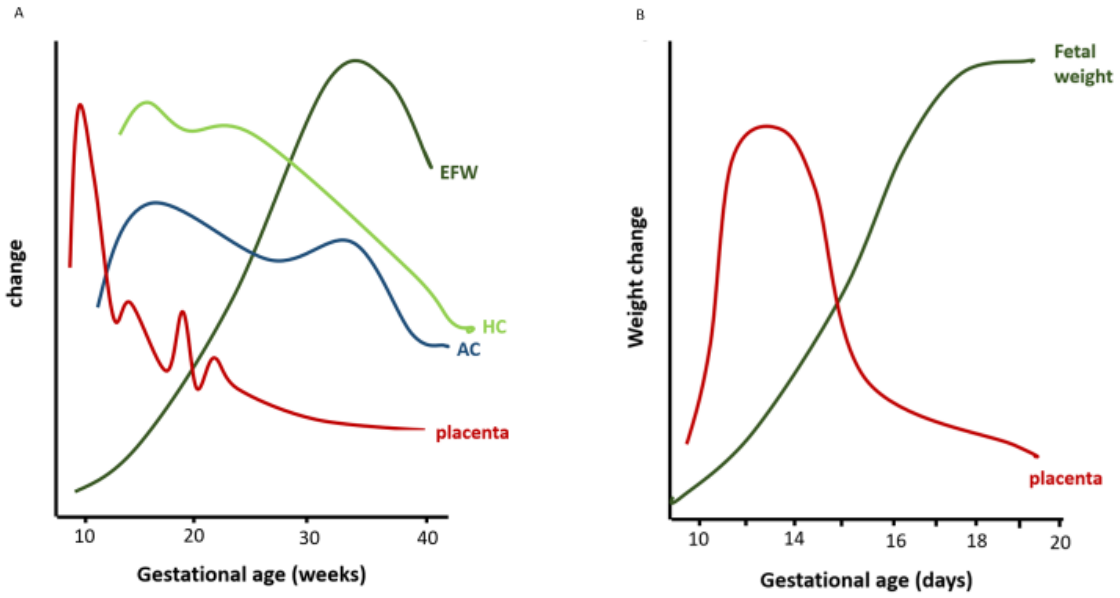

Figure 1.3: Growth velocities in human and murine pregnancy

(A) Graphs are adapted to show the change in placental weight (red), estimated fetal weight (EFW, black), head (HC, green) and abdominal circumference (AC, blue) in a human pregnancy[136,137]*. (B) The weight change of the placenta and the fetal weight in a murine placenta is shown*[138]*.*

1.6 Gestational diabetes mellitus (GDM)

1.6.1 Prevalence and pathophysiology of GDM

Hyperglycaemia affects approximately 16% of pregnancies worldwide[139]. This includes both types of hyperglycaemia during pregnancy: pre-existing diabetes (type 1 and type 2) and GDM (which develops during pregnancy). GDM is defined as glucose intolerance that only presents itself during pregnancy and usually vanishes after delivery. It is an increasing problem worldwide and across the globe the prevalence ranges from 1 – 30% with the highest prevalence in the Middle East, North Africa and South-East Asia (Figure 1.3A). The high variability in the diagnostic criteria used makes it challenging to compare prevalence between countries (Figure 1.3B). Section 1.6.4 discusses in more detail the missing consensus regarding diagnostic criteria for GDM.

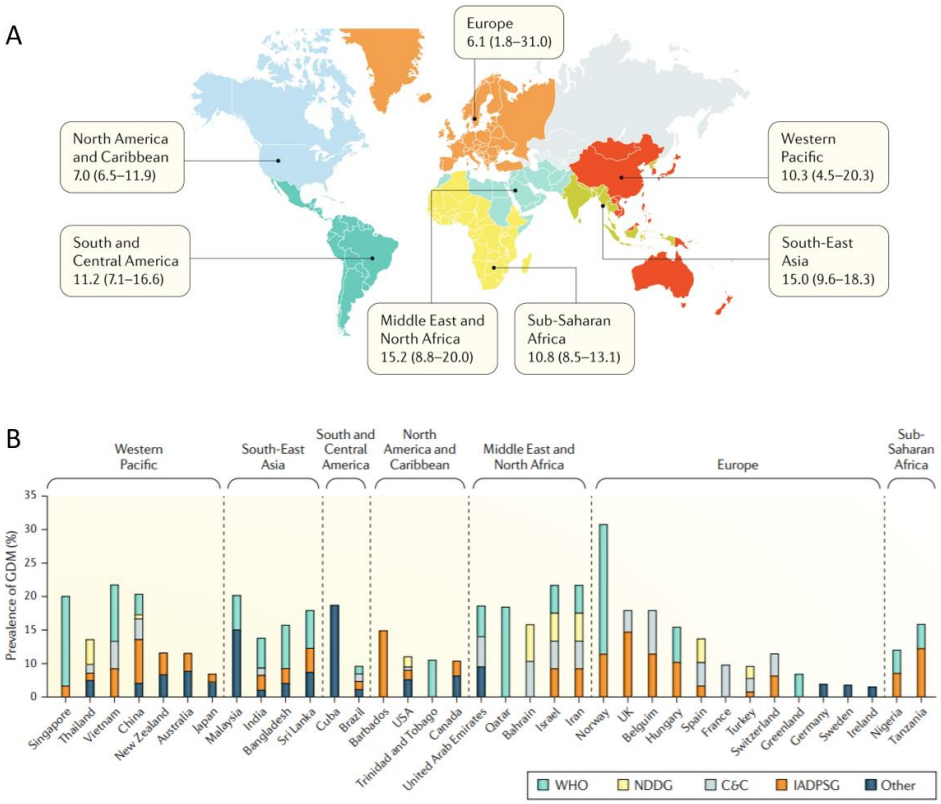

Figure 1.4: GDM prevalence varies worldwide

(A) GDM prevalence is shown as median percentage and interquartile range in brackets in 2005 – 2018 [140]*, permission for use of figure has been obtained. (B) Use of different diagnostic criteria and therefore prevalence is shown* [140]*, permission for use of figure has been obtained.*

First described by the German doctor Bennewitz in 1824[141], it was debated until the 1960s whether the diabetic state in pregnancy is pathological or physiological[142]. Even in a healthy pregnancy a state of insulin resistance is induced. In early pregnancy insulin sensitivity ensures that sufficient glucose stores are built up in maternal adipose tissue to support fetal growth in later pregnancy[105]. At the end of the second trimester (around week 20)[143] insulin resistance is induced by local and placental hormones (estrogen, progesterone, leptin, cortisol, placental lactogen, growth hormone)[144]. The resulting high blood glucose levels along with free fatty acids (FFAs) (due to fat store breakdown resulting from resistance to the anti-lipolytic action of insulin) allow high glucose and FFAs to be transported to the fetus that is now growing rapidly. During this time hyperplasia and hypertrophy of pancreatic β-cells compensate to produce more insulin and ensure normal glucose homeostasis (Figure 1.4A)[105]. Within one to two days after delivery the placental hormones that have a short half-life have cleared from the maternal circulation, allowing the mother to return to her pre-gestational insulin sensitivity state[143]. This whole circle of compensatory β -cell adaptation during pregnancy-induced insulin resistance fails during GDM pregnancies, resulting in hyperglycaemia (Figure 1.4B).

Hyperglycaemia usually resolves after delivery but can persist, especially if glucose homeostasis was already mildly impaired prior to pregnancy[105]. Multiple risk factors for GDM (such as obesity, unhealthy diet, maternal age) interfere with insulin signalling/insulin sensitivity (Figure 1.4C) or β-cell function prior to pregnancy so that the pregnancy-induced changes can lead to a manifestation of insulin-resistance, β-cell-dysfunction and impaired glucose homeostasis[105].

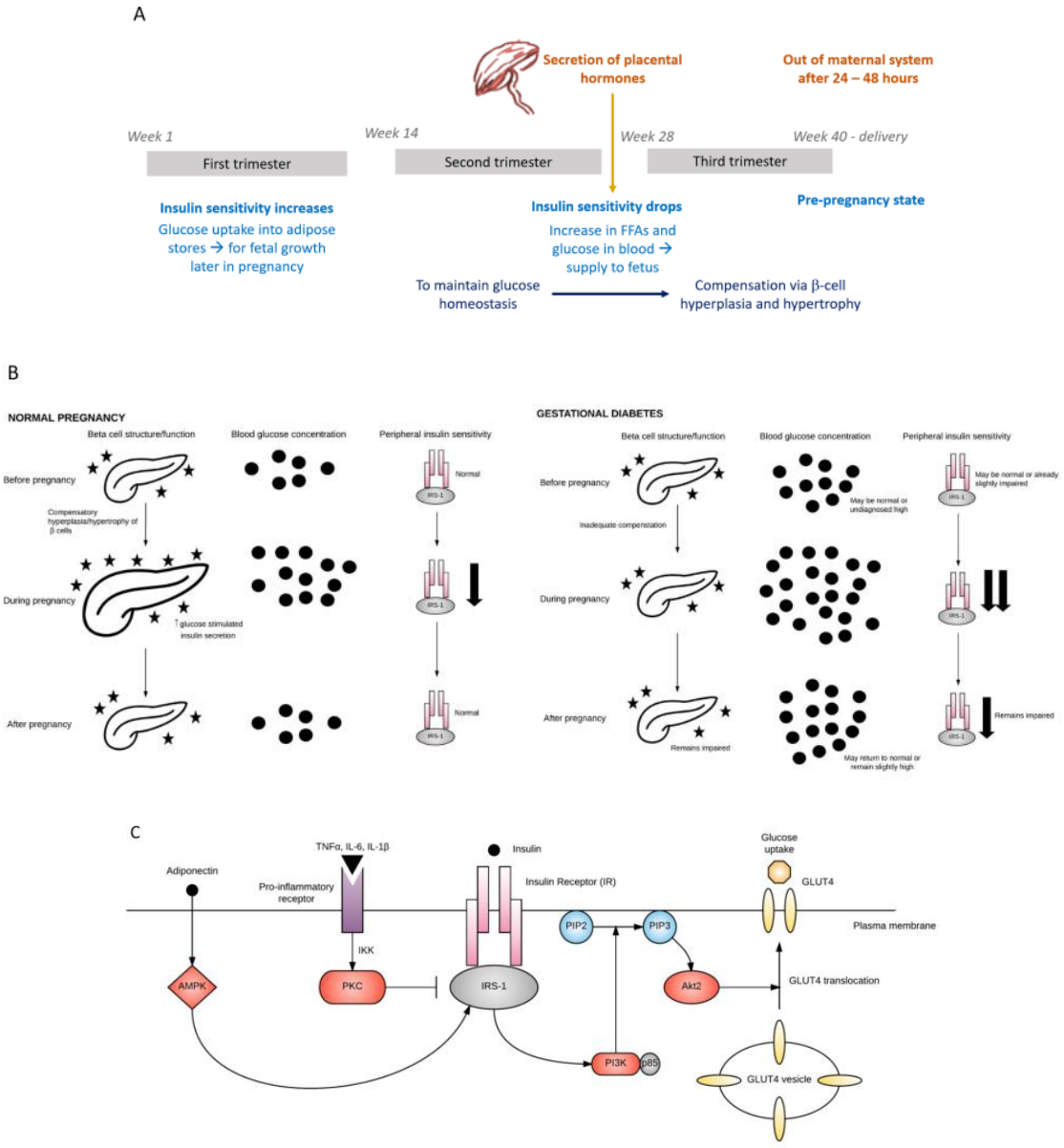

Figure 1.5: The pathogenesis of GDM

(A) Physiological changes occur across pregnancy. (B) The difference in the ability of preventing hyperglycaemia in a normal vs. a GDM-complicated pregnancy is shown with stars indicating insulin and circles showing glucose[105], figure used with permission (CC-BY licence). (C) Insulin signalling is impaired by the presence of pro-inflammatory cytokines and adiponectin, both affected by obesity[105], figure used with permission (CC-BY licence).

1.6.2 Effects of GDM on mother and child – human observations

It is well known that diabetes in pregnancy leads to maternal and fetal short-term complications and detrimental long-term outcomes. A lot of observational data comes from women with pre-gestational (T1 or T2) diabetes, which is known to have more severe adverse effects (e.g. congenital malformations or stillbirth) on pregnancy outcome and fetal health than GDM, perhaps because the glucose intolerance is present from the point of conception.

Women with GDM and pre-existing diabetes are more prone to complications such as hypertension or preeclampsia during pregnancy[105]. Often babies are delivered earlier, especially if GDM is not well controlled, to avoid longer exposure of the fetus to hyperglycaemia[145]. Delivery is more commonly performed via caesarean section (C-section) to reduce harm for mother and the baby due to the often macrosomic fetus[146]. After a GDM pregnancy women are more likely to develop T2D and CVD themselves later in life. Thereby a GDM diagnosis has consequences for the maternal long-term health and may represent a good indicator that early interventions to prevent T2D development would be particularly beneficial.

Fetuses born to mothers with GDM or pre-gestational diabetes are more likely to be macrosomic or, in cases with vascular complication, growth-restricted. Furthermore, neonatal respiratory distress syndrome, neonatal polycythemia and hyperinsulinemia in the fetus are also often reported. High levels of maternal glucose, which freely crosses the placenta, induce hyperinsulinemia in the fetus and consequently often hypoglycaemia in the neonate. Increased oxidative stress and impaired placental development are associated with diabetic pregnancies and contribute to an increased risk for long-term health effects in the offspring[147]. Increased stimulation of fetal pancreatic β-cells to produce more insulin makes the offspring prone to develop diabetes later in life. Offspring from diabetic women are more likely to develop cardiovascular and renal diseases as well as obesity and T2D.

1.6.3 Animal models of GDM

Animal models have helped to elucidate the underlying mechanisms of adverse health outcomes for mother and child in GDM pregnancies. Commonly used in diabetes research, β-cells can be destroyed by injection of alloxan or streptozotocin (less unspecific effects compared to alloxan)[148]. Depending on the dose a mild or severe diabetic phenotype can be induced. Often these models mimic pre-gestational diabetes as the injections are usually done before the pregnancy to avoid adverse effects on the fetus by the chemical itself. Large animals such as pigs, sheep and non-human primates (NHP) were used in a limited number of studies with induction of diabetes by alloxan injections showing similar maternal and fetal phenotypes to human diabetes[149].

More often rodent, especially mouse models are used. Apart from chemical models, genetic and dietary models of T2D are used to investigate pre-gestational and gestational diabetes. Genetic models include the non-obese diabetic mouse (NOD), an inbred strain that develops diabetes spontaneously

and can be used as a T1D model [150]. A liver-specific insulin receptor knock-out model (LIRKO) presents hyperinsulinemia before pregnancy but displays glucose intolerance and hyperglycaemia during pregnancy[151]. The adiponectin knock-out (Adipoq$^{-/-}$) develops glucose intolerance during pregnancy returning to the pre-gestational glucose status postpartum. Most used is a heterozygous leptin receptor mutation model (Lepr$^{db/+}$), which also only presents with hyperglycaemia during pregnancy. Additionally dietary interventions like high-fat diet (HFD) feeding are used as models of obesity often showing signs of impaired insulin sensitivity and glucose tolerance. Section 1.9 will give an overview of the effects of diabetes in these models on the mother, the placenta, the fetus and the offspring.

1.6.4 Diagnostics of GDM

To avoid the detrimental effects of GDM on mother and child described above effective screening is needed to intervene as early and as efficiently as possible in human pregnancy. The best way to screen for diabetes is heavily debated[152]. Figure 1.5A describes the history of diagnosis of GDM. In 1964, the first screening criteria were proposed by O'Sullivan and Mahan in Boston[142]. A 100 g glucose load 3 hour oral glucose tolerance test (OGTT) was performed during the first obstetric visit of the women to predict the risk of the women developing T2D later in life. This risk was based on OGTTs that were performed periodically for eight years after the pregnancy. Therefore threshold values for GDM diagnosis were established based on the future risk of developing T2D[142]. In 1973 O'Sullivan et al. introduced a two-step test, including a 1 hour and a 3 hour OGTT to ascertain their results[153].

In the 1990s multiple institutions (see table in Figure 1.5B) recommended performing one screening test with a 75 g glucose load and glucose measurements at fasting and 2 hours into the OGTT. The WHO changed the thresholds to make a cut-off that can be used to detect diabetes with and without pregnancy. All these different recommendations and the fact that so far all thresholds of glucose levels are based on the future risk of the mother developing T2D showed that further studies were needed.

The Hyperglycaemia and Adverse Pregnancy Outcomes study (HAPO) was the first systematic analysis of the association between maternal hyperglycaemia and adverse pregnancy outcomes[154]. Started in 2002 the study was the basis of the conference of the International Association of Diabetes in Pregnancy Study Groups (IADPSG) in 2009[142]. They used the study results to base the glucose thresholds on the glucose levels associated with an increased risk of large for gestational age (LGA) babies, increased neonatal body fat and increased cord blood c-peptide levels. The HAPO study demonstrated a continuous relationship between maternal glycaemia and adverse outcomes, thus

establishing a direct biological relationship between the two. Thereby the thresholds set for GDM diagnosis are by nature an arbitrary threshold[154].

A

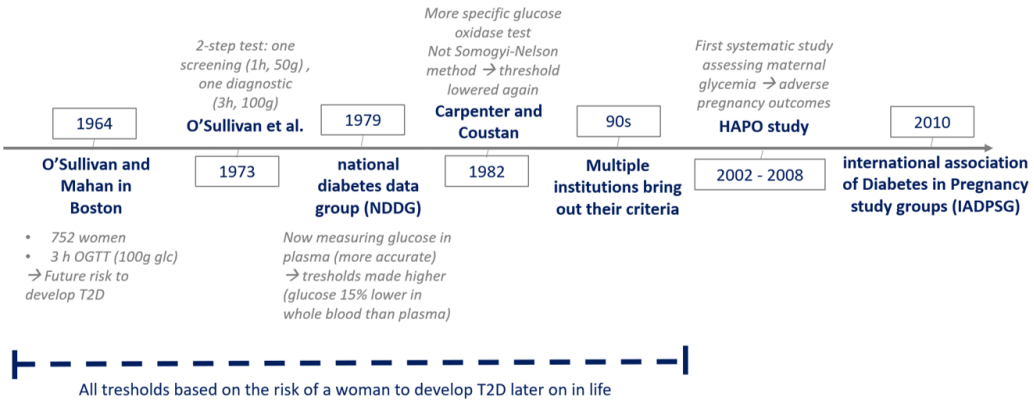

B

	Sample	Steps	OGTT load	No. abnormal	Fasting mg/dl (mmol/l)	1 h mg/dl (mmol/l)	2 h mg/dl (mmol/l)	3 h mg/dl (mmol/l)
O'Sullivan 1964 [6]	B	2	100 g	≥2	90 (5)	165 (9.2)	145 (8.1)	125 (6.9)
NDDG 1979 [11]	P	2	100 g	≥2	105 (5.8)	190 (10.6)	165 (9.2)	145 (8.0)
C&C 1982 [12]	P	2	100 g	≥2	95 (5.3)	180 (10)	155 (8.6)	140 (7.8)
EASD1996 [15]	P	1	75 g	≥1	108 (6)	X	162 (9)	X
ADIPS1998 [16]	P	1	75 g	≥1	100 (5.5)	X	144 (8)	X
WHO 1999 [17]	P	1	75 g	≥1	126 (7)	X	140 (7.8)	X
IADPSG 2010 [4]	P	1	75 g	≥1	92 (5.1)	180 (10)	153 (8.5)	X

Figure 1.6: The development of diagnostic criteria for GDM

(A) Timeline of changes in GDM diagnostic criteria from 1964 to 2010 (based on several publications[142,152,155,156]). (B) Thresholds and diagnostic test types from different institutions, P=plasma, B=whole blood, X=not applicable [142], figure used with permission (CC-BY licence).

There is no current consensus and a lot of different guidelines, test types and thresholds for glucose levels exist within and especially between countries [152]. These different testing approaches and thresholds explain the huge variation in the prevalence of GDM across the world (see Figure Figure 1.4A). Multiple studies also stress that mild hyperglycaemia needs to be treated to reduce the risk of fetal overgrowth, C-section and hypertensive disorders during pregnancy[156]. It has been suggested that older and obese patients in particular may benefit from an earlier screening and detection of GDM [157].

The ideal way to screen for diabetes in pregnancy needs to consider the best outcome for mother and child, feasibility, cost-effectiveness as well as intervention time and method. In addition, whether every woman should be tested for GDM or only those at higher risk remains unclear. Common risk factors include age over 35 years, overweight or obesity, polycystic ovary syndrome (PCOS), prior GDM, family history, high-risk ethnicity and previous still birth. In some countries (e.g. Germany) a non-fasting glucose challenge test (GCT) is performed in all women and only if that GCT shows an abnormal result or the woman is in a high risk group an OGTT performed[158]. Other guidelines (The National Institute for Health and Care Excellence (NICE) in the UK) recommend to only test high risk women as early as possible via an OGTT[159]. Recent studies suggest that the use of biomarkers in early pregnancy to predict later onset of GDM could be valuable[160].

1.6.5 Risk factors for GDM

Women who are over 40 years old have a two-fold increased risk of developing GDM compared to women under 30[140]. A meta-analysis showed that women who are pregnant with a boy have a 4% increased relative risk of developing GDM [161,162]. Smoking, exposure to environmental pollutants and depression during pregnancy are associated with an increased GDM risk[140]. Multiple studies have confirmed an effect of ethnicity with Asians having a very high risk of GDM compared to the Caucasian population. The Middle East and Africa are additional countries with a high GDM risk[163] which might be related to differences in adiposity, lifestyle[140] and genetic susceptibilty[164]. Genetic analyses show that small nucleotide polymorphisms (small changes in the DNA nucleotide sequence), in genes related to the regulation of insulin secretion are associated with GDM. Failure of β-cells to maintain glucose homeostasis via hypertrophy and increased insulin secretion is a key step in the pathogenesis[165]. Women with PCOS are also more likely to develop GDM. PCOS is characterised by high androgen levels, fertility difficulties and high susceptibility to develop obesity, insulin resistance and metabolic problems. The most significant risk factor associated with GDM is a BMI ≥ 25, an unhealthy lifestyle with little activity and a high intake of saturated fats, refined sugars and processed meat[105,166]. Nowadays 86 % of cases of hyperglycaemia in pregnancy are GDM cases, likely reflecting the worldwide obesity epidemic[155,167]. Obese/overweight women probably already have impaired insulin sensitivity or secretion or even undiagnosed diabetes before pregnancy. In low-income countries obesity is becoming an increasing problem, leading to high prevalence of GDM (see high risk in ethnic groups in Asia and Africa)[147]. This is particularly concerning as in many of these populations screening and treatment can't be provided sufficiently[168, 169].

1.7 Maternal obesity

1.7.1 Prevalence of maternal obesity

As detailed in section 1.1, obesity is a global health burden affecting all age groups in the population, including women of childbearing ages (Figure 1.6A). Therefore around 50% of women worldwide enter pregnancy with an unhealthy high body weight (i.e. overweight or obese)[170]. This has been highlighted in an Annual Report of the Chief Medical Officer for England with over half of pregnant women in the UK being either overweight or obese, Figure 1.6B shows the high numbers of babies who are exposed to an obese or severely obese (BMI > 40) environment *in utero* in the UK. In addition to recommendations for a healthy pre-pregnancy weight, gestational weight gain (GWG) is also important and therefore recommendations by the National Academy of Medicine (former Institute of Medicine) have been made. They recommend healthy weight gain depending on the BMI class of the woman. Underweight (12.5 – 18 kg) and normal weight (11.5 – 16 kg) women are thereby advised to gain more weight than overweight (7 – 11.5 kg) and obese women (5 – 9 kg)[171]. Excessive weight gain in early pregnancy in particular has been associated with detrimental long-term effects on the mother (weight retention, high blood pressure)[172] and child (adiposity, high blood pressure)[173]. Multiple studies stress however that pre-pregnancy BMI is a strong predictor of adverse pregnancy outcomes[174–176]. It is therefore very important to establish and improve pre-conceptional counselling and intervention to reduce detrimental effects on mother and child induced by maternal obesity.

A

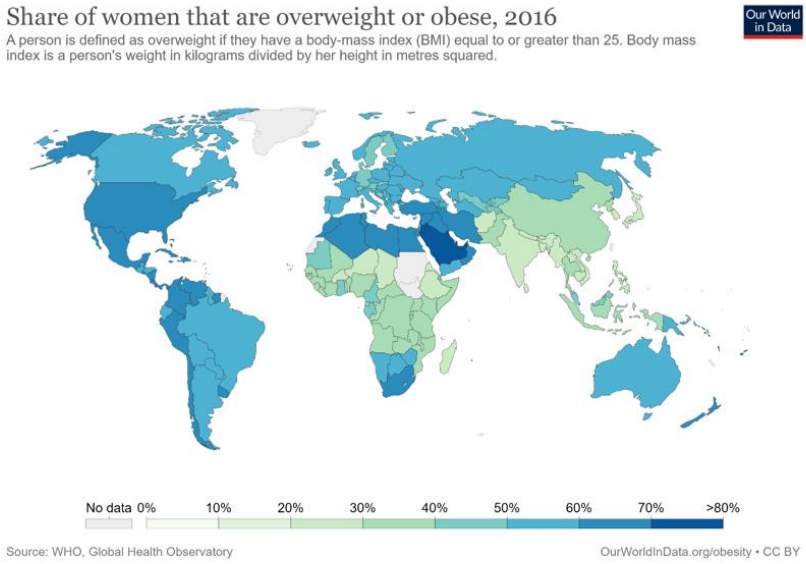

B

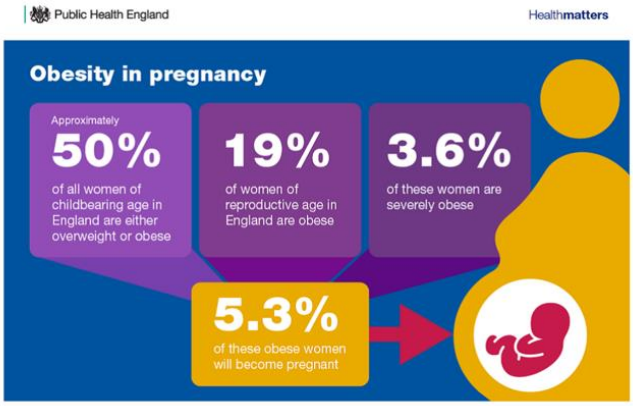

Figure 1.7: Maternal obesity is a critical and rapidly increasing health problem worldwide

(A) Percentage of women over 18 years that have a BMI above 25 [20], figure used with permission (CC-BY licence). (B) UK governmental guidance on pregnancy health highlights the importance of addressing the problem of increasing maternal obesity [177], figure used with permission (Open Government Licence).

1.7.2 Effects of maternal obesity on mother and child – human observations

As outlined in section 1.6.1 maternal obesity is the main risk factor for development of GDM. Obesity also increases the number of women entering pregnancy with pre-existing T2D[178]. Obesity often leads to chronic hypertension and reduced insulin sensitivity, being obese before pregnancy and having these conditions thereby increases the risk of developing preeclampsia as well as GDM[105,179]. Mainly due to these two common complications of maternal obesity, obese women are more likely to experience stillbirth[178]. Early pregnancy loss is also commonly observed in obese women. Accurate assessment of fetal growth and fetal abnormalities via ultrasound is significantly impeded by maternal obesity delaying the identification of abnormal development that increases risk of stillbirth[180]. As with GDM, C-section, induction of labour and increased complications during and after delivery are more

frequently seen in obese women[181]. Obese women are also more likely to show poor health outcomes after delivery with increased risk of depression during and after pregnancy and long-term development of T2D and CVD[178]. Babies born to obese women also show increased complications including macrosomia (due to overnutrition/high glucose) in the womb and also growth restriction (especially at a high BMI when vascular complication like preeclampsia occur more frequently)[182]. Therefore, obese women deliver more babies at both ends of the birth weight spectrum. Long-term risks for the offspring are very similar to the effects of GDM including T2D, obesity, CVD, higher susceptibility to allergies and delay in neurocognitive development[37].

1.7.3 Animal studies of maternal obesity

Animal models are very helpful in proving causality of relationships between maternal obesity and offspring health and in dissecting out the underlying mechanisms. A limited number of studies exist using larger animal models like sheep or NHP. Overfeeding of sheep before and during gestation has been shown to cause increased risk of adiposity and impaired glucose tolerance in the offspring[183]. Studies in NHPs show similar effects. Japanese macaques fed a HFD (32% fat) for four years showed reduced placental blood flow and uterine artery dysfunction and increased stillbirth[184]. Even though larger animals resemble the human situation more closely regarding the litter size, gestation length and placenta type (see section 1.8.2, p.33), rodent models are more commonly used. They have a shorter gestation time (20 days) as well as a shorter life span (allowing studies across the lifecourse) and modifications and interventions can be done more easily.

The range of phenotypes and dietary models used in rodents is very broad. Models differ regarding the fat content of the diet (40 or 60% fat in the diet), the timing of the start of the diet feeding (at weaning, 4 weeks of age or 8 – 12 weeks of age), the duration of feeding (4-10 weeks, 10 – 16 weeks, lifelong) and the bodyweight differences observed between the control and obese/HFD-fed group (less than 5 g difference or more than 5 g difference). Additionally, some models don't only use a diet high in fat but supplement it with sugar water or condensed milk to mimic a so-called westernized diet (high in simple sugars and high in fat). A summary of the outcomes for mother, placenta, fetus and postnatal offspring in all these models is presented in section 1.9.

Our lab uses a model of a 45% HFD supplemented with condensed milk (55 % sugar) fed to the future dam from weaning. After 6 weeks the animals are mated for a first pregnancy that is used to ensure good breeding and good postnatal care by the mum. Mating for the experimental pregnancy is initiated when the animals reach a bodyweight of over 35 g, thereby being on average 10 g heavier than the chow control group. The obese dams have a higher fat mass and are hyperinsulinemic, but only become glucose-intolerant during pregnancy, mirroring a model of GDM.

This shows that as for the human situation animal models of maternal obesity often coexist with diabetic phenotypes, some resembling GDM-phenotypes (such as our model), others report pre-

pregnancy glucose tolerance impairments [185,186] and other studies only poorly characterise maternal metabolic health.

1.7.4 Maternal obesity and GDM

Human observations and animal models highlight the close relationship between maternal obesity and GDM. Therefore, multiple studies have attempted to dissect out the relationship between hyperglycaemia and obesity on adverse outcomes. Some studies have shown that maternal lipids rather than glucose are a stronger predictor of fetal size[187,188]. Interestingly placental changes induced by GDM mainly occur in lipid pathway genes (67%) rather than glucose pathways (9%)[105]. The HAPO study highlighted a strong relationship between maternal BMI (independent of glycaemia) and fetal adiposity and hyperinsulinemia[182]. A Finnish study reported the same association regarding outcomes including increased cord blood c peptide and macrosomia[189]. The authors stressed that some obese women might become hyperglycaemic after the usual screening period and therefore might need more follow-up later in gestation. As obesity alone is a huge driver of adverse pregnancy outcomes it has been suggested to monitor obese pregnancies more closely, much like GDM-complicated pregnancies[189]. Because GDM and maternal obesity are so closely related, both are part of the same intergenerational vicious cycle (Figure 1.7) and present the same adverse pregnancy outcomes, therefore they will be considered together in the following sections of the introduction.

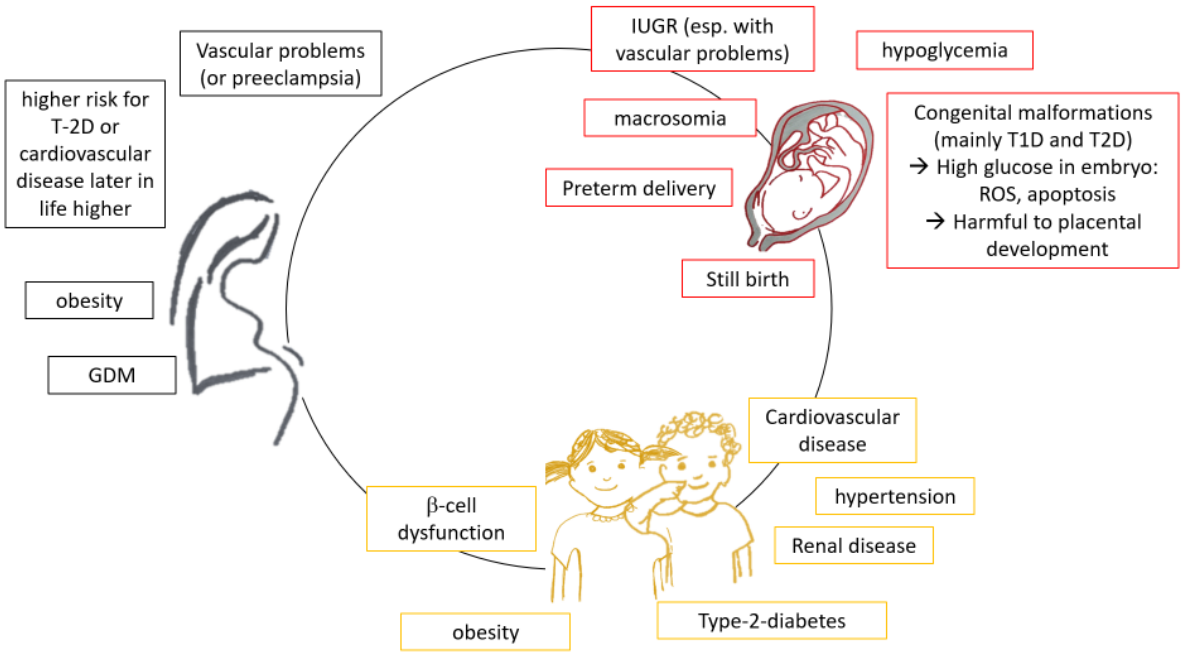

Figure 1.8: Intergenerational cycle associated with maternal obesity and GDM

GDM and obesity in pregnancy do not only lead to complications during pregnancy and in the fetus, but the offspring is also more prone to develop obesity, β-cell dysfunction or even diabetes. As parents of the next generation they are very likely to carry these health risks further into the following generations, closing a vicious cycle of diabetes and obesity.

1.8 The placenta

1.8.1 Placental functions

Despite just being a transient organ for only nine months in humans, the placenta is capable of many different functions and is highly adaptable aiming to ensure healthy fetal development (Figure 1.8). Even though the placenta only contributes to 10-20 % of the uterine mass it uses 40-60% of oxygen and glucose delivered to the uterus[190]. This highlights that the placenta not only connects the fetus to the uterine wall but accomplishes important and energy-consuming tasks. It facilitates nutrient and waste exchange, has endocrine and protective functions and serves as an environmental sensor by adapting to the environment and integrating maternal supply and fetal demand.

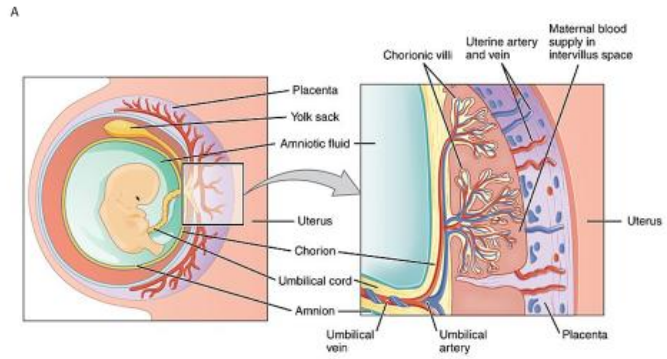

Visualisation of exchange between mother and child via the placenta, redacted for copyright reasons

Figure 1.9: The placenta is the key interface between mum and fetus with essential functions

(A) Fetal blood coming from the umbilical cord and maternal blood coming from the uterine artery are in close proximity in the placenta (B) facilitating exchange of nutrients, oxygen and waste products. (Source: https://pediaa.com/what-is-the-difference-between-chorion-and-placenta/ (figure used with permission (CC-BY licence) and https://ib.bioninja.com.au/higher-level/topic-11-animal-physiology/114-sexual-reproduction/placenta.html)

For transport the main layers that separate maternal and fetal blood that need to be crossed in rodents and humans are the syncytiotrophoblast layer(s) of the placenta and the endothelial cells of the fetal capillaries. Small hydrophobic molecules, such as carbon dioxide, oxygen and alcohol, can cross the placenta easily by diffusion. Maternal and fetal blood flow and the concentration gradient determine the diffusion rate, oxygen is delivered to the fetus and carbon dioxide removed from the fetal circulation into the maternal circulation. The uptake of oxygen into the fetal circulation is supported by fetal haemoglobin and its high oxygen affinity. In the murine placenta the flow of maternal blood is counter-current to the fetal blood flow, further enhancing transport efficiency[191,192] (see Figure 1.9A). Transport of hydrophilic molecules needs to be facilitated. Glucose is the main energy source for both, the placenta and the fetus. Its transport is enabled via glucose transporters (GLUT). A high density of the transporters is seen on the placental side facing the maternal circulation (often referred to as the apical side or the microvillous membrane). This reflects that the placenta itself utilises a lot of glucose

and the expression of GLUTs on the side facing the fetal circulation (basal side, basal membrane) is rate-limiting for glucose transfer to the fetus. GLUT1 is the main transporter, but GLUT3 is also found on the apical side and the fetal capillary endothelium, whereas GLUT4 is only present in the cytosol of the syncytiotrophoblast and thought to be regulated and inserted into the membranes upon insulin stimulation[193].

For transport of amino acids the placenta expresses 15 different transporters. Well-characterised are the system-A and system-L transporters. System A transporters transport small, neutral amino acids like alanine, serine and glycine via sodium-dependent accumulative transporters. These transporters are called small neutral amino acid transporters (SNATs). The system L transporters (called LATs) on the other hand use a sodium-independent exchange mechanism and transport large neutral amino acids across in exchange for non-essential amino acids.

Lipid supply to the fetus is possible via transfer of lipoproteins or FFAs. Triglycerides can be packed into lipoproteins and receptors for the different types of lipoproteins (very low density, low density and high density lipoproteins (VLDL, LDL, HDL)) are present on the apical and basal placental membrane. The expression of VLDL and LDL receptors increases across gestation[194]. Triglycerides can also be cleaved into FFAs by lipases present on the apical side of the placenta. FFAs can then be transported via the fatty acid transport proteins (FATP1-6) on the apical side and the fatty acid translocase (FAT, also called CD36) facilitates transfer across the apical and basal side. A schematic overview of facilitated transport across the placenta can be found in Figure 1.9B. Another well-known substrate for transfer across the placenta are IgG antibodies conferring first immunity to the neonate before the development of its own immunity. IgGs cross the placenta via transcytosis[195]. It is suggested that other proteins and even micronutrients and vitamins such as transferrin-bound iron, Vitamin D and folate are taken up by the placenta via endocytosis, with the membrane protein megalin as an important mediator of the process, but data is still scarce[196–198].

The endocrine functions of the placenta are well-known. In humans very early on in the first trimester the syncytiotrophoblast secretes human chorionic gonadotropin, which maintains progesterone secretion from the corpus luteum. Progesterone is also secreted from the second trimester onwards by the placenta. Progesterone maintains the pregnancy and leads to an increase in maternal appetite and leptin resistance, leading to depositions of maternal reserve. The secretion of placental growth hormone stimulates insulin-like growth factor 1 (IGF1) secretion from the maternal liver which stimulates placental cell proliferation and blood flow to the placenta. Hormones associated with hypoxia, such as erythropoietin and angiotensin II are also secreted from the placenta. In the second half of gestation the placenta produces serotonin from tryptophan. Serotonin is important for neurodevelopment and could explain why children born prematurely suffer from autism and anxiety as they are missing the serotonin supply in this critical time period[190].

The placenta was long depicted as the perfect barrier, which is why drugs were freely prescribed to pregnant women until the 1960s[199]. The placenta is indeed a protective barrier, not only physically but also due to the high abundance of macrophages in the placental stroma, efflux transporters and clearance enzymes. Efflux transporters are present on the apical side of the placenta, thereby being important for efflux of drugs back into the maternal circulation. ATP binding cassette transporter family (ABC transporters), the multidrug resistance protein family (MRPs), organic anion (OAT) and cation transporters (OCTs) along with norepinephrine and serotonin transporters (NET and SERT) can be found in the human placenta[200]. Placental enzymes such as cytochrome P-450, alcohol dehydrogenase or 11β-HSD protect the fetus from alcohol or excessive glucocorticoid exposure that would harm development. However, the barrier is not perfect: alcohol dehydrogenase can't cope with too much alcohol exposure as seen with fetal alcohol syndrome. Also, a change in haemodynamics in the placenta (e.g. due to uterine blood flow changes) leads to shear stress and damages the protective physical barrier of the placenta[194]. The efflux transporters can be used by drugs to enter the placenta and the fetus. Some compounds such as carnitines even inhibit or modulate their transporter function[200].

The placenta aims to adapt to its environment by sensing environmental changes and challenges as will be discussed in section 1.8.4. Additionally, the placenta is the interface between mother and child. Its secretion of hormones and cytokines helps the mother adapt to pregnancy and modulates the immune system of the mum to enable tolerance to the implanting embryo and fetus. Extracellular vesicles (EVs), membrane-bound vesicles from the syncytiotrophoblast, are secreted by the placenta and are thought to modulate maternal immune functions[201]. In recent years they have also been shown as candidates of bidirectional maternal-fetal communication across the placenta via their cargos such as microRNAs (miRNAs), proteins or lipids[202]. Additional communication between mother and fetus occurs via imprinted genes such as Igf2 that help in aligning maternal supply and fetal demand[203]. Communication between the fetus and the placenta is also evident with a recent study showing that fetal Igf2 is able to regulate placental development and vascularisation to match placental supply to fetal growth[204]. Maternal and fetal signals can thereby regulate placental structure, function and transport capacity to balance resource allocation[205].

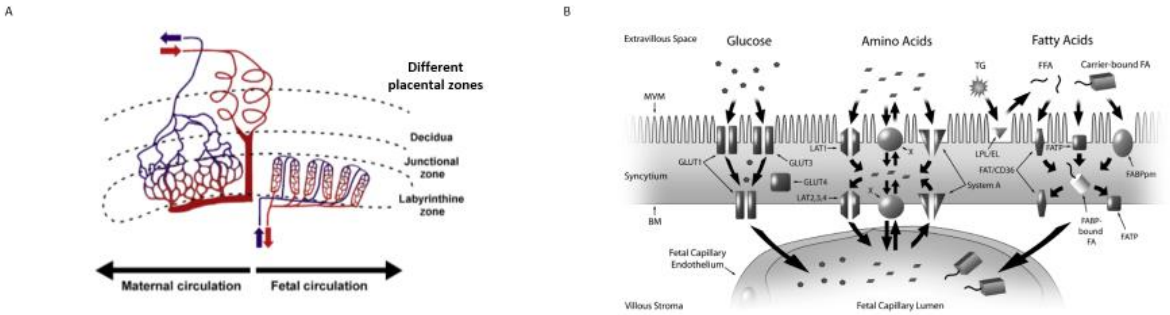

Figure 1.10: The placenta enables oxygen and nutrient delivery to the fetus

(A) In the murine placenta maternal and fetal blood flow are in counter-current to make nutrient and oxygen more efficient[206], figure used with permission. (B) Glucose, amino acids and fatty acids are transferred across the placenta to the fetal capillaries by facilitated transport as described in the text[207], figure used with permission (CC-BY licence).

1.8.2 Species differences

A lot of different placental types exist across mammalian species. The main structural differences between species are the degree of invasion into the maternal uterus and the composition of the layers separating maternal and fetal blood. The placenta from rodents and humans is a chorioallantoic placenta, which describes the fact that chorion and allantois fuse to build the placenta. The chorion is a fetal membrane surrounding the embryo and contacting the uterus. The allantois is a sac-like protrusion of the embryo, which builds vascular structures of the placenta. Three common placental types are the epitheliochorial placenta in ruminants, the endotheliochorial type in carnivores and the haemochorial placenta in humans and rodents. The names specify the type of barrier between mother and fetus. The degree of invasion in ruminants is very low and maternal and fetal blood are still separated by epithelium. This is not the case for the human or rodent placenta where maternal and fetal blood are only separated by layers of differentiated trophoblasts. These layers are made of cytotrophoblast and syncytiotrophoblast, the latter being a multinucleated cell layer created by fusion. In humans, maternal blood and fetal blood are separated by one layer of cytotrophoblasts and one layer of syncytiotrophoblasts. In mice there is a layer of trophoblast giant cells and two layers of syncytiotrophoblasts (see Figure 1.10) but with advancing gestation the syncytiotrophoblast layers present gap junctions and the fact that GLUT1 transporters are only expressed on the apical side of one layer and the basal side on the other layer shows that the two layers can be functionally regarded as one. Thereby human and murine maternal-fetal exchange zones in the placenta are very similar to each other[194].

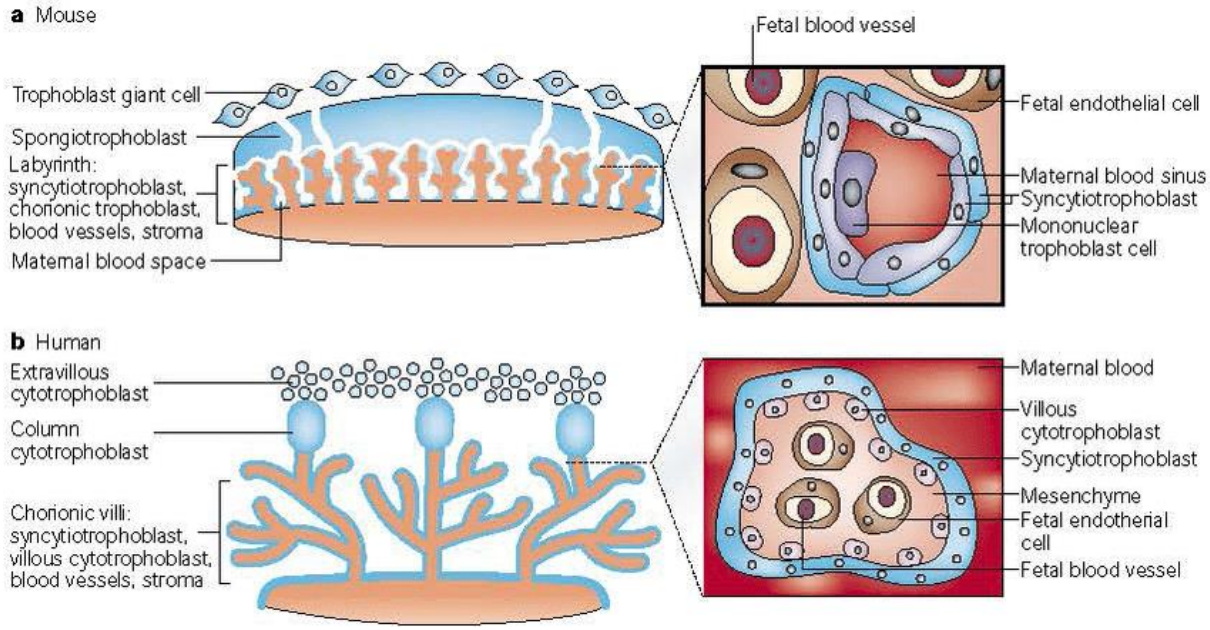

Figure 1.11: Placental structure differs between species

Structural differences between the murine and human placenta in detail, permission for use of figure has been obtained.[208]

1.8.3 Development of the placenta

Mouse development starts with the successful mating that is visible to the researcher by the appearance of a vaginal plug. The day of the vaginal plug is usually defined as embryonic day 0.5 (E0.5) from which onwards the days of the murine pregnancy can be counted. Depending on the mouse strain gestation length is 19 - 21 days. In the first days, the murine blastocyst differentiates into the inner cell mass (ICM) becoming the embryo and the trophoectoderm (TE). Signalling via the hippo pathway, that can differentiate between external vs. internal cells leads to pluripotency in the ICM by protein expression of the transcription factors Oct4 and Nanog[209,210]. After implantation at E4.5 the TE develops into the ectoplacental cone (EPC) and the extraembryonic ectoderm (ExE) that later develops into the placenta (Figure 1.11A). The ExE develops into the chorion and the labyrinthine structure by fusing to the allantois. At E8.5 fetal capillaries branch out from the allantois induced by the chorioallantoic fusion leading to the establishment of the labyrinthine layer by E10 (Figure 1.11B). Until then the fetus relies on histiotrophic nutrition via endometrial secretions and the yolk sac placenta, before haematotrophic nutrition is established. The EPC gives rise to trophoblast giant cells (TGCs) with sinusoidal and spiral artery TGCs playing a key role in spiral artery remodelling. Spiral arteries are the branches of the uterine arteries that are in the innermost layer of the uterus, the endometrium. Spiral artery TGCs replace maternal endothelial cells on spiral arteries and sinusoidal TGCs can create vascular tubes *de novo*. These processes ensure supply from maternal spiral arteries to the labyrinthine layer of the placenta where fetal capillaries can encounter the maternal blood. Fetal capillaries are

thereby now not separated by maternal endothelial cells anymore but only by trophoblast layers (two syncytiotrophoblast layers and the TGCs that remodelled the vessels). The placenta reaches its maximum weight at E16.5 with the peak of fetal growth just before the end of gestation at E18.5[194]. An overview of the developmental steps of the murine placenta can be found in Figure 1.11C.

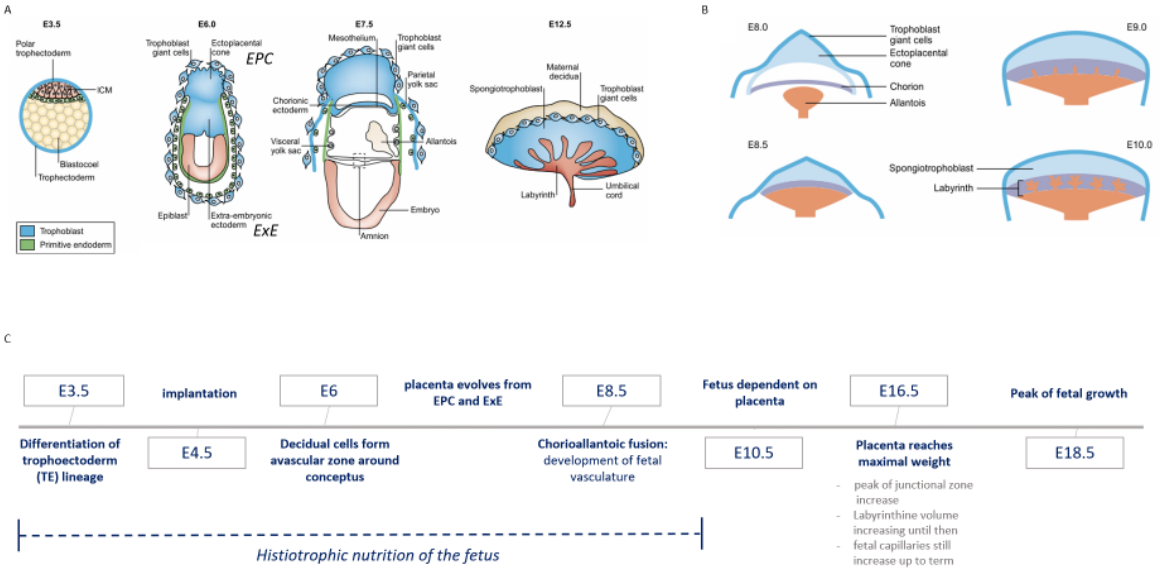

Figure 1.12: Placental development in the mouse

(A) Development from E3.5 (implantation of the blastocyst) until E12.5[208], permission for use of figure has been obtained. (B) The layers separate in the mouse placenta with establishment of the vasculature upon allantoic fusion at E8.5 with fetal vessels branching out[208], permission for use of figure has been obtained. (C) Timeline of events in the development of the murine placenta is shown.

Human pregnancy is usually around 40 weeks long and can be divided in three trimesters: the first trimester from conception to week 14, the second trimester from week 14 to week 28 and the third trimester continuing from week 28 until birth. In the first trimester the human blastocyst implants at day 8 after conception (Figure 1.12A). Until the 8-cell stage the cells are metabolically autonomous cells without gap junctions, in these initial days the sensitivity to stressors is therefore high[194]. Shortly after implantation a first wave of syncytialization occurs, from this syncytiotrophoblast layer cytotrophoblast cells invade the uterine tissue. In contrast to the mouse these cells do not only invade into the endometrium but the inner parts of the muscular uterine layer as well, the myometrium. The invading trophoblasts are termed extravillous trophoblasts (EVTs) and remodel maternal spiral arteries via endothelial mimicry (Figure 1.12B). Similarly to spiral artery TGCs in the mouse, the EVTs displace maternal endothelial cells on the spiral arteries. Interestingly these EVTs plug the remodelled maternal vessels therefore no maternal blood flow in the placenta is observed in the first trimester. This is the

reason why the human embryo relies on histiotrophic nutrition from endometrial secretions in the first trimester. It is thought that for a successful placental development low oxygen levels in the first trimester play a crucial role. Thereby glycolysis and polyol pathways are the dominating forms of energy production in the first trimester placenta. At the end of the first trimester the plugs on the spiral arteries are removed leading to the switch to haemotrophic nutrition. The placental vasculature is now established with spiral arteries opening above the villi of the placenta with fine branches of the villi being surrounded by maternal blood (Figure 1.12C). The villous branches are highly vascularised with fetal capillaries, which are separated from maternal blood by the syncytiotrophoblast layer and EVTs that are scattered around. Figure 1.12D makes clear that both species, mice and humans, first rely on histiotrophic nutrition until the definitive placenta is formed in the second half of the first trimester. It needs to be noted that in humans the blood circulation in the placenta is not established until the end of the first trimester even though the definitive placenta is established before.

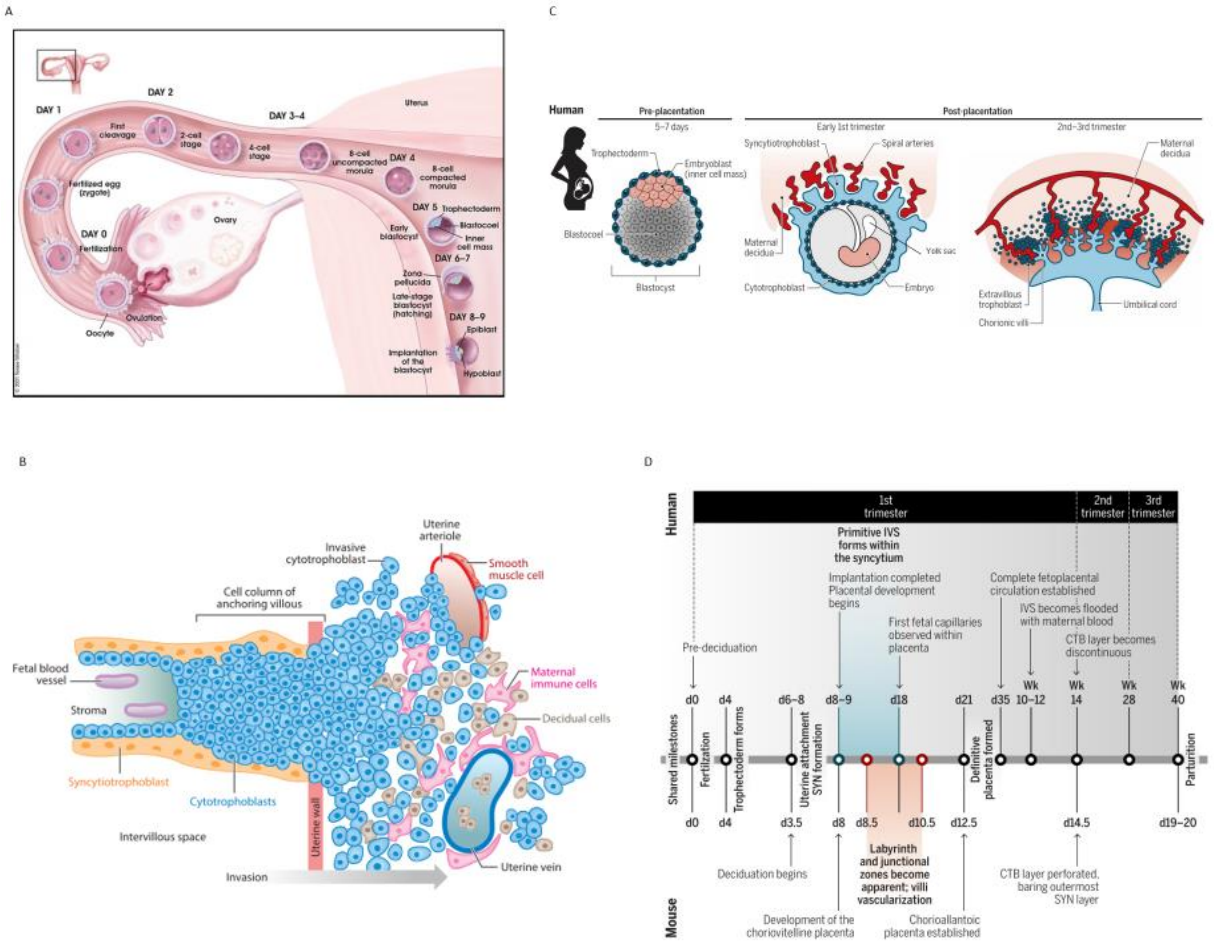

Figure 1.13: Placental development in the human

(A) Development from fertilization until implantation of the blastocyst at day 8-9 (Source: https://embryology.med.unsw.edu.au/embryology/index.php/Implantation, permission for use of figure has been obtained (© 2001Terese Winslow LLC)) (B) Cytotrophoblasts invade the uterus and remodel the uterine spiral arteries[190], permission for use of figure has been obtained. (C) Development of the placenta and its

vascularisation across gestation is visualised[211], figure used with permission. (D) Timing of mouse and human embryo and placental development are compared[211], figure used with permission.

1.8.4 Environmental influences on the placenta

As one can imagine many of the steps described above can be influenced by the environment. Starting before implantation it has been shown that women with a high BMI show accelerated development of the blastocyst with lower number of TE cells, potentially impacting development of the placenta[212]. Equally it has been shown in mice that a low protein diet during preimplantation increased the number of TE cells and their mobility, which is interpreted as a compensatory mechanism to allow a more extensive invasion[213]. Potentially also the phase of histiotrophic nutrition can be subject to developmental programming. Burton et al.[194] hypothesize that the reason that women born small for gestational age (SGA) are more likely to have SGA babies could be attributed to their lower uterine size and thereby potentially lower uterine gland density and reduced endometrial secretions[214].

More firm evidence exists for the influence on the placenta itself. Observations from Barker and Osmond regarding infant and fetal health and death from coronary heart disease and stroke in Hertfordshire and Sheffield showed the relationship between placental efficiency and death rate from coronary heart disease in adult life[215]. Placental efficiency can be calculated by the ratio of placental to fetal weight. It is a crude measure but commonly used to estimate how efficiently the placenta supplies the fetus and supports its growth[135]. The association between placental inefficiency and death from coronary heart disease was U-shaped, showing that both extremes of the placental efficiency spectrum are detrimental for long-term cardiovascular health[216]. But how the placenta is involved in fetal programming can't be answered by looking solely at the weight. In 1992 it was shown that food restriction in guinea pigs led to changes not only in placental and fetal weight but also in placental structure, shown by a reduced labyrinthine area[217]. They showed subsequently that the exchange surface area was reduced and placental barrier thickness for exchange increased, yielding direct explanations for the reduced growth of the fetuses in the undernutrition model[218] .It is now known that the placenta not only influences fetal development via effects on nutrient and oxygen transport but also by altering the secretory and protective functions of the placenta and even via direct mechanical forces[194]. The effect of the mechanical impact is a result of the placental vasculature being the main impedance to the fetal circulatory system. Thereby increases in placental vascular resistance increase the afterload against which the fetal heart needs to pump. These could result in hypertrophy *in utero* impacting long-term cardiovascular health[219,220]. As mentioned above altered vascular properties due to impaired remodelling of maternal vessels can change the haemodynamics within the placenta, damaging the protective layer of the placenta[194]. This makes the placenta and the fetus conversely more prone to be exposed to infections or environmental toxins or drugs.

As described above the placenta can function as an environmental sensor, thereby environmental stressors can impact on placental transport and secretory function. The placenta can sense hypoxia and adaptively increases its diffusion capacity. The oxygen sensors are prolyl-4-hydroxylase enzymes that can hydroxylate hypoxia-inducible factors (HIFs) when oxygen is present and thereby mark them for ubiquitination. In the hypoxic environment in early pregnancy HIFs are important for regulating trophoblast proliferation, invasion and migration, thereby allowing successful placental development. If exposure to hypoxia occurs later as described for high-altitude pregnancies it can impact multiple mechanisms. mRNA stability can be affected by oxygen abundance as can the activity of demethylases that need oxygen, thereby oxygen levels can affect epigenetic processes. Equally protein disulfide isomerases need oxygen and are necessary for protein folding. Low oxygen levels can thereby also induce the unfolded protein response that in turn leads to blocking of RNA translation. It is also known that HIF-2α can initiate translation of a subset of hypoxia-responsive mRNAs[221]. This could also change the placental secretome[194].

The secretome of the placenta can change in response to hypoxia or high glucose altering secretion of EVs and their miRNA cargo as potential programming factors. Additionally, stressors like obesity lead to an inflammatory state in the placenta leading to the secretion of pro-inflammatory cytokines. Obesity in ewes was shown to reduce CYP11A1 enzyme from the cytochrome p450 family in the placenta, leading to altered progesterone biosynthesis and thereby reduced secretion of progesterone and placental lactogen by the placenta[222].

In addition to secretory functions metabolism of the placenta can be affected by the same stressors (hypoxia, obesity). Mitochondria respond to hypoxia by high production of reactive oxygen species that can damage the cell. Maternal obesity is also associated with a lower mitochondrial DNA content and reduced complex I activity[223,224]. Key mediators regulating placental metabolism are mTOR and AMP kinase (AMPK) pathways. mTOR complex 1 is regulated by amino acid and glucose abundance thereby presenting a sensor of the maternal nutritional status. mTOR is a potent influencer of fetal and placental development by regulating protein synthesis, placental growth and the potential to regulate amino acid transport. The mTOR pathway has been shown to be one of the most sexually dimorphic ones regarding its gene expression in the placenta which could contribute to differential growth rates in male and female fetuses[225]. AMPK, activated by a high ratio of AMP to ATP, indicative of low cellular energy reserve, can inhibit mTOR signalling. AMPK activity can equally be influenced by environmental factors and influences the use of lipids versus glucose metabolism. Hypoxia, which can also activate AMPK, can lead to a metabolic switch using more glucose, thereby less glucose can be transferred to the fetus reducing growth. The maternal environment can thereby influence all functions of the placenta, which will be discussed below for maternal obesity and GDM.

1.9 Effects of maternal obesity and GDM (animal studies)

Effects on the mother, placenta, fetus and offspring in maternal obesity models (Figure 1.13) and GDM models (Figure 1.14) are summarized below.

1.9.1 Effects on the mum

Models of maternal obesity characterise the metabolic health of the mum to a varying degree. Some report no differences in fasting glucose or insulin[226] with others showing impaired glucose tolerance before[227] or during[228] pregnancy. In our mouse model the dams are hyperinsulinemic and glucose-intolerant at the end of pregnancy (E18.5) but unpublished data from the lab shows that glucose intolerance is not present after weaning despite being hyperinsulinemic[229,230]. The dams in our model also present hyperphagia, reduced insulin signalling in white adipose tissue and increased liver fat content with the hyperinsulinemia thought to lead to increased lipogenesis[231]. Wu et al. investigated maternal obesity with a genetic model, the Blobby strain which leads to induction of hyperphagia resulting in obesity on a chow diet. The dams show increased insulin and cholesterol but not glucose levels before pregnancy[232]. A model of HFD-induced obesity that only led to a 2 g body weight difference in the female mice before mating showed the induction of an inflammatory state in the mums showing increased cytokine levels[233]. As discussed above in human obese pregnancies maternal obesity is tightly linked to hypertension and preeclampsia. Douglas et al. provide an interesting link showing that maternal obesity led to impaired uterine natural killer cell functions[234]. These cells are crucial for initiating uterine vascular modification, thereby resulting in suboptimal vascularisation upon HFD[234].

Similar metabolic and physiologic changes in the dams are observed in GDM models. Mice heterozygous for a spontaneous loss-of-function mutation in the leptin receptor gene present increased body weight and insulin resistance[235], along with oxidative stress in the liver[236] and impaired uterine artery function indicated by an increased resistance index[237]. The LIRKO model shows hyperinsulinemia and glucose-intolerance despite no differences in the body weight of the dam[151]. As expected destroying the β-cells via streptozotocin or alloxan injection leads to high blood glucose levels in the dams before[238,239] or during pregnancy[240]. The inbred NOD mouse strain that developed diabetes spontaneously in the study from Aasa et al. showed impaired adaptation regarding cardiac output from the mums, thereby affecting utero-placental circulation[150].

1.9.2 Effects on placenta

One parameter analysed in many studies is the placental weight, which is reduced, unchanged or increased in weight dependent on the model. The placenta to fetal weight ratio as mentioned in section 1.8.4 is often used to assess placental efficiency. Reduced efficiency has been observed due to HFD feeding[241,242]. In both, GDM and obesity models, many changes in placental phenotype can be observed including reduction in labyrinthine area[233], reduced vascular density[243] increased vascular

lesions[150], increased lipid droplets [243] and reduced mTOR signalling[241]. Additionally apoptosis[226] and inflammation[244] have been reported. The increased apoptosis is thought to impact on the invasion of the placental cells. In our mouse model maternal obesity was shown to reduce expression of genes involved in invasion and vascular adaptations of the uterine vessels[245]. Previous studies in our mouse model have shown increased lipid deposits in the placentae from obese dams and increased HIF-1α protein abundance - indicative of placental hypoxia[229]. Similarly to other studies the labyrinthine area was reduced at E12.5 which persisted until E18.5[245].

1.9.3 Effects on fetal development

In some of the GDM and maternal obesity models postnatal catch-up growth is observed[151,246–248] following fetal growth restriction during pregnancy[150,151,242,249,250]. However, in some models birth weight is increased (see Figure 1.13 and 1.14) and therefore can mimic the macrosomic phenotype of obese and GDM human pregnancies but in most birth weight is either unchanged or reduced. Machado et al. suggested that the shorter fetal period in comparison to the embryonic period in rodents compared to humans could explain the increased rates of intrauterine growth restriction (IUGR) upon HFD or GDM exposure in rodent models compared to humans[238]. The fetal period is the period of major growth, thereby human fetuses might be able to compensate and adapt leading eventually to overgrowth. It can be expected that models that lead to vascular impairments (such as blunted cardiac output increase or reduced uterine artery flow) can induce reduced fetal growth. This is likely also the cause for growth restriction in human obese or diabetic pregnancies. Unfortunately, not all mouse models are that well characterized regarding the maternal glycaemic state and vascular phenotype. Therefore, no clear explanation for the differences in the fetal size across different models can be found. In our mouse model fetal weight is reduced at E12.5 and E18.5 in pregnancy[245].

Fetuses from obese dams are mainly characterised via their weight but it is also shown that they have increased body fat percentage[228] and increased lipogenic gene expression and hyperinsulinemia[250]. In GDM models malformations are often observed that can be the result of increased tumor necrosis factor α (TNFα) and inducible nitric oxide synthase (iNOS) levels[150,239]. iNOS is known to induce neural tube defects[251]. Congenital heart defects are also commonly observed[252]. As fetal changes can directly explain and influence phenotypes seen in the offspring later in life the study of the fetal changes is an important field to investigate further and in more detail in these animal models.

1.9.4 Effects on offspring

Models of maternal obesity and impaired glucose tolerance mirror observations from human pregnancies with long-term effects on the health of the offspring such as an increased risks for CVD, renal diseases, obesity and T2D. Even on a control diet the offspring from obese dams have increased body and liver fat [253]. White adipocyte differentiation is increased at the expense of brown adipose

tissue function[254]. Reduced β-cell function and increased levels of glucose, leptin and insulin are some of the metabolic disturbance observed in the offspring of obese dams[151,255]. Additionally offspring from obese dams has been shown to have an altered circadian rhythm set in the hypothalamus that can explain altered feeding behaviour leading to obesity in these animals[256].

Sex differences in response to programming have become increasingly recognised in recent years. In our mouse model male glucose homeostasis seems to be more affected by maternal obesity[257]. Females were shown to be primed to cope better with a postnatal obesogenic environment[258]. In a study from Dahlhoff et al. metabolic disturbance in 5 and 9 months old offspring in response to HFD was only seen in male offspring[259]. Our mouse model has investigated four main timepoints (8 weeks, 12 weeks, 6 and 12 months) showing metabolic disturbances and cardiovascular dysfunction. The offspring from obese mice showed cardiac hypertrophy, dysfunction and hypertension at 8 weeks of age[260–262]. A sympathetic dominance in the heart[263] and increased systolic blood pressure was still evident at 12 weeks[257] and females showed reduced ovarian reserve[264]. Even at 6 months of age effects are still seen in the form of increased leptin, cholesterol and systolic blood pressure (SBP) and low insulin and hyperglycaemia[257]. At 12 months of age offspring from obese dams show significantly increased body weight and liver steatosis[265]. Many studies also show that offspring from obese mums are particularly vulnerable to metabolic stressors in their own adult life, such as HFD[266–269].

Similar effects are also seen in the offspring from GDM models: increased body fat and fasting insulin in females at 6 months[270], impaired glucose tolerance[271] and reduced β-cell numbers and increased adipocyte size[151]. Spermatozoa methylation and thereby potentially next generations were affected by GDM[272]. In one study CD1 mice were injected with streptozotocin and some of these mice were additionally fed an HFD, interestingly methylation changes in spermatozoa differed in offspring from obese vs. diabetic mums[272]. Effect on the kidneys were seen by Hokke et al., showing lower glomeruli numbers at postnatal day 21 (P21) but adaptive changes restoring glomerular volume was evident by 6 months[273]. The similarity of outcomes seen in GDM and obese mouse models confirms observations in the human situation (see section 1.7.4). Many maternal obesity mouse models might model GDM or glucose impairment in pregnancy or even glucose impairment prior to gestation, but such data is often not reported.

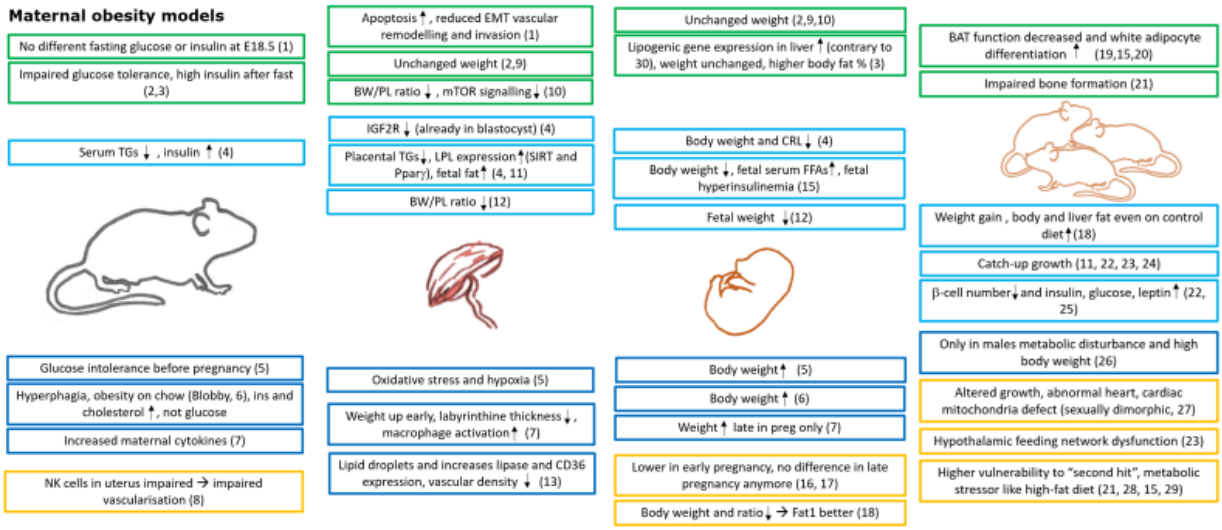

Figure 1.14: Observations in mouse maternal obesity models

Main outcomes of murine models observed in dams, placentas, fetuses and offspring are summarized. References can be found in the supplement (supplement 1, page 214). Studies either showed unchanged fetal body weight (green boxes), reduced body weight in response to maternal obesity (light blue boxes) or increased body weight (dark blue). Studies in yellow boxes showed reversal of body weight changes by the end of pregnancy or don't report the fetal body weight.

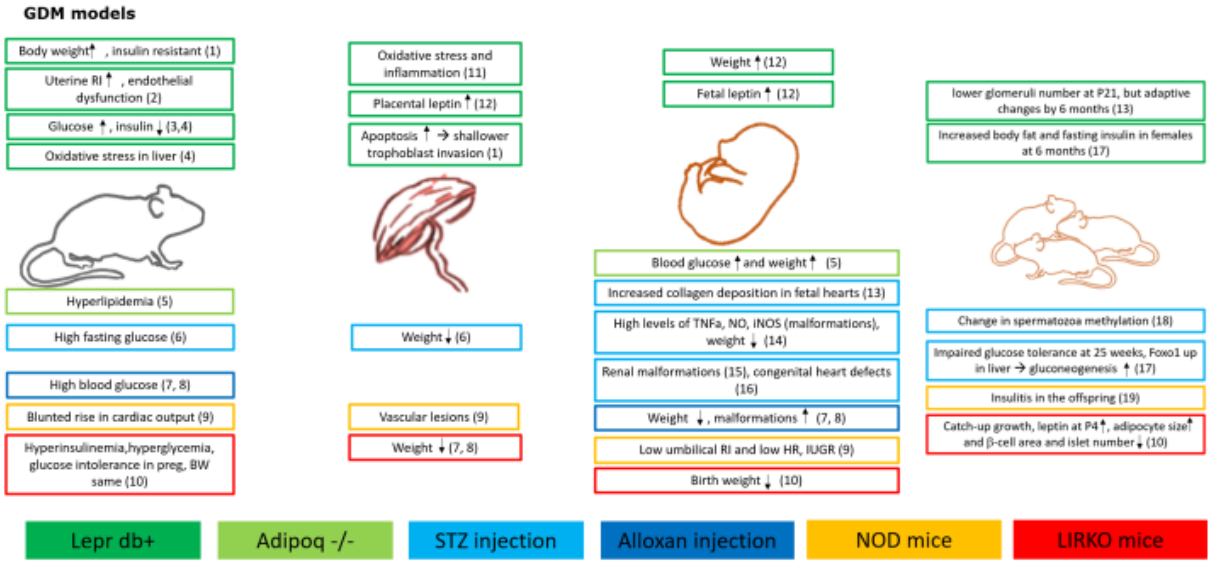

Figure 1.15: Observations in mouse GDM models

Main outcomes of murine models observed in dams, placentas, fetuses and offspring are summarized. References can be found in the supplement (supplement 2, page 216). Colours of boxes indicate the GDM animal model used as indicated in the Figure.

1.10 Interventions for maternal obesity and GDM

1.10.1 Diet and lifestyle

Upon diagnosis with GDM the first line treatment is usually a lifestyle and diet intervention aiming to lower blood glucose levels. If glucose homeostasis can't be achieved pharmacological treatment as

outlined below is necessary. Lifestyle and diet intervention usually encompass physical activity advice and counselling either by a doctor or a dietician encouraging healthy nutrition as outlined by the American College of Obstetricians and Gynaecologists (ACOG)[274]. The recommendations for physical activity are the same as in the non-pregnant setting. The aim should be 30 minutes of moderate intensity of aerobic exercise (e.g. walking, swimming, low impact aerobics) at least 5 days a week. The minimum should be 150 minutes per week. Barakat et al. highlight that the exact type, length and intensity need to be investigated in more detail in further trials, research on higher intensity exercise in particular is needed[275]. A Cochrane review summarized the results from 45 randomized controlled trials (RCTs) looking at these lifestyle interventions in GDM pregnancies[276]. The interventions include dietary changes, physical activity, education and self-monitoring of blood glucose. It was shown that LGA and neonatal adiposity were reduced in the intervention group, along with a reduction in postnatal depression and postnatal weight gain in the mum. They highlight the need for more trials assessing long-term outcomes which are poorly reported in the RCTs so far. Diet and physical activity have also been studied isolated from each other. Yamamoto et al. showed in a systematic review assessing diet interventions in 18 studies that postprandial glucose and birth weight could be reduced with the interventions[277]. Women in the assessed RCTs were advised to eat a low glycaemic index diet, low carbohydrate diet, a diet modified in fat and fibre content, an energy-restricted diet or the DASH diet (Dietary Approach to Stop Hypertension). The systematic review highlighted that the quality of the evidence for their findings was low and comparisons between the different diets could not be made due to a limited number of studies and participants in the existing studies. A review assessing diet alone reported no effects in the outcomes studied[278], whereas a review assessing exercise alone reported reduced fasting and postprandial glucose in the GDM women[279]. Tight control regarding the adherence to the recommendation is difficult in dietary interventions which a recently launched study called DiGest tries to circumvent by providing foodboxes for a low and a high energy intake group with follow-up of mothers and offspring at 3 months, 1, 2 and 3 years post-birth[280,281].

Interestingly lifestyle interventions were also investigated as a tool to prevent diabetes progression after a pregnancy with GDM up to 17 years later. The DPP (Diabetes Prevention Program) study showed that lifestyle intervention (aim of 7% weight loss and >150 minutes moderate exercise per week) could prevent the development of diabetes in women with and without GDM history[282].

Obesity is a major risk factor for GDM and preventing excessive weight gain in pregnancy and promoting a healthy lifestyle can therefore be important in improving outcomes of obese pregnancies. The DALI study (Vitamin D and lifestyle intervention) assessed the impact of healthy eating and/or physical activity in women with a BMI >29 kg/m^2 [283]. Gestational weight gain was reduced in the exercise and diet intervention group and neonatal adiposity and leptin levels were reduced in the

combined intervention and the exercise alone group. However, GDM was not prevented. Similarly UPBEAT (UK pregnancies better eating and activity trial) advising an exercise regimen (supplied with a DVD) and dietary changes to pregnant women with a BMI >30 kg/m^2 showed reduced gestational weight gain and reduced adiposity in the offspring at 6 months and beneficial effects on the maternal VLDL and fatty acid profiles but no prevention of GDM[284,285]. The TOP (Treatment of Obese Pregnant women) study, an RCT from Copenhagen using activity and diet or an activity only intervention in women with a BMI > 30 kg/m^2, showed improvements in inflammatory markers in the women of the two intervention arms[286]. The ETIP (Exercise training and weight gain in obese pregnant women) trial assessed just exercise alone in 91 pregnancies with a BMI >28 kg/m^2 and showed no difference in GDM incidence, gestational weight gain, but a reduction in systolic blood pressure[287]. In the ETIP study it was clear that GDM diagnostic criteria influence the results heavily. Adopting the old WHO 2009 definitions rather than the IADPSG definitions changed the difference in GDM incidence between the exercise and the control group. Simmons therefore highlights that it is important in studies assessing GDM interventions to adapt one single GDM diagnostic definition with the IADPSG criteria being the best that is currently available and that studies need to account for different subgroups in GDM women[288]. Most women develop GDM early, but others only develop it later in pregnancy and therefore might benefit from a different treatment. Simmons suggests that women with elevated fasting glucose might benefit from metformin treatment whereas women with high postprandial glucose should receive dietary interventions[288]. The article also highlights the challenging nature of lifestyle studies in humans as women participating in these lifestyle trials are usually willing to adapt to a healthier lifestyle, possibly confounding results in the control groups. Thereby mouse studies are important in studying diet and exercise effects.

Multiple nutritional supplementation studies exist in mice which won't be assessed here. The simplest diet intervention mirroring the wish of women before or during pregnancy to eat healthily or reduce weight is switching the HFD to a chow diet before or immediately after conception. Fu et al. changed mice from a 60% HFD to a chow diet 1 week prior to mating with no weight loss achievement in the mums[289]. Female offspring of these mice who were fed a HFD after weaning were more prone to develop obesity if the mother's diet was changed before pregnancy. The authors speculate that the rapid diet change induces a dietary restriction phenotype during pregnancy, like undernutrition. Other studies have shown improved offspring phenotypes. For example change to chow diet during pregnancy and lactation reduced maternal leptin and insulin levels and lowered body weight and fat weight of the offspring at P21[290].

In mice different types of exercise have been trialled. Voluntary running wheels in the cage are often used but Pearson et al. showed that wheel running under supervision and on a motorized platform to control for the speed and length of the exercise might be a better tool as free wheel running in the

cage is also used as a model of obsessive-compulsive-type behaviour possibly confounding results[291]. Studies have investigated exercise in non-obese (chow-fed) pregnant mice showing improved mitochondrial function in the fetal heart[292] and improved fetal brown adipose tissue function, protecting offspring from metabolic dysfunction induced by HFD feeding[293]. Exercise before pregnancy improved mitochondrial metabolism in embryos *in vitro* and led to epigenetic reprogramming improving embryonic development[294]. In a genetic preeclampsia model exercise (voluntary running) four weeks prior to mating normalised proteinuria and blood pressure reducing placental necrosis and restoring placental and fetal development[295]. A study in mice investigating a forced swimming exercise before and during pregnancy showed a negative effect on the development of the neurogenic niche in the offspring[296]. Forced swimming is studied as an aerobic exercise that challenges metabolism and the immune system, thereby posing the question already mentioned in human trials, how much exercise and what intensity regarding high intensity levels can be recommended in pregnancy.

Exercise has also been studied in the context of HFD assessing the prevention of detrimental effects of maternal obesity. Voluntary wheel running throughout pregnancy reduced insulin in the offspring of exercised obese dams compared to dams only fed HFD (for 9-10 weeks)[297]. Additionally, Interleukin 6 signalling in white adipose tissue and hypothalamus was reduced potentially explaining the improved glucose metabolism in the offspring. Glucose homeostasis improvement in the offspring was also observed in male and female offspring studied by Goodyear et al. in a model using treadmill exercise in mice one week before and during pregnancy[298]. Placental inflammation and lipid accumulation in the placenta was reduced, placental vascularisation restored and AMPK activated. In their model HFD feeding induced fetal overgrowth and inhibition of AMPK. Effects of exercise on the mum where shown by Pearson et al. with a reduced body weight[299]. This is not consistently shown in murine exercise intervention studies. In our mouse model we used a treadmill exercise intervention, starting one week before mating and ending at E16.5 five times a week with a standardized training protocol. Our lab has shown no effect of the exercise on the maternal weight, but exercise partially restored maternal insulin and white adipose tissue insulin signalling[230]. Equally glucose tolerance in the dams at E17.5 was improved and placental lipid content and placental hypoxia were restored[229]. In 8-week male offspring fasting serum insulin and adipose tissue insulin receptor substrate 1 (IRS-1) levels were restored. Offspring cardiac dysfunction (hypertrophy, reduced ejection fraction) induced by maternal obesity was prevented by maternal exercise, but hypertension could not be improved[261]. Little of these offspring long-term outcomes are studied in the human situation, highlighting further need for these long-term studies[300].

1.10.2 Insulin

For 25-30% of women with GDM diet intervention is not successful and pharmacotherapy is required[301]. In the treatment of GDM, insulin has been used for more than four decades. Despite the

increasing use of oral antidiabetic medications (see below) insulin is still recommended by the American Diabetes Association (ADA) and multiple other organisations as the first-line therapy for gestational diabetes[274].

The most apparent negative outcome of GDM is macrosomia. An early paper from 1985 demonstrated the beneficial effects of insulin treatment, the authors reviewed six studies that compared a diet intervention and an intervention comprised of diet and insulin treatment[302]. Fetal macrosomia was significantly reduced in the insulin groups in 5 studies. In the same year (1985) Lindmark et al. analysed the use of insulin in almost a prophylactic manner as a supplement to diet interventions in 119 women and showed reduced macrosomia rates and no adverse effects[303]. They highlighted a previous study in Pima Indians, a population of Native Americans that show a high incidence of T2D. This study showed that babies from women who only develop diabetes years after the pregnancy, delivered babies with a slightly higher body weight. Lindmark et al. thereby concluded that it could be beneficial to treat subtle glucose impairments in pregnancy. This is still a matter of debate, with Landon et al. stating in 2009 that treatment of mild hyperglycaemia is beneficial[156]. In 2008 the US preventive services task force (USPSTF) did not see the benefit of screening asymptomatic women to potentially identify early slight glucose impairments, with new guidelines from 2014 still stating that there is not enough evidence for screening before 24 weeks to be beneficial[304]. However, they do recommend screening for asymptomatic women after 24 weeks.

A lot of different regimens for insulin dosing exist. Depending on the length and timing (post- or pre-prandial) of hyperglycaemic episodes fast-, intermediate- and long-acting insulin versions are administered just before a meal or at certain times in the day[274]. Nowadays many studies compare insulin with the more recently emerged oral alternatives, which will be discussed below.

Only a few animal studies tested the direct effect of insulin treatment in pregnancy. One model used streptozotocin in pregnancy at E6 and E12 to induce GDM[305]. With a mini-osmotic pump a group of these mice was then treated with insulin from day 14.5/15 onwards. Insulin therapy led to a decline in maternal blood glucose and it normalized the weight trajectory, serum glucose and lipid metabolism in the offspring at 20 weeks[305]. However, when the offspring were challenged with HFD itself, insulin therapy did not improve metabolic health compared to the offspring from GDM pregnancy without intervention, especially in male offspring. A paper from 1983 investigated the effects of insulin on embryonic development *in vitro*. Whole embryos were cultured in serum from diabetic rats that received insulin, in serum from diabetic rats where insulin was just added to the culture medium and in serum from control rats where insulin was added. Growth retardation and malformations were shown to be reduced when the embryos were cultured in medium from rats that were dosed with insulin[306].

Insulin has been considered a safe treatment in pregnancy since it does not cross the placenta. With insulin, postprandial hyperglycaemic periods can be well managed as insulin can be injected. However, short hyperglycaemic periods can impact fetal development[307]. The use of insulin is more costly, needs patient education, requires injection and cold storage and decreased patient compliance can be a problem[301]. These problems can be circumvented by the following orally applied agents.

1.10.3 Glyburide

Glyburide (glibenclamide) is a second-generation sulfonylurea used in T2D treatment as it stimulates insulin secretion from β-cells. It binds to sulfonylurea receptor 1 on β-cells, which leads to closure of a potassium channel, thereby leading to a cell membrane depolarisation inducing insulin secretion. It is highly protein-bound and metabolized by cytochrome 450 enzymes in the liver, where it is broken down into its active metabolites[301]. Even though it is not officially licensed for use in pregnancies due to limited long-term data, it is used as an alternative to insulin mainly in the US. Here a large rise in its use from 2001 (use in 7.4% of women with GDM) until 2011 (64.5%) was reported[308]. This is despite little data on long-term effects, even animal studies are very scarce. Animal studies mainly investigated the pharmacokinetics. Retro-orbital injection of glyburide into mice showed higher clearance of glyburide in pregnancy due to the increased activity of a hepatic cytochrome[309]. It is well-known that in pregnancy pharmacokinetics change due to increases in hepatic blood flow and glomerular filtration and a change in the expression of drug-metabolizing enzymes. The same group reported that clearance of glyburide and the expression of breast cancer resistance protein (BCRP) and p-glycoprotein (p-gp) in the placenta changes with gestational age[310]. These efflux transporters, BCRP and P-gp, were shown to decrease in the placenta with progression of pregnancy. They are thought to protect the fetus from glyburide exposure, it is thereby likely that the fetus is exposed differently depending on its gestational age.

The earliest human study from 2000 showed no difference in maternal and perinatal outcomes between insulin and glyburide treatment. Glyburide was thereby deemed a good alternative to insulin and only 4% failed the treatment with glyburide and needed insulin[311]. It was long thought that only little glyburide transfer occurs across the placenta, but in 2009 Hebert et al. showed that up to 70% of the maternal serum concentration can be measured in fetal cord blood[312]. A small study by Bertini et al. showed that glyburide treatment led to increased rates of neonatal hypoglycaemia and macrosomia compared to insulin treatment[313]. A higher neonatal hypoglycaemia rate was also seen in an RCT by Sénat et al. [314]. It is hypothesized that as glyburide can cross the placenta it can induce fetal insulin secretion explaining the high hypoglycaemia rate[315].

Maternal fasting glucose can be controlled very well with glyburide[313,315,316]. One retrospective study reported higher preeclampsia rates in women treated with glyburide[316]. A meta-analysis of 42 RCTS

comparing metformin, insulin and glyburide showed that glyburide was not more effective compared to insulin. The authors highlighted that the data quality is very poor, a lot of RCTs are poorly designed or very small and urged that more and larger multi-centre trials are needed. It is thereby difficult to assess the optimal treatment for GDM taking maternal, fetal and long-term outcomes into account. This comes also apparent when assessing metformin as an increasingly used oral GDM treatment across the whole world.

1.10.4 Metformin

Metformin (1,1-dimethylbiguanide hydrochloride) is a biguanide, first shown by Jean Sterne in 1957 to be a potent drug to treat diabetes[317]. It is now the most common glucose-lowering agent for T2D patients. Initial use of metformin in pregnancy was unintended, resulting from continuation of metformin use in early pregnancy in women with pre-existing diabetes, with clinical observations not showing any safety concerns [318,319]. The first active use of metformin during pregnancy was reported in a study from 1979 in South Africa which assessed the use of metformin during pregnancy in women with pregestational and gestational diabetes and deemed it safe for use in pregnancy[319]. In the late 1990s Nestler and Jakubowitz proposed the use of metformin for PCOS[320,321]. Women with PCOS suffer from reduced fertility and increased rates of spontaneous abortions in the first trimester which are significantly improved with metformin treatment before conception and during pregnancy[322,323]. A growing number of studies have therefore assessed the use of metformin in pregnancy on maternal health. Initial studies in mouse PCOS models confirmed the data from Nestler et al. showing improved estrous cycles[324,325] and reduced rates of embryonic resorption following metformin treatment[326]. In 2004 Glueck et al. published results from a prospective cohort study in PCOS women highlighting metformin's benefits on improving insulin sensitivity and reducing body weight and GDM incidence[327]. Additionally follow-up of the children showed no difference in growth and development in the first 18 months of life[328]. Given the benefits for the mother and the good safety profile considerations of the use of metformin in GDM pregnancies were increasing. However caution was urged in an ADA letter in 2006 highlighting that too little is known about metformin use in pregnancy which is crucial especially as metformin can cross the placenta[329].

In the following years multiple studies systematically assessed the use of metformin in pregnancy. From 2005-2009 Vanky et al. ran a study with 257 PCOS women treated with metformin from gestational week 5-12 onwards. Despite beneficial effects shown in the mother such as lower GWG[330] and lowered insulin levels[331], children from metformin-exposed mothers had an increased BMI at 6 months, 4 and 7 years of age[332,333]. Additionally they showed that under- and overweight women treated with metformin delivered babies of lower birth weight[334]. This highlighted the potential for adverse effects of metformin on the offspring short- and long-term.

However, metformin use in pregnancy outside of the PCOS setting has increased worldwide. In 2008 the NICE guidelines in the UK recommended metformin as first-line treatment for GDM[335]. Multiple RCTs looking at metformin use in GDM pregnancies compared the use of insulin with the use of metformin and showed beneficial effects. These studies showed reduced GWG[336], lower risk for preeclampsia[337] and similar glycaemic control[338] in metformin- compared to insulin-treated GDM women. A study in women with GDM comparing insulin and metformin showed that metformin is generally preferred by the women themselves: in the MiG (Metformin in GDM) trial from Rowan et al. patient acceptance of metformin was higher than for insulin likely due to metformin being taken orally rather than injected[339]. Many studies however report a high failure rate of up to 50% of women who do not achieve glycaemic control with metformin, leading to many women requiring additional insulin[340]. A recent meta-analysis from our lab summarized human studies comparing metformin and insulin treatment of GDM and reported overall reduced birthweight in babies born to GDM mothers treated with metformin rather than insulin[341]. However later in life offspring from metformin-treated mothers had increased weight at 1.5 – 2 years of age and increased BMI at 5-7 years of age. The use of metformin in pregnancy is thereby controversially discussed[318].

Due to promising weight reductions with metformin treatment in GDM pregnancies metformin is increasingly trialled for the use in obese pregnancies. The Metformin in Obese non-diabetic Pregnancies (MOP) study treated women with a BMI of over 35 with metformin from week 12-18 until delivery and showed that GWG and preeclampsia rate were reduced[342]. The EMPOWaR study (Efficacy of Metformin in Pregnant Obese Women, a Randomised Controlled Trial) treated women in a similar time window with a BMI of over 30 and showed no significant changes in GWG and a trend for a reduced GDM rate[343]. Both studies showed no difference in the birth weight of the babies. Human studies in both PCOS and GDM treatment showed the potential impact of metformin on fetal growth and increased offspring adiposity in later life. However data on effects of metformin on the fetus and the placenta is scarce[341].

This is an important lack of knowledge as in contrast to insulin, metformin can cross the placenta and reaches the fetal circulation at high levels[340]. One of the few human studies to address metformin action on the placenta compared exercise and lifestyle intervention with metformin treatment in GDM women and focussed specifically on placental structure[344]. Metformin treatment reduced chorangiosis and syncytial knots in the placenta that were induced by GDM. Chorangiosis is hypervascularisation in the villi of the human placenta and is thought to be a response to a hypoxic environment that could e.g. be a result of impaired uterine artery blood flow and preeclampsia[345]. Syncytial knots are also often associated with preeclamptic placentas and are a sign of premature placental ageing. The improved placental structure following metformin treatment could thereby be attributed to the potential of metformin to prevent and improve preeclampsia-like phenotypes. There is more data from rodent and

in vitro studies regarding the impact of metformin treatment on placental tissue and cells (Table 1.1). Several new studies have emerged since the design of this study in summer 2018. However, despite the unclear effects of metformin on the placenta raised in multiple reviews no additional human studies looking at the placenta have emerged in the last three years. Most of the rodent studies assessing metformin treatment in mice fed a high fat and/or high sugar diet showed improved placental vascularisation and reduced placental inflammation shown by measurements of cytokines in the placenta[346,347]. In these studies metformin was only administered during pregnancy, however another study gave metformin together with a high fat diet 6-8 weeks prior to mating and throughout pregnancy and showed improved mitochondrial biogenesis indicated by increased promoter methylation and expression of PGC1α and increased protein levels of the mitochondrial transcription factor TFAM[348]. One recent study however showed detrimental rather than beneficial effects of metformin on the placenta as it exacerbated placental insufficiency induced by a high fat-sucrose diet together with streptozotocin treatment in rats[349]. Metformin was administered together with glyburide and this did not improve placental vascularisation but improved other structural changes in the placenta such as necrosis in spongiotrophoblast cells. Overall, a high variety of different metformin treatment regimes and models exist. A few models assessed metformin use in those unrelated to obesity and/or GDM as they looked at genetic models known for their high risk of preterm birth[350], impaired trophoblast invasion[351] or spontaneous miscarriage[352]. As Table 5.1 shows many *in vitro* studies either in cell lines or primary cultures of murine or human placental tissue recapitulate the findings from the *in vivo* rodent studies showing reduced inflammation, improved mobility and angiogenesis[347,353,354]. Studies using primary cultures of human trophoblasts from first trimester placentas showed that metformin reduced apoptosis[353]. On the other hand metformin reduced cell viability in a study of an immortalized human trophoblast cell line (HTR-8/SVneo)[355]. It needs to be noted that most of the *in vitro* studies only see effects at high concentration of metformin such as 1 mM. This is several orders of magnitude higher than those concentrations reported in pregnant women administered metformin (2000 – 7000 nM)[356]. The requirement for high levels of metformin may be explained by the low levels of metformin transporters in cell lines compared to primary cells[350]. The use of high metformin concentrations is a limitation of metformin studies *in vitro*[357]. It is hypothesized that a complete inhibition of oxidative phosphorylation seen *in vitro* due to metformin, only occurs at supraphysiological concentrations and more likely just a suppression of oxidative phosphorylation is present *in vivo* at clinically relevant concentrations[358].

Overall Table 5.1 demonstrates the lack of systematic placental analyses in human studies and the focus on a few key pathways when assessing metformin in *in vivo* and *in vitro* models. The mechanisms of metformin action in pregnancy thereby need careful further assessment, especially given the increased use of metformin in pregnancy across the world.

Study	Model	Metformin dosage	Observed effect
Alzamendi et al. (2012)[346] 	Rats fed a fructose rich diet (during pregnancy only)	50 mg/kg/day in drinking water (in gestation)	- Improved placental vessel area
Desai et al. (2013)[347]  	High fat/high sugar diet in rats (5 weeks prior to mating and in pregnancy) Human placental choriocarcinoma JAR cells	300 mg/kg/day (in gestation) 0.01- 2.5 mmol/L for 24 h	-reduced placental TNFα levels -reduced TNFα-induced Il6 secretion -no effect on cell viability
Wang et al. (2014)[352]	human extra- villous cytotrophoblast cell lines (HTR-8/ SVneo and HPT-8)	n.a.	- Reduction of mitochondrial dysfunction in gC1qR overexpressing cells
Deng et al. (2016)[350]   	p53$^{d/d}$ mice → model of preterm birth culture of mouse uterine stromal cells (day 4) Human uterine fibroblast (HuF) cell line	(1 mg/kg BW per dose) on E8, 10, 12 1, 10 mM for 24 h 0.1-2.5 mM for 24 h	-improved decidual thickness, increase pAMPK signalling - increased pAMPK (10mM), reduced pS6 levels (1 mM) - increased pAMPK (1 mM), reduced pS6 levels (2.5 mM)
Arshad et al. (2016)[344] 	62 GDM women	500 mg - 1500 mg	- reduced chorangiosis and syncytial knots
Pettker et al. (2016)[359] 	first trimester trophoblast cell line (Sw.71), glucose treated	0.5mM for 72 h	- reduced secretion of cytokines - no rescuing effect on migration and angiogenic factor
Correia-Branco et al. (2018)[355] 	HTR-8/SVneo cells (immortalized human trophoblast cells)	0.01–1 mM for 24 h, most effects seen at 1mM	- Reduction in cell viability, growth and migration - mTOR, JNK and PI3K involved in these negative effects
Vega et al. (2019)[353] 	Human trophoblasts from first trimester placentas, insulin treated	10 µM for 24 – 72 h	- reduced apoptosis
Hastie et al. (2019)[360] 	primary cytotrophoblast from preeclamptic vs. normotensive women	500, 750 µM and 1mM for 48 h	-increased pAMPK, reduced mitochondrial respiration (1 mM) - reduced sFlt secretion (750 µM)
Jiang et al. (2020)[348]  	Placental explants from 23 diabetic women (GDM + T2D) High fat diet in mice (6-8 weeks)	1 mg/ml (=7.7 mM) for 18 h 2 mg/ml or 4 mg/ml (6-8 weeks before mating and in pregnancy)	- Increased AMPK and PGCα signalling - improved placental efficiency, increased PGC1α and TFAM

Sun et al. (2020)[354] 	HUVECs isolated from umbilical cords from diabetic women	100 µM for 72 h	- Improved cell migration and angiogenesis (via downregulation of Nrf2 and p65)
Yan et al. [351] (2021) 	HTR-8 and B6Tert-1 cells (immortalized human trophoblast cells), ADAM7 knockdown	200 ng/ml (=1.5 µM) for 24 h	- Reversal of negative effects (reduced cell proliferation)
Zhang et al. (2021)[361] 	High fat diet in mice (1 week prior mating)	600 mg/kg/day (E11.5 – E18.5)	- increased AMPK, pAkt, Ki67, pACC and GLUT3 localisation rescued back to plasma membrane
Hosni et al. (2021)[349] 	Rats fed fat-sucrose diet and treated with streptozotocin STZ	Glyburide and metformin together (0.6 and 100 mg/kg/day, 1 week before and during gestation)	- exacerbated placental insufficiency - impaired placental vascularisation not improved - protection from structural abnormalities

Table 1.1: Summary of studies assessing the effects of metformin on the placenta

Model type (: mouse/rat study, : human study, : cell line experiment, : primary culture/explants), dose of metformin and the observed effects on the placenta are shown. The thick line divides the studies into studies published before the design of this PhD study and studies after the design of this study. Images created with BioRender.com.

1.11 Aims and hypotheses

The overall aim of this thesis is therefore to understand the effects of metformin treatment during an obese pregnancy on maternal, fetal and placental health using our mouse model of diet-induced maternal obesity. This will be achieved via four main objectives, presented in four results chapters (see Figure 1.15).

Aim 1 (chapter 3): To determine how maternal obesity affects maternal metabolic health and uterine artery function and to assess whether metformin treatment prevents any impact of maternal obesity on these parameters.

This will be achieved using our mouse model of maternal diet-induced obesity together with addition of metformin to the diet and assessing maternal metabolic health via body weight, body composition and food intake measurements, intraperitoneal glucose tolerance tests, assessment of liver steatosis and blood pressure measurements. Uterine artery function will be assessed via ultrasound.

Aim 2 (chapter 4): To investigate the effect of maternal obesity and metformin exposure *in utero* on the fetus and the placenta.

This will be achieved by carrying out fetal biometrical measurements, placental structural analyses, fetal ultrasound (assessing placental and fetal vessels) and metformin measurements in the fetus.

Aim 3 (chapter 5): To explore molecular mechanisms that could mediate potential direct effects of metformin treatment during an obese, glucose-intolerant pregnancy on the placenta.
This will be achieved using omics approaches with bulk RNASeq and lipidomics analysis of the placenta.

Aim 4 (chapter 6): To develop a method for isolation and characterisation of placental extracellular vesicles (EVs) and to determine their potential to be involved in fetal programming by maternal obesity.
This will be achieved by isolation and characterisation of EVs from placental explant supernatants and assessing the miRNA content of the isolated EVs by small RNASeq.

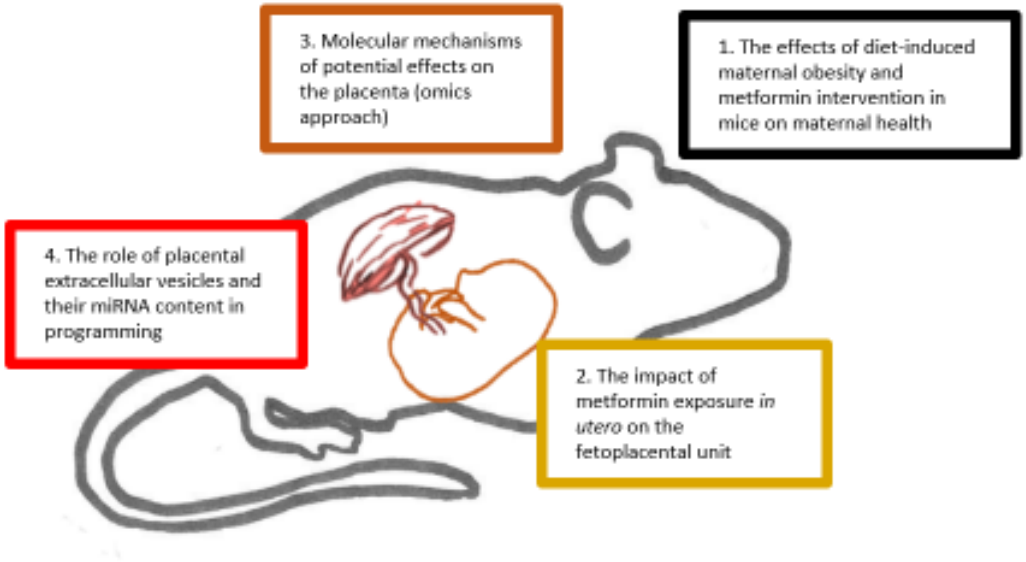

Figure 1.16: Overview of the four objectives addressed in this thesis

2 General methods

In this chapter general methods that are used in more than one of the subsequent results chapters are described. Every results chapter has its own methods section describing the methods specific to the analyses in the chapter. Unless specified further all work is my work.

2.1 Mouse model

All animal work was reviewed and approved by the University of Cambridge Animal Welfare Ethical Review Body (AWERB) and was performed according to the UK Animals Scientific Procedures Act 1986. Thanks to Claire Custance for maintaining all animals on a day-to day basis. The work in this thesis is based on a model of maternal diet-induced obesity, which is well-established in our laboratory[260]. Breeding was performed in house with stock mice used for generating the experimental dams being purchased from Charles River Laboratories. Female C57Bl6/J mice were randomly subjected to their experimental diet at weaning (3 weeks of age). Mice were fed *ad libitum* either a control chow diet (801002, Special Dietary Services) or an obesogenic diet (824053, Special Dietary Services) supplemented with condensed milk (12029969, Nestlé) and a mineral mix (AIN93G, MP Biomedicals). Further details of the diets are shown in Table 2.1. At 6 weeks of age mice were mated for a first pregnancy. At weaning the litters of this first pregnancy were culled. This initial pregnancy is used to prove that the dams are good breeders, a feature that was and is needed for other studies in the lab that are working on the offspring. For consistency the same protocol is also followed for embryonic studies. After this first pregnancy animals were given at least one week of rest and weighed weekly to determine when the females are mated for the second experimental pregnancy. Mice fed a control diet were mated with a body weight of ≤25 g and females on an obesogenic diet were either dosed with metformin (see 2.2) or mated when a body weight of ≥35 g was reached. The mating for the second pregnancy was therefore approximately at 20 weeks of age in all animals. The day of the plug is counted as embryonic day 0.5 (E0.5). Food intake and weights were monitored throughout pregnancy and dams and their fetuses killed at embryonic day E13.5 or E18.5. At these timepoints maternal and fetal tissues were collected as specified further in the following respective results chapters. In this thesis no metformin-treated control-diet fed animals were included as the purpose of the study is the assessment of metformin intervention in a pregnancy complicated by obesity and glucose intolerance. This is the most clinically relevant situation as metformin is not used in lean women. Therefore, the experimental design used is in line with the ARRIVE guidelines and complied with the 3Rs to reduce animal use.

	RM 1	Obesogenic diet	Condensed milk
Atwater free energy (kcal/g)	3.28	4.54	3.26
Energy (% kcal)			
- Fat	- 7.4	- 44.7	-
- Protein	- 17.5	- 20.3	-
- Fibre	- 75.1	- 35.0	-
Composition (%w/w)			
- Fat	- 3	- 20	- 8
- Protein	- 15	- 23	- 8
- Simple sugars	- 7	- 10	- 55

Table 2.1: Diet composition details

2.2 Metformin dosing

Half of the females fed an obesogenic diet were dosed with Metformin one week before mating for the second pregnancy and continued during the pregnancy (Figure 2.1). Metformin (0215169-CF, MP Biomedicals) was administered in the condensed milk aiming for a dose of 300 mg/kg/day, based on allometric scaling this equates to 1.7 g of metformin in a 70 kg man[362]. Weighing of the condensed milk twice a week to estimate milk intake of each individual animal and body weight measurements allowed adjustment of metformin content in the milk to ensure the required dose was achieved. The metformin dose was dissolved in 1 ml of water which was mixed into a milk pot filled with 75 g of condensed milk. Due to the addition of the water caloric content is decreased from 3.26 kcal/g to 3.22 kcal/g, previous analyses in the lab have shown however that the addition of water itself does not change the palatability of the condensed milk.

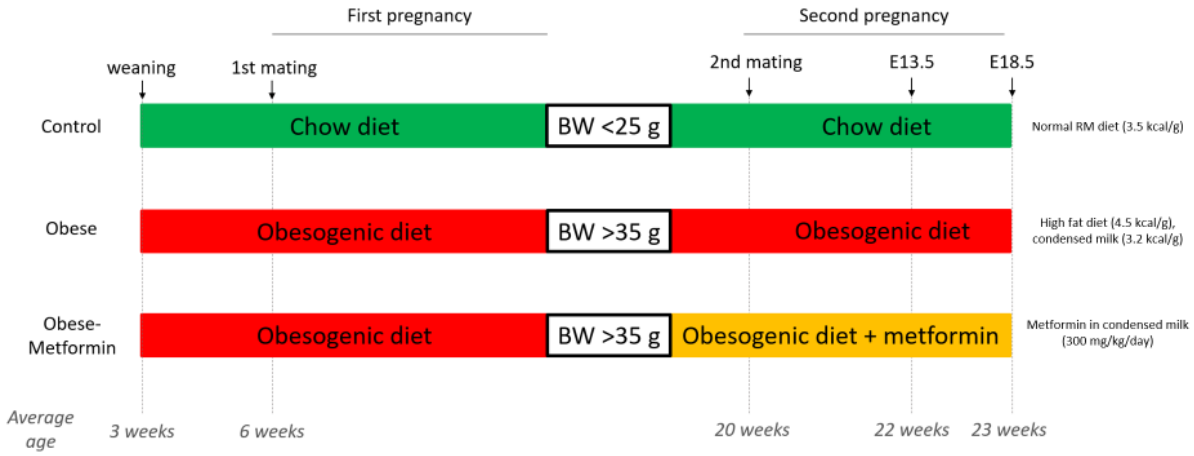

Figure 2.1: Schematic of our mouse model of diet-induced maternal obesity and metformin intervention

2.3 Metformin liquid chromatography mass spectrometry (LC-MS)

Metformin was measured in various tissue and liquid samples (amniotic fluid, serum, plasma) via LC-MS. This was performed by Dr. Benjamin Jenkins from the Core Metabolomics and Lipidomics

Laboratory (CMaLL) at the University of Cambridge. The protocol has been described previously[363,364]. In brief, samples were homogenised in 400 µl of a chloroform:methanol (2:1) solution and homogenised using a Biorep-24-1004 homogeniser (4.5m/s for 60 sec). Then 100 µl of 1 µM metformin-d6 were added together with 600 µl chloroform:methanol (2:1) solution and 300 µl of water. After vortexing and centrifugation (21000 g, 5 minutes) the aqueous phase was dried down with an Eppendorf Concentrator Plus (60°C, 180 minutes). Reconstituted samples (in 100 µl of chromatography starting conditions) were analysed using an HPLC system (Scherzo SM-C18 column, 40°C). Mobile phase A consisted of 30 mM ammonium acetate in 0.02% acetic acid in water and mobile phase B was 20% acetonitrile in 0.8% acetic acid in water. The following gradient was used at a flow rate of 0.5 ml/min: 0 minutes 10% phase B, 20 seconds 10% phase B, 80 seconds 99% phase B, 5 minutes 99% phase B, 5 minutes 10 sec 10% phase B, 8 minutes 10% phase B. Subsequently samples were then analysed with the Exactive Orbitrap mass spectrometer with a heated electrospray ionisation source (positive mode, full-scan range of m/z 100 – 200, resolution: 2 Hz). Thermo Xcalibur Quan Browser was used to process the data.

2.4 SDS-PAGE

SDS-PAGE was performed for placental tissue (section 4.2.6) and EVs (section 6.2.5). 7.5% gels were used for proteins with a high molecular weight (e.g. mTOR with molecular weight of 289 kDa) whereas high percentage gels (e.g. 12%) were used for detection of proteins with a low molecular weight (e.g. Bax with a molecular weight of 20 kDa). Table 4.2 summarizes the composition of the gel mixtures for the different percentages used for the gels. The stacking gel was prepared by using 13 % Protogel (National Diagnostics, EC-890), 25% Protogel Stacking B (National Diagnostics, EC-893) in water with addition of 0.5% of 10% APS and 0.1% TEMED. After loading of the samples into the gel and addition of a protein ladder (5 µl, Thermo Scientific, 26617) the gel was run with 1x running buffer (National Diagnostics, B9-0032) at 180V until the samples entered the resolving gel. Then the voltage was lowered to 30V to run the gel overnight. If the gel was run during the day the voltage was kept at 180V and the gel ran for 4 hours.

	7.5 % gel	**8 % gel**	**10% gel**	**12 % gel**
Protogel (ND, EC-890)	25%	27%	33%	40%
Protogel Resolving buffer (ND, EC-892)	25%	25%	25%	25%
Filled up with water				
10% APS	1.35%			
TEMED	0.135%			

Table 2.2: Composition for the resolving gels

The first gel of a study was stained for Coomassie to check equal loading of the samples. For that purpose, the gel was washed in water (3 x 10 minutes) and then stained in Coomassie solution overnight. The gel was then de-stained in de-staining solution (10% acetic acid and 50% ethanol in water) until the background was removed and the gel was then imaged on the Bio-Rad ChemiDoc Imager.

2.5 Western blotting

After the SDS-PAGE proteins were transferred onto a PDVF membrane as described in the respective sections of the thesis (section 4.2.6 and 6.2.5). Blots were then blocked in 5% BSA in 1xTween-10 in TBS (1 hour), washed (3 x 10 minutes) in T-TBS and incubated with the primary antibody overnight at 4°C. After washing the membrane with T-TBS (3 x 10 minutes) the blot was incubated with the secondary antibody and after additional washes with T-TBS (3 x 10 minutes) detected with HRP substrate (WBLUF0100) on the ChemiDoc MP Imaging System. The gel was stained with Coomassie (1610436, Biorad) after the transfer overnight and imaged after de-staining in de-staining solution (10% acetic acid, 50% ethanol, 40% water) for 10 minutes, washing in distilled water (3 x 10 minutes) and drying of the membrane. This was used to check the loading of the gel[365].

2.6 Agarose gel

For the sexing of fetal tissue (section 4.2.3) and the assessment of RNA (section 4.2.4) agarose gels were used. A 2 % agarose solution was prepared in TAE buffer (0.04 M Tris base, 0.02 M acetic acid and 1 mM EDTA), dissolved via heating and poured into a gel mould with the addition of SYBR safe and let to solidify. Samples were loaded into the gel along with a ladder (NEB DNA ladder) and the gel run at 80 V for 40 minutes.

2.7 RNA extraction

RNA was extracted from the fetal tissues (section 4.2.4), placentas (section 5.2.3) and EV samples (section 6.2.7) with the QIAGEN miRNeasy Micro kit (QIAGEN, 217084) according to the manufacturer's protocol. In brief for the QIAGEN kit 5 volumes of Qiazol were added to the concentrated EV sample, one volume of chloroform added and the mixture vortexed and incubated (room temperature, 3 minutes) before centrifugation (12000 g, 15 minutes, 4°C). The aqueous phase was mixed with 1.5 volumes of 100% ethanol and subjected to the extraction column for centrifugation (8000 g, 15 seconds). The columns were then washed with RWT buffer, RLT buffer, 80% ethanol and air-dried before elution of the RNA with 14 µl of RNase-free water.

2.8 Hematoxylin and eosin (H&E) staining

After fixation and embedding of tissues sections were cute. For the H&E stain sections were deparaffinised with xylene (2 x 5 minutes), rehydrated in ethanol (2 x 5 minutes) and washed under

running water (5 minutes). Slides were then stained with hematoxylin for 10 minutes, washed under running water (4 minutes) and counterstained with eosin (10 seconds). By dipping into water slides are briefly washed before being dehydrated with ethanol (2 x 30 seconds), penetrated with Xylene (first 2 minutes, then at least 5 minutes) and mounted.

2.9 Statistics

Data is shown as mean ± standard error of the mean (SEM), unless stated otherwise, and n numbers are indicated below each Figure. N numbers always refer to the dam which is used as the statistical unit in the field of developmental programming. For all data statistical outliers identified via Rout testing were removed. Maternal data analysis with comparisons between two or three groups is performed via t-tests or One-Way ANOVAs after testing for equal variance with the Brown-Forsythe test and normal distribution with the Shapiro-Wilk test. Some data (as indicated) showed unequal variances and was therefore analysed with a Welch ANOVA. Significant differences in the main factor were followed up via Tukey's multiple comparison test. For analyses over time within the same animal (such as body weight or blood pressure data) a mixed effects model followed by Tukey's multiple comparison test in case of significant effects was used. These analyses together with Pearson correlation analyses were performed in GraphPad Prism 9.0.0 Software.

Heatmaps and organisation of data as well as the RNASeq and lipidomics analysis (see chapter 5) were performed in R Studio (Version 1.4.1106) with R (Version 4.0.5). Most of the fetal data was analysed using a linear model including all fetuses in a litter to account for the dam as a random effect, with sex and experimental group as fixed effects. This is described further in chapter 4. For some fetal data, such as the fetal ultrasound, too little data existed to fit a good model so that a Two-Way ANOVA with group and fetal sex as independent variables was used and Tukey's comparison test performed as the post hoc test. Blinding for the physiological analyses was not possible due to the clear differences in body weight in the dams. However, all histological analyses were performed blinded.

3 Physiological characterisation of our mouse model of maternal diet-induced obesity and metformin treatment

3.1 Introduction

3.1.1 Our mouse model

The adaptations that usually occur in a healthy pregnancy as described in section s1.5.1 are more likely to fail in an obese compared to a lean pregnancy[366]. In general, as highlighted in the general introduction, obesity during pregnancy has detrimental effects not only leading to pregnancy complications such as GDM, preeclampsia or stillbirth but impacting fetal development and growth as well as offspring health long-term. Our diet-induced maternal obesity mouse model allows assessment of these effects. Previous data shows an obese phenotype and metabolic disturbance such as hyperinsulinemia, hyperleptinemia and glucose intolerance in the obese dams of our model[229,257] (Figure 3.1). The dams do not only have placental dysfunction and fetuses of lower birthweight but the offspring develop a wide range of cardiometabolic disturbances such as impaired glucose tolerance, cardiac hypertrophy and hypertension[258,260,261]. We thereby need to understand how an obese environment affects the pregnancy in detail and why a healthy pregnancy can't be achieved in our obese dams.

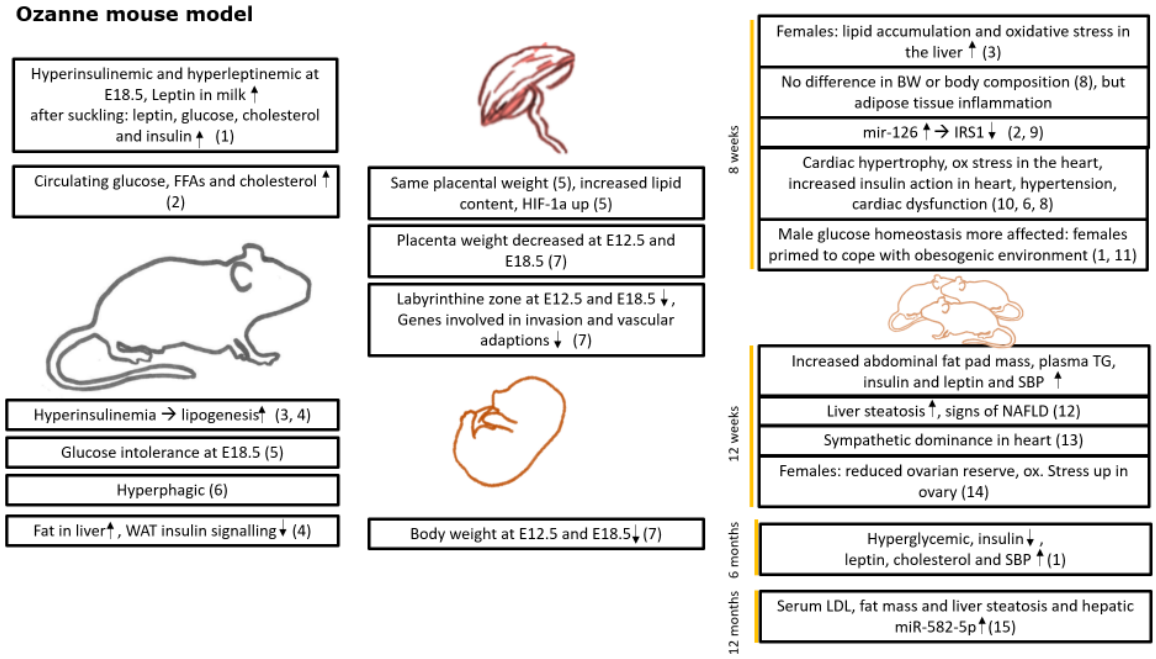

Figure 3.1: Observations from our Ozanne lab mouse model

Main outcomes observed in dams, placentas, fetuses and offspring are summarized. References can be found in the supplement (supplement 3, page 217).

3.1.2 Metformin

Due to the detrimental effects of GDM and obese pregnancies, successful interventions are urgently needed. Metformin is a cheap and easy intervention in pregnancy. It is currently the most-prescribed glucose-lowering agent with a consensus statement of the American Diabetes Association and the European Association for the Study of Diabetes stating metformin as the first line treatment together with lifestyle modifications for T2D patients[367]. Since 2009 the prescription rate of metformin in the US has risen considerably not only for treatment of patients with T2D but also for treatment of endocrine and cardiovascular diseases and cancer[368].

In the past decade the use of metformin in pregnancy has been studied more and more with the potential to be a treatment during pregnancy for GDM, obesity and even PE. In comparison with insulin treatment, metformin was shown to be equally efficient in reducing glucose but had lower rates of hypoglycaemic episodes[339]. Despite its frequently reported side effects like bloating and diarrhoea it is also reported that women preferred the use of metformin over insulin. Metformin can be taken orally and does not need to be stored refrigerated. Many countries such as the UK have now introduced metformin as the first line treatment for GDM once lifestyle interventions have failed. Metformin is also increasingly introduced for use in GDM pregnancies worldwide (Figure 3.2). However, knowledge on the effects of metformin exists mainly from data outside of pregnancy and the exact molecular mechanisms of its actions are still unknown[369].

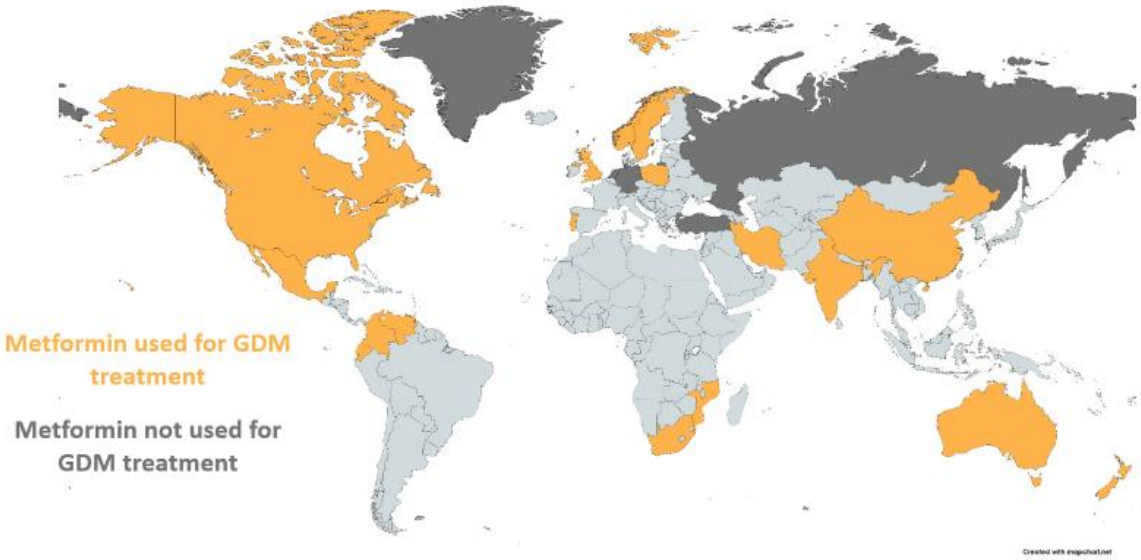

Figure 3.2: World map of metformin use in GDM treatment

Based on the most recent guidelines (see detailed Table in Supplement 4, p.218) the map shows where metformin treatment during pregnancy is (in orange) or isn't used (grey), for countries coloured in light grey no guidelines have been found or looked up. Stand: 08.12.2021, map created with mapchart.net.

From studies in T2D patients it is known that metformin reduces body fat and reduces or at least does not increase body weight unlike other oral hypoglycaemic agents or insulin[370]. The major uptake of metformin (70%) is via the duodenum and jejunum, with the rest being excreted via the faeces[371]. In the intestine metformin is thought to lead to changes in the microbiome and increases the secretion of glucagon-like peptide 1 (Glp1) leading to reductions in glucose levels upon metformin treatment [372–374]. The liver is thought to be one important organ of metformin action, here AMPK is activated either via inhibition of mitochondrial complex I at high concentrations or via a cytoplasmic serine-threonine kinase LKB1 or a lysosomal pathway[371,375]. High AMP/ATP ratios and AMPK activation lead to increased glucose uptake and inhibition of gluconeogenesis and lipid synthesis. In skeletal muscle, insulin sensitivity and glucose uptake are increased following metformin treatment[376]. A recent paper highlighted that metformin increases growth differentiation factor 15 (GDF-15) which could explain increased energy expenditure and decreased food intake[377]. GDF-15, a member of the TGFβ family, has been previously researched as a general stress-inducible cytokine, e.g. often elevated in cancer patients and in response to tissue injury, but recent years also highlight the link to metabolic diseases[378]. Metformin clearance is facilitated via the kidney, where renal cells take up metformin via multidrug and toxic compound extrusion (MATE 1 and 2) transporters. Metformin uptake and effects are summarized in Figure 3.3.

During pregnancy pharmacokinetics of drugs can change drastically. The adaptions to pregnancy in the cardiovascular system (e.g. increased plasma volume) can lower concentrations of an equivalent drug dose in the plasma compared to non-pregnant individuals. Lower intestinal motility and gastric acid secretion have also been shown in pregnancy, which could alter drug absorption[379]. However very little of this has been investigated experimentally with two thirds of women receiving drugs during pregnancy with dosing regimes based on non-pregnant data. For metformin it has been shown that renal clearance of metformin is increased in pregnancy[340,380].

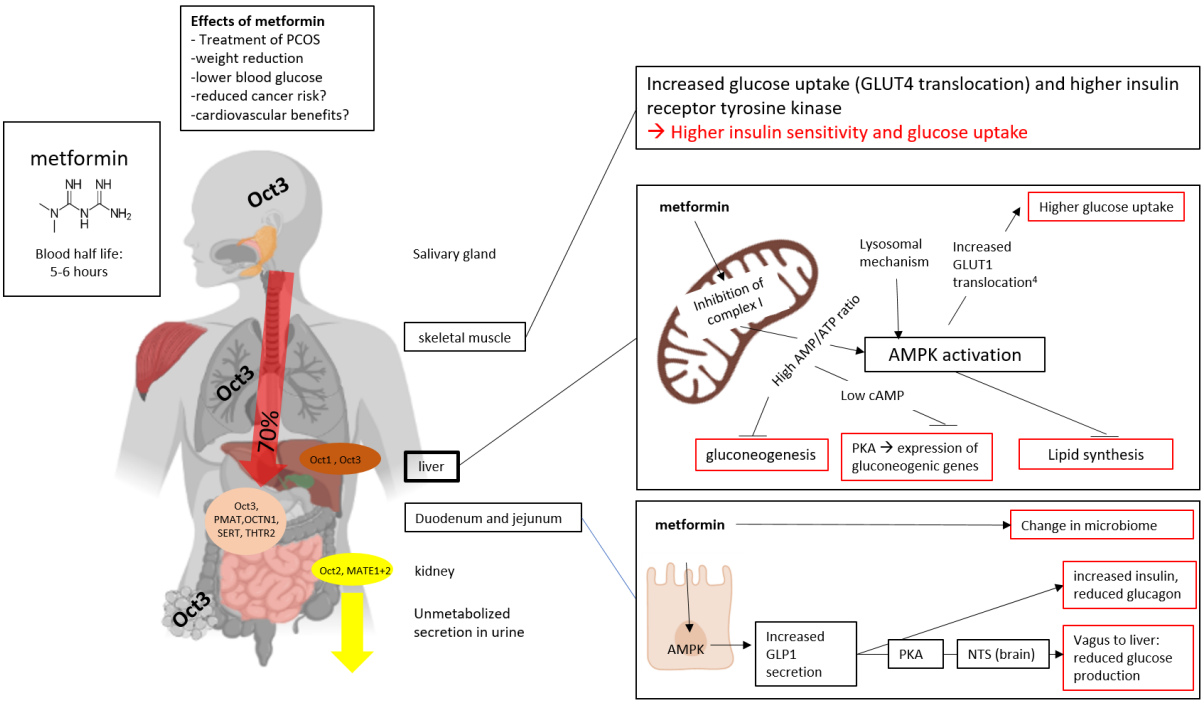

Figure 3.3: Actions of metformin in a non-pregnant individual

Uptake of metformin and its action on the skeletal muscle, liver and the intestine are shown. Known expression of metformin transporters in the brain, lung, liver, intestine, fat and kidney is shown on the body scheme and on the right-hand metformin's actions for the skeletal muscle, the liver and the duodenum and jejunum are further specified. Figures created with BioRender.com.

3.1.3 Aims

The aims of this chapter are:

- To characterise basic maternal health and physical characteristics in our mouse model of maternal diet-induced obesity (bodyweight, fat mass, glucose tolerance).
- To assess successful adaptation to pregnancy in our model of maternal obesity (maternal haemodynamics).
- To investigate the effect of metformin in obese pregnancy on the maternal outcomes stated in the previous two aims.

3.2 Methods

3.2.1 Dam phenotyping

The mouse model outlined in the general methods was used.

In the first main cohort food (Figure 3.4A), milk and dam were weighed twice weekly. Time Domain Nuclear Magnetic Resonance measurements (TD-NMR, Bruker minispec) were performed on the day of the plug (E0.5), E4.5 and E18.5 to assess body composition. In the middle of the study time this equipment broke and could not be used. Therefore, unfortunately body composition data is not available for all animals. In this cohort dams were killed after the ultrasound measurements at E18.5 (see section 3.2.5), cardiac puncture was performed under 2% isoflurane anaesthesia and death confirmed by cervical dislocation.

In the second cohort the aim was to assess food intake in obese untreated and obese metformin-treated dams daily. Food, milk and the dam were thereby weighed every day between 7 and 9 am. As shown in Figure 3.4B in comparison to the first main cohort this second cohort did not include a control group as we aimed to specifically investigate the effect of metformin on food and milk intake and weight gain. In contrast to the first main cohort single-housing was performed 1 week prior to dosing of the dams so that accurate daily food and milk weighing could be performed in individual animals before dosing, in the dosing week prior to mating and during pregnancy. Mice that did not mate successfully were also included to assess body weight and food intake in both groups in a non-pregnant state. In this cohort half of the mice were killed on day E13.5 and the other half on day E18.5 with CO_2 exposure and death confirmed via cervical dislocation.

For the analysis of the food pellet and milk pot weighings in both cohorts any datapoints with over 4 g food intake (equals 19.2 kcal) and datapoints with over 6 g milk intake (equals 18 kcal) were excluded as this intake would be clearly higher than the expected daily kcal intake of a C57BL/6 mouse and therefore the result of a technical error[381]. These errors are likely caused by the mouse playing with the food and pulling it through the hopper and powdering it.

For both cohorts, data is shown per weeks of pregnancy with week 1 (E0.5 – E5.5), week 2 (E6.5 – E12-5) and week 3 (E13.5 – E18.5).

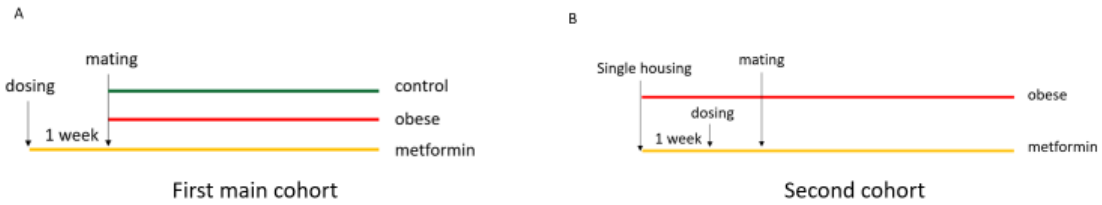

Figure 3.4: Designs of the two cohorts

(A) A main cohort investigated control, obese untreated and metformin-treated dams during pregnancy. (B) In a second cohort only obese untreated and metformin-treated dams were analysed to specifically address effects on food intake, also investigating them prior to pregnancy.

3.2.2 Liver histology

The left lateral liver lobe was cut of the liver and immersion-fixed in 10% formalin for up to 1 year until further processed and embedded in paraffin, which was performed by Tom Ashmore. 5 µm mid-sections were stained with hematoxylin and eosin (H&E) as described in section 2.8 of the general methods. Images were acquired with the Zeiss Axioscan microscopy slide scanner and analysis of the liver fat vacuoles was performed with HALO software (Indica labs). Vessels were manually delineated on the pictures taken so that the software could be taught via artificial intelligence to exclude vessels so that fat content in the livers could be quantified. For the analysis of the fat content the vacuole setting in HALO was used that has been designed to quantify and calculate the area of white space in a tissue section.

3.2.3 Glucose tolerance measurement

On day E17.5 of pregnancy dams were fasted in the morning for 4 hours. Glucose (1 mg/kg) was intra-peritoneally injected and glucose measured in tail blood at 0, 15, 30, 60 and 120 minutes (AlphaTRAK, Abbot Logistics, Netherlands). Capillary tubes were used for blood collection at 0 and 15 minutes for future measurement of insulin concentrations later via an enzyme-linked immunoassay (ELISA, Crystal Chem Mouse Insulin ELISA (Ultra-Sensitive) kit). Due to the high variation of intraperitoneal GTT (ipGTT) data and thereby the need for higher n numbers for this measurement compared to others, data from a previous cohort assessing metformin treatment in obese dams was included to provide sufficient statistical power. Both cohorts were established and maintained in the same way. To account for the use of two cohort in this data, analysis of the glucose excursion curves is presented as the difference to the starting glucose (Δ glucose). Animals for which glucose rose less than 50% between fasting and the measurement at 15 and/or 30 minutes after glucose injection were excluded from the analysis. In these cases, the GTT was considered a failed GTT due to a failed injection with a slightly higher failure rate in the control group (23%) but similar rates in the obese (9%) and the metformin-treated group (5%). In total 14% needed to be excluded which fits which the literature that states that the error rate of ipGTTs is 10-20%[382].

3.2.4 Blood pressure measurements

Systolic blood pressure and heart rate were measured via non-invasive tail cuff plethysmography (BP-200 system, Visitech) which measures via transmission of light through the tail. Animals are restrained in the machine in a little container and their tails placed and secured in a cuff that allows the measurement of blood pressure by inflating and deflating. Before mating dams were trained on two consecutive days, then the pre-pregnancy blood pressure measurement was performed. Blood pressure was additionally measured on day E4.5 and E16.5 to provide longitudinal data. On each day blood pressure measurements were performed in the morning (7.30 – 9 am) and evening (5 – 6.30 pm) to cover the light and dark phases.

3.2.5 Uterine artery Doppler

Thanks to Dr. Colin Murdoch, Dr. Norman Shreeve and Dr. Dieter Fuchs for the help in setting up and establishing pregnancy ultrasound in the lab. On day E18.5 uterine artery Doppler was performed (FUJIFILM VisualSonics, Canada, Vevo3100). Anaesthesia was induced with 2% isoflurane which was reduced to 1.5% after 10 minutes for the duration of the assessment. Animals were positioned on a heated platform to maintain a constant body temperature of 36°C throughout. Body temperature was measured via a rectal probe and measurements from one animal were excluded as the temperature fell below 36°C multiple times. Via electrodes on the platform the ECG was also recorded to monitor the animal under anaesthesia. The bladder was used as a landmark, at this height the abdominal splits into the iliac artery from which the uterine artery branches off (Figure 3.5A) [383]. The probe was moved further downwards so that the uterine artery could be observed as a clear streak. Here the Doppler measurement is taken showing the typical uterine artery waveform in Figure 3.5B. From the systolic, minimum diastolic velocity and the velocity time integral (VTI, measure for the mean velocity) the pulsatility and resistance index were calculated.

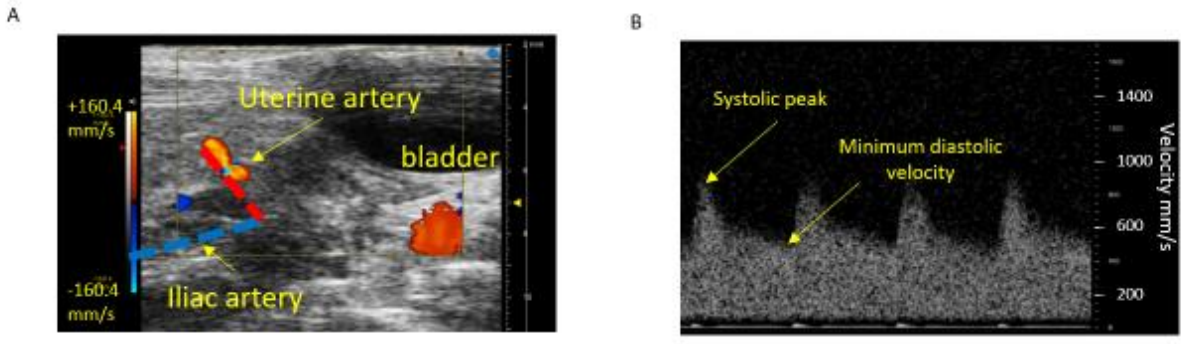

Figure 3.5: Uterine artery Doppler measurements

(A) Ultrasound allows the detection of the bladder as a landmark to see the branching of the iliac and the uterine artery, where the Doppler measurement is taken in the uterine artery, (B) showing the typical waveform of the uterine artery.

3.2.6 Serum analysis

Blood samples of the dams were left at room temperature for at least 30 minutes before centrifugation (1500 g for 5 minutes, twice) to obtain clean serum. Serum was aliquoted and stored at -80°C until used for the assays below.

3.2.7 sFlt measurements

sFlt (VEGF-R1), a typical marker for preeclampsia, was measured in maternal serum by ELISA according to the manufacturer's instructions (R&D Systems, Cat #MVR100). The kit already provides an antibody coated plate, so samples (dilution 1:35, in single) are added to the wells in the provided assay diluent for incubation (2 hours, room temperature). After washing with provided wash buffer the sFlt antibody conjugated to horseradish peroxidase is added and incubated for 2 hours (room temperature). The plate is then washed and incubated with substrate solution for 30 minutes (room temperature, away from light). The stop solution is then added and the plate read with a plate reader at a wavelength of 450 nm (wavelength correction at 540 nm). A standard curve was used to interpret results from the samples.

3.2.8 GDF-15 measurements

GDF-15, previously identified to increase with metformin treatment, was measured in the dam serum by the Core Biochemical Assay Laboratory, Cambridge University Hospitals with the Mouse GDF-15 DuoSet ELISA (DY6385)[377]. In brief, GDF-15 antibodies are coated onto MesoScale Discovery (MSD) microplates, after washing the plates are then blocked with MSD blocker A. 40 µl of assay diluent and standards/QCs/sample (undiluted, in duplicates) were incubated on the plate for 2 hours (room temperature). Goat anti-human GDF-15 detection antibody (biotinylated) diluted in MSD diluent 100 incubated on the plate for 1 hour on a plate shaker (room temperature). The plate was washed and Sulpho-TAG labelled Streptavidin (MSD) in MSD diluent 100 incubated on the plate for 30 minutes. The plate was washed again, MSD read buffer added and the plate read with the MSD s600 plate reader.

3.3 Results

3.3.1 Dam bodyweight across pregnancy

Obese untreated and obese metformin-treated dams had a significantly increased bodyweight throughout pregnancy compared to control dams (Figure 3.1A). However, all dams showed an increase in body weight from the day of the plug (E0.5) until day E18.5. As visible in Figure 3.6A the slope in body weight gain is steeper in the control dams compared to the animals on an obesogenic diet. Total GWG expressed as the % of starting bodyweight was significantly higher in the control group (Figure 3.6B). Metformin treatment had no effect on body weight or GWG but reduced maternal fat mass significantly at the end of pregnancy compared to obese untreated dams (21.2 ± 2.3 g in obese untreated vs. 17.58 ± 3.0 g in obese metformin-treated, p=0.02, Figure 3.6C).

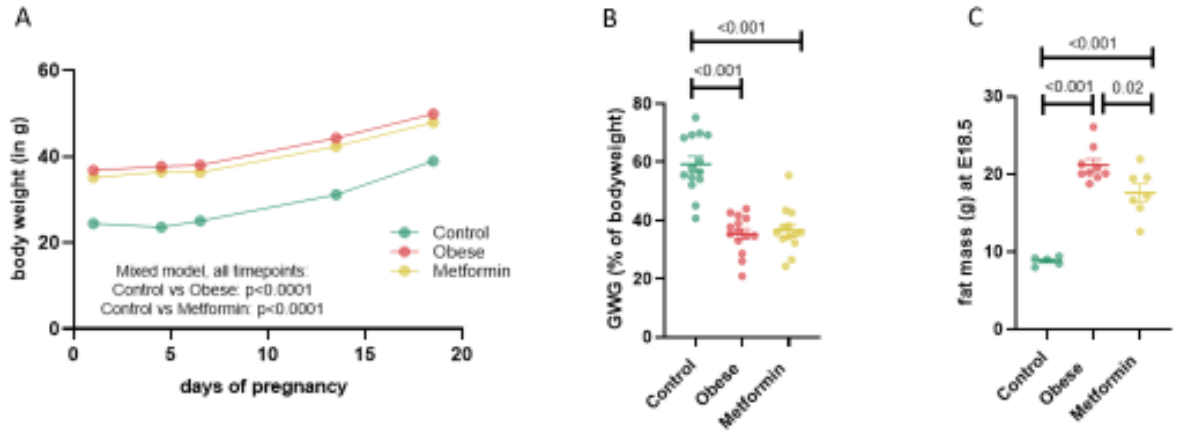

Figure 3.6: Bodyweight was increased in the obese untreated and obese metformin-treated dams

(A) Body weight was measured throughout pregnancy (n = 14 for control, n = 14 for obese, n = 13 for metformin dams; mean ± SEM and mixed model analysis shown) and (B) gestational weight gain as a % of the body weight calculated (n = 14 for control, n = 14 for obese, n = 13 for metformin dams). (C) TD-NMR measurements allowed measurement of fat mass in the dams (n = 5 for control, n = 9 for obese, n = 7 for metformin dams). One-Way-ANOVA followed by Tukey's multiple comparison test and mean ± SEM are shown.

To adress the effect of metformin treatment on maternal body weight more precisely a second cohort was established where daily measurements comparing obese untreated and obese metformin-treated animals in the pregnant and non-pregnant state were performed. Both, the obese untreated and obese metformin-treated pregnant animals, gained similar weight during pregnancy, comparable to the data from the first cohort (Figure 3.7A). Daily tracking of bodyweight however showed that from the second half of the dosing week onwards obese metformin-treated dams showed a slight reduction in bodyweight. This remained through pregnancy with the obese metformin-treated dams tracking below the bodyweight of the obese untreated dams. The effect of metformin treatment on body weight reduction becomes clear when looking at the divergence of the graphs for the non-pregnant obese untreated and obese metformin-treated animals (Figure 3.7A).

Analysis of bodyweight change by week showed a significant bodyweight reduction pre-pregnancy upon dosing in the obese metformin-treated animals compared to the obese untreated animals (-0.5 ± 0.3 g in obese untreated vs. -2.8 ± 0.6 g in obese metformin-treated dams, p=0.001, Figure 3.7B). In pregnancy obese metformin-treated dams still gained less weight in the first week of pregnancy (3.2 ± 0.3 g in obese untreated vs. 1.0 ± 0.4 g in obese metformin-treated dams, p=0.006, Figure 3.7C). This effect was not observed in the last two weeks of pregnancy where both groups gain a similar amount of body weight in each week. Non-pregnant obese metformin-treated females also gained less weight compared to the obese untreated animals as expected (Figure 3.7C).

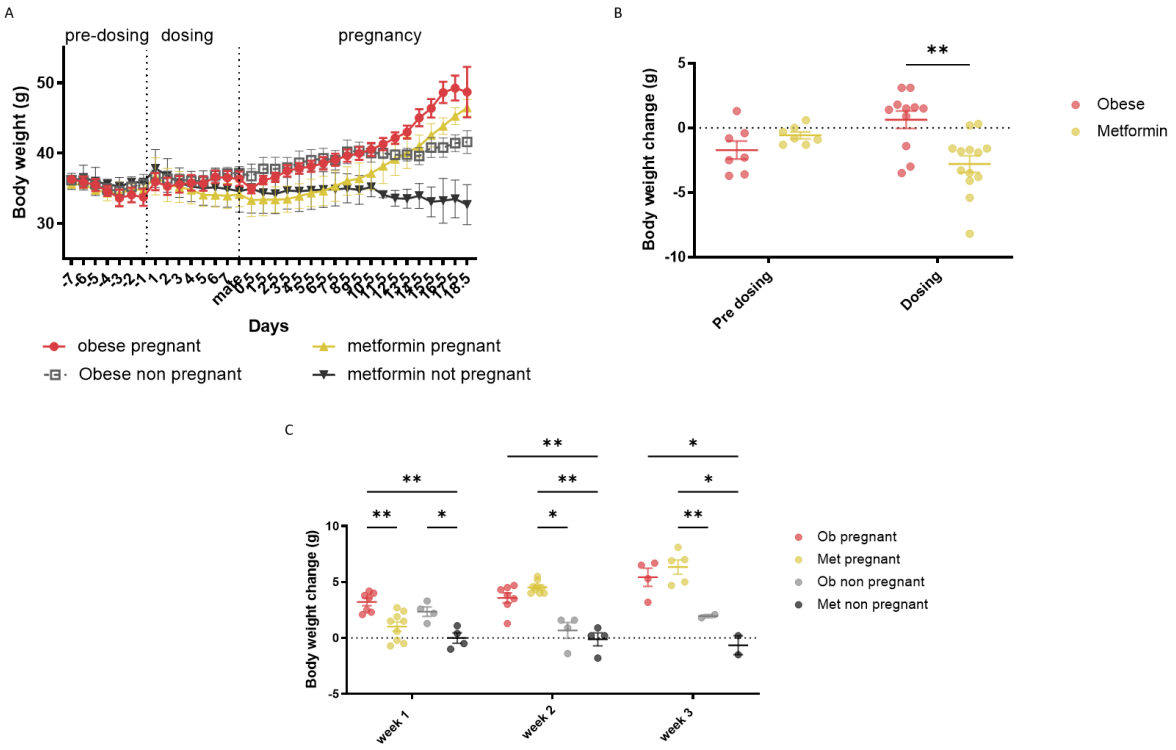

Figure 3.7: Body weight in the second cohort was tracked daily

(A) Body weight was measured throughout pregnancy in obese untreated and obese metformin-treated pregnant and non-pregnant animals. Body weight change per week is shown (B) prior to mating (pre-dosing: n=7 for obese dams, n=11 for metformin dams, dosing: n=7 for obese dams, n=13 for metformin dams) and (C) after mating (week 1: n=7 and 4 for obese pregnant and non-pregnant animals, n=9 and 4 for metformin pregnant and non-pregnant animals, week 2: n=7 and 4 for obese pregnant animals, n=9 and 4 for metformin pregnant and non-pregnant animals, week 3: n=4 and 2 for obese pregnant and non-pregnant animals and n=5 and 2 for metformin pregnant and non-pregnant animals.). Mixed effects model ANOVA followed by Tukey's multiple comparison test and mean ± SEM are shown (: p<0.05, **: p<0.01, ***: p<0.001, ****: p<0.001).*

3.3.2 Food intake

Food intake was first analysed in the main cohort, here average total food intake in kcal/day during pregnancy was doubled in the obese untreated and obese metformin-treated dams compared to dams

on a control diet (Figure 3.8A). In the last week of pregnancy this difference disappears with all three groups taking in around 20 kcal/day on average. Pellet food intake was not significantly different across the three groups with the obese metformin-treated dams taking in significantly more kcal of food pellets per day than the obese untreated dams in week 2 of pregnancy (Figure 3.8B). The milk intake however showed slightly lower milk kcal intake per day in the obese metformin-treated dams compared to the obese untreated dams (Figure 3.8C), but this difference was not significant.

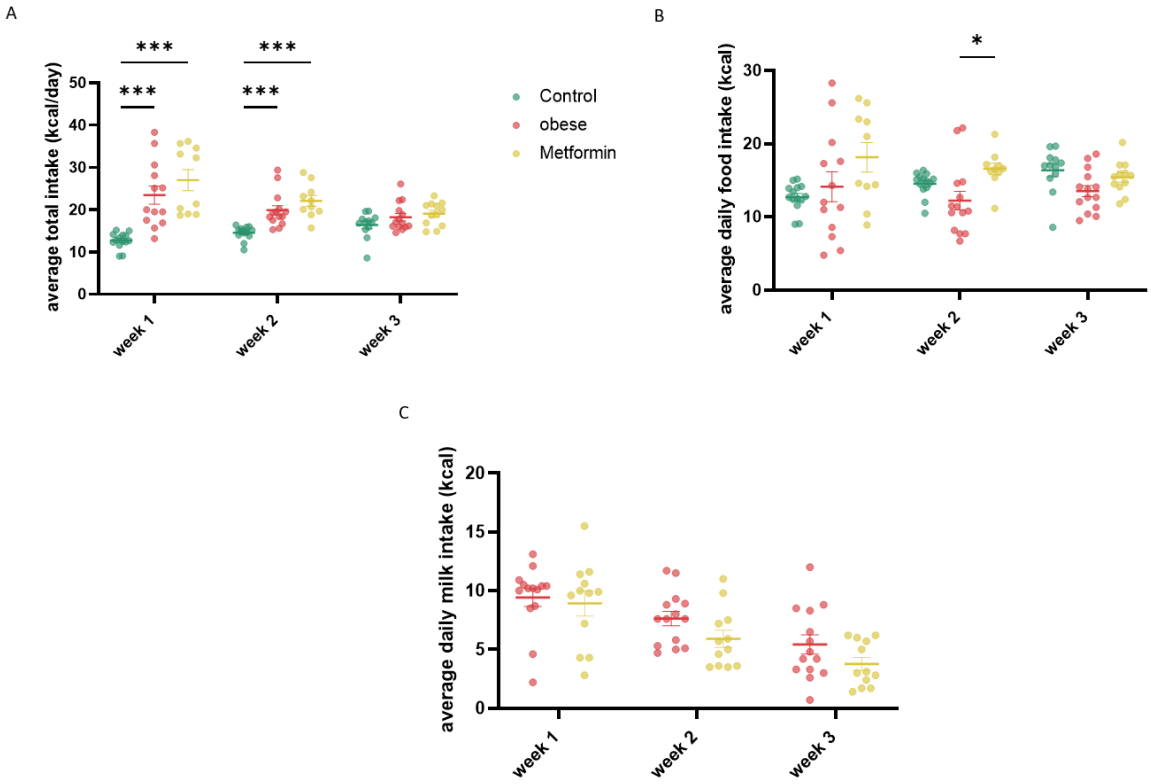

Figure 3.8: Daily total food intake was increased in the obese untreated and metformin-treated dams in early pregnancy

(A) Total daily food intake was averaged over the three weeks of pregnancy in the control, obese untreated and obese metformin-treated group. The different ingredients of the diet are shown separately as well: (B) averaged daily food intake and (C) averaged daily milk intake. All graphs show for week 1: n=14 for control and obese and n=12 for metformin dams, week 2: n=13 for control, n=14 for obese and n=14 for metformin dams, week 3: n=10 for control and obese and n=12 for metformin dams. Mixed effects model ANOVA followed by Tukey's multiple comparison test and mean ± SEM are shown (: p<0.05, **: p<0.01, ***: p<0.001, ****: p<0.001).*

To investigate this phenotype more closely and accurately via daily rather than weekly weighings the second cohort was used. Prior to pregnancy animals dosed with metformin showed an increase in daily food intake upon dosing (Figure 3.9B). However, the milk intake per kcal is reduced upon metformin treatment (Figure 3.9 C) with the whole average daily kcal intake being reduced (total daily food intake

of 16.6 ± 0.7 kcal in obese untreated vs. 14.2 ± 0.9 kcal in obese metformin-treated, p=0.04, Figure 3.9A).

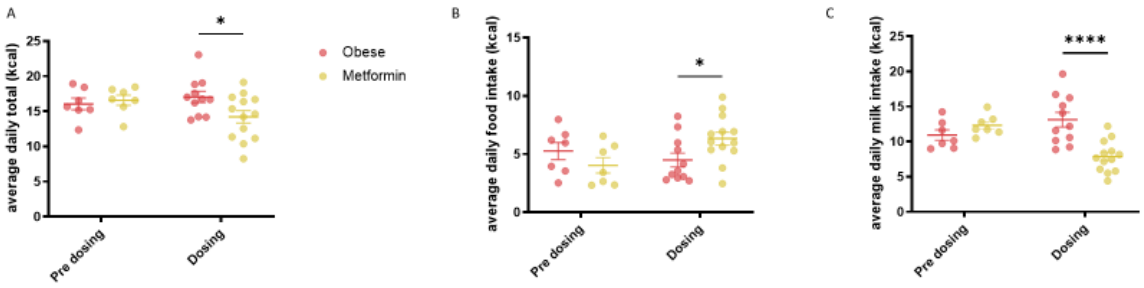

Figure 3.9: Prior to pregnancy averaged total daily food intake is reduced in obese animals upon metformin treatment

(A) Total daily food intake was averaged in the week before metformin dosing and in the week of metformin dosing. The different ingredients of the diet are shown separately as well: (B) averaged daily food intake and (C) averaged daily milk intake. All graphs show pre dosing: n=7 for obese and metformin dams, dosing: n=11 for obese and n=13 for metformin dams. Mixed effects model ANOVA followed by Tukey's multiple comparison test and mean ± SEM are shown (: p<0.05, **: p<0.01, ***: p<0.001, ****: p<0.001).*

During pregnancy average total daily kcal intake was similar across groups. Only in week 1 of pregnancy the total average daily kcal intake was lower in the pregnant obese metformin-treated compared to the obese untreated dams (Figure 3.10A). In week 3 of pregnancy average total kcal intake is even slightly higher in the obese metformin-treated animals, in the non-pregnant animals metformin seems to still reduce total kcal intake even after 4 weeks of treatment.

In contrast pellet food intake was increased in the pregnant obese metformin-treated dams in week 1 and 2 of pregnancy in comparison with the obese untreated dams (Figure 3.10B). The food intake increased in both groups with advancing gestation, showing a clear difference to the non-pregnant animals who have a lower food intake throughout. Daily milk intake decreased overall across gestation (Figure 3.10C). In the non-pregnant animals, no change in milk intake was seen across the weeks. As shown in the week of dosing, intake of milk was significantly reduced in both the pregnant and non-pregnant obese metformin-treated dams compared to their obese untreated counterparts in the first week of pregnancy/the second week of dosing.

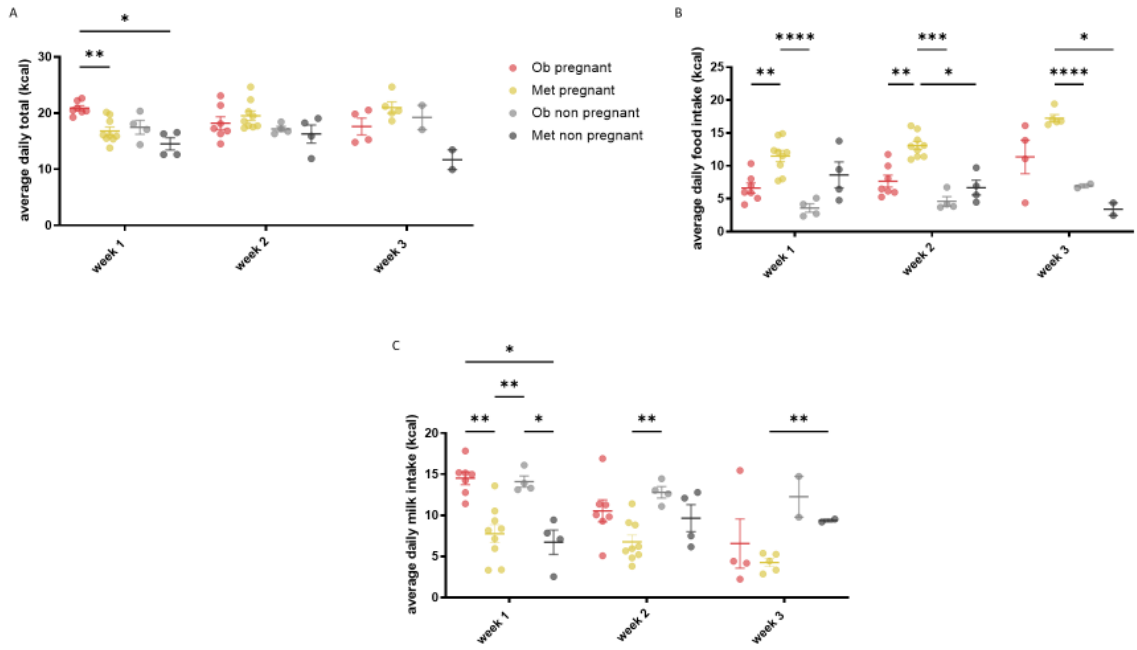

Figure 3.10: During pregnancy food intake is averaged across the three weeks of pregnancy

(A) Total daily food intake was averaged per week in the pregnant and non-pregnant obese untreated and obese metformin-treated animals. The different ingredients of the diet are shown separately as well: (B) averaged daily food intake and (C) averaged daily milk intake. All graphs show for week 1: n=7 and 4 for obese pregnant and non-pregnant animals, n=9 and 4 for metformin pregnant and non-pregnant animals, week 2: n=7 and 4 for obese pregnant animals, n=9 and 4 for metformin pregnant and non-pregnant animals, week 3: n=4 and 2 for obese pregnant and non-pregnant animals and n=5 and 2 for metformin pregnant and non-pregnant animals. Mixed effects model ANOVA followed by Tukey's multiple comparison test and mean ± SEM are shown (: p<0.05, **: p<0.01, ***: p<0.001, ****: p<0.001). Ob=Obese, Met=Metformin*

3.3.3 Metformin dosing

Based on the milk intake calculated in the food intake data, metformin intake was assessed. As expected from the milk intake data metformin intake in mg/kg/day reduces with pregnancy progression from pre-pregnancy to week 3 of pregnancy (Figure 3.11A). Total average metformin dose was 255 ± 13.3 mg/kg/day and thereby above the lowest dose threshold that we set at 200 mg/kg/day to achieve sufficient metformin exposure (Figure 3.11B).

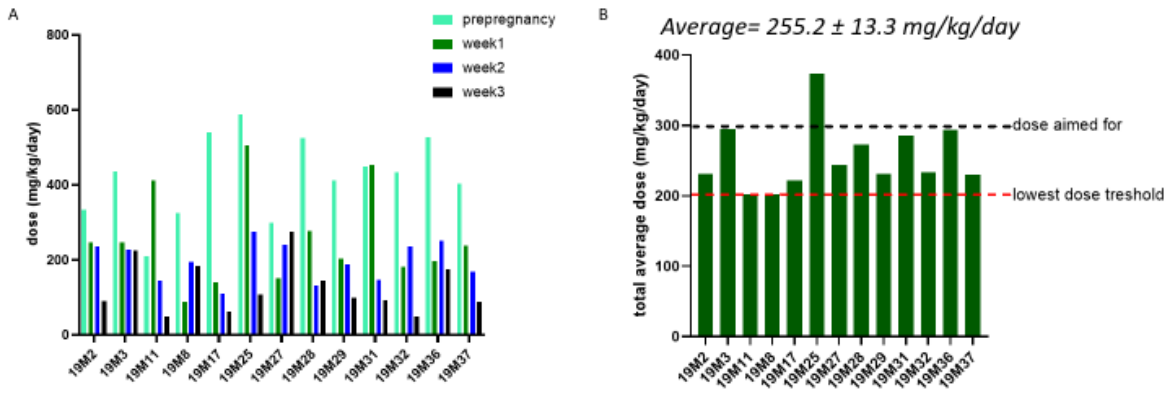

Figure 3.11: All dams received sufficient amounts of Metformin based on their milk intake

(A) Metformin dose received by the animal was averaged over the first week of dosing before pregnancy and three weeks of pregnancy. (B) Averaged dose across the whole dosing time shows that all dams received a dose within a range of 200 – 300 mg/kg/day.

Equally the second cohort shows the same trajectory (data not shown here).

Metformin was additionally measured in the serum via LC-MS. In the initial main cohort, the concentrations showed a range from 0.10 to 5.96 nmol/ml in the 13 dams with an average of 1.67 ± 0.57 nmol/ml.

3.3.4 GDF-15 measurements

GDF-15 levels were significantly increased in the metformin-treated obese dams compared to both, the obese untreated and the control group (Figure 3.12A). Due to unexpectedly high levels of GDF-15 compared to data from the literature it was hypothesized that anaesthesia could be an underlying cause of the increased GDF-15 levels. Evidence for this could be the strong correlation between approximate time under anaesthesia and GDF-15 levels (Figure 3.12B).

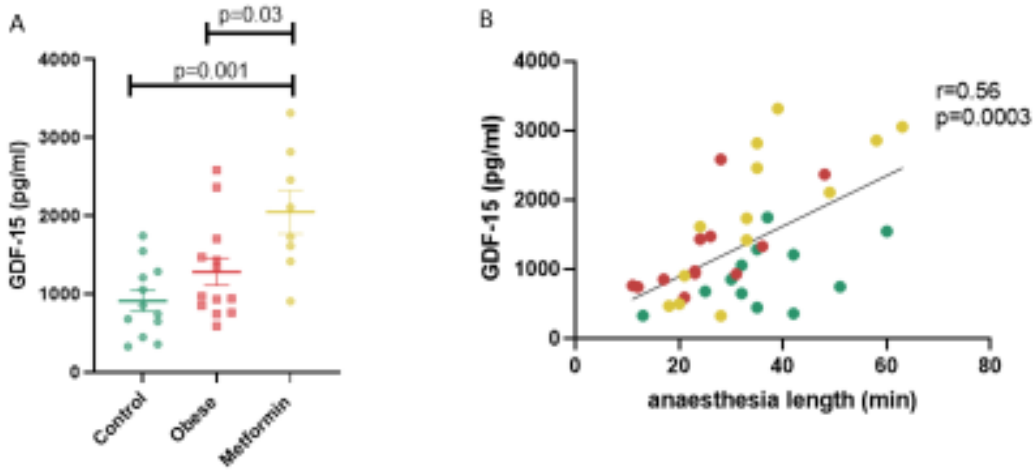

Figure 3.12: GDF-15 levels are increased in metformin-treated obese dams but correlate with anaesthesia length

(A*) GDF-15 levels are measured in dam serum, One-Way-ANOVA followed by Tukey's multiple comparison test and mean ± SEM are shown. (B) GDF-15 serum levels were correlated against approximate length of the animal under anaesthesia, linear regression and Pearson correlation coefficient r are shown. N=12 for control, n=13 for obese and n=8 for metformin dams was shown.*

3.3.5 Liver steatosis

As the liver is a key metabolic organ, maternal livers were weighed and showed significant differences with the livers being significantly heavier in the obese dams. The obese metformin-treated dams however had a significantly reduced liver weight compared to the obese untreated dams (Figure 3.13A). This led us to hypothesize that liver fat is reduced in obese dams with metformin-treatment compared to obese untreated dams despite the same obesogenic diet and livers were therefore further analysed. H&E staining was performed (Figure 3.13B) which showed increased fat content in livers from obese untreated dams compared to dams on a control diet (8.5 ± 0.5% in obese untreated vs. 1.3 ± 0.2% in controls $p < 0.0001$, Figure 3.13C). As expected from the liver weight data fat content was significantly reduced in obese metformin-treated dams compared to obese untreated dams (6.5 ± 0.7% in obese metformin treated group, p=0.01, Figure 3.13C).

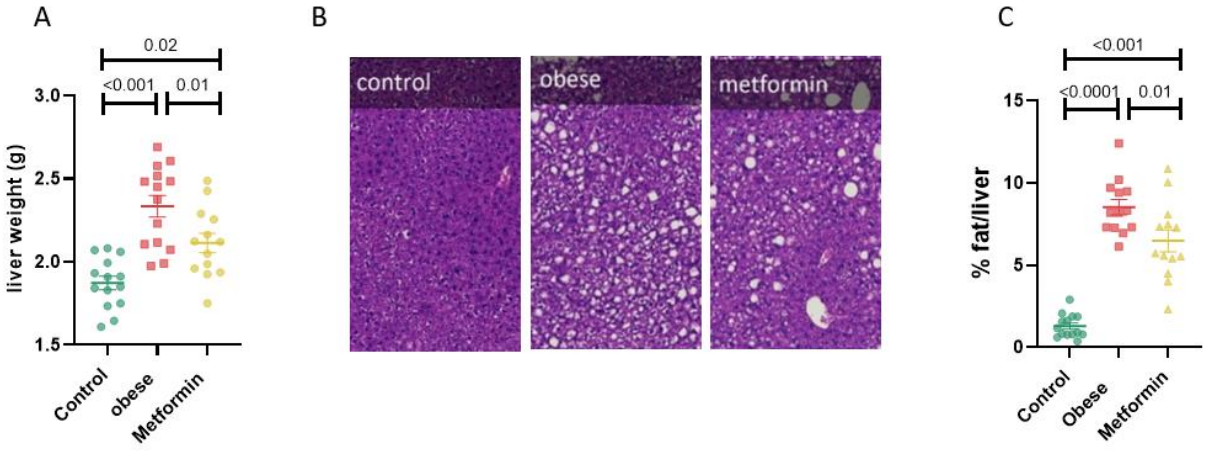

Figure 3.13: Liver steatosis is increased in obese untreated dams but improved with metformin-treatment

(A) Livers were weighed at the time of dissection on E18.5, n=14 for control and obese dams and n=13 for metformin dams and One-Way-ANOVA followed by Tukey's multiple comparison test with mean ± SEM are shown. (B) H&E staining of the liver section (representative images) allowed (C) calculation of percentage of fat in the liver, n=14 for control and n=13 for obese and metformin dams and Welch-ANOVA followed by Dunnett's multiple comparison test and mean ± SEM are shown.

3.3.6 Glucose tolerance

Glucose tolerance was impaired in the obese untreated dams with the area under the curve (AUC) being significantly increased in the obese untreated dams compared to control dams (Figure 3.14A and B). Metformin-treatment in obese dams improved glucose tolerance. The AUC tended to be reduced with metformin-treatment compared to obese dams without treatment (p=0.01 for obese untreated vs. controls and p=0.07 for obese metformin treated vs. obese untreated, Figure 3.14B).

Insulin levels in the dams were measured after a 4 hour fast prior to the ipGTT and 15 minutes after glucose injection. Both, at time 0 and time 15, insulin levels were significantly increased in the obese untreated dams compared to control dams (Figure 3.14C and D). At both timepoints metformin-treatment in obese dams reduced insulin levels but this was only statistically significant at the 15 minute timepoint.

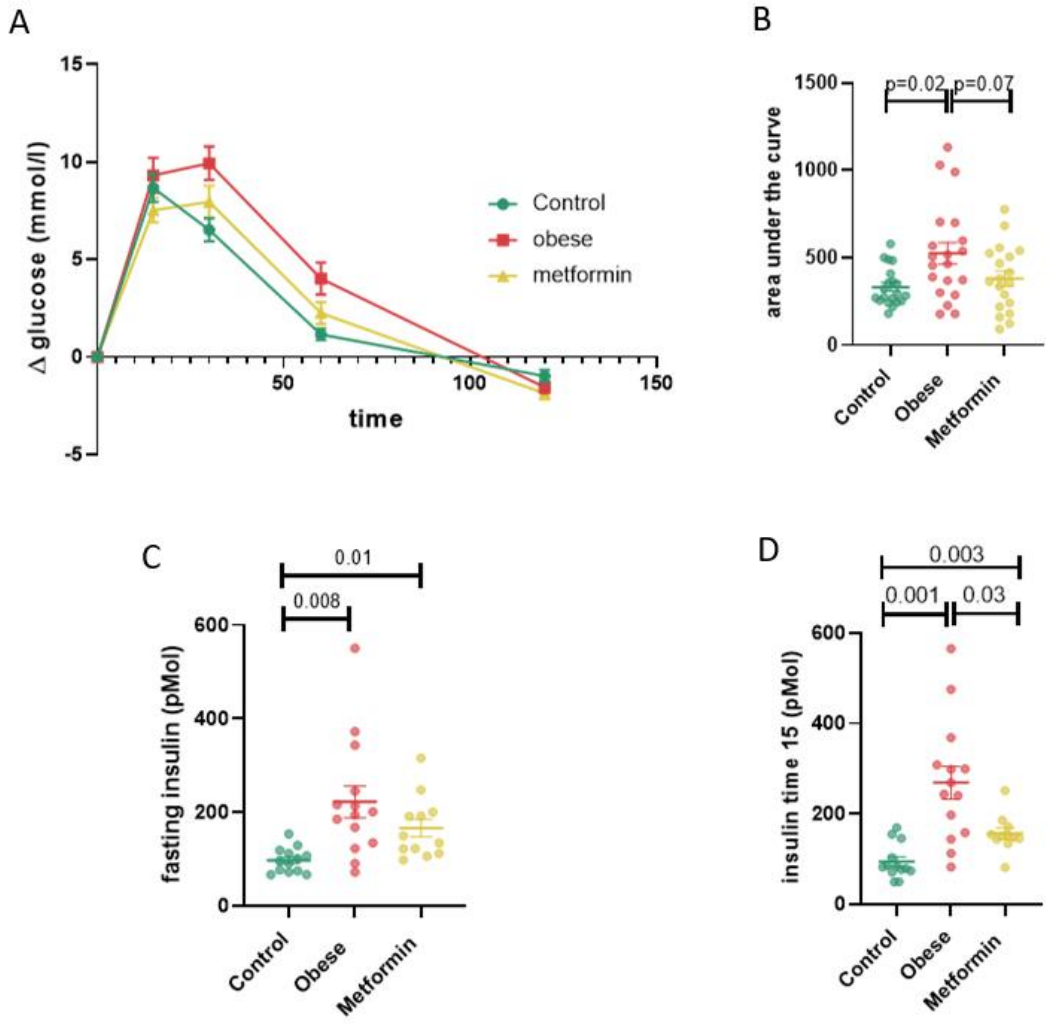

Figure 3.14: Impaired glucose tolerance induced by maternal obesity is improved with metformin treatment

(A) Glucose excursion curves are shown as difference of glucose levels to the starting glucose and (B) AUC is calculated. N=20 for control and obese and n=19 for metformin dams are shown for A and B. (C) Fasting insulin and (D) insulin at 15 minutes after glucose injection were measured. N=13 for control, n=14 for obese and n=12 for metformin dams, Welch-ANOVA followed by Dunnett's multiple comparison test and mean ± SEM are shown.

3.3.7 Blood pressure

Heart rate was significantly increased in the obese untreated dams compared to the control dams prior to mating, at E4.5 and E17.5 when measured in the morning (Figure 3.15A). Measurements in the evening only revealed this significant difference prior to mating and at E17.5 (Figure 3.15B). Obese metformin-treated dams showed a trend for a lower heart rate than the obese untreated at time of mating when measured in the morning (p=0.07). The heart rate of obese metformin-treated dams was significantly higher than in the control dams at E4.5 when measured in the morning and at E17.5 when measured in the evening. Measurements for the systolic blood pressure were generally not

significantly different between the groups (Figure 3.15C and D). The only significant difference observed was in the obese metformin-treated animals measured in the morning prior to mating when SBP was significantly reduced compared to controls. Overall, linear modelling assessing the effect of treatment, day of gestation and time of the day showed that heart rate (coefficient: -38.8, p<0.001) and SBP (coefficient: -4.3, p=0.03) were lower when measured in the evening.

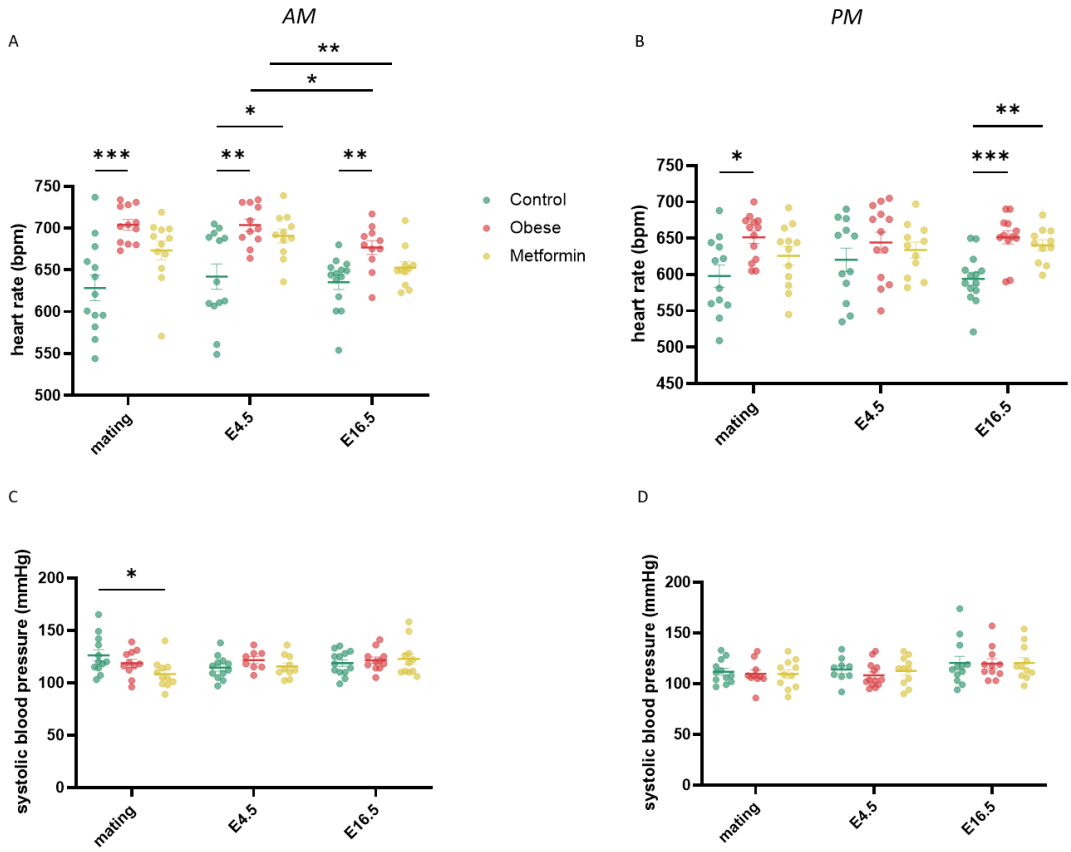

Figure 3.15: Heart rate is increased in obese untreated dams with reductions via metformin-treatment

(A) Heart rate measurements before mating, at E4.5 and E16.5 were performed in the morning (n=13-14 for control, n=11-12 for obese and n=11-12 for metformin dams) and (B) evening (n=12-14 for control, n=12-13 for obese and n=11-12 for metformin dams). (C) Equally systolic blood pressure was recorded at the same timepoints in the morning (n=11-12 for control, n=10-12 for obese and n=11-13 for metformin dams) and (D) the evening (n=9-12 for control, n=9-13 for obese and n=11-12 for metformin dams). Mixed effects model ANOVA followed by Tukey's multiple comparison test and mean ± SEM are shown.

3.3.8 Uterine artery Doppler

Uterine artery pulsatility and resistance index were calculated. They were both significantly negatively correlated with the maternal heart rate recorded during the ultrasound (Figure 3.16A and B). This was previously reported in a study in sheep which suggested the need for correction of uterine artery Doppler by the maternal heart rate[384,385]. Thereby uterine artery PI and RI were corrected for maternal heart rate according to the following formula presented by Ochi et al. [384,385]: PI = ($intercept_{correlation}$ –

$slope_{correlation}$ * heart rate) * $PI_{measured}$.

The corrected PI and RI were both significantly increased in the obese untreated dams compared to control dams (Pulsatility index: p=0.001 obese untreated vs. controls, Figure 3.16C and D). Metformin-treatment of obese dams reduced the PI and RI significantly (p=0.04 and p=0.03 compared to obese untreated animals).

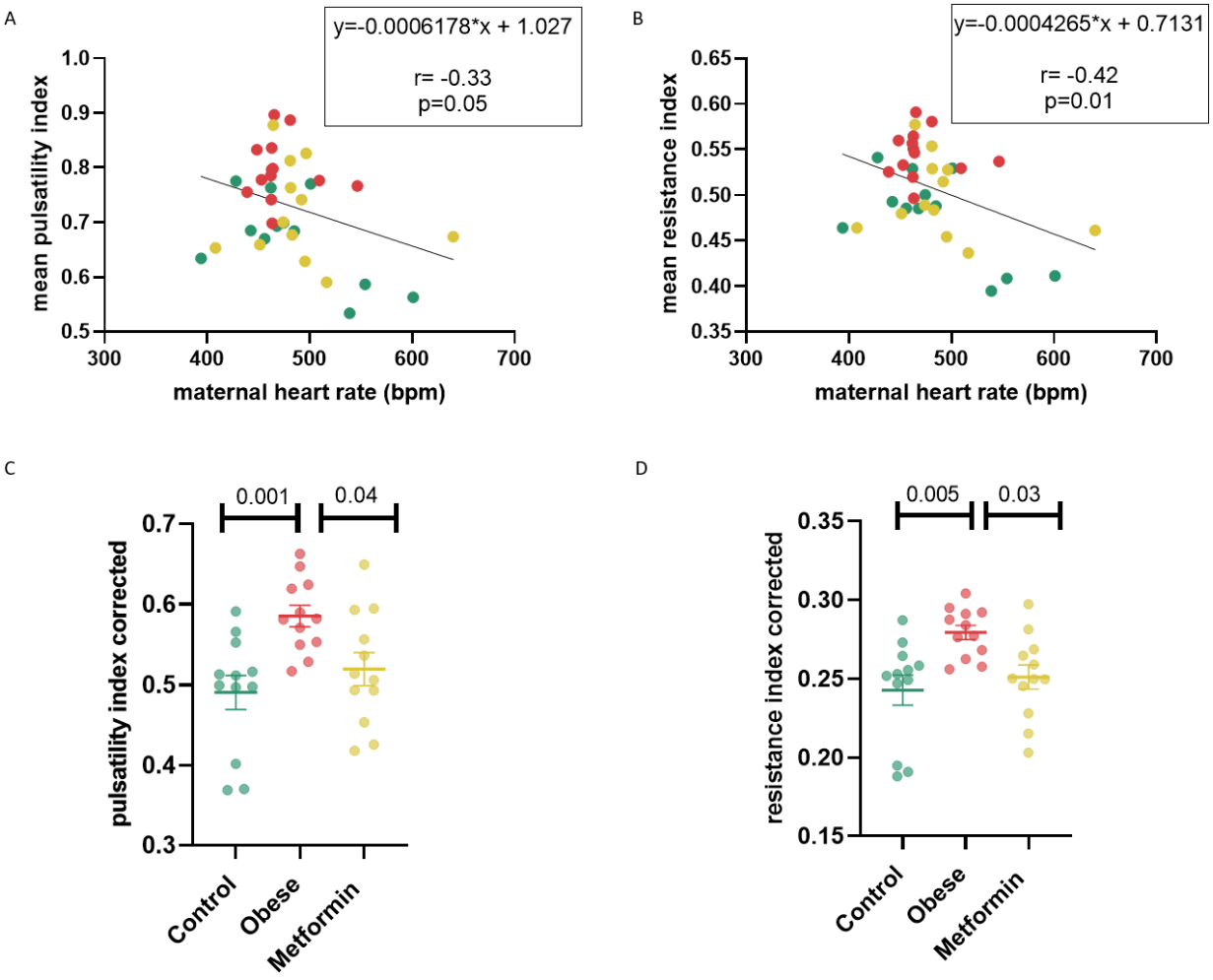

Figure 3.16: Uterine artery compliance is impaired in obese untreated but rescued in obese metformin-treated dams

(A) Uterine artery PI and (B) RI were correlated to the maternal heart rate recorded during the ultrasound. Via the intercept and the slope of the regression line uterine artery (C) PI and (D) RI were corrected and are presented here for all three groups. N=12 for all groups, One-Way-ANOVA followed by Tukey's multiple comparison test and mean ± SEM are shown. For correlation analyses linear regression and Pearson correlation coefficient r are shown.

The uterine artery PI correlated with insulin at both timepoints, fasting and 15 minutes after glucose injection (r=0.51, p=0.001 and r=0.43, p=0.02, Figure 3.17A and B). A similar correlation was seen between the RI and insulin levels (data not shown).

Levels of sFlt were measured as a marker of preeclampsia in maternal blood at E18.5 and were shown to be significantly increased in the obese untreated dams compared to control dams (control vs. obese untreated p=0.04, Figure 3.17C). Metformin treatment of obese dams reduced serum sFlt with levels being no longer different compared to control dams (Control vs. Metformin-treated obese p=0.7).

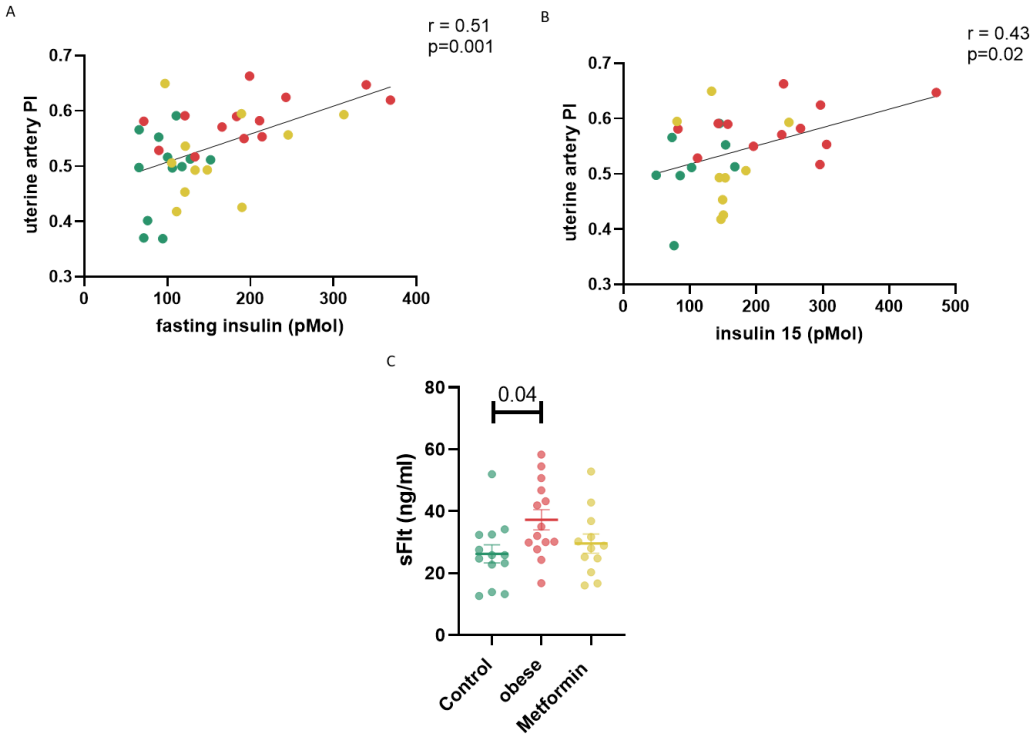

Figure 3.17: Uterine artery compliance correlates with insulin levels

(A) Correlation of the uterine artery PI with insulin at fasting and (B) with insulin at 15 minutes after glucose injection are shown. Linear regression and Pearson correlation coefficient r are shown. (C) Serum sFlt levels were measured at E18.5, n=13 for control, n=14 for obese and n=13 for metformin dams and One-Way-ANOVA followed by Tukey's multiple comparison test and mean ± SEM are shown.

3.4 Discussion

The global initial aim of this chapter was to characterise the maternal phenotype of our diet-induced maternal obesity model in detail, looking at body composition outcomes, metabolic health and adaptation to pregnancy. This showed that our model mirrors the human situation of obese and glucose-intolerant pregnancies, making it a suitable model to assess the effect of a metformin intervention in an obese pregnancy as a second aim.

3.4.1 Body composition and food intake

We have previously shown in our model that feeding mice a diet high in fat and sugar diet prior to and throughout pregnancy leads to hyperphagia, increased body weight and fat mass[257,261,262]. The data in this chapter confirms the robustness of our model, leading to increased bodyweight and fat mass at the end of pregnancy in obese dams compared to dams fed the control diet. Due to the feeding of the diet on average 4-5 months prior to mating and a first pregnancy obese dams, although age matched to controls, start the experimental pregnancy with an average bodyweight of 36.8 g and 47% body fat compared to 24.5 g and 21% body fat in the controls.

Compared to other mouse models of maternal obesity this obesity phenotype is clinically obese when compared to human obesity where body fat percentage above 40% is classed as obese[386]. Many other models show a subtle bodyweight difference at the beginning of pregnancy of 2 – 8 g between the obese and control animals which is closer to a model for an overweight phenotype[185,226,387–389]. All these models are equally clinically relevant with the numbers of overweight, obese and severely obese women entering pregnancy increasing worldwide as highlighted in section 1.7.1 of the general introduction. It also needs to be noted that our model uses a high fat diet combined with high sugar content via the condensed milk, mimicking the so-called western diet rather than simply a high fat diet.

Studies using metformin in human GDM pregnancies have shown a reduction in GWG[390]. Therefore metformin has been trialled in obese human pregnancies in recent years, where it showed reduced GWG (4.6 kg in metformin-treated vs. 6.3 kg in untreated obese women)[342]. A recent study in T2D pregnant women also showed reduction of weight gain with metformin treatment[391]. We observed that fat mass at the end of pregnancy was reduced in the obese metformin-treated compared to the obese untreated dams. The daily weighings of the dams in the second additional cohort highlighted the weight reducing effect of metformin in pregnant and not-pregnant dams.

Our obese dams had on average double the intake of kcal per day compared to dams fed a control diet. Towards the end of pregnancy however average total food intake reduces gradually in the obese but not the control dams. Institute of Medicine (IOM) recommendations for human pregnancy highlight that kcal intake should increase from the first to the third trimester. Energy requirements are

not based on weight maintenance as for the non-pregnant population but on appropriate GWG. Due to the increased maternal body mass in pregnancy and fetal metabolic demand energy requirements increase by 390 kcal/day in the second and third trimester of human pregnancy[392]. A recent study highlighted that these guidelines are not suitable for obese women, in which lower kcal intake than their energy expenditure needs to be achieved in order to avoid excessive GWG[393].

Metformin treatment reduced total kcal intake in the first week of treatment prior to pregnancy and during the first week of pregnancy. A reduced food intake was postulated by Coll et al. as a possible mechanism of metformin's action via GDF-15 to reduced body weight[377]. We demonstrated increased GDF-15 levels in the metformin-treated obese dams. Interestingly GDF-15 levels were very high overall amongst all groups and higher than expected from metformin-treated non-pregnant animals with current publications reporting a range of 200-300 pg/ml[377,394]. Even though pregnancy increases GDF-15 serum levels independent of metformin treatment we did see levels even above 2000 pg/ml. Interestingly a correlation with length of anaesthesia and thereby length of exposure to isoflurane could be observed. Other researchers of the Institute of Metabolic Science have recently also come across this phenomenon in their non-pregnant mouse models (personal communication), this could be of clinical interest given the notion that GDF-15 is a nutritional stress marker.

In our study the food intake reduction was primarily related to reduced milk intake. As the reduction of milk intake upon metformin dosing is evident in both pregnant and non-pregnant animals it is not possible to exclude the possibility that the addition of metformin to the milk reduces its palatability rather than the metformin directly reducing hunger/increasing satiety. Based on the current data we also can't exclude that metformin might lead to a change in food preference, leading the animals to avoiding the sugar-dense condensed milk and preferring the high fat diet. Total kcal intake was significantly reduced with metformin prior to pregnancy and in early but not in late pregnancy, in late pregnancy metformin treatment even seemed to slightly increase total kcal intake. This might be different in non-pregnant animals, where metformin treatment consistently shows a trend for a reduced total kcal intake. Therefore, metformin might regulate food intake differently in the pregnant compared to the non-pregnant state. Little data exist regarding food intake in pregnancy in rodents, early reports from 2001 highlighted that food intake in the rat slightly decreases in early pregnancy but then increases with advancing gestation, this could explain different effects of metformin in early and late gestation in our study[395]. In humans food intake is thought to increase by 10-15% in pregnancy[395]. Food intake in metformin-treated pregnancies in humans has not been assessed but could be an interesting additional parameter to investigate aiming to understand metformin's effects in pregnancy further.

3.4.2 Metformin treatment

Metformin intake was estimated and adapted based on the milk intake to achieve a metformin dose of 200 – 300 mg/kg/day for each animal. This dose was chosen based on previous papers and mirrors the dose given in humans as it equates to 1700 mg of metformin in a 70kg man based on the allometric body surface method[396,397]. A recent meta-analysis from our lab highlighted that metformin doses for women with GDM show a wide range from 500 to 3000 mg per day[341]. The chosen dose in our mouse models therefore lies in the middle of this range. The reduction of metformin intake in mg/kg/day with advancing gestation due to reduced milk intake towards the end of pregnancy can be translated into the human situation where women are not given an increased dose of metformin adjusted for their increased weight at the end of pregnancy leading to a reduced metformin intake in mg/kg/day towards the end of gestation as well.

We confirmed metformin concentration in the maternal circulation to be within the clinically observed range. Our data shows a range of 0.10 to 5.9 nmol/ml. Pharmacokinetic analysis of metformin (500 mg) in GDM vs T2D patients showed a peak of metformin concentration at around 2 hours after drug administration at 7.7 nmol/ml in the pregnant GDM women. Around 12 hours after administration serum concentrations were on average at 2 nmol/ml. Thereby our measurements lie within the ranges observed in GDM women. A wide range of metformin serum concentrations is found in clinical studies due to the time of measurement after drug administration[398]. Similarly in our study the high range of metformin concentrations in the different dams is likely to be due to different times the dams last took in metformin via the milk. Overall, the metformin dosing in our model mirrors the human situation of metformin treatment in obese and/or glucose-intolerant pregnancies.

3.4.3 Metabolic health

Previous data from our model has highlighted that the obese dams show glucose intolerance and are hyperinsulinemic[229]. This glucose intolerance is only present during pregnancy and not present at the time of weaning[399], making our model a good model of an obese GDM pregnancy. Impaired glucose tolerance was shown in the obese dams in this chapter. Additionally, increased hepatic lipid content was observed in the obese dams. Previous data highlighted increased lipogenic proteins especially in the liver in the obese dams from our model[230]. The study showed a correlation between plasma insulin and the liver fat content suggesting that hyperinsulinemia and glucose intolerance stimulate fat accumulation in the liver, which has been shown previously in non-pregnant animals fed a sucrose-rich diet[400]. Altogether this data highlights major metabolic dysfunction in our obese dams.

Metformin treatment improved metabolism in the obese dams. The GTT AUC and insulin levels were not fully rescued but improved with metformin treatment of the obese dams. Other mouse studies using metformin in T2D or HFD models have shown an improvement in glucose tolerance and reduction in insulin and glucose levels during pregnancy[362,401,402]. In human GDM pregnancies

metformin treatment can be equally efficient in glycaemic control as glyburide and insulin though metformin is unable to control glycaemia in some women[390]. Additionally, GDM incidence in obese and PCOS pregnancies treated with metformin has been shown not to be reduced[330,403].

A careful look at the insulin levels in the dams shows that metformin didn't lower insulin levels in all dams. Repeatedly human studies have reported a high failure rate of 30 – 50% with metformin interventions in pregnancy requiring supplementation of insulin to lower blood glucose [340,390]. Thus some authors urge for a more individualistic approach and that metformin might be only useful in a subset of women[288].

3.4.4 Haemodynamics

Heart rate was consistently increased in the obese untreated and metformin-treated dams before and during pregnancy. Higher rates of tachycardia during pregnancy have been observed in women with a higher BMI. Obesity-associated hyperinsulinemia can stimulate the sympathetic nervous system, leading to a higher heart rate[404]. The authors of a meta-analysis looking at the correlation between heart rate and BMI hypothesized that this imbalance of the sympathetic nervous system can lead to a less adaptive haemodynamic system in obese mums[404]. Thereby these women are less able to cope with the adaptations needed in a healthy pregnancy, such as further heart rate and cardiac output increase.

In the current study obese dams receiving metformin treatment present a slightly lower heart rate than the obese untreated dams at all measurement timepoints, however this effect is not significant. No major differences were detected in blood pressure either due to treatment group or due to pregnancy. A detailed analysis of blood pressure during mouse pregnancy via telemetry implants identified a pattern of 5 phases showing mean arterial pressure (MAP=1/3 systolic blood pressure + 2/3 diastolic blood pressure) decreases from gestation day E5.5 onwards to a nadir at E9.5[110,111]. At that timepoint the final murine placenta is built and the MAP increases to baseline level again[111]. Based on this it would be expected to not see an effect of time on the blood pressure in our analysis as the timepoints were when the MAP change is expected to be only very minor. Assessment of maternal blood pressure at the nadir point around E9.5 and comparing the difference across groups would be of interest. However, one also needs to take into account the high variability of restrained non-invasive blood pressure measurement. The data from the detailed blood pressure analysis mentioned above detected small changes (in mice only 5 mmHg from baseline to nadir), but this was performed via telemetry. Here mice are not stressed due to the handling in the restrainer cuff but have an implanted blood pressure measuring probe which measures blood pressure continuously. We minimised handling stress and variability via training the animals two times before the actual measurement, handling them frequently during the whole study time and taking many measurements at a time. However small differences are still unlikely to be detectable by this method. In our study SBP and heart rate were

lower in the evening, which is the onset of the active phase of the mouse. Circadian analyses show that heart rate and SBP are increased in the dark and active phase and thereby many highlight a slight increase in these parameters in the evening preparing for the onset of the active phase[405,406]. However other studies also highlight a slight increase in heart rate and SBP just before the onset of the light phase in the morning and the increase in heart rate and SBP only shortly after the onset of the dark phase[407]. Thereby our data presented in this chapter might have mainly picked these two timepoints in the circadian pattern of heart rate and SBP in the mouse. It can also be hypothesized that the mouse is less stressed in the evening measurements as the mouse already had a measurement performed in the morning of the same day.

The current study showed that maternal obesity leads to an impaired uterine artery compliance. In both mice and humans the uterine artery PI and RI are reduced with advancing gestation. This resistance drop is significantly smaller in overweight women as shown by a recent prospective cohort study from our lab[408]. Human studies highlight in general that overweight women have a high risk for an abnormal uterine artery PI[409,410]. Equally women with GDM present impaired endothelium-dependent vasorelaxation and endothelial dysfunction[411–413]. Other mouse models of diabetes during pregnancy (a streptozotocin-induced and $Lepr^{db/+}$ GDM), showed impaired vasorelaxation and increased uterine PI in the dams [237,414]. Impaired uterine artery compliance is likely a key contributor to pregnancy complications such as fetal growth restriction and stillbirth[415].

It is encouraging that metformin reduced the uterine artery PI back to control levels in the current study. Many human studies investigated the effect of metformin on uterine vascular function in women with PCOS. As PCOS is characterised by high spontaneous abortion rate, sufficient uterine artery adaptations are investigated as a potential reason for the increase of successful pregnancies with metformin treatment. Metformin-treated PCOS women presented a larger decrease in the uterine artery PI between 12 and 19 weeks gestation and in general a reduced uterine artery PI at 20 weeks of gestation[416,417]. However, the PregMet PCOS studies did not find a difference in uterine PI upon metformin treatment, but they did observe a significant positive correlation between serum glucose and uterine artery PI[418]. In our model uterine artery PI correlated with insulin levels in the dams. One of the first PCOS studies by Jakubowicz et al. showed that insulin reduction induced by metformin treatment leads to an enhanced uterine vascularisation[419]. Insulin not only leads to sympathetic nervous system activation as outlined above but increases nitric oxide (NO) production leading to vasorelaxation and thereby vasodilation[420]. In insulin-resistant subjects this insulin-mediated vasodilation is impaired. Nitric oxide is synthesized by NO synthase (NOS), which is present in the endothelium of uterine arteries (endothelial NOS, eNOS). An increase of eNOS across gestation is observed in mice and humans[421,422]. ENOS knock-out studies in pregnant mice have shown that the

knock-out leads to reduced uterine artery blood flow[423]. It is therefore likely that the hyperinsulinemia in our obese dams and the reduction of insulin with metformin is a key contributor to the observed effects on uterine artery compliance.

There is also promising evidence that metformin prevents preeclampsia based on studies in GDM or obese pregnancies and reduced sFlt secretion from human placental explants[342,424,425]. As outlined in the introduction poor cardiovascular health and increased uterine artery resistance (e.g. due to impaired spiral artery remodelling) can lead to preeclampsia. It is thereby important that metformin improved haemodynamics and lowered sFlt serum levels in the dams in our obesity model.

3.4.5 Conclusion

The data presented in this chapter demonstrates that our model mirrors the physiological and metabolic status of human pregnancies complicated by obesity and/or GDM. Feeding a diet high in sugar and fat not only lead to increased bodyweight, but impaired glucose tolerance in pregnancy and induced hyperinsulinemia, liver steatosis, increased heart rate and impaired uterine artery compliance. Thereby our model is a good tool to investigate interventions such as metformin commonly used in human GDM-complicated pregnancies. Metformin treatment of the obese dams improved basic metabolic health such as reducing fat mass, improving glucose tolerance and insulin levels and also led to beneficial haemodynamic changes. Heart rate was lowered with metformin and uterine artery compliance significantly improved. This shows that metformin is not only benefical in GDM treatment but can improve other pregnancy outcomes such as reduce the rate of preeclampsia. Additionally, the reduction in GWG likely leads to a healthier weight after the pregnancy which can be beneficial for subsequent pregnancies as it might thereby also reduce weight gain between pregnancies. Interpregnancy weight gain has been associated with adverse fetal outcomes such as a low APGAR score and increased obesity in the offspring[426,427]. However, as pregnancy involves two individuals, mother and child, the effect of metformin on the fetus and the placenta will be assessed carefully in the next chapter.

Key findings

- Dams on an obesogenic diet are glucose-intolerant, have increased insulin levels and an increased fat mass and present liver steatosis. Metformin treatment can improve all these parameters in the obese dams.
- Metformin was administered in the diet and reached clinically relevant concentrations in the maternal circulation.
- Increased heart rate was observed in the obese dams prior to and during pregnancy which was non-significantly reduced with metformin treatment at all timepoints.

- Uterine artery function is impaired in the obese dams along with increased levels of serum sFlt, mimicking a preeclampsia-like phenotype. Metformin improved uterine artery function and reduced sFlt levels.

4 The impact of metformin exposure *in utero* on the fetus and its placenta during obese pregnancy

4.1 Introduction

4.1.1 The placenta

In both human and mouse pregnancies the placenta is vital for a successful pregnancy. As outlined in section 1.8.4 many environmental cues have been found to influence placental structure and function. However, despite its vital role many processes underlying placental development, how it communicates with fetus and mother and how it responds to the *in utero* environment are still poorly understood. The National Institutes of Health described the placenta as the least understood organ and thereby launched the Human Placenta Project[428,429]. This is particularly relevant in the context of the topic of this thesis as it is now recognise that the placenta is not only crucial for healthy fetal development but for the long-term health of mother and offspring. Therefore, more research in this area is more important than ever.

The general architecture of the whole placenta is different in humans and in the mouse as highlighted in section 1.8.2. In the human placenta villi branch out into the so-called intervillous space which is filled with maternal blood. The terminal branches of the villi then harbour fetal capillaries where the exchange between maternal and fetal circulation can occur. Cytotrophoblast and syncytiotrophoblast, exerting the endocrine functions of the placenta, coat the villi. The murine placenta is ordered in different layers with the labyrinthine layer facilitating exchange between the maternal and fetal circulation. Here fetal capillaries branch out and build a highly branched network of fetal capillaries that are in contact with isolated maternal blood sinuses rather than bathed in maternal blood as in the intervillous space in the human placenta. Next to this is the so-called junctional zone with glycogen cells and spongiotrophoblasts that exert the endocrine function of the murine placenta. Both species have the chorionic layer on the fetal side of the placenta and the attachment side of the placenta on the uterine side is called the decidua, where drastic tissue remodelling takes places to enable fetal-maternal nutrient transfer.

The human and murine placenta are often compared as the mouse is a key model organism in many research fields. Schmidt et al. highlighted in their review some features that are not comparable between the murine and the human placenta[430]. This includes the observation that, in primates chromosome 19 harbours a placental specific miRNA cluster (C19MC cluster), which is not present in the murine placenta. Equally the secretion of the hormone human chorionic gonadotropin is unique to the human placenta. The invasion degree into the uterus is more shallow in the mouse placenta and mice do not usually develop the common human complication preeclampsia. It should also be noted that in the first half of pregnancy mice have an initial primitive placenta, the inverted yolk sac placenta,

which is established around day 8[211]. This placenta is a choriovitelline placenta built by the fusion of the yolk sac and the chorion. This first placenta nurtures the developing embryo by supplying it directly with secretions from the uterine glands, so called histio-trophic nutrition. Around day 11 to 12.5 the final chorioallantoic placenta replaces the initial primitive placenta. In the human such an initial placenta does not exist, however, as in the mouse, in the first trimester the exchange between maternal and fetal blood is not yet established. Up to week 12 no significant maternal blood flow through the placenta can be observed. Thereby the main nutrients are also supplied by histio-trophic nutrition, which consist of endometrial secretions, also termed uterine milk[431]. The yolk sac in humans is not attached to the chorion, but is also important for nurturing the embryo in the first weeks of gestation including providing hematopoiesis[432]. It is later, around week 8, incorporated into the gut of the embryo. As the yolk sac placenta in mice and the yolk sac in the human provide the initial hematopoiesis they are crucial for embryonic development and the later establishment of the vascularisation of the definitive placenta[433]. Once the final circulations within the placenta are established in the murine and human placenta the circulation and exchange mechanisms are very similar between the two species[206,208].

4.1.2 Metformin

A recent meta-analysis from our lab analysed the outcome of human GDM-pregnancies treated with metformin compared to treatment with insulin and showed that babies born to metformin-treated mothers are smaller at birth and present postnatal catch-up growth with a higher BMI in childhood compared to those from insulin-treated mums[341]. This is consistent with the follow-up studies in PCOS pregnancies (PedMet)[333]. The same was observed in the recent MiTy (Metformin in women with type 2 diabetes in pregnancy) study in women with T2D that had metformin or placebo added to their insulin treatment regimen[391]. Women having additional metformin added had better glycaemic control, needed less insulin and had lower weight gain but delivered more SGA babies and babies of lower birth weight than the placebo group. While many women are now given metformin to treat PCOS or GDM long-term effects on mothers and their babies are still unknown. Although more and more follow-up data suggest that metformin-exposed babies are smaller and show higher adiposity and/or BMI in childhood, underlying mechanisms are poorly understood. There is also a surprising lack of data regarding effects on fetal growth. This is particularly relevant as one major difference between the long used insulin and metformin is that metformin can cross the placenta readily shown in *in vitro* studies and hence detected in the fetal circulation in human and mouse studies[340,362,398,434,435]. It reaches concentrations in the fetus that are similar to those in the maternal circulation or even higher. As described in chapter 3 metformin inhibits the key growth signalling mediator mTOR. One can thereby hypothesize that it could impact fetal growth. Furthermore metformin activates AMPK , which is known to regulate histone deacetylases thereby potentially having epigenetic effects[436]. Metformin

can lead to Vitamin B12 deficiency leading to reduced nucleotide availability via the folate trap[437]. Additionally, metformin has been shown to induce apoptosis in cancer studies [438,439]. However little is known about these possible direct effects of metformin on the fetus[318,440].

Starting in 1994 metformin's safety in pregnancy was assessed in mouse models. Teratology analyses highlighted no major defects in fetal development[306]. In the following years mouse models of PCOS were used to assess metformin effects. Studies highlighted improved blastocyst health and reduced embryonic resorption[326]. From 2014 onwards more and more studies assessed the use of metformin in mouse models of maternal obesity and/or GDM in line with the expansion of its use clinically. Here improvements such as increased placental vascularisation and placental mitochondrial biogenesis were found along with reduction of embryopathies induced by diabetes[348,441,442].

In relation to fetal growth, different findings have been reported with metformin some increasing[441] and some decreasing[443,444] body weight compared to controls at the end of the murine gestation[362]. In an obese mouse model, offspring from obese metformin-exposed dams showed improved metabolic health with increased adipose tissue browning[362]. Interestingly the same group, when giving metformin to lean dams during pregnancy showed impaired glucose tolerance and increased body weight in the offspring compared to those from lean untreated dams, when offspring were fed a HFD[396]. A summary of the studies assessing metformin use in murine pregnancy can be found in Figure 4.2, showing the controversy between some outcomes and highlighting that further information is needed regarding the exact effects on the fetus and placenta under different metabolic conditions.

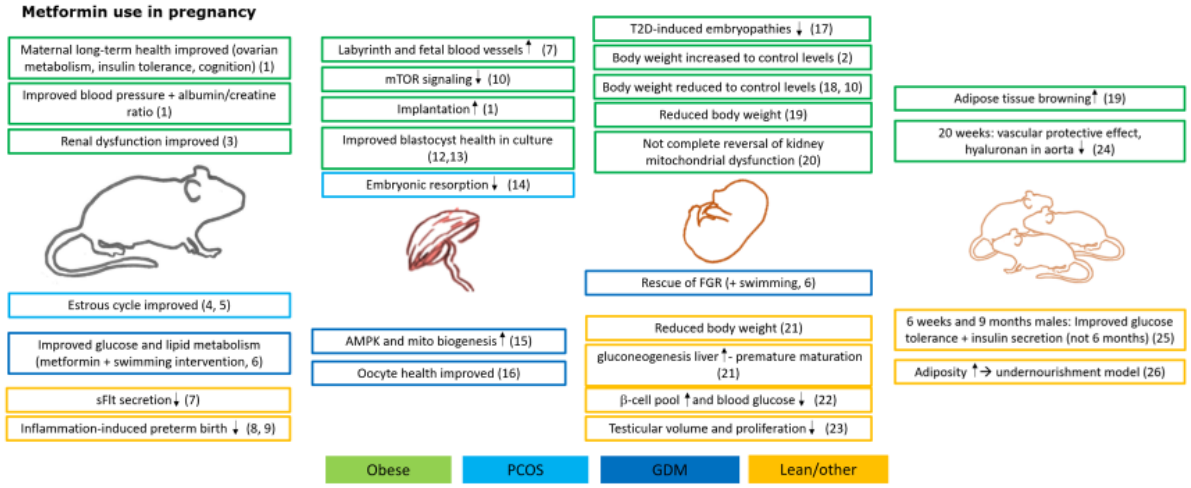

Figure 4.1: Observations in pregnancy mouse models with metformin treatment

Main outcomes observed in dams, placentas, fetuses and offspring are summarized. References can be found in the supplement (supplement 5, page 220). Colours of boxes indicate the animal model used as indicated in the Figure.

4.1.3 Aims

The aims of this chapter were therefore:

- To assess fetal and placental physiology and growth in our model of maternal obesity and to establish how it is affected by maternal metformin administration. This was achieved by fetal biometry, fetal ultrasound and analysis of placental structure.
- To measure uptake of metformin into the placenta, the fetal circulation and tissues. This was achieved by metformin measurements via LC-MS and assessment of metformin transporter expression in the placenta and fetal tissues.

4.2 Methods

4.2.1 Fetal ultrasound

After the Doppler analysis of the uterine artery at E18.5 (as described under 3.2.5) fetal ultrasound was performed. The probe was moved across the fetuses and for those that were accessible fetal measurements were taken. To minimise the anaesthesia time but still get sufficient data 2-3 fetuses per dam were scanned. The umbilical artery was scanned in a free loop of the umbilical cord rather than at the insertion point into the placenta or the egression point at the fetal naval for consistency[445]. Figure 4.3A shows the paw and placenta of the fetus with the umbilical artery and vein intertwined. The typical waveform of the umbilical artery can then be seen (Figure 4.3C). For the MCA measurement the fetus and the adjustment of the probe needed to allow a transversal view on the top of the fetal head. In that way the MCA can be measured at the level of the circle of Willis (Figure 4.3B) to obtain the typical MCA reading (Figure 4.3.D)[446]. The fetuses that were scanned were marked on the shaven belly of the dam so that upon opening of the dam the fetuses could be identified and sexed.

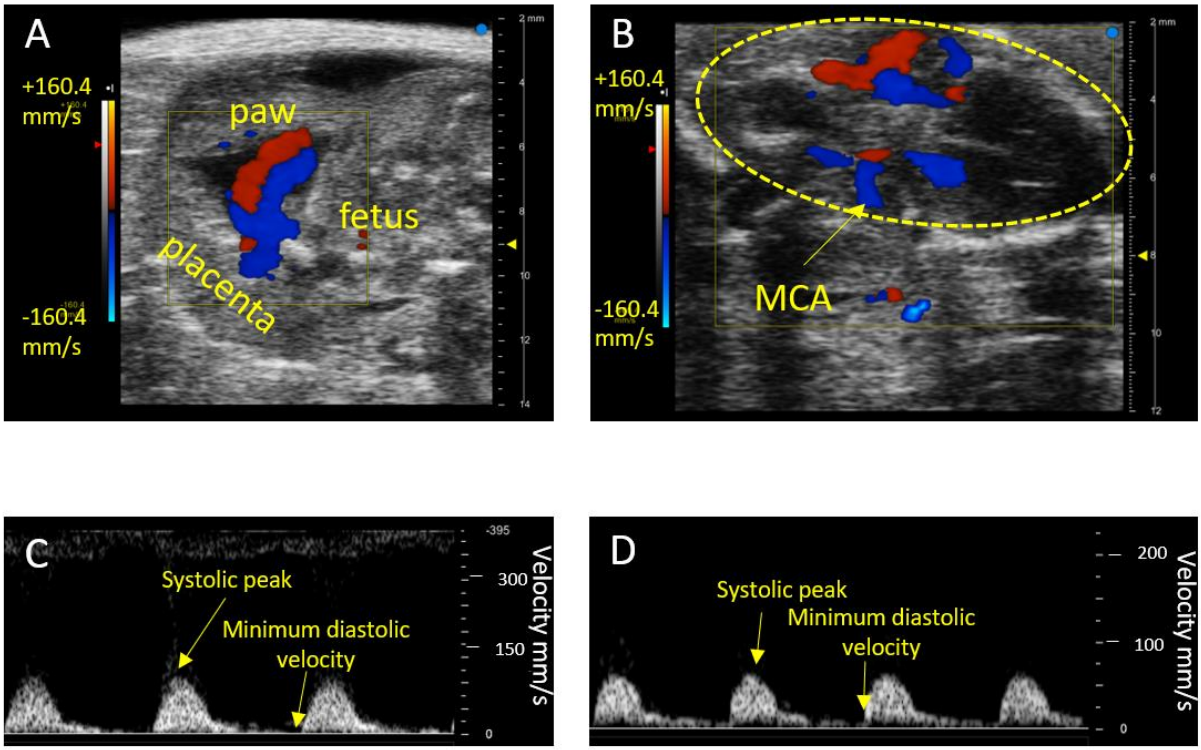

Figure 4.2: Performance of fetal ultrasound

(A) Fetal umbilical cord and (B) the MCA are identified to obtain waveforms for the (C) umbilical and (D) MCA. Systolic peak and minimum diastolic velocity can be measured to calculate the pulsatility index.

4.2.2 Fetal dissection

After killing of the dam (see section 3.2.1) the uterus with the fetuses was taken out and placed on ice. Before dissection of the fetus the amniotic sac was kept intact so that amniotic fluid could be aspirated

with a syringe. Afterwards the amniotic sac was removed and placenta and fetus dissected apart from each other and weighed individually. Fetal sex was determined via visual inspection of a black spot between the genital tubercle and the tail in males[447]. For those fetuses where further histological or molecular analysis was performed sex was validated molecularly as described in section 4.2.3. Via a caliper CRL, BPD, HL and ATD were measured. The head was removed to obtain fetal blood in capillary tubes (Hirschmann-Laborgeräte, Germany), which were later centrifuged to obtain plasma and the haematocrit determined using a haematocrit capillary tube reader. From one male and one female fetus the whole body and the placenta were fixed (separately) in formalin. From the other fetuses liver, brain, kidney and heart were dissected out and frozen. All frozen samples including fetal plasma were stored at -80°C. Half of the samples from the second smaller cohort looking at obese untreated and metformin treated dams only (see chapter 3) were collected at E13.5 to assess an earlier point in gestation.

4.2.3 Fetal molecular sexing

A small piece of fetal tissue was used for sexing via a method previously published[448]. Genomic DNA was isolated by incubation of the tissue with a Chelex mixture [5 % Chelex (Instagene Matrix-Biorad 732-6030), 0.1% Tween-20 and 0.1% Proteinase K] at 50°C for 1 hour. Subsequently the mixture was heated to 95°C for 15 minutes, Chelex resin was spun down briefly and the supernatant cooled to 4°C or frozen at -20°C for later use. The PCR reaction was performed with GO Taq G2 DNA polymerase (Promega) with the following primers for Sly (Y chromosome)/Xlr (X chromosome), that share multiple homologous regions: SX_F, 5'-GATGATTTGAGTGGAAATGTGAGGTA-3'; SX_R, 5'-CTTATGTTTATAGGCATGCACCATGTA-3'. Figure 4.4A and B shows the pipetting scheme of the reaction and the PCR reaction conditions, the concentration of genomic DNA (gDNA) was not measured at this stage but just 6 µl from the supernatant of the Chelex mixture used for the PCR. On the an agarose gel the male samples display a band at 280 bp, the female samples show 2-3 bands (480 bp, 660 bp, 685 bp) as shown in Figure 4.4C.

A

	1x
5x green GoTaq reaction buffer	2 µl
PCR nucleotide mix (10mM)	0.2 mM
Fwd + Rv primers (5x mix)	0.5 µM
GoTaq G2 DNA Polymerase	0.05 µl
gDNA	6 µl
Nuclease free water	1.25 µl
Total	**10 µl**

B

temp	time (min)	
95°C	2	
95°C	1	40 x
57°C	1	
72°C	1	
72°C	5	
4°C	∞	

C

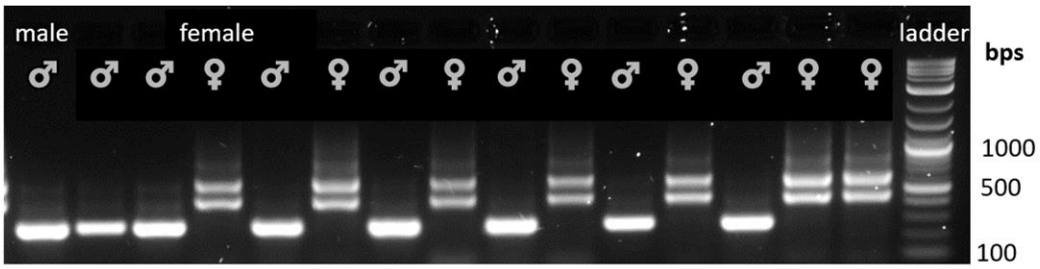

Figure 4.3: Sexing of the fetuses

(A) GoTaq DNA polymerase was used for the PCR reaction according to the pipetting scheme (gDNA amount was not measured and 6µl of extracted gDNA used for all samples) and (B) the reaction protocol. (C) Samples were run on a 2% agarose gel and the different fragments of the Sly (male) or Xlr (female) gene dependent on the sex of the samples become apparent.

4.2.4 Quantitative PCR

RNA was extracted from placentas, fetal liver and kidneys (n=3 per group and sex was used for all tissues) via the miRNeasy Micro kit (Qiagen) as described in the general methods. Carry-over genomic DNA was digested on a column using the Qiagen DNase kit. RNA concentration and the absorption ratio A260/280 to check for contamination of the samples were measure on the Nanodrop. All samples had A260/280 ratios above 2 and dilutions of 100 ng/ul were made and boiled at 65°C for 5 minutes to destroy secondary structures. Samples were run on an agarose gel to assess RNA integrity (Figure 4.5A). Samples that presented a strong smear (and therefore were degraded) were excluded and RNA extraction repeated. If the smear was as shown below (see arrows in Figure 4.5) these samples were monitored to check that they were not outliers in the following qPCRs. Integrity was further checked

by expression of the housekeeping gene and none of the smeared samples showed expression levels outside of the range of the other samples. 10 ng of the RNA dilution were used to perform reverse transcription with the Revert Aid First Strand cDNA synthesis kit (Thermo Scientific) according to the pipetting schedule and the reaction scheme outlined in Figure 4.5B and C.

QPCR was performed with Taqman assays for metformin transporters (Mm00457739, Mm00840361, Mm00525575, Mm00488294, Mm00456303, Mm02601013, Mm00472657, Mm00457295, Mm00441468, Mm00439391, Mm00436661, see Table 4.1). For the reaction (in total 7 µl) 1x Taqman master mix (Thermo Scientific, Cat #4304437) were mixed with 21 ng cDNA and 1.4 µl Taqman probe (1:4 dilution of the probe in water). QPCR was performed in duplicates on a QuantStudio 7 Flex Real-Time PCR system (384 wells) according to the cycling conditions shown in Figure 4.5D. For the analysis of all metformin transporter across different tissues raw CT values were used, but for the comparison of transporter expression between different gestational ages Sdha was used as a housekeeping gene. Sdha has been shown to be a good housekeeping gene in the placenta[449] and showed stable expression in our analysis. CT values for Sdha were subtracted from the CT values of the genes of interest (ΔCT). The mean of the male placenta, fetal kidney and liver respectively at E13.5 was used as a reference and subtracted from all DCT values ($\Delta\Delta$CT) and fold change expressed as $2^{-\Delta\Delta CT}$ analysed.

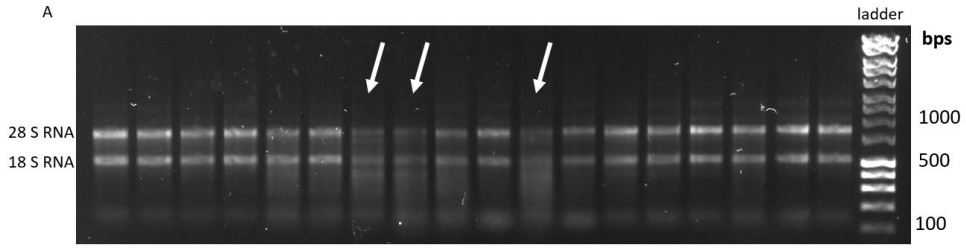

B

	1x (ul)
RT buffer	4
Ribolock	1
dNTP	2
RT	1
Random primer	1
water	1
Total	**10**

+ 10 µl of 100ng/µl RNA

C

temp	time
25°C	5 min
42°C	60 min
70°C	5 min

D

temp	time	
50°C	2 min	
95°C	10 min	
95°C	15 sec	40 x
60°C	1 min	

Figure 4.4: Quantitative PCR protocol

(A) RNA integrity was checked on an agarose gel, (B) then cDNA was obtained by reverse transcription according to the shown pipetting scheme and (C) reaction settings. (D) QPCR was performed according to the shown cycling conditions.

Gene symbol	Accession number	Assay ID	Amplicon length
Slc22a4	NM_019687.3	Mm00457739	73 bp
Slc47a1	NM_026183.5	Mm00840361	80 bp
Slc29a4	NM_146257.2	Mm00525575	82 bp
Slc22a3	NM_011395.2	Mm00488294	70 bp
Slc22a1	NM_009202.5	Mm00456303	69 bp
Slc47a2	NM_001033542.2	Mm02601013	64 bp
Slc19a3	NM_030556.2	Mm00472657	72 bp
Slc22a2	NM_013667.2	Mm00457295	85 bp
Slc22a5	NM_011396.3	Mm00441468	74 bp
Slc6a4	NM_010484.2	Mm00439391	72 bp
Slc6a2	NM_009209.3	Mm00436661	90 bp
Sdha (endogenous control)	NM_023281.1	Mm01352366	82 bp

Table 4.1: Taqman probes and their details

4.2.5 Placental histology

Placentas were immersion-fixed in formalin, processed and mid sections of 5 µm thickness were cut, which was performed by Thomas Ashmore. For immunohistochemistry staining, sections were deparaffinised with xylene (2 x 5 minutes) and rehydrated in ethanol (2 x 2 minutes) and water (3 minutes). Sections were then incubated at 60°C in water for 15 minutes after which antigen retrieval (Vector, H-3301, pH=9) was used for 20 minutes at 97°C. After blocking for 1 hour (animal-free blocking solution, Vector, SP-5030) the slides were incubated with the endothelial cell marker CD31 (Cluster of Differentiation 31) and the trophoblast cell marker Tpbpa (trophoblast-specific proteins α) antibodies (AF3628, R+D, 1:40 dilution and ab104401, abcam, 1:1000, in antibody diluent (Vector, SP-5035)) overnight at 4°C. Slides were washed with 0.5% Tween in TBS (T-TBS) five times. Secondary antibody was applied subsequently at room temperature for 1 hour each with three washes in T-TBS (first: NL557 (R+D) at 1:200, then Alexa 488 at 1:1000). After three washes in T-TBS and two washes in PBS the slides were incubated with DAPI (1:2500) for 10 minutes in the dark. Autofluorescence was then quenched with the Vector TrueVIEW autofluorescence kit (1:1:1 mix of the supplied reagents A, B and C, Vector, SP-4800) for 4 minutes in the dark. Slides were washed five times with PBS and mounted with Vectashield hard set anti-fade mounting medium (Vector, H-1400) and stored at 4°C. After imaging of the slides with the Zeiss Axioscan microscopy slide scanner, the HALO software (Indica labs) was used to delineate the placental layers (chorion, labyrinth, junctional zone and decidua) manually and calculate the percentages of the respective layers.

For the staining with the macrophage marker F4/80 sections were deparaffinised in xylene and rehydrated in ethanol and water as described above but then rinsed with wash buffer (Dako, S3006)

before incubation in antigen retrieval (Vector H-3300, pH=6) for 20 minutes at 97°C. The retrieval solution with the slides was then cooled at -20°C for 15 minutes. After rinsing in wash buffer (Dako, S3006) the slides were incubated with Bloxall peroxidase blocking solution for 10 minutes at room temperature (Vector, SP-6000). Slides were then washed in wash buffer (2 x 3 minutes) and subsequently blocked (animal-free blocking solution, Vector, SP-5030) for 30 minutes. The slides were then incubated with primary F4/80-antibody (MCA497, Bio-Rad, 1:20 dilution) at 4°C overnight. After washing the slides with wash buffer (2 x 3 minutes) the secondary antibody (A110-322A, Bethyl, 1:250 dilution) was added for a 1 hour incubation at room temperature. Slides were washed with wash buffer (2 x 3 minutes) and then incubated with the ImmPRESS horseradish peroxidase (HRP) labelled polymer for 30 minutes (Vector, MP-7451). After another set of washes with the wash buffer (3 x 5 minutes) ImmPACT DAB (Vector, SK-4105) was added for 5 minutes at room temperature. Slides were washed with wash buffer (2 x 3 minutes) and then counterstained with Hematoxylin QS for 10 seconds. Slides were then rinsed with water and wash buffer and dehydrated in ethanol (2 x 2 minutes) and immersed in xylene (2 x 2 minutes) to be mounted with synthetic mountant and slides scanned with the Zeiss Axioscan microscopy slide scanner.

Alizarin Red staining was performed to assess placental calcification. Sections were processed as described above. Slides were then dewaxed and placed in 100% ethanol (2 times for 5 minutes) and then 95% ethanol (for 5 minutes). Slides were left to air dry. Once dry, sections were incubated in Alizarin red solution for 5 minutes (1% aqueous solution pH=6.4, ammonium hydroxide). Slides were then rinsed with distilled water and counterstained with Fast Green (0.05% Fast Green solution in 0.2% acetic acid) for 15 seconds. After washing thoroughly with water the slides were dehydrated to be mounted in synthetic resin. Images were taken with the Zeiss Axioscan microscopy slide scanner and analysis was performed with the HALO software (Indica labs) that was taught to classify areas of the strong red Alizarin stain against the pale background as the stain of interest. Thereby the area of calcification as a percentage of the whole placenta can be calculated. Thanks to James Warner from the histology core of the Institute of Metabolic Science and Dr. Betania Mahler-Araujo (Histopathology Addenbrookes) for the help with the finding of calcium in the placenta.

The apoptosis stain was performed with a terminal deoxynucleotidyl transferase mediated dUTP nick end labelling (TUNEL) kit (Takara, MK500). The kit was used according to the manufacturer's instructions, the protocol for detection via light microscopy rather than fluorescence microscopy was used. In brief, slides were dehydrated and deparaffinised as in the instructions and 20 µg/ml Proteinase K added to the slide for 15 minutes at room temperature. Endogenous peroxidase was inactivated via 3% H_2O_2 addition for 5 minutes. After this the slides were washed in PBS and incubated with a reaction mix of 5 µl terminal deoxynucleotidy transferase (TdT) enzyme and 45 µl labelling buffer in a 37°C

humidified chamber for 90 minutes. The reaction was terminated by washing the slides with PBS (3 x 5 minutes). 70 µl of HRP conjugate were added subsequently for incubation at 37°C for 30 minutes. After washes in PBS (3 x 5 minutes) the slides were incubated with DAB for 15 minutes at room temperature. The reaction was terminated via rinsing under water and counterstain performed with Hematoxylin for 10 seconds, after which the slides were washed in water again. Then slides were dehydrated, penetrated, and mounted with synthetic mountant and slides scanned with the Zeiss Axioscan microscopy slide scanner.

4.2.6 Western blotting

Due to the limited size of the gel only eight samples could be run on a gel per group and sex, additionally male and female samples needed to be run on separate gels and therefore required separate analysis. Placentas were used picked from those litters where the average of the body weight of the male and female fetuses in the litter was in the average range for the respective group to not randomly bias or dilute effects of the molecular analysis by picking those litters where bodyweights were all on the lower or upper end of the weight range. Placental tissue was homogenized in lysis buffer [50 mM HEPES (pH 8), 150 mM sodium chloride, 1 mM sodium orthovanadate, 30 mM sodium fluoride, 10 mM sodium pyrophosphate, 10 mM EDTA, 1% Triton X-100, protease inhibitor cocktail III (Calbiochem Novabiochem biosciences, Nottingham, UK)]. After protein concentration determination via a BCA assay, 20 µg of protein, prepared in 1x Laemmli buffer [5x: 20% glycerol, 2% SDS, 62.5 mM Tris-HCl (pH 6.8), 100 mM DTT, some Bromophenol blue] and heated for 5 minutes at 95°C, were loaded onto the SDS-PAGE. Separate gels were used for male and female samples. For the SDS-PAGE the SE 600 Ruby Standard Dual Cooled Vertical Unit was used and gels prepared as specified in section 2.4 of the general methods. For blotting of the gel, the TE70XP Semi-Dry Transfer Unit was used. PDVF membrane was activated in 100% methanol (1 minute), then washed in water (1 minute) and transferred into transfer buffer [20% methanol and 1 x transfer buffer (National Diagnostics, B9-0056) in water]. For high molecular weight proteins like mTOR only 5% of methanol was used in the transfer buffer as methanol slows the transfer process. Three filter papers soaked in transfer buffer were laid onto the transfer unit, then the activated PDVF membrane was added and the gel carefully placed on top. After addition of three additional pre-soaked filter papers bubbles trapped in the stack were removed by rolling over the stack. Depending on the size of the protein of interest and the number and size of blots in the transfer unit the settings of the transfer were chosen. Usually for two gels (male and female) from the SE 600 Ruby Standard Dual Cooled Vertical Unit SDS-PAGE the transfer was performed at 400 mA for 1.30 – 1.45 hours.

The blots were prepared as described in section 2.5 of the general methods and probed for the following primary antibodies: anti-apoptotic protein Bcl-2 (B-cell lymphoma 2, Cell Signalling 3498), the pro-apoptotic protein Bax (Bcl-2 associated X protein, Cell Signalling, 2772), the inactivated form

of the protein kinase AMPK (adenosin monophosphate activated protein kinase) involved in energy homeostasis (Cell Signalling, 2532), the activated phosphorylated form of the protein kinase called pAMPK (Cell Signalling, 2535), the inactivated form of the protein kinase mTOR (mammalian target of rapamycin) involved in cell growth and proliferation (Cell Signalling, 2972) and the activated phosphorylated form of the protein kinase called mTOR (Cell Signalling, 2971). All antibodies were diluted at 1:1000 in 1% BSA in 1x T-TBS and the blots incubated in primary antibody solution at 4°C overnight. After washing blots were incubated with the following secondary HRP-conjugated antibodies: Goat Anti-Rabbit IgG HRP (abcam, ab6721) and Rabbit Anti-Mouse IgG HRP (abcam, ab6728) and blots imaged on the Bio-Rad ChemiDoc Imager as described in section2.5 of the general methods. After detection blots were stained with Coomassie overnight as stated in section 2.5 of the general methods, which was used for normalisation in the subsequent analysis performed on ImageLab[365].

4.2.7 Statistics - Fetal data analysis

Fetal data is complex as it includes information from all fetuses from one litter with 3 different experimental groups and two sexes. As shown with the example of the fetal body weight a Two-Way-ANOVA assessing sex and the group can be used (Figure 4.5A). Here the mean of female and male fetuses respectively per litter is used for the analysis. However as shown in Figure 4.5B this analysis could miss sex effects as the litter (the maternal ID) is not taken into account. Linear model analyses can be used to reveal an effect of the litter ID. Thereby a linear model was used to account for the litter as a random effect. This identified significant sex effects previously not picked up in the ANOVA analysis (Figure 4.5C). Therefore, where possible fetal data was analysed with a linear model (lme4 package in R). This was not possible for datasets with missing data (which was the case for umbilical artery and MCA analysis) so for these a Two-Way-ANOVA was used.

A

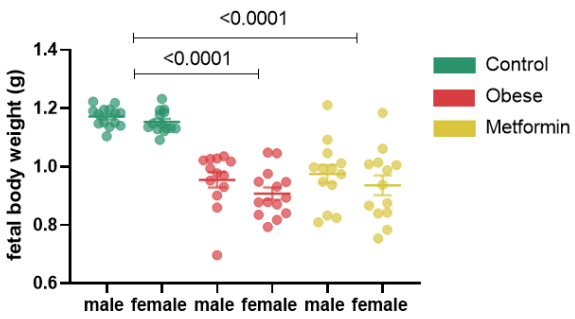

B

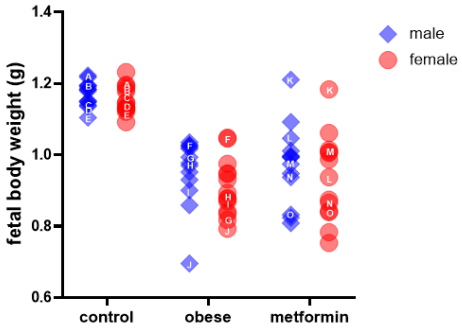

C

	ANOVA		Lmer model	
Measure	**P sex**	**P group**	**P sex**	**P group**
Bodyweight	0.0722	<0.0001	<0.0001	<0.0001
CRL	0.2747	<0.0001	0.0009	<0.0001
BPD	0.0287	<0.0001	0.003	<0.0001
HL	0.3779	<0.0001	0.148	<0.0001
ATD	0.9733	<0.0001	0.5415	<0.0001
Placental weight	<0.0001	0.0099	<0.0001	0.0415
BW/PL ratio	0.0246	<0.0001	<0.0001	<0.0001
Labyrinth %	0.7054	<0.0001	0.7137	<0.0001
Calcium %	0.8627	<0.0001	0.7959	<0.0001

Figure 4.5: Analysis of fetal data – ANOVA vs. linear mixed model

(A) Fetal body weight can be analysed by a Two-Way-ANOVA with the mean bodyweight per sex and group calculated and compared with each other, this does not consider the effect of the litter. (B) Or fetal body weight can be anaylsed by a linear mixed model that takes into account the litter as a random effect. This could bring out unseen sex effects as additional comparison between males and females within one litter (here mean bodyweight per sex and group plotted) can highlight a true sex effect, exemplarily a few litters are marked with letters A to O to highlight male and female measurements from the same mother. This visualises the lower bodyweight in females compared to males across groups that only comes apparent when taking the litter into account. (C) Comparison of the Two-Way-ANOVA and the linear mixed model is shown. Changes between the two analysis types regarding sex effects are highlighted in yellow.

4.3 Results

4.3.1 Fetal body weight and biometry

Body weight was significantly reduced in fetuses from obese untreated and obese metformin-treated dams (Figure 4.6 A). Biometrical measurements of fetal size including CRL, BPD, HL and ATD were similarly reduced in the obese group with no correction by metformin-treatment (Figure 4.6 B-F). In all groups the female fetuses were lighter than the male fetuses and had reduced BPD and CRL.

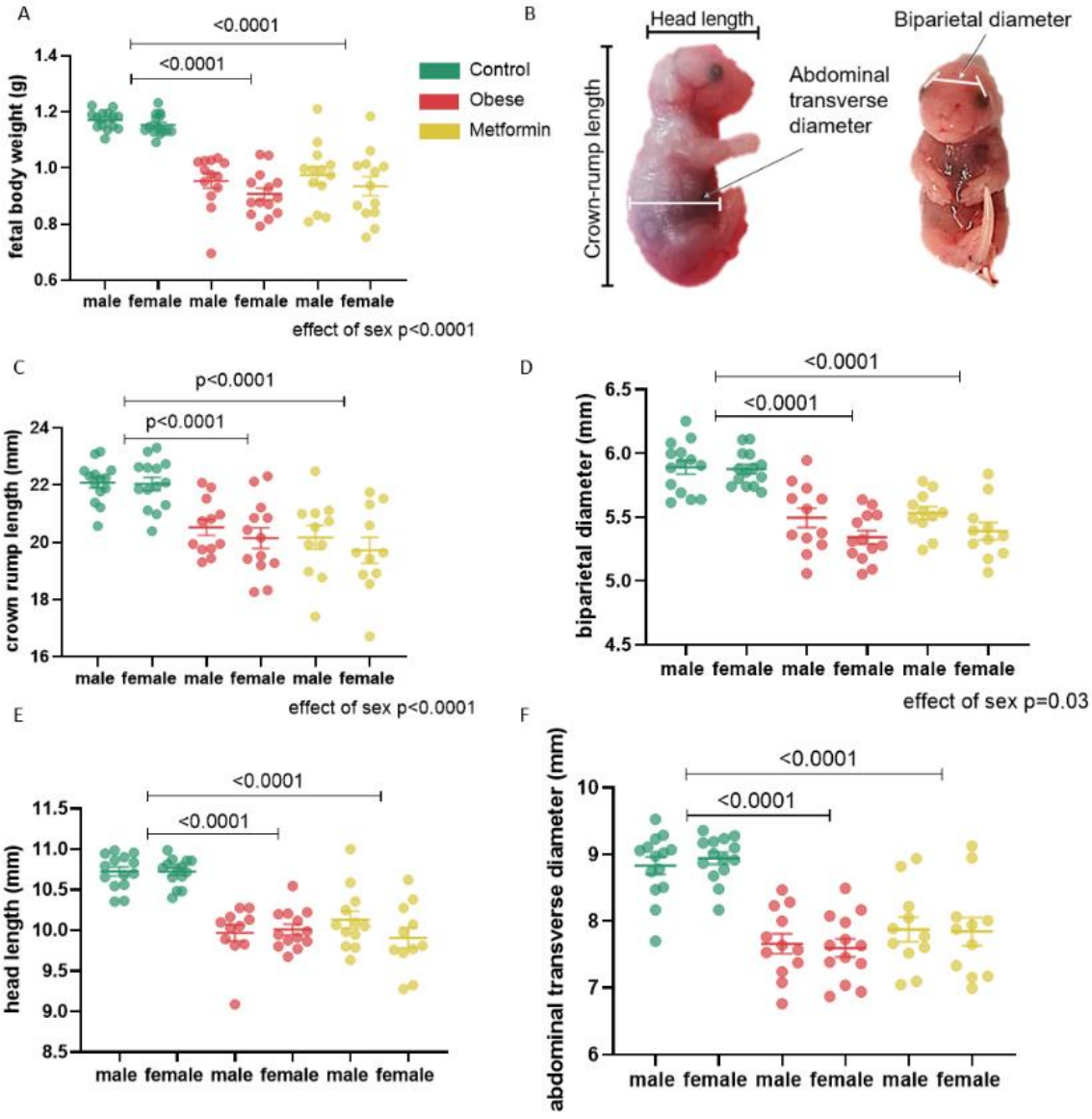

Figure 4.6: Fetal bodyweight is reduced in fetuses from obese untreated and obese metformin-treated dams

(A) Upon dissection fetal bodyweight (n = 14/14 dams for male/female control, n = 13/14 dams male/female obese and n = 13/13 dams for male/female metformin fetuses) and (B) fetal biometry was measured. (C) Measures of crown rump length, (D) biparietal diameter, (E) head length and (F) abdominal transverse diameter were taken. In fetal biometry measurements n= 14/14 dams for male/female control, n = 12/13 dams for male/female obese and n = 11/11 dams for male/female metformin fetuses was used. Linear mixed model analyses and mean ± SEM are shown.

Brain and liver weights of fetuses from obese and obese metformin-treated dams were significantly reduced compared to controls (Figure 4.8A and B). The ratio of brain to liver weight was increased significantly in fetuses from obese dams and showed a borderline significant increase (p=0.058) in fetuses from obese metformin-treated dams compared to control dams (Figure 4.8C). Haematocrit was reduced in fetuses from obese untreated and metformin-treated dams (Figure 4.8D).

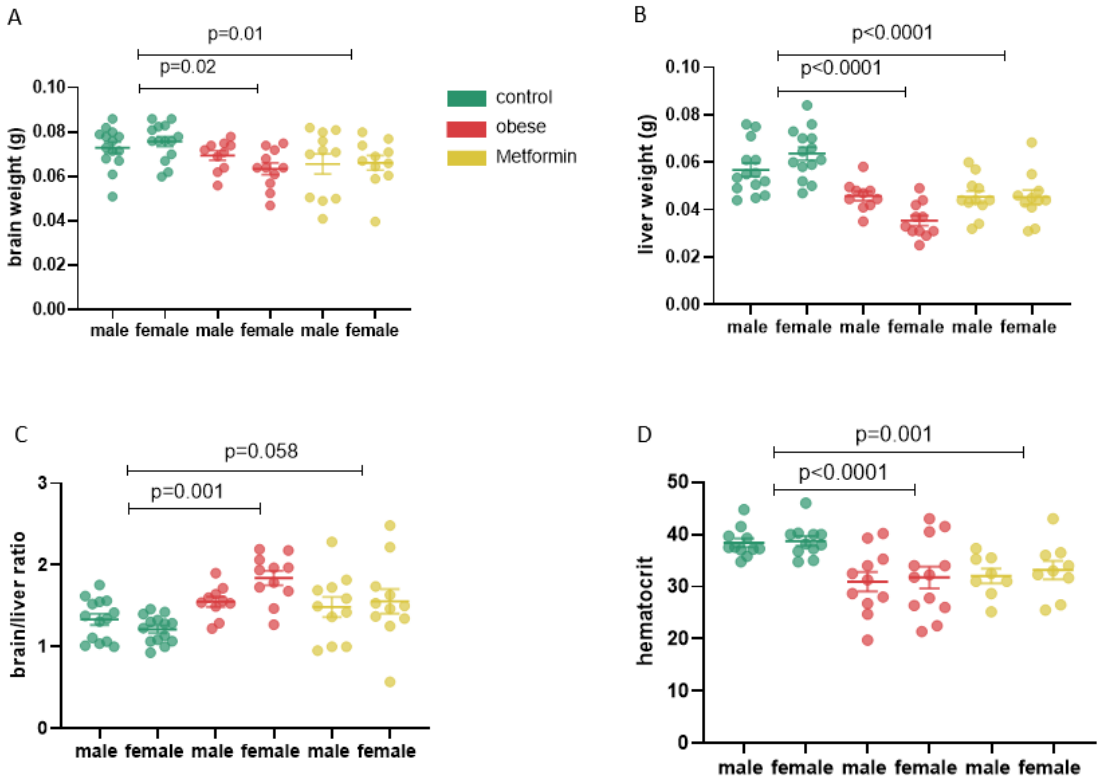

Figure 4.7: Fetuses from obese untreated and obese metformin-treated dams show reduced organ weights and hematocrit

(A) Fetal brains and (B) livers were weighed to calculate the (C) brain-to-liver-ratio. For A, B and C n = 14/14 dams for male/female control, n = 10/11 dams male/female obese and n = 11/11 dams for male/female metformin fetuses was used. (D) Additionally the haematocrit of the fetuses was measured in the blood samples (n = 11/11 dams for male/female control, n = 11/12 dams male/female obese and n = 8/9 dams for male/female metformin fetuses). Linear mixed model analyses and mean ± SEM are shown.

4.3.2 Fetal ultrasound

Pulsatility index (and resistance index, not shown) of the umbilical artery and the middle cerebral artery were not significantly different across groups or between sexes and neither was the cerebroplacental ratio (Figure 4.9A, B and C). Based on data for the uterine artery blood flow (see chapter 3) and the umbilical blood flow, the placental pulsatility index (PPI) was calculated (Figure

4.9D). The PPI was significantly increased in the obese untreated group compared to the controls. This increase was not observed in the obese metformin-treated group.

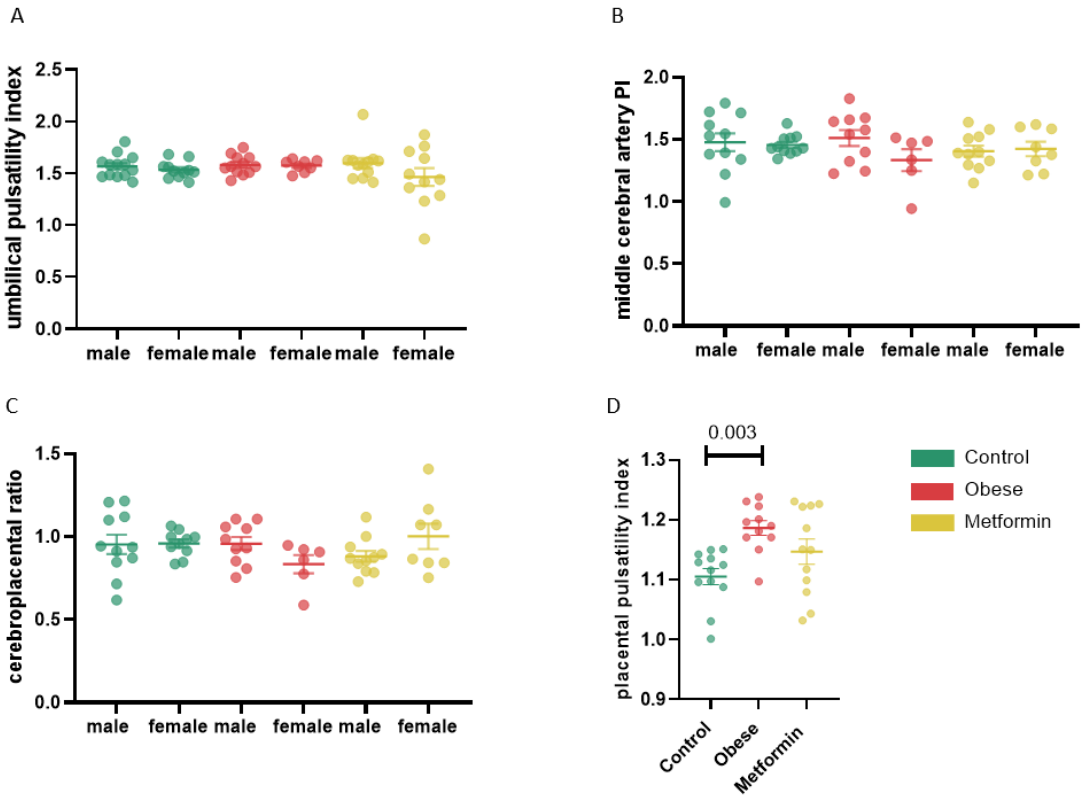

Figure 4.8: Fetal ultrasound did not show abnormalities in any of the groups

(A) Umbilical artery (n = 13/11 dams for male/female control, n = 12/8 dams male/female obese and n = 12/11 dams for male/female metformin fetuses) and (B) MCA pulsatility index (n = 11/11 dams for male/female control, n = 10/6 dams male/female obese and n = 11/8 dams for male/female metformin fetuses) were calculated and (C) the ratio of the two calculated in form of the cerebroplacental ratio. (n = 11/10 dams for male/female control, n = 10/6 dams male/female obese and n = 11/8 dams for male/female metformin fetuses) (D) With the umbilical artery and uterine artery pulsatility index the placental pulsatility index is calculated in all three groups and One-Way-ANOVA analysis shown (n = 12 for control, n = 11 for obese and n = 11 for metformin dams). Two-Way-ANOVA assessing effects of the experimental group and the fetal sex and mean ± SEM are shown for the fetal ultrasound data.

The umbilical artery pulsatility index correlated with the body weight in males (p=0.058) and more strongly in females (p<0.003) (Figure 4.10A and B). The raw uterine artery pulsatility index predicted fetal body weight (averaged per litter) less well in both males and female (Figure 4.10C and D) compared to the PPI which takes placental perfusion into account and showed a strong correlation especially in females (Figure 4.10E and F).

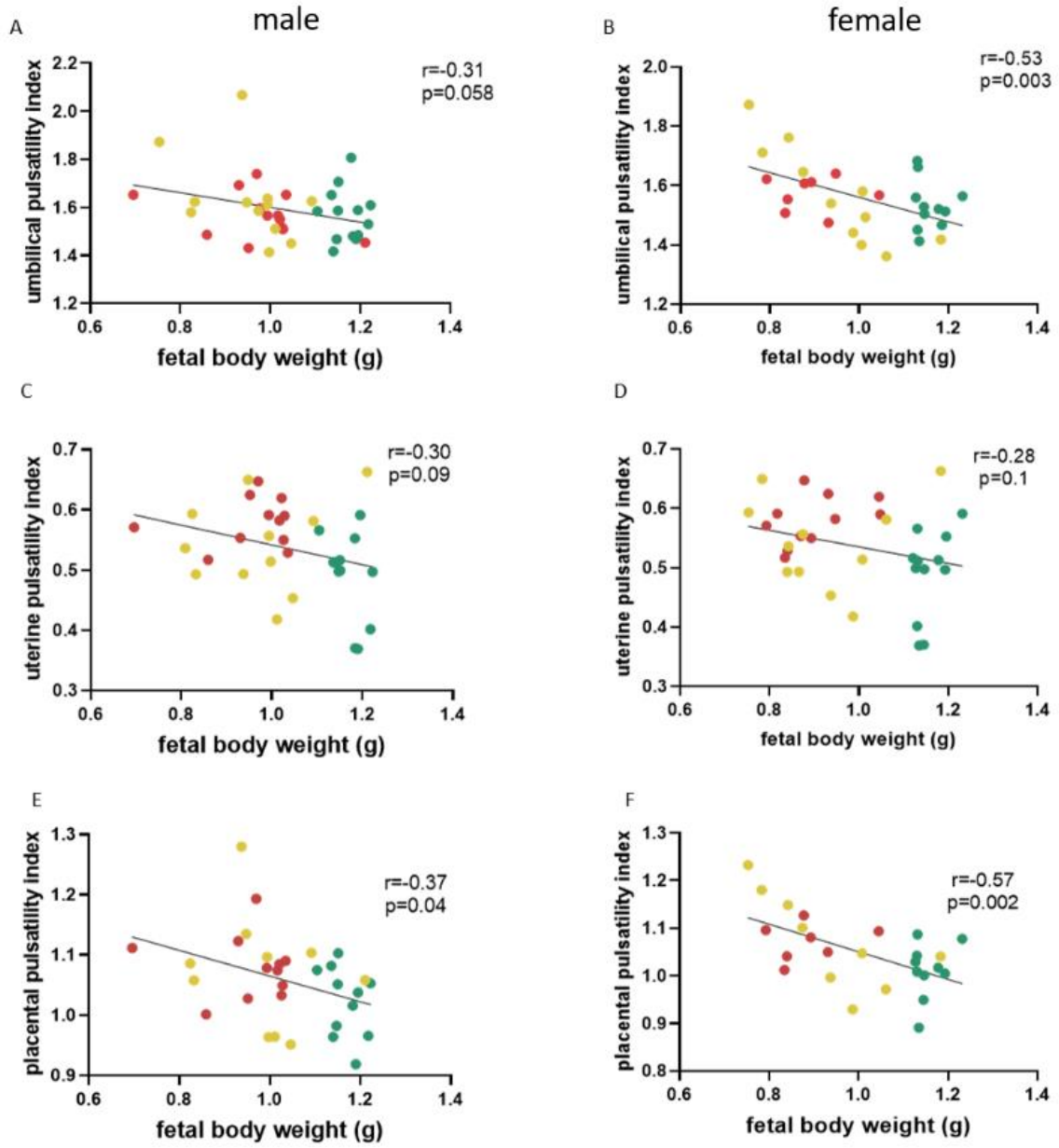

Figure 4.9: Ultrasound data can predict fetal bodyweight

(A*) Fetal body weight is correlated with the umbilical artery pulsatility index (A) in males and (B) females. The same correlation analysis is performed for the uterine artery (C) in males and (D) in females and the placental pulsatility index (E) in males and (F) in females, with the averaged litter body weight as the uterine artery is the same for the whole litter. Linear regression and Pearson correlation coefficient r are shown, green= fetuses from control dams, red=fetuses from obese dams, orange=fetuses from obese metformin-treated dams.*

4.3.3 Placental weight

Placentas from obese dams had an increased weight compared to the control dams but this increase was not observed in the metformin group (Figure 4.11A). Overall fetal sex had a significant effect on the placental weight with female placentas being lighter than their littermate male siblings. However, placental efficiency, calculated via the ratio of body weight to placental weight, was reduced in both

the obese untreated and obese metformin-treated group and overall increased in female fetuses compared to male fetuses (Figure 4.11B).

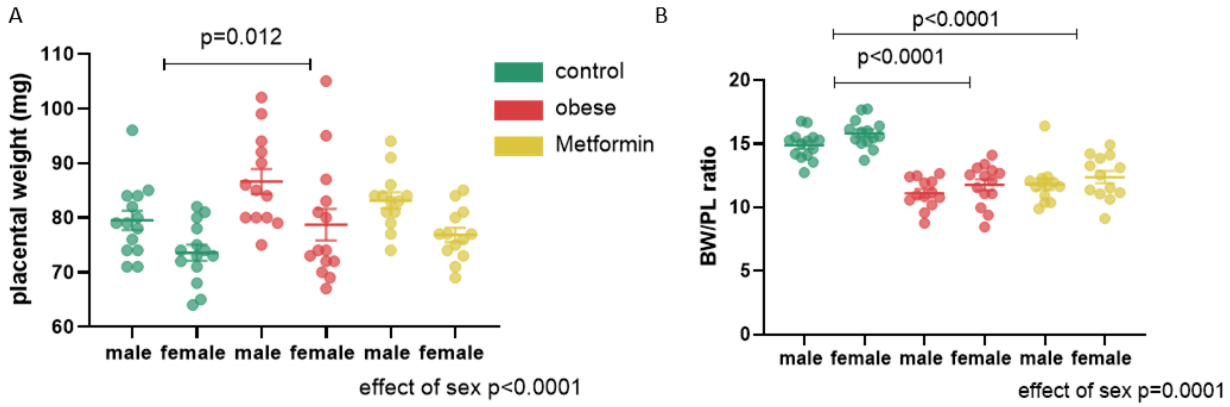

***Figure 4.10**: Placental efficiency is reduced in obese untreated and obese metformin-treated dams*

(A) Placental body weight was measured and together with the fetal bodyweight the (B) placental efficiency was calculated. N= 14/14 dams for male/female control, n = 13/14 dams male/female obese and n = 13/13 dams for male/female metformin placentas, linear mixed model analyses and mean ± SEM are shown.

4.3.4 Placental structure

Placentas were stained for an endothelial cell marker (CD31) and a marker of the junctional zone (Tpbpa, Figure 4.12A). This stain allowed quantification of the percentage of the labyrinthine area which was reduced in the placentas from obese untreated and obese metformin-treated dams (Figure 4.12B).

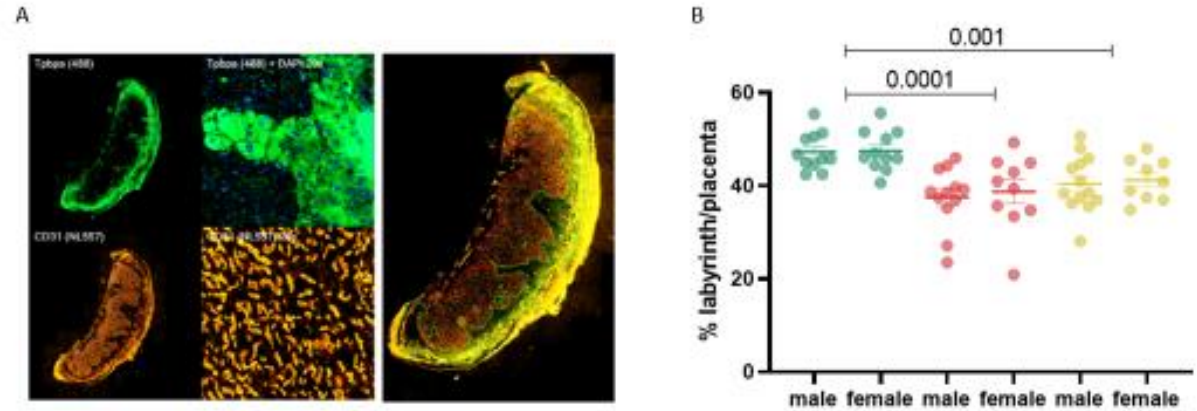

Figure 4.11: Placental structure is affected by maternal obesity which is not rescued by metformin

(A) Placentas were stained via immunohistochemistry for CD31 and Tpbpa (B) to calculate the percentage of the labyrinthine area. N= 11/11 dams for male/female control, n = 12/10 dams male/female obese and n = 13/9 dams for male/female metformin placentas, linear mixed model analyses and mean ± SEM are shown.

Alizarin Red staining demonstrated calcification in placentas from obese untreated and obese metformin-treated dams but not in those from controls (Figure 4.13A and 4.12B). Calcification was not present in obese placentas at E13.5 but could be seen from E15.5 onwards (Figure 4.13C) Staining of serial sections showed that in calcified areas F4/80 staining (macrophages) was visible and that the labyrinthine structures was destroyed in areas with calcification (Figure 4.13D). Overlap of areas with calcification and apoptotic areas could also be seen (Figure 4.13D).

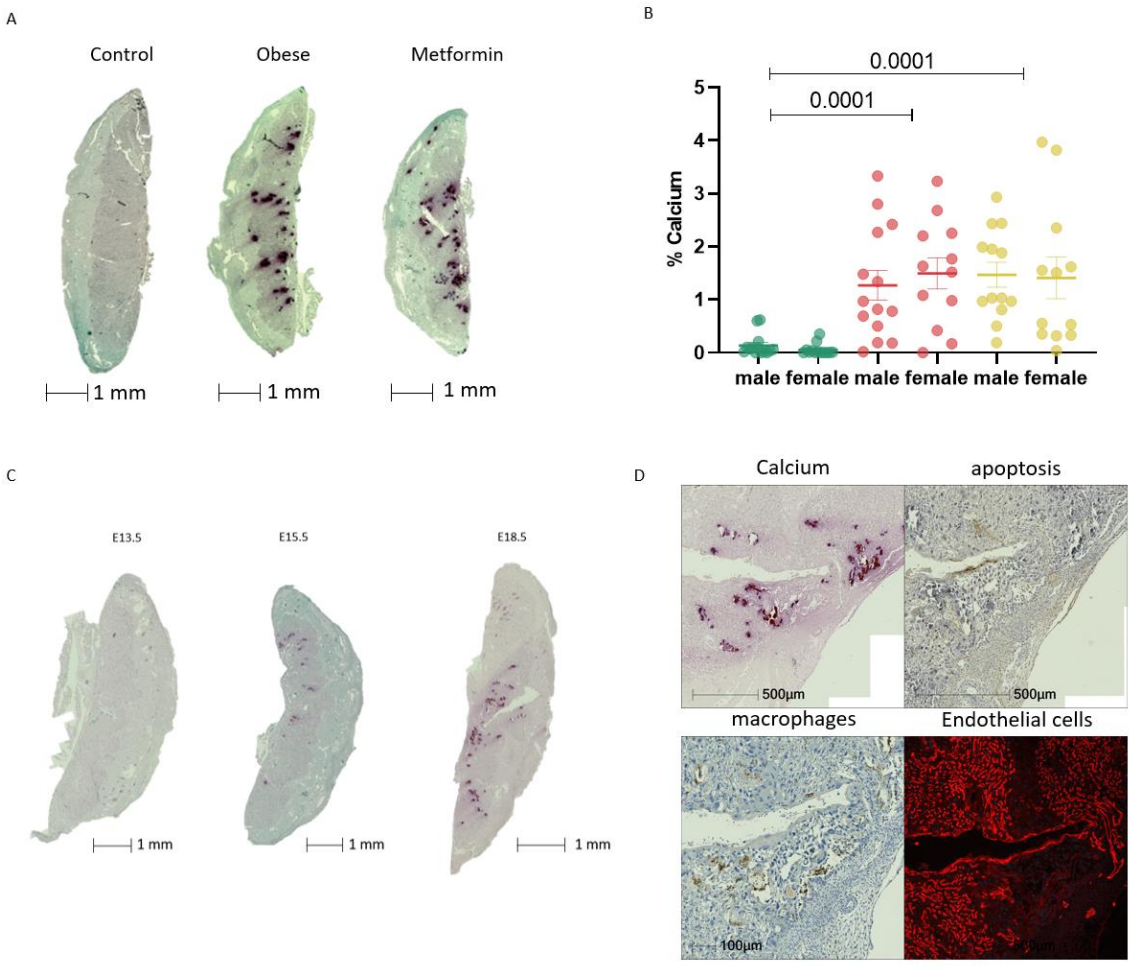

Figure 4.12: Placentas from obese untreated and obese metformin-treated dams are calcified

(A) Alizarin Red staining highlighted Calcium deposits, (B) so that the percentage of calcification in the placenta could be quantified (n= 14/13 dams for male/female control, n = 14/12 dams male/female obese and n = 13/12 dams for male/female metformin placentas.) (C) Obese placentas were stained for Alizarin Red at E13.5, E15.5. and E18.5. (D) Direct comparison of serial sections allowed staining for apoptosis (TUNEL), macrophages (F4/80) and the labyrinth (CD31) in areas of calcification.

4.3.5 Metformin in the fetoplacental unit

LC-MS quantification of metformin revealed strong correlations between metformin in the maternal circulation and the concentration in the fetal plasma (Figure 4.14A) and the placenta (Figure 4.14B) at

E18.5 of pregnancy. High quantities of metformin were detected in the fetus, especially the kidney (189.3 ± 84.8 nmol/g) and the amniotic fluid (21.89 ± 11.52 nmol/ml) on E18.5 (Figure 4.14C). Already at E13.5 metformin could be detected in the placenta (143.8 ± 59.1 nmol/g, n=4), fetal liver (63.0 ± 49.1 nmol/g, n=2) and amniotic fluid (2.0 ± 0.9 nmol/ml, n=2).

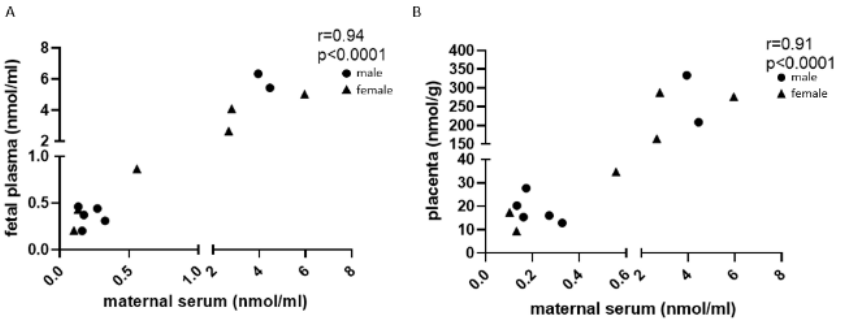

C

Sample type	Metformin conc (mean ± SEM)
fetal kidney (n=6)	189.3 ± 84.8 nmol/g
fetal liver (n=6)	17.9 ± 8.8 nmol/g
fetal heart (n=3)	32.6 ± 21.8 nmol/g
fetal brain (n=3)	16.9 ± 8.1 nmol/g
Placenta (n=13)	109.7 ± 34.8 nmol/g
amniotic fluid (n=6)	21.89 ± 11.52 nmol/ml
Fetal plasma (n=13)	2.06 ± 0.65 nmol/ml
Maternal serum (n=13)	1.67 ± 0.57 nmol/ml

Figure 4.13: High concentrations of metformin can be found in the placenta and the fetus at E18.5

(A) Metformin was quantified by LC-MS in fetal plasma and (B) the placenta and correlated with the concentration in the maternal circulation. Linear regression and Pearson correlation coefficient r are shown, squares indicate male fetuses (n=7) and circles female fetuses (n=6). (C) Metformin was measured in a range of fetal tissues and the amniotic fluid. n=6: 3 male and 3 female fetuses, n=3: 3 male fetuses, n=13: 7 male and 6 female fetuses.

4.3.6 Metformin transporter expression

RNA expression of known transporters of metformin was detected at E18.5 in the placenta, fetal kidney and liver. Out of the 11 metformin transporters explored RNA for six transporters was present in the placenta at E18.5 with a CT value below 30 (Figure 4.15A). These were in order of decreasing expression: Slc22a3 (Oct3), Slc6a2 (Net), Slc6a4 (Sert), Slc22a5 (Octn2), Slc22a4 (Octn1) and Slc19a3 (Thtr2). In contrast in the kidney RNA for the following seven transporters was expressed at E18.5, listed from high to low expression (Figure 4.15A): Slc22a2 (Oct2), Slc47a1 (Mate1), Slc22a1 (Oct1),

Slc6a4 (Sert), Slc22a5 (Octn2), Slc22a3 (Oct3), Slc29a4 (PMAT). Consistent with the lower levels of metformin in the liver (p=0.02 for kidney *vs*. liver comparison via Mann-Whitney test) RNA for only only three transporters was detected in the fetal liver at E18.5 (Figure 4.13A): Slc22a4 (Octn1), Slc47a1 (Mate1), Slc6a4 (Sert).

The same six transporters that were expressed at E18.5 in the placenta were also detectable with CT values below 30 in the placenta at E13.5. Comparison between the transporters at E13.5 and E18.5 showed that most transporters (Slc6a4, Slc19a3 and Slc22a4) increased their expression clearly from E13.5 to E18.5 (Figure 4.15B). One transporter (Slc6a2) decreased its expression slightly at E18.5 compared to E13.5.

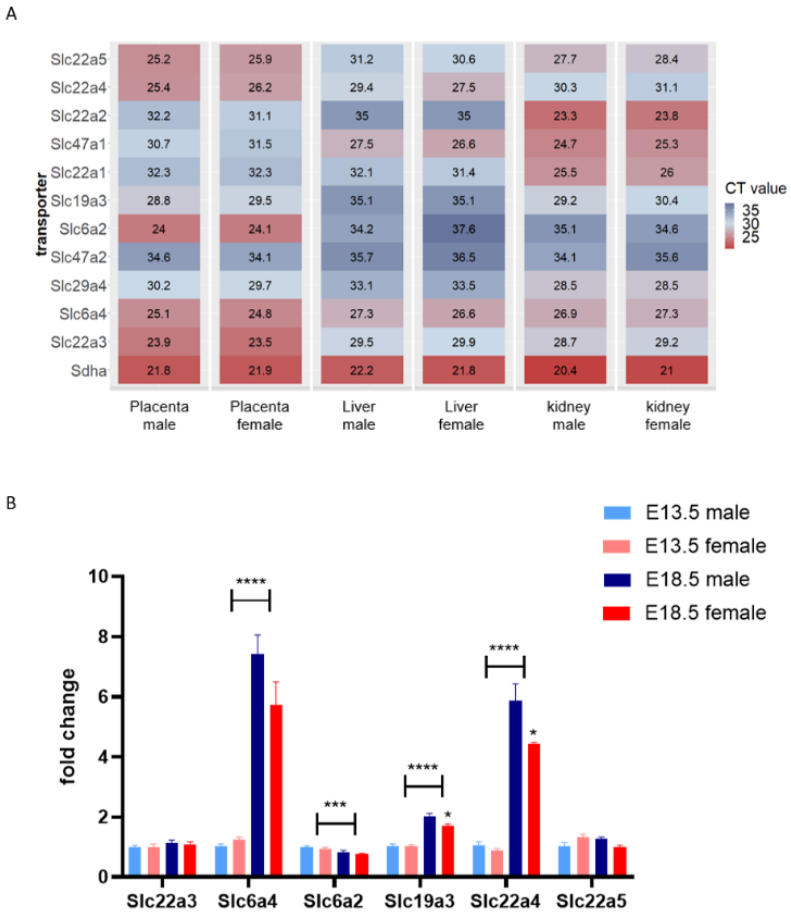

***Figure 4.14*: Metformin transporter are expressed in the placenta and the fetus**

(A) Metformin transporter expression was assessed in placentas, fetal livers and fetal kidney at E18.5 shown as a heatmap, mean CT values are shown in the heatmap (n=3 per tissue and sex respectively, all from control animals). (B) Expression of the transporters in the placenta was compared between E13.5 and E18.5, normalisation is performed against the reference gene Sdha and fold change calculated as $2^{-\Delta\Delta CT}$. Two-Way-ANOVA is performed for each individual gene with the factors time and sex (: p<0.05, **: p<0.01, ***: p<0.001, ****: p<0.001). A sole star indicates significance between sexes, the bar across the two timepoints highlights significance between E13.5 and E18.5.*

4.3.7 Metformin action in the placenta

Given the potential of metformin to enter the placenta in high quantities and to affect apoptotic, mTOR and AMPK pathways analysis of key mediators in these pathways was performed via western blotting analysis in placental tissue.

Total mTOR (males/females: 100 ± 4 %/100 ± 6 % in control, 94 ± 6 %/99 ± 4% in obese untreated and 98 ± 5 %/94 ± 5 % in obese metformin-treated placentas) and phosphorylated mTOR (pmTOR, males/females: 100 ± 7 %/100 ± 5 % in control, 95 ± 9%/101 ± 6% in obese untreated and 103 ± 11 %/93 ± 8 % in obese metformin-treated placentas) were not significantly different in either male or female placenta as shown in blots in Figure 4.16A. Similar results were found for total AMPK (males/females: 100 ± 12 %/100 ± 20 % in control, 96 ± 15 %/102 ± 19 % in obese untreated and 102 ± 10 %/94 ± 15 % in obese metformin-treated placentas), which was not changed between the groups. Phospho AMPK (pAMPK, 100 ± 5 % in control, 101 ± 5 % in obese untreated and 94 ± 6 % in metformin-treated placentas) levels were not different between groups in the male placenta (Figure 4.16B). In females pAMPK was significantly reduced in the obese untreated and the obese metformin-treated obese group compared to the control group (100 ± 7 % in control, 80 ± 4 % in obese untreated and 72 ± 4 % in obese metformin-treated placentas, Figure 4.14B). Bcl-2 (100 ± 8 % in control, 124 ± 8 % in obese untreated and 135 ± 10 % in obese metformin-treated placentas) and Bax (100 ± 9 % in control, 115 ± 5 % in obese untreated and 137 ± 9 % in metformin-treated placentas) were both increased in the obese metformin-treated placentas in males only (Figure 4.16C and D). In the female placenta Bcl-2 and Bax levels were not changed (Bcl-2: 100 ± 5 % in control, 111 ± 9 % in obese untreated and 116 ± 16 % in obese metformin-treated placentas, Bax: 100 ± 13 % in control, 105 ± 8 % in obese untreated and 127 ± 18 % in obese metformin-treated placentas).

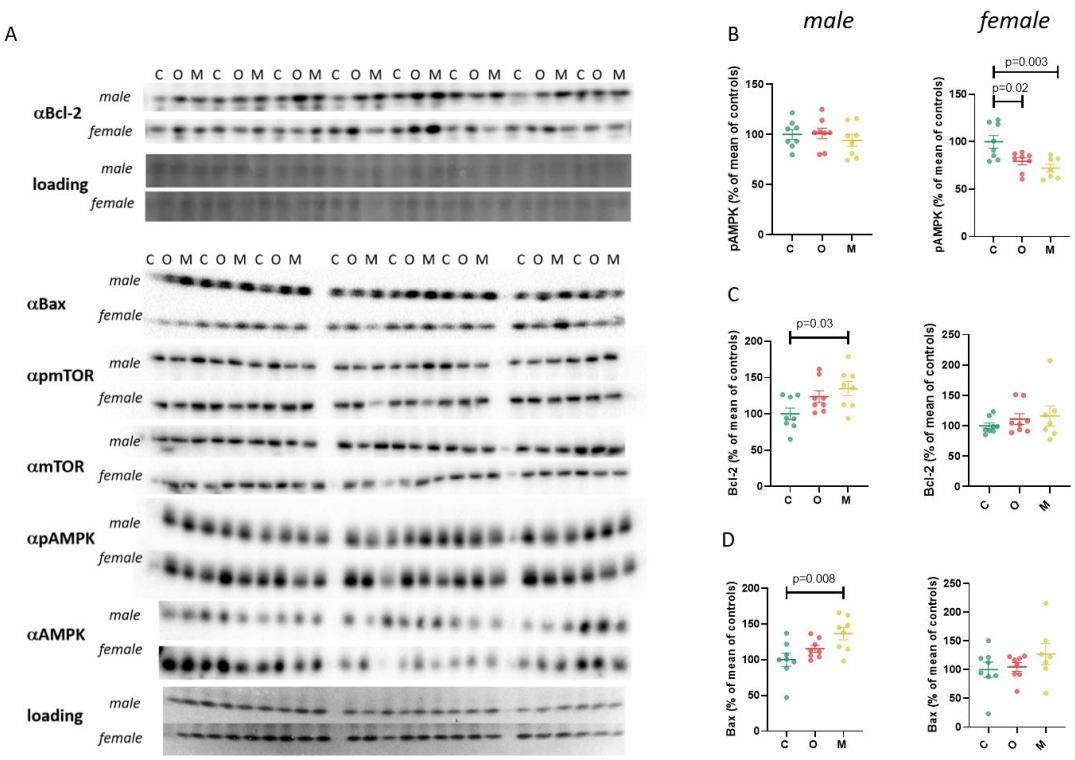

Figure 4.15: In male placentas from obese metformin-treated dams protein levels of Bax and Bcl-2 are increased

(A) Western blots of placental protein were probed for Bcl-2, Bax, phosphorylated and total AMPK and phosphorylated and total mTOR. As a normalisation a Coomassie of the blot was used (see loading). (B) Intensity of bands for pAMPK, (C) Bcl-2 and (D) Bax were quantified, normalised to loading and expressed here as a % of the mean of the control, male and female samples were separately analysed on two gels. One-Way-ANOVA followed by Tukey's multiple comparison test and mean ± SEM are shown, n=8 per group and sex (expect for female metformin placentas n=7). C=Control, O=Obese, M=Metformin.

4.4 Discussion

The aim of this chapter was to characterise fetal and placental physiology in our model of maternal diet-induced obesity. As outlined in the first chapter metformin was explored as a promising intervention as it improved negative obesity-associated impacts on the pregnant dams. However, as metformin has the potential to cross the placenta and act directly on the fetus, it is important to establish how metformin treatment in pregnancy affects the placental-fetal unit.

4.4.1 Fetal growth

We have shown previously that fetuses in our maternal obesity model at both E12.5 and E18.5 have a reduced body weight[245]. However, by weaning the offspring from the obese mums have caught up in weight and were heavier than the offspring from control dams[262]. In line with this data fetuses from obese untreated dams in this study had a reduced body weight at the end of pregnancy (E18.5). The growth restriction was symmetric as all other measurements including head length, crown rump length and abdominal diameter were equally reduced. Metformin treatment in obese dams did not prevent this growth restriction despite improving maternal metabolic health and uterine artery compliance as described in the previous chapter. Liver and brain weights were both reduced in fetuses from obese untreated and obese metformin-treated dams. However, whereas the ratio of brain to liver weight was increased in the fetuses from obese compared to controls, this significant increase was not observed in metformin-treated dams compared to controls. An increased ratio generally indicates asymmetric growth restriction, highlighting that the brain is favoured in its supply and growth at the expense of other organs such as the liver. However, the fetal ultrasound analysis did not detect changes indicative of asymmetric growth (e.g. an increased cerebroplacental ratio) and there was no increase in haematocrit (generally expected to occur as a consequence of brain sparing in response to hypoxia). In fact, fetuses from obese untreated and metformin-treated dams showed a reduced haematocrit. A low haematocrit could be the result of impaired erythropoiesis. Marks et al. showed in a mouse model of HFD-induced maternal obesity impaired erythropoiesis in the fetal liver and reduced self-renewal of the hematopoietic stem cells (HSPCs) in the liver[450]. According to their experiments the HSPCs egress the liver prematurely and start differentiating to myeloid cells or B-cells rather than increasing the pool of HSPCs by self-renewal. This observation warrants furter investigation in our model.

4.4.2 Placental phenotype

Obese untreated and obese metformin-treated dams showed major placental defects leading to reduced placental efficiency in both groups. Previous mouse models of maternal obesity and GDM have highlighted decreased labyrinthine zones, lipid accumulation in the placenta and increased secretion of pro-inflammatory cytokines and oxidative stress[233,244,451,452]. In our mouse model we have previously shown downregulation of angiogenesis markers, hypoxia and increased lipid content in the

placentas from obese dams[229,245]. These features have also been reported in the human placenta in obesity- and/or GDM-complicated pregnancies[453]. The presence of calcium in the placenta is a well-known occurrence in human obese pregnancies[454,455]. With advancing gestation calcification of the placenta is a physiological process, however early calcification is a sign of a failing placenta which is associated with an increased risk of stillbirth and IUGR[456,457]. Thereby the presence of calcium in the placentas of the obese dams in our study shows that our model resembles the human situation. Both, the reduced labyrinthine area and the presence of calcium deposits were not rescued by metformin treatment. Despite placental calcification being frequently described in human pregnancy in obstetric care its aetiology is not known[458]. Three types of calcification exist, the metastatic type with calcification in healthy tissue due to high levels of calcium and phosphate, the dystrophic type in dead tissue and the physiological calcification known from bone formation. In our mouse model calcification can be observed from E15.5 onwards but not earlier in pregnancy at E13.5. Our data leads us to hypothesize that mechanisms similar to vascular calcification like in atherosclerosis could play a role in placental calcification. Our analysis of serial sections showed a high overlap of calcium deposits with F4/80 staining. In atherosclerosis it is now well-established that macrophages play a crucial role in the progression of vascular calcification and the progression of the disease[459].

4.4.3 Metformin transport and accumulation in the fetal and placenta

The fetal circulation and the placenta showed high concentrations of metformin. Fetal metformin concentrations were as high as those in the maternal circulation, as has been reported previously in humans[340,398]. The human placenta is thought to facilitate metformin transport across the placenta via the serotonin transporter (SERT, Slc6a4), organic cation transporters novel 1 and 2 (OCTN1 and 2, Slc22a4 and 22a5) and norepinephrine transporter (NET, Slc6a2). These transporters are found on the apical side whilst OCT2 and 3 are the main transporter on the basal side facing the fetus (Figure 4.15 A)[460, 340]. In the current study, we demonstrated expression of Oct3, Sert, Net, Octn1, Octn2 and thiamine transporter 2 (Thtr2) in the mouse placenta (Figure 4.17A). This is in line with genome-wide expression profiling in the murine placenta[461]. Lee et al. proposed in a paper from 2018 that metformin transport in the human placenta could be facilitated by transport of metformin across the maternal-facing membrane via OCTN1 and 2, SERT and NET together with p-gp and BCRP[462]. The researchers showed OCT3 presence only at the fetal-facing placental membrane and the fetal endothelium, so transport across these barriers could be facilitated via Oct3. Assuming a similar localisation and given the transporter expression shown in this study a similar model can be proposed for the transport of metformin across the murine placenta (Figure 4.17). But exact localisation of these transporters in the mouse placenta needs further assessment. Many of these transporters were already expressed in early gestation (E13.5) and increased in expression levels with advancing gestation.

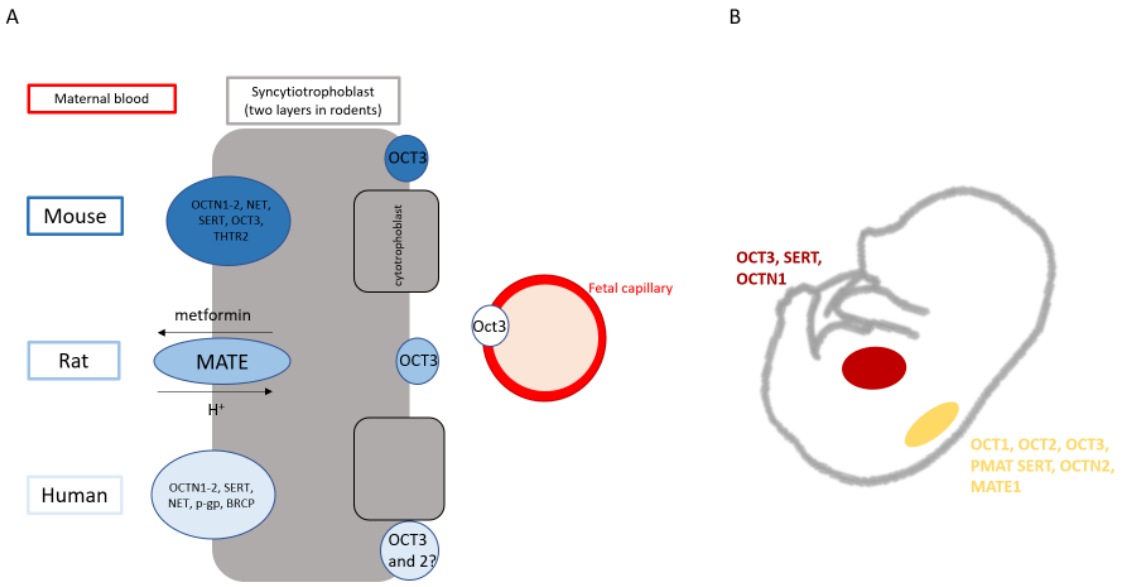

Figure 4.16: Metformin transport across the placenta and into the fetus

(A) The different routes of metformin transport across the placenta are shown in mouse, rat and human based on the current knowledge (including that established in this chapter). This is only a schematic, rodent placentas consist of two syncytiotrophoblast layers[335,340,460,463] *(B) The transporters found in our study in the fetal kidney (yellow) and fetal liver (red) are shown.*

Although uptake of metformin into and across the placenta and into the fetal circulation has been reported previously, little is known about which fetal tissues can take up metformin. Liver and kidney were shown to express metformin transporters (Figure 4.17B) and presented high levels of metformin. Both, transporter expression and metformin concentrations, were higher in the fetal kidney compared to the fetal liver. The amniotic fluid showed high levels of metformin as well, especially in late gestation (E18.5). Amniotic fluid consists of fetal urine excretion and nasal and pulmonal fluids from the fetus. The high concentration of metformin in the fetal kidney could suggest that high concentrations of metformin are secreted into the amniotic fluid by the fetus as the kidney is the main excretion organ for metformin in the adult[464]. However the main pathway for waste elimination in the fetus is via the placenta[465]. The placenta itself could thereby also lead to the metformin accumulation in the amniotic fluid. Figure 4.18 highlights the production of the amniotic fluid and shows that the fetus is repeatedly taking in amniotic fluid and presumably metformin.

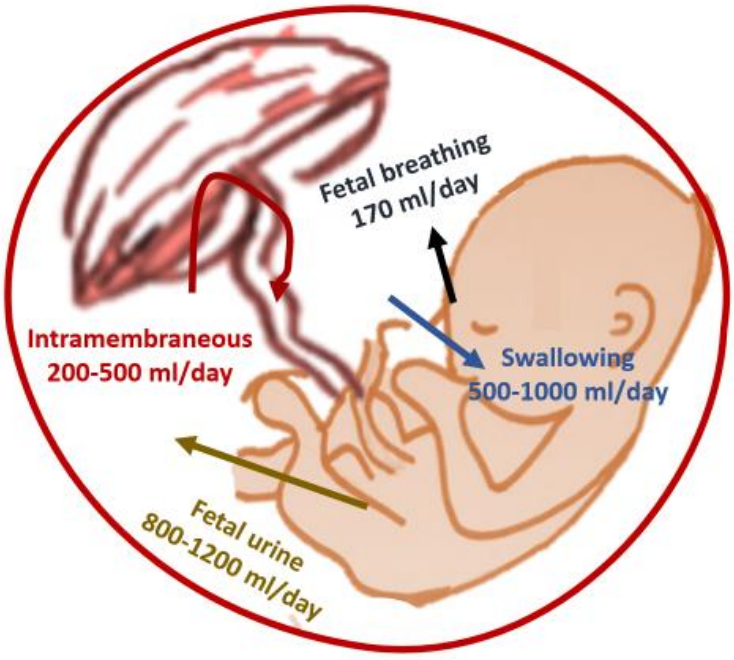

Figure 4.17: Amniotic fluid composition and turn-over

Amniotic fluid is constantly exchanged between fetus and placenta. The fetus urinates and breathes lung fluid into the amniotic sac. Uptake of the amniotic fluid into the fetus takes place via active swallowing of the fetus and the intramembraneous pathway across the placental membranes. All the exchange rates are based on human data at the end of pregnancy, schematic is adapted based on previous publications[466,467].

4.4.4 Direct effects of metformin

Analysis of the effects of metformin treatment on the obese dams showed clear benefits on metabolic and cardiovascular health including uterine artery function as detailed in chapter 3 of this thesis. It is therefore at first surprising that fetal growth can't be rescued with metformin treatment as a reduced uterine artery function likely explains the reduced fetal growth in the obese group. Given the high quantities of metformin that reach the fetus and the placenta it is therefore likely that metformin has direct effects on the fetus and the placenta that explain the sustained growth restriction. As the placenta plays a key role in regulation of fetal growth and development, we assessed effects of metformin on the placenta. Metformin, at least at high concentrations, is known to activate AMPK and inhibit mTOR. We observed no effects on mTOR or pmTOR in either male or female placenta. However, in the female placenta pAMPK was reduced in both the obese untreated and obese metformin-treated placenta. Reduced levels of activated AMPK have previously been reported in placentas from obese women, which then also showed increased mTOR signalling likely explaining overgrowth in the fetus[468,469]. Sex differences regarding this effect have not been investigated. Our data shows that pAMPK reduction in an obese maternal environment is specific to the female placenta, however we did not observe a change in mTOR signalling and saw reduced rather than increased fetal

growth. Additionally metformin did not increase pAMPK levels as previously shown in placental *in vivo* and *in vitro* studies[350,360].

Another previously established effect of metformin is its potential to induce apoptosis, which has been especially shown in cancer studies[438,439]. In human breast cancer cell lines metformin induced mitochondrial dysfunction and upregulated Bax[470]. Metformin treatment increased levels of the pro-apoptotic protein Bax and the anti-apoptotic protein Bcl-2 in male placentas. It is unexpected that both the pro- and the anti-apoptotic proteins show a change in the same direction. Only a few studies exist that report a similar phenotype. A study from 1999 in glioblastoma cells showed that Bcl-2 only inhibited apoptosis at low expression levels whereas when overexpressed it activated apoptosis by inducing mitochondrial damage[471]. Another study also showed that Bax and Bcl-2 were increased in fetal brains upon cocaine exposure *in utero* and suggest that the increase in Bcl-2 could be a compensatory mechanism trying to avoid apoptosis[472]. Interestingly the increase in Bax and Bcl-2 was only observed in the male placentas which could highlight the increased vulnerability of male fetuses. Human studies show differences in the susceptibility of males and females to an adverse *in utero* environment (such as obesity or GDM) with males being more vulnerable with poorer long-term cardiometabolic health[59]. Sex-specific differences are also reported in animal models, in our mouse model male offspring from obese mums show earlier onset of cardiac dysfunction and their pancreatic islets were more compromised than from their female siblings[258]. When assessing offspring in the metformin model presented in this thesis our lab showed that increased adiposity in the offspring from metformin-treated obese mothers at 8 weeks of age specifically occurred in the male offspring[473]. Given this offspring data and the effect on apoptosis in the male placentas sexually dimorphic effects of metformin treatment *in utero* require further investigation.

4.4.5 Conclusion

The data presented in this chapter shows that exposure to obesity *in utero* has detrimental effects for the fetus and the placenta. In the obese group fetal weight is significantly reduced and placental perfusion and structure impaired as shown by the calcium deposits. The impaired uterine artery function and preeclampsia-like phenotype in the obese dams is highly likely to cause the reduced fetal growth in the presented model. It is thereby striking that metformin could not rescue fetal growth despite improved uterine artery function. We can thereby only speculate on the exact pathway leading to fetal growth restriction and placental pathologies in the metformin-treated pregnancies. Metformin crosses the placenta from E13.5 onwards and can be detected at high levels in the placenta and fetal tissues. We thereby hypothesize that direct effects of metformin could play a role in the sustained fetal growth restriction despite maternal improvements. No effects of metformin were observed on AMPK or mTOR signalling. However male placentas presented upregulation of apoptotic signalling upon metformin treatment. The data presented could potentially indicate that metformin has indeed

detrimental effects on the placenta and thereby fetal development which may be different between males and females.

Key findings

- Fetal growth is symmetrically reduced in fetuses from obese-untreated dams which is likely caused by reduced uterine artery compliance in the dams. Fetal growth is not improved by metformin treatment despite improvement in uterine artery function in the dams, highlighting the potential that fetal growth restriction occurs via different pathways in obese untreated and obese metformin-treated fetuses.
- Placentas from obese untreated and obese metformin-treated dams both present reduced placental efficiency compared to placentas from controls. The reduced efficiency is likely caused by a reduced labyrinthine area and placental calcification that is not corrected by metformin.
- The placental calcification highlights that our mouse model of maternal obesity mirrors the human situation where calcium deposits are often found in pregnancies complicated by obesity, GDM and PE.
- Metformin can cross the placenta in high quantities and is detected from E13.5 onwards in the placenta, fetal tissues and the fetal circulation.
- Metformin likely has direct effects on the placenta, such as increased apoptosis. This was only found in the male placentas.

5 Exploration of the molecular mechanisms that could mediate potential direct effects of metformin exposure on the placenta during an obese, glucose-intolerant pregnancy

5.1 Introduction

5.1.1 The multiple mechanisms of metformin action

As highlighted in the previous chapters key pathways of metformin action, until recently, were thought to be mainly related to AMPK signalling with the liver being the main organ of action[371]. However, this view has been challenged in recent years and multiple possible pathways on which metformin can act have been identified. Glucose-lowering effects via reduction of hepatic glucose production are thought to not only be AMPK-mediated as metformin maintains its glucose lowering effect in AMPK knock-out mice[474]. Subsequent studies have shown effects of increased levels of AMP (resulting from metformin's inhibitory action on mitochondrial complex I) could be causative for the acute hypoglycaemic effects of metformin[475]. In a study by Hunter et al. AMP was shown to inhibit fructose-1,6-bisphosphatase-1, which is a key enzyme in gluconeogenesis[475]. AMP also inhibits adenylate cyclase and thereby reduces cAMP levels and consequently reduces protein kinase A activity leading to reduced glucagon signalling in the liver[476]. In recent years it has been proposed that the gut is also an important site of metformin action as studies using PET scanning with 18F-fluoro-deoxyglucose showed that metformin increased glucose uptake into the intestine[477]. This was first observed in 2007 in studies that highlighted that due to the high glucose uptake into the bowel induced by metformin, its use during bowel tumour screening could lead to false-positive results[478]. In addition, Stepensky et al. showed in 2002 that the glucose-lowering effect of metformin is most pronounced when given intraduodenally or orally in diabetic rats[479]. Studies in recent years have therefore assessed the effect of metformin on the gut. Data from 2021 highlights that metformin causes mitochondrial dysfunction in intestinal cells leading to increased glucose uptake, increased glycolysis and increased GDF-15 secretion in the intestine[480]. In this study RNASeq analysis detected transcriptional changes in intestinal cultures treated with 1 mM of metformin but not at lower concentrations. Overall, the exact actions of physiological metformin concentrations in the clinic are not fully understood.

Interest in metformin action has increased in recent years as its use is now not limited to T2D treatment but has expanded to use in cancer treatment and is even suggested as an anti-ageing treatment[481]. As a potential anti-ageing drug, metformin has been shown in human studies to reduce ageing-induced inflammation via, paradoxically, improving mitochondrial function[482]. However Espada at al. showed that metformin is only beneficial in young C-elegans improving metabolic health and longevity, however in old C-elegans metformin was toxic and increased ageing-associated mitochondrial dysfunction making the authors question its benefits as an anti-ageing drug[483]. Additionally, metformin

can reduce cancer growth and inhibit lipogenesis in prostate tumours via activation of AMPK and inactivation of Acetyl-CoA-Carboxylase, the first enzyme needed for fatty acid synthesis[484].

There is very limited data regarding metformin action on the placenta as described in Table 1.1 in the general introduction. If metformin actions on the placenta are similar to those previously identified in adult tissues, then it can be hypothesised that metformin action on the placenta could lead to altered placental and fetal growth and metabolism (Figure 3.1). The meta-analysis from our lab comparing metformin and insulin treatment of gestational diabetes highlighted the scarcity of data regarding effects of metformin on the fetus and the placenta[341]. Overall there is a lack of systematic placental analyses in human studies and the focus on only a few key pathways when assessing metformin in *in vivo* and *in vitro* models. However as described metformin could have many yet unknown actions on different pathways. Not many studies have used explorative approaches with no studies assessing the effects of metformin on the lipidome despite the known effects of metformin on lipid metabolism highlighted above. Additionally, only one rat study assessed transcriptomic changes in response to treatment with metformin and glyburide[349].

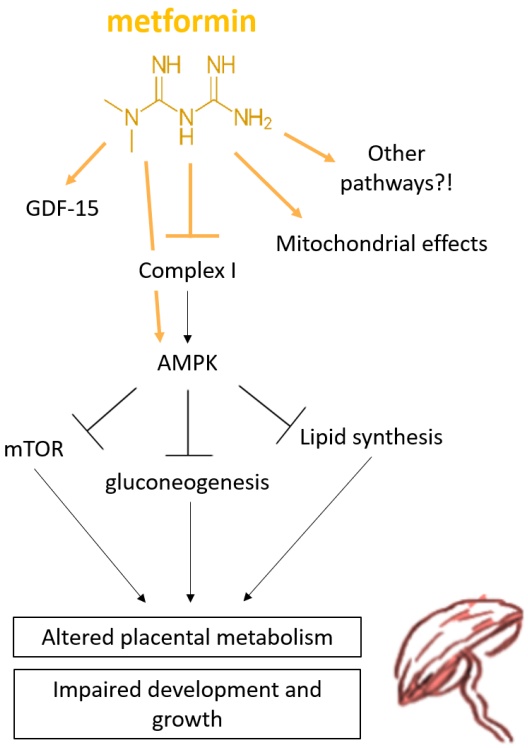

Figure 5.1: Potential effects of metformin on the placenta and the fetus

5.1.2 Aims

The aims of this chapter were therefore:

- To assess the effect of metformin on the lipid profile of the obese placenta. This was achieved by performing lipidomic analyses comparing the obese untreated and obese metformin-treated placentas.
- To determine changes of gene expression induced by metformin treatment. This was achieved by bulk RNA sequencing analysis comparing the obese untreated and obese metformin-treated placentas.

5.2 Methods

In this chapter placentas from the main cohort described in section 2.1 and 4.2.2 were used, but only obese untreated and obese metformin-treated placentas were included.

5.2.1 LC-MS analysis of lipids

Lipidomics (a specialist methodology) were performed by Dr. Benjamin Jenkins from the Core Metabolomics and Lipidomics Laboratory (CMaLL) at the University of Cambridge. Placentas (n=6 per group and sex, 24 in total) were homogenised as described in section 2.3 for the LC-MS analysis of metformin. Instead of the aqueous phase used for metformin analysis, the lower organic fraction was taken for lipidomic analysis. The organic fraction was dried down in a Concentrator Plus system (60°C, 90 minutes). After reconstitution of the sample in 100 ml of 2:1:1 propan-2-ol:acetonitrile:water the sample was subjected to LC-MS analysis. Chromatographic separation was achieved via the Shimadzu HPLC System with subsequent mass spectrometry analysis on the Thermo Scientific Orbitrap with a heated electrospray ionisation source. The LC-MS was performed as described previously[363].

5.2.2 Analysis of lipidomic data

R Studio (Version 1.4.1106) with R (Version 4.0.5) was used for analysis of the lipidomic data. Lipid species where more than 20% of the samples showed no abundance were excluded from the analysis. Sums of lipid species per lipid class were generated to assess the broad lipidomic spectrum. Assessment of the effect of sex and diet was performed via a linear mixed model assessing the effect of sex and diet and their interaction as variables and incorporating the dam ID as a random effect. With the same linear mixed model regulation of individual lipid species in each lipid class was determined with the lipidomeR package. All analyses show n=6 per group and sex.

5.2.3 Library preparation for RNA sequencing

RNA was extracted from 35-45 mg of placental tissue (n=6 per group and sex, 24 in total) using the QIAGEN miRNeasy micro kit as described in the general methods. Extraction was performed according to the manufacturer's instructions with an additional DNA digestion step with a QIAGEN DNAse kit. Nanodrop analysis showed a A260/280 ratio above 2 and a yield of 1500 – 2500 ng/µl for all samples. Analysis with the Agilent Bioanalyser 2100 system (Agilent RNA 6000 Nano Kit) confirmed RNA integrity (RIN) values above 8 for all 24 samples. Total RNA (400 ng) was used for library construction with the Illumina's TruSeq Stranded mRNA Library Prep Kit. Library preparation was performed by Dr. Marcella Ma (Genomics/Transcriptomics Core Facility from the Institute of Metabolic Science, University of Cambridge) as described previously[485]. In brief, mRNA was enriched before reverse transcription. After synthesis of double stranded cDNA, adenylation and barcode ligation was performed. Enrichment of ligated libraries was obtained via limited amplification. Indexed libraries were normalized, pooled and sequenced on the NovaSeq 6000 (50bp paired-end) at the Genomics Core Facility, Cancer Research UK Cambridge Institute.

5.2.4 Analysis of RNA sequencing data

Using STAR, sequence reads were mapped to the GRCm38 reference genome with ≥90% mapping efficiency for all samples and counted. RNA sequencing (RNASeq) analysis was performed using R Studio (Version 1.4.1106) with R (Version 4.0.5). Gene annotations were downloaded via BioMart to replace the Ensembl IDs with gene names. Differential expression was analysed using DESeq2 after excluding genes where more than half of the samples had a count of less than 5. The variance stabilizing transformation (VST) function was used to normalize the count data and allow principal component analysis (PCA) analysis which was plotted using ggplot. Volcano plots were also visualised via ggplot, the log fold change shrinking function within DESeq2 was used to compensate for the fact that lowly expressed genes appear to show a greater fold change[486]. Statistical analyses were performed in DESeq2 using each of the following models: sex as a single variable (model: ~sex), group as a single variable (model: ~group), an additive model of sex and diet (model: ~sex+diet), or the additional interaction between sex and treatment (model: ~sex+treatment +sex*treatment). Models were compared to each other with the likelihood ratio test (LRT) function in R which showed that the additive model (model: ~sex+diet) was the best fit for the data as no interaction was found between sex and treatment. Genes with an adjusted p value of <0.05 were considered differentially expressed, no threshold for the fold change was used. Pathway enrichment analysis was performed with the gene ontology resource http://geneontology.org/. All analyses show n=6 per group and sex. Thanks a lot to Dr. Christopher Smith, Dr. Lucas Pantaleão and Dr. Brian Lam for being so helpful and always so kindly and promptly replying to my questions when I performed this RNA sequencing analysis.

5.3 Results

5.3.1 Total placental lipid profiles

As shown in the PCA plot in Figure 5.2A no clear-cut clustering of the samples can be observed by eye. However, addition of ellipses marking where 95% of the samples lie shows that the clearest separation can be seen between the female obese-untreated and female obese metformin-treated placentas, with less separation between the male groups (Figure 5.2B). Relative changes in response to metformin treatment in total lipid classes showed significantly reduced carnitine, lysophosphatidylcholine (lyso-PC) and phosphatidylserine (PS) levels in the female obese metformin-treated placentas compared to the female obese untreated placentas (Figure 5.2C). In the males however total PS along with sphingosine were significantly increased. It can be noted that all lipid classes (except for sphingosine which were unchanged in female placenta) were reduced with metformin treatment in the female placentas. This global reduction was not observed in the male placentas, where several lipid classes were significantly increased by metformin exposure, but none were significantly decreased (Figure 5.2C). A strong interaction between sex and treatment can be seen for PS which is upregulated in the male placenta and downregulated in the female placenta in response to metformin treatment.

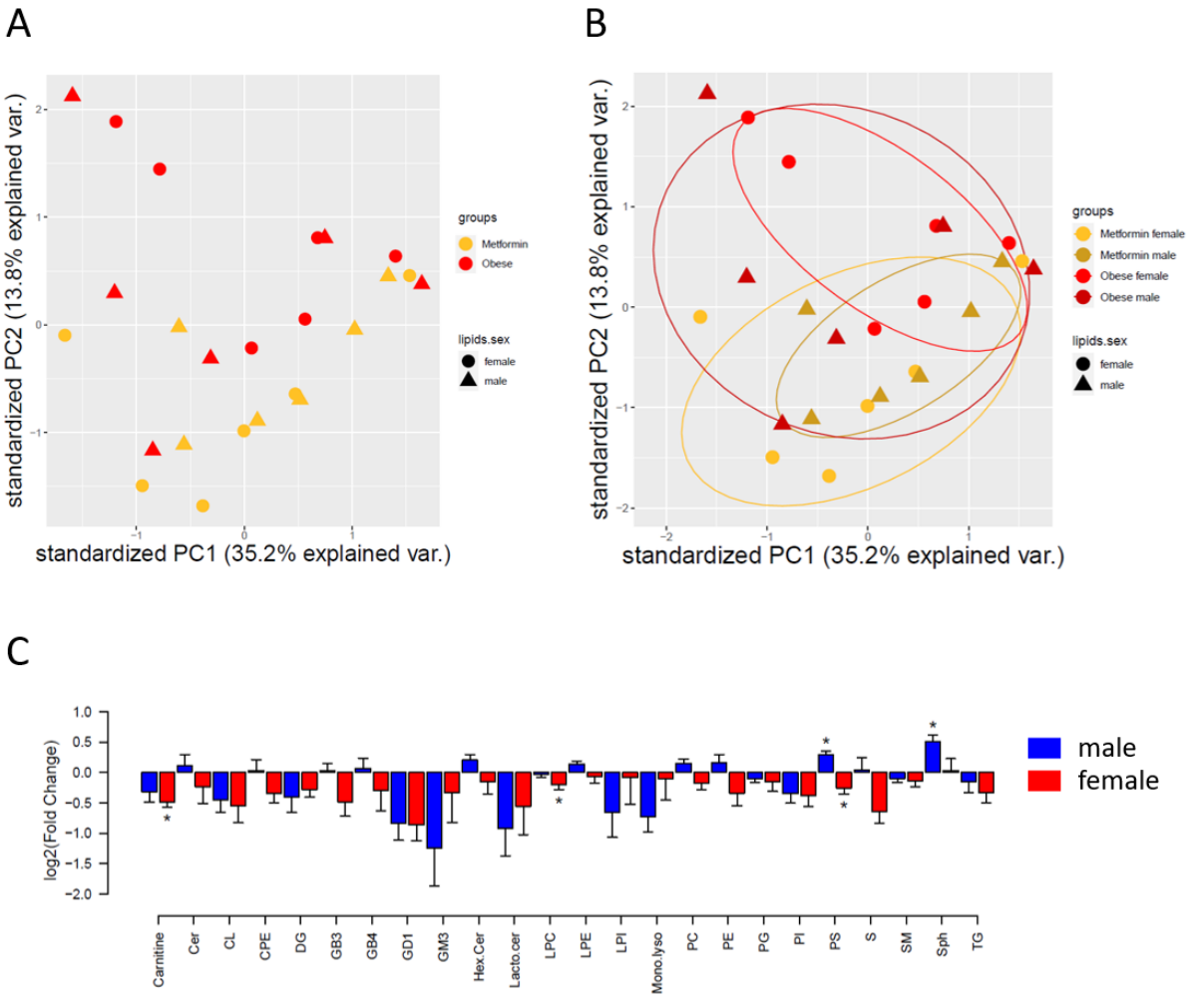

Figure 5.2: Total lipid classes are changed in a sexually dimorphic manner in response to metformin

*(A) PCA plots showing PC1 and PC2 scores for the lipidome of obese untreated and obese metformin-treated placentas, separated by sex and with (B) PCA ellipses (95% confidence interval) visualizing the clustering of the samples. (C) Relative changes in lipid classes (as log2) are shown for male and female placentas in response to metformin treatment, mean + SE is shown and p<0.05 marked with *. This Figure 5.2C has been provided by Dr. Lucas Pantaleão, Cer: ceramides, CL:cardiplipins, CPE:ceramide phophatidylethanolamines, DG=di-acylglycerides, GB: GB gangliosides, GD: GD gangliosides, GM: GM gangliosides, Hex.Cer:Hexosyl-ceramides, Lacto.cer:Lactosyl-ceramides, LPC: lyso-hopsphatidylcholines, LPE: lyso-phosphatidylethanolamines, LPI: lyso-phopshatidylinositol, Mono.lyso: Mono-lyso-cardiolipins, PC:phosphatidylcholines, PE: phosphatidylethanolamines, PG: phosphatidylglycerol, PI: phosphatidylinositol, PS: phosphatidylserines, S: sulfatides, SM: Sphingomyelins, Sph: sphingosines, TG: triglycerides*

5.3.2 Detailed view on the lipid profiles

The previously identified lipids (carnitine, sphingosin, PS and lyso-PC) that showed significant changes with metformin treatment were plotted and analysed with a linear mixed model that assessed the effect of sex and treatment and their interaction, while taking into account the dam ID as a random effect as explained in section 4.2.7. Carnitines were overall decreased in the obese metformin-treated placentas (Figure 5.3A) and this was driven by a reduction in free carnitine rather than acylcarnitines (Figure 5.3B and C). Consistent with the overview data presented above, there were sexually dimorphic effects of metformin treatment on sphingosine and PS (Figure 5.3D and E). It needs to be noted that only one sphingosine, sphingosine (18:0), was detected in the placental samples, therefore this lipid class only consists of one sphingosine species. The PS levels were increased with metformin treatment in the males whereas the opposite effect was observed in the females. Lyso-PCs were overall reduced with metformin treatment, however this effect was more pronounced in the females.

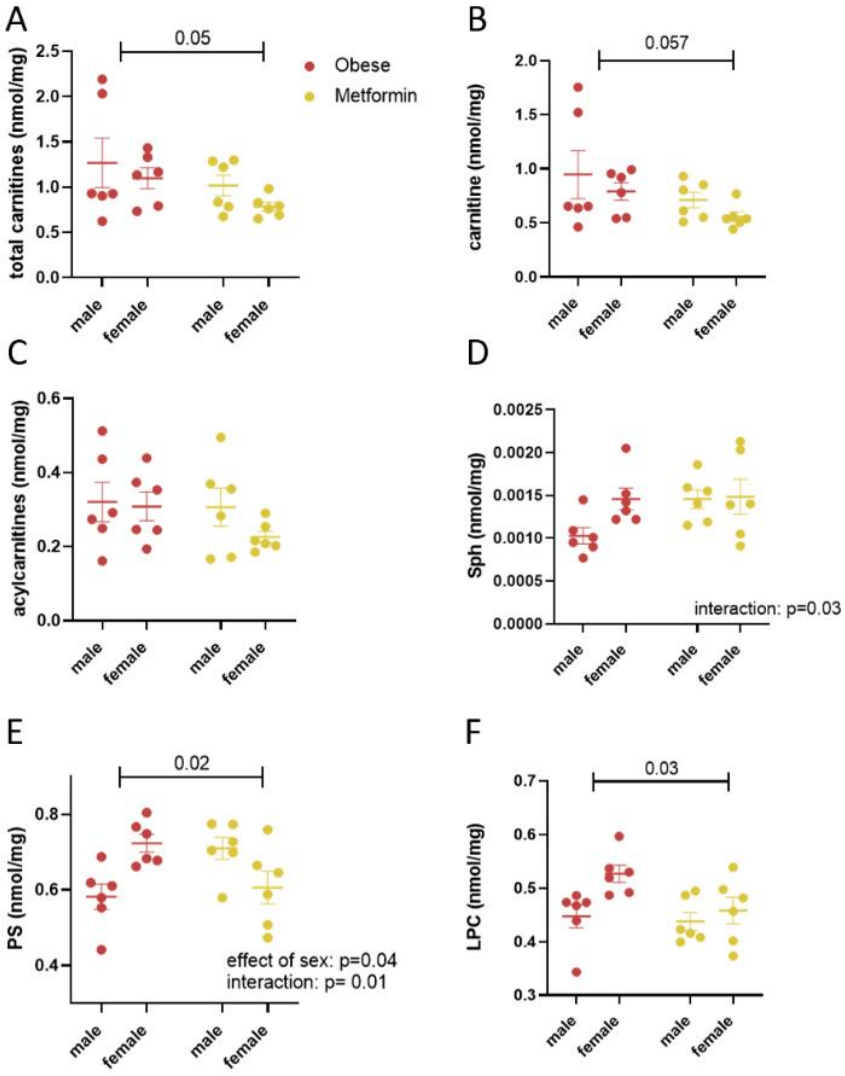

Figure 5.3: Detailed analysis of lipid classes shown to be changed in Figure 5.2

Levels in nmol/mg are shown for (A) total carnitines, (B) just carnitine, (C) acylcarnitines, (D) sphingomyelins, (E) phosphatidylserines and (F) lysophosphatidylcholines. Mean ± SEM are shown together with p values from linear mixed model analysis (group and sex as factors and the dam ID as a random effect).

Despite no differences in total triglycerides (Figure 5.4A), triglycerides with lower total numbers of C atoms (35 – 55) were significantly reduced with metformin treatment as shown by the negative correlation (blue) in the correlation matrix (Figure 5.4B). These triglycerides thereby likely have medium (6-12 carbon atoms) to long (3-21 carbon atoms) fatty acids attached to them. Unsaturated, monounsaturated and polyunsaturated triglycerides were reduced with metformin treatment equally. Detailed analysis of lyso-PC levels showed that lyso-PC (16:0) and lyso-PC (18:3) are reduced in the male placentas (Figure 5.5). Lyso-PC (22:6), having docosahexaenoyl acid (DHA) important for fetal brain development incorporated, was reduced with metformin treatment but only marginally and not significantly.

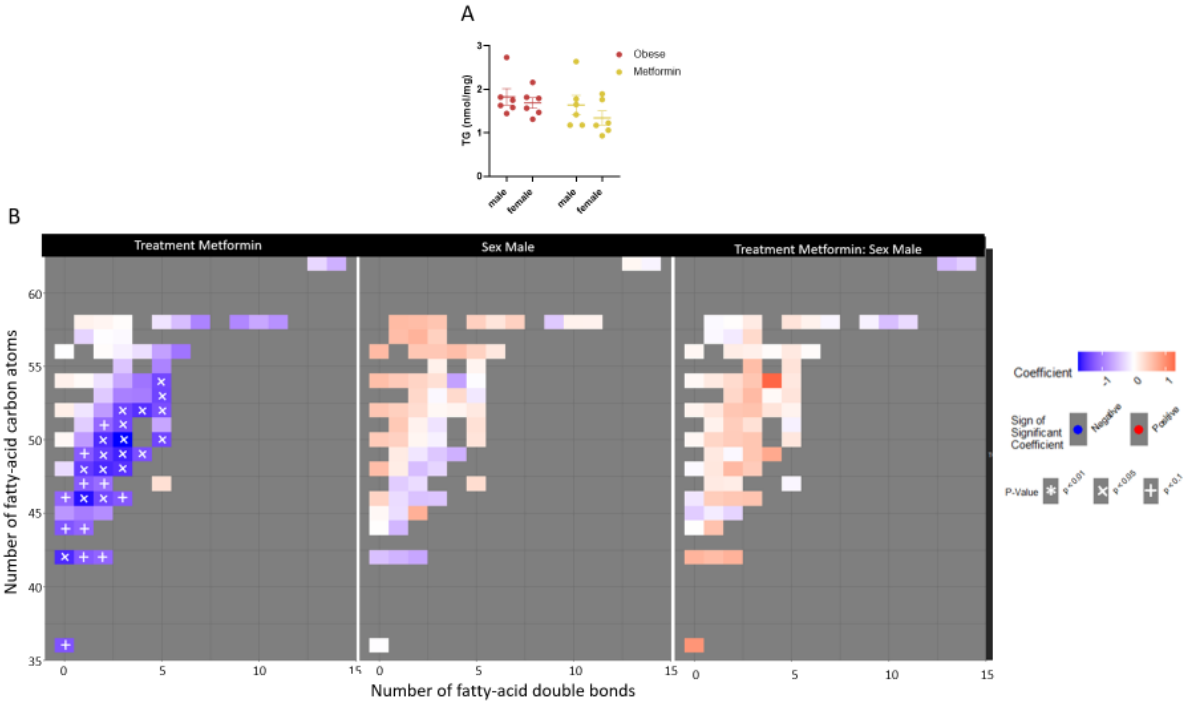

Figure 5.4: Changes of triglycerides in response to metformin

(A) Total triglyceride levels are shown as mean ± SEM together with p values from linear mixed model analysis (group and sex and their interaction as factors and the dam ID as a random effect). (B) Heatmap for all triglyceride species based on a regression model taking group, sex and dam ID as a random effect into account. On the x-axis number of fatty-acid double bonds (saturation level of the fatty acids) and on the y-axis the number of total fatty acid carbon atoms can be found.

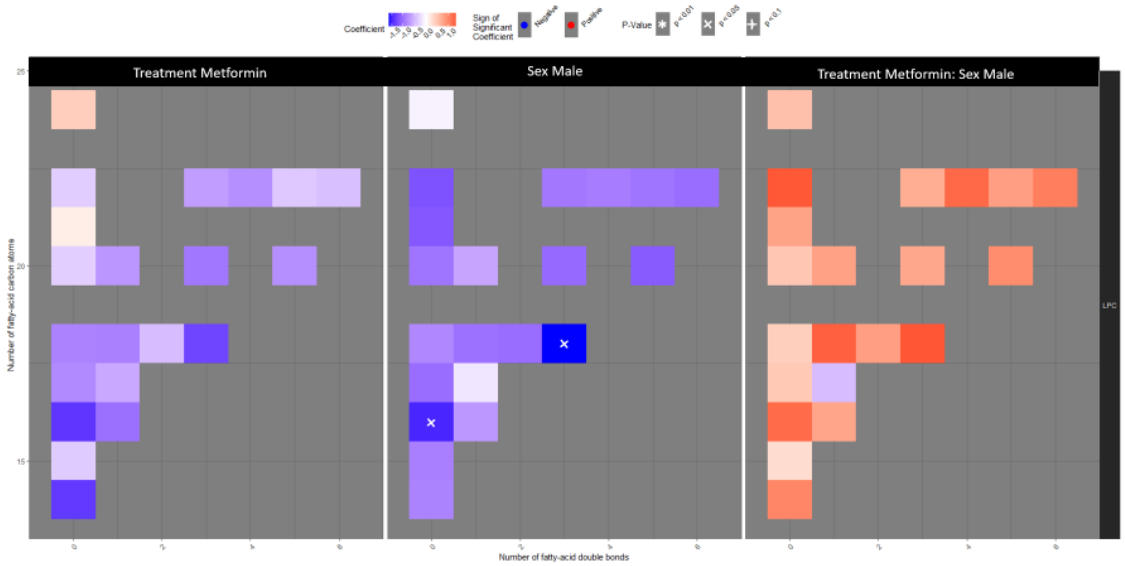

Figure 5.5: Changes of lyso-PCs in response to metformin

(A) Heatmap for all lyso-PC species based on a regression model taking group, sex and dam ID as a random effect into account. On the x-axis number of fatty-acid double bonds (saturation level of the fatty acids) and on the y-axis the number of total fatty acid carbon atoms can be found.

5.3.3 Transcriptomic analyses of the placentas

The transcriptomic analysis identified 16110 transcripts that were expressed in the placenta. Out of these 16100 transcripts 1911 (11%) can be mapped to long non-coding RNAs (lnRNAs), pseudogenes and uncharacterised genes predicted to be protein coding, identified in the RIKEN (ending on "Rik") and Mouse Genome Informatics (MGI, starting with "Gm") projects[487]. The rest of the transcripts were mapped to the characterised coding genome. Comparison of different models used for differential expression analysis showed that an additive model assessing the effects of treatment and sex fitted the data best, with no interaction between treatment and sex observed. The PCA plots show that no outliers were identified and that no striking clustering can be observed between the four groups (Figure 5.6A). Some clustering can be seen between male and female placentas when adding ellipses which encompass 95% of the samples (Figure 5.6B).

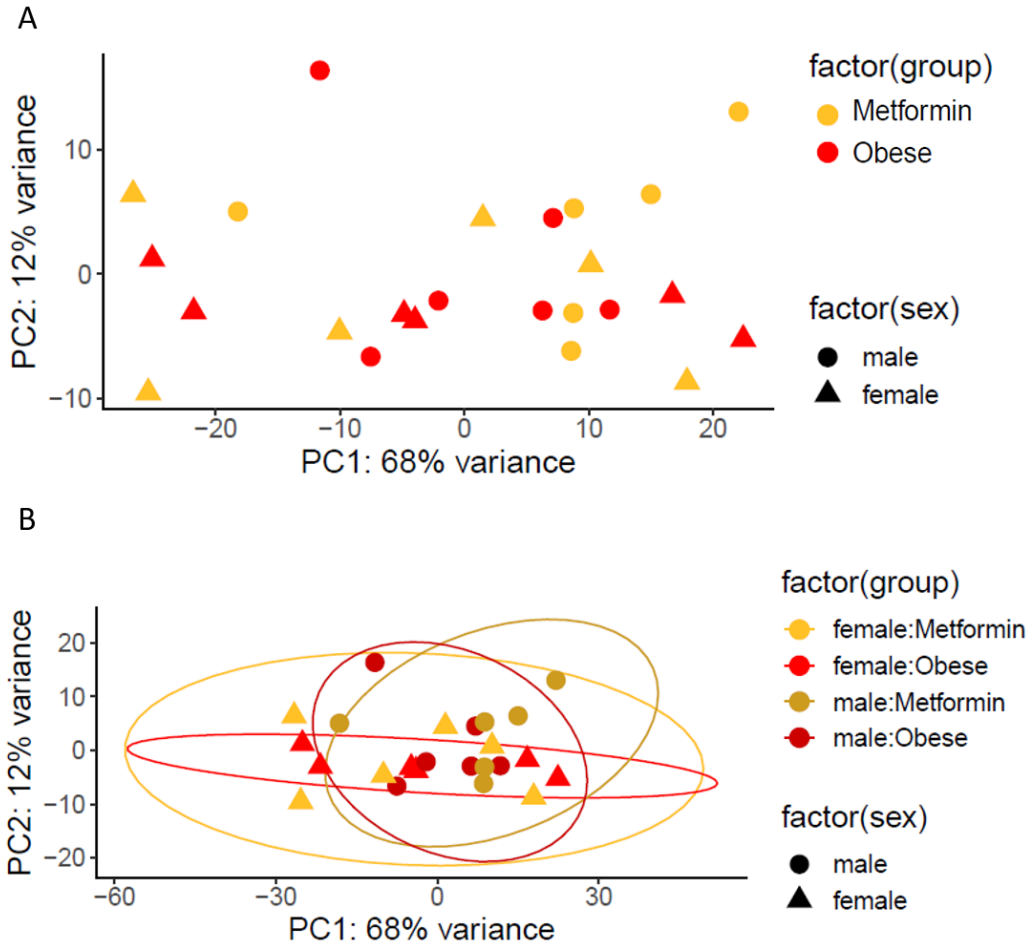

Figure 5.6: Effects of sex and metformin treatment on the placenta

(A) PCA plots showing PC1 and PC2 scores for the lipidome of obese untreated and obese metformin-treated placentas separated by sex, (B) addition of ellipses (95% confidence interval).

5.3.4 Transcriptomic differences with metformin treatment

With an adjusted p value (padj) of <0.05 only seven genes were significantly differentially expressed with metformin treatment: two prolactin genes (Prl2c5, Prl4a1), the ribonuclease protein Rpp38, the long non-coding RNAs Gm26899 and Gm27786, the gene Syn3 encoding Synapsin protein and the predicted gene Gm9 encoding an, as yet, uncharacterized protein (Figure 5.7A). All seven genes had reduced expression with metformin treatment. When applying a threshold of padj <0.1, 32 more genes showed significant differential expression. Among the enriched genes with the highest fold change were Cntn2 encoding contactin 2 and genes encoding calponin 1 and a sodium channel (Figure 5.7B). Genes that are reduced in metformin-treated placentas include, in addition to those mentioned above with a p<0.05, the pseudogene 1810014B01Rik and genes encoding for a signal-recognition particle, a lectin-like receptor and long non-coding RNAs (lncRNA, Figure 5.7B). A list of all genes and their fold changes and padj values can be found in the supplement (Supplement 6, p.222). Overall, the transcriptomic changes in response to metformin are small.

A

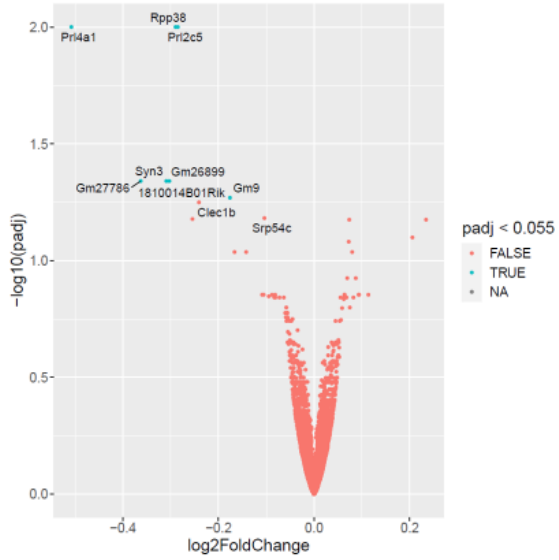

B

gene_name	Fold change	padj	transcript information/encoded protein
Cntn2	2.49	0.09	Contactin 2, cell ahesion
Cnn1	2.08	0.14	calponin1, role in placental vascular development
Scn3b	1.94	0.14	sodium voltage-gated channel
Fam171a2	1.67	0.14	Family with sequence similarity 171 member A2
Tppp	1.62	0.08	Tubulin polymerization promoting protein
Gldc	1.61	0.07	glycine decarboxylase, mitochondrial
Adamtsl4	1.36	0.14	Metalloproteinase
Bgn	1.36	0.14	proteoglycan
Tril	1.33	0.14	TRL4 interactor
Ank2	1.25	0.12	ankyrin B, interaction with ion channels
Armh4	1.20	0.14	armadillo like helical domain containing 4
Cpt1a	1.17	0.14	carnitine palmitoyltransferase
Gm14586	0.63	0.09	long non-coding RNA
Gm10790	0.62	0.09	long non-coding RNA
Clec1b	0.62	0.07	calcium-dependent lectin-like receptor
Srp54c	0.61	0.07	signal recognition particle,
1810014B01Rik	0.60	0.06	pseudogene
Gm9	**0.56**	**0.05**	**uncharacterised protein**
Gm27786	**0.54**	**0.05**	**non-coding RNA**
Syn3	**0.53**	**0.05**	**Synapsin 3, regulation of neurotransmitter release**
Gm26899	**0.52**	**0.05**	**long non-coding RNA**
Prl2c5	**0.47**	**0.01**	**prolactin**
Rpp38	**0.47**	**0.01**	**ribonuclease P subunit**
Prl4a1	**0.42**	**0.01**	**prolactin**

Enriched with metformin

Reduced with metformin

Figure 5.7: Metformin does not have major effects on the placental transcriptome

(A) Volcano plot showing the log2 fold change (shrinking applied) and the -log10 of the adjusted p value comparing obese metformin-treated placentas to obese untreated placentas as the baseline. (B) Summary of differentially expressed genes with padj <0.1, sorted by fold change and separated into up- and downregulated transcripts, the samples with the 12 highest fold changes above 1 and the 12 lowest fold changes below 1 are shown. Genes with a padj < 0.05 are highlighted in bold and a short description of the gene or encoded protein provided. A complete list can be found in the supplement (Supplement 6, p.222).

5.3.5 Sex differences in the placental transcriptome

Of the transcripts analysed from this dataset 456 genes (2.8%) showed significant ($p<0.05$) differential expression between male and female placentas (Figure 5.8). Not applying a threshold to remove genes which are not expressed in more than 50% of samples validates our dataset, as Y-chromsome-located genes (Ddx3y, Eif2s3y, Kdm5d and Uty) show a high fold change as they are not expressed in the female placenta (Figure 5.9A). Thresholding removes these genes (as they are not expressed in the female tissue) (Figure 5.9B). 24 genes located on the X chromosome are among the significantly differentially expressed genes, one of them, the lncRNA Xist, has been removed in Figure 5.9C to allow better visualisation of the volcano plot (Figure 5.9C). The volcano plot shows reduced expression of several prolactins in the male placenta and enrichment of the genes Ogt, Taf (both located on the X chromosome) and Eif2s3x in the female placenta. The majority (432/456) of genes that were identified as being differentially expressed were not located on the sex chromosomes.

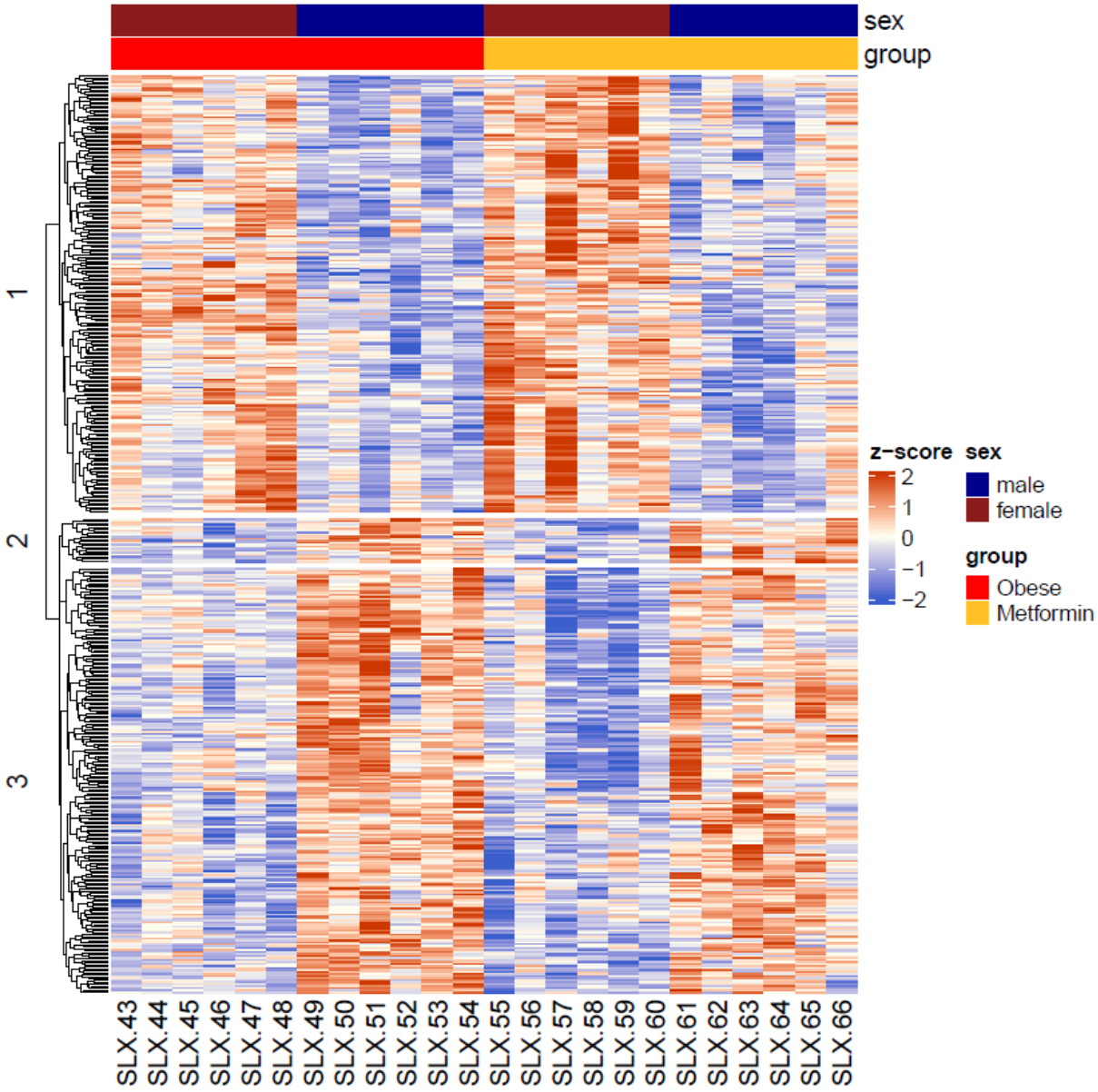

Figure 5.8: The placental transcriptome is sexually dimorphic

Heatmap showing the 456 genes that are significantly different (padj<0.05) between male and female placentas.

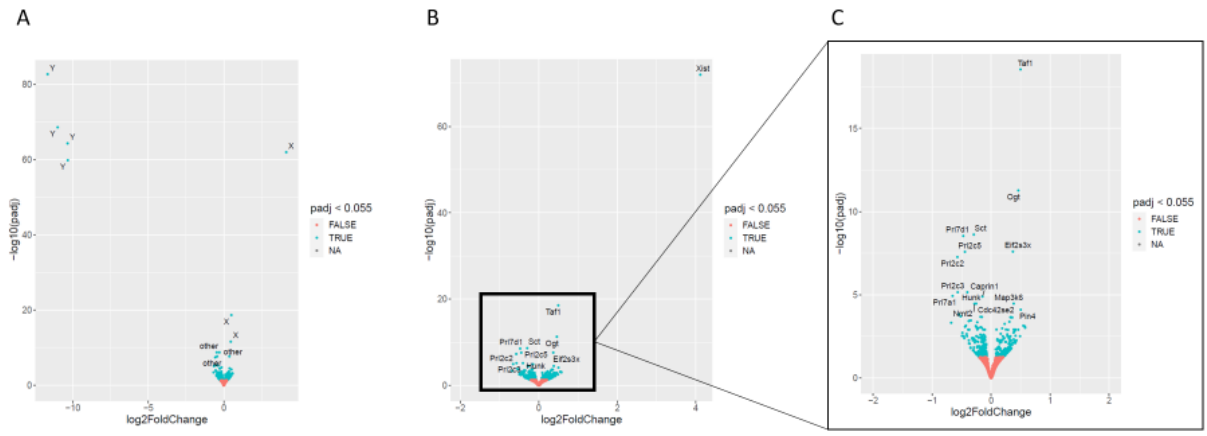

Figure 5.9: Overall sex differences across all groups

(A) Volcano plot with all genes without thresholding to remove genes not expressed in more than 50% of samples, showing X- and Y-linked genes. (B) Analysis was performed with application of the threshold: volcano plot showing the log2 fold change (shrinking applied) comparing female placentas with male placentas that are used as the baseline with (C) X-linked Xist removed to zoom into the volcano plot.

Of the significantly differentially expressed genes 234 had reduced expression in the female placenta whereas 222 genes were enriched in the female compared to the male placenta. A list of all 456 genes with their fold change and padj can be found in the supplement (Supplement 7, p.223). Out of the list of differentially expressed genes between male and female placenta those with the 15 highest and lowest fold changes are presented in Table 5.2. Highest fold change observed between the male and female placenta is 2.2 and lowest fold change is 0.39. In the female placenta genes including Igha encoding an immunoglobin constant and Cftr encoding a cystic fibrosis transmembrane conductance regulator are enriched. In the male placenta genes such as Cxcl1, encoding a chemokine ligand attracting neutrophils, Il1α encoding interleukin 1α and multiple prolactin genes (Prl2c3, Prl4a1, Prl7a1) are enriched (i.e. downregulated in female placenta).

Ontology analysis of all differentially expressed genes (padj<0.05) showed that pathways that were enriched in the female placenta were related to regulation of Notch and Wnt signalling, leukocyte differentiation and angiogenesis (Figure 5.9A). In the male placenta key enriched pathways are the negative regulation of natural killer cell cytotoxicity and the positive regulation of JAK-STAT signalling (Figure 5.9B).

gene_name	fold change	padj	chromsome	transcript information/encoded protein
Xist	17.61	1.1E-72	X	lncRNA
Gm8488	2.23	4.8E-03	autosomal	predicted gene
Prkg2	2.19	0.03	autosomal	cGMP-dependent protein kinase
Igha	2.11	1.0E-03	autosomal	processed pseudogenes
Cftr	2.08	0.01	autosomal	cystic fibrosis transmembrane conductance regulator
Arsj	2.07	0.02	autosomal	sulfatase
Cck	2.02	0.01	autosomal	cholecystokinin
Camk2a	2.01	0.03	autosomal	calmodulin-dependent protein kinase
Zfp618	1.99	6.9E-03	autosomal	zinc finger protein
Clic3	1.98	0.05	autosomal	chloride intracellualr channel
2410004P03Rik	1.95	0.03	autosomal	uncharacterised protein
Abcc8	1.90	0.03	autosomal	ATP binding casette subunit
Paqr5	1.88	8.4E-04	autosomal	progesterone receptor
Ccdc160	1.87	0.02	X	coiled-coil domain containing
Ptprr	1.86	0.02	autosomal	protein tyrosine phosphatase receptor
Il1a	0.63	3.2E-03	autosomal	interleukin 1a
Myo16	0.63	1.7E-02	autosomal	myosin 16
Prl2c3	0.62	7.5E-06	autosomal	prolactin
Prl4a1	0.62	1.6E-04	autosomal	prolactin
Gm38393	0.62	2.0E-03	autosomal	predicted gene
Gm20541	0.61	3.4E-02	autosomal	pseudogene
Zcchc18	0.57	2.2E-02	X	Zinc Finger CCHC-Type Containing protein
Pcdhgc4	0.54	5.3E-02	autosomal	protocadherin
Prl7a1	0.54	1.2E-05	autosomal	prolactin
Gm11427	0.51	3.3E-02	autosomal	pseudogene
Hoxd13	0.50	3.1E-03	autosomal	Homeobox D13
Otoa	0.50	9.2E-03	autosomal	Otoancorin
Cxcl1	0.49	4.3E-03	autosomal	C-X-C Motif Chemokine Ligand 1
Tmem114	0.44	5.7E-03	autosomal	Transmembrane Protein 114
Sohlh2	0.39	5.1E-04	autosomal	Spermatogenesis And Oogenesis Specific transcription factor

Upregulated in females

Downregulated in females

Table 5.2: Differentially expressed genes between male and female placenta

The 15 genes with the highest fold change and greatest decrease respectively are shown together with the adjusted p value (padj<0.05), the gene name, chromosomal location (sex chromosome or autosome) and a short description of the gene or encoded protein, the complete table can be found in the supplement (Supplement 7, p.223).

A

enriched in the female placenta

GO biological process complete	fold enrichment	FDR
cardiac septum morphogenesis (GO:0060411)	7.78	3.4E-02
regulation of Notch signaling pathway (GO:0008593)	7.07	4.7E-02
Notch signaling pathway (GO:0007219)	6.91	1.1E-02
cardiac septum development (GO:0003279)	6.75	1.1E-02
cell-cell signaling by wnt (GO:0198738)	4.29	3.3E-02
Wnt signaling pathway (GO:0016055)	4.29	3.3E-02
regulation of canonical Wnt signaling pathway (GO:0060828)	4.2	3.6E-02
regulation of leukocyte differentiation (GO:1902105)	3.95	1.8E-02
angiogenesis (GO:0001525)	3.89	2.1E-02
cell surface receptor signaling pathway involved in cell-cell signaling (GO:1905114)	3.87	3.5E-02
blood vessel development (GO:0001568)	3.86	3.7E-04
regulation of cellular response to growth factor stimulus (GO:0090287)	3.83	3.6E-02
vasculature development (GO:0001944)	3.83	3.1E-04
blood vessel morphogenesis (GO:0048514)	3.81	3.7E-03
regulation of hemopoiesis (GO:1903706)	3.45	3.1E-02

B

enriched in the male placenta

GO biological process complete	fold enrichment	FDR
protection from natural killer cell mediated cytotoxicity (GO:0042270)	55.02	3.7E-05
positive regulation of lactation (GO:1903489)	33.62	8.5E-07
regulation of lactation (GO:1903487)	32.42	5.5E-07
negative regulation of natural killer cell mediated cytotoxicity (GO:0045953)	29.42	4.5E-05
negative regulation of natural killer cell mediated immunity (GO:0002716)	28.24	4.9E-05
glomerular epithelial cell differentiation (GO:0072311)	23.73	1.8E-02
glomerular visceral epithelial cell differentiation (GO:0072112)	23.73	1.8E-02
renal filtration cell differentiation (GO:0061318)	23.73	1.7E-02
negative regulation of leukocyte mediated cytotoxicity (GO:0001911)	23.53	1.3E-04
glomerular epithelium development (GO:0072010)	21.23	2.2E-02
negative regulation of cell killing (GO:0031342)	20.17	2.1E-04
positive regulation of receptor signaling pathway via STAT (GO:1904894)	16.53	9.7E-06
positive regulation of receptor signaling pathway via JAK-STAT (GO:0046427)	16.5	3.9E-05
positive regulation of pri-miRNA transcription by RNA polymerase II (GO:1902895)	13.16	1.3E-04
negative regulation of lymphocyte mediated immunity (GO:0002707)	13.01	4.2E-04

Figure 5.9: Ontology analysis of the differentially expressed genes between male and female placentas

Gene ontology biological processes and the fold enrichment is shown together with the false discovery rate for pathways enriched in the (A) female and (B) male placenta. Only the first 15 hits with the highest fold enrichment are exemplarily shown here, a complete table can be found in the supplement (Supplement 8, p.233). Analysis was performed with http://geneontology.org/

5.4 Discussion

The aim of this chapter was to explore the potential effects of metformin on the placenta which could explain why metformin exposed fetuses remained growth restricted despite normalisation of maternal metabolism and uterine artery function. Given the scarcity of data on metformin's effects on the placenta and given the multiple different pathways of metformin action described to date in adult tissues, an explorative approach was used. Transcriptomic analyses did not show major differences between the obese untreated and obese metformin-treated placenta. But the transcriptomic analysis highlighted sex differences in the placenta which is of growing interest in the field of developmental programming. Lipidomic analysis also showed sex differences and sexually dimorphic responses to metformin treatment. Specifically in the female placenta metformin treatment led to reduced carnitine levels together with reduction of lyso-PCs and PS. In the male placenta however PS levels were increased upon metformin treatment as was sphingosine (18:0).

5.4.1 Lipid metabolism of the placentas

In both the male and female placenta metformin treatment led to reduced levels of triglycerides with lower total carbon atom number. The analysis performed here does not provide the exact identification of fatty acid species attached to the glycerol in the triglyceride, it is thereby difficult to hypothesize on the biological explanation for the specific reduction in triglycerides with lower carbon atoms. However, the heatmap also showed that even for those triglycerides with higher carbon atom numbers a trend for a reduction with metformin treatment could be seen despite not being significant. Reduction of placental triglycerides with metformin treatment is likely due to reduced fat mass and liver steatosis in the dams, indicative of improved metabolic health. Maternal lipoproteins are taken up by the placenta as a whole or maternal triglycerides are hydrolysed by lipases and fatty acids transferred across to the placenta via fatty acid transporters[488]. In the placenta fatty acids are then esterified for storage to triglycerides, with fatty acids being released to the fetus if needed. For a long time glucose was thought to be the key nutrient transferred across the placenta but recent years have highlighted the importance of fatty acid transfer to the fetus for fetal growth and brain development, especially in the third trimester[489]. It has been shown that placentas from obese and glucose-intolerant women have increased levels of trigylcerides[490,491]. This is hypothesized to be a protective mechanism protecting the fetus from lipotoxicity via placental lipid storage[492]. In placentas from obese women proteins involved in lipid metabolism and storage such as fatty acid transporters and perilipin coating lipid droplets are increased[490]. In trophoblast cultures insulin and oleic acid (a long-chain fatty acid) can induce changes in placental lipid handling, highlighting the role of maternal metabolic health in placental lipid handling[490].

Based on the current findings, the reduction in placental triglyceride content likely reflects a beneficial change of metformin action. The reduction in lipid content could explain the observation that only

obese untreated placentas but not obese metformin-treated placentas were heavier compared to control placentas (chapter 4). Despite this potentially beneficial effect other detrimental obesity-induced placental structural changes and fetal growth restriction (chapter 4) were not corrected with metformin treatment, this could be linked to other effects of metformin on the placenta that are not necessarily beneficial.

A notable effect of metformin was to reduce carnitine levels in the placenta, which might not reflect a positive change. Total carnitine levels were specifically reduced in the female placentas. However detailed analysis showed that specifically free carnitine, needed for shuttling fatty acids into mitochondria for fatty acid oxidation, was reduced with metformin treatment in both sexes. Carnitine is transported into the placenta via OCTN2, which is also involved in metformin transport[493] (see chapter 4). No data exists regarding metformin's potential to competitively inhibit the OCTN2 transporter, but a cancer drug (etoposide) a substrate of OCTN2, has been shown to reduce carnitine transport via competitive inhibition[494]. Therefore, the common transporter of metformin and carnitine could be an explanation for reduced carnitine levels in the placentas from obese metformin-treated dams, which could in turn lead to a reduced supply of carnitine to the fetus. Reduced carnitine levels in the fetus have been linked to preterm birth and fetal growth restriction[495,496]. Carnitine is important for the fetus to enable sufficient fatty acid oxidation with energy production via fatty acid oxidation being important during fetal development[497]. Given the reduced carnitine levels in the obese placentas treated with metformin this could partially explain the reduced fetal growth (observed in both sexes) despite improved uterine artery blood flow and maternal metabolic health with metformin treatment. Additionally it could also explain the reduced birthweight found in human studies in babies from GDM mothers treated with metformin rather than insulin[341]. Interestingly two human studies, one retrospective study and the Metformin in Gestational diabetes (MiG) trial, showed a higher rate of preterm birth with metformin treatment[339,498]. It is therefore important to follow this up further by assessing carnitine levels in placentas and babies from mothers treated with metformin.

Metformin treatment led to a significant reduction of lyso-PC in the female placenta. Reduced lyso-PC levels in serum from healthy individuals after metformin treatment were suggested as a biomarker for metformin use[499]. Lyso-PCs have also been previously shown to be reduced with metformin treatment (at 1mM and 0.5mM respectively) in primary hepatocytes[500]. One of the roles of lyso-PCs in the placenta is thought to be the transfer of the fatty acid DHA to the fetus as DHA (C22:6) is mainly found in lyso-PCs in the placenta[501]. DHA is important for fetal brain development. Further analysis of the lyso-PCs showed that the specific lyso-PC(22:6) was reduced with metformin treatment, however this was not statistically significant.

Sphingosine (18:0) was increased with metformin treatment in the male placenta. Altered sphingolipid metabolism has previously been observed in preeclamptic placentas with increased levels of

sphingomyelins and reduced sphingosine intermediates in placental vessels[502]. These changes are thought to lead to reduced levels of sphingosine-1-phosphate, which is known to regulate endothelial function[502]. In line with beneficial effects of metformin on the preeclampsia-like phenotype shown in chapter 3, metformin increased sphingosine levels in male placentas. Interestingly in the obese untreated placentas a trend for reduced sphingosine levels is present in the male compared to the female placentas at baseline. This could be associated with an increased preeclampsia risk for the male fetus. In human pregnancies male fetuses are more likely affected by specifically late-onset preeclampsia[503]. The mechanisms behind these effects of metformin on lyso-PC and sphingosine in metformin-treated placentas remain to be elucidated but they show that direct effects of metformin on the placenta are possible. The sex-specific effects seen here suggest that the observed lipid changes in the placenta can be driven via direct effects of metformin rather than solely via effects of metformin on maternal lipid metabolism.

Another sexually dimorphic effect was observed regarding phosphatidylserine levels. In female placentas phosphatidylserine levels were reduced with metformin treatment, whereas the opposite effect was seen in the male placentas. Phosphatidylserines are well-known for their role in regulation of apoptosis where exposure on the cell membrane leads to phagocytosis of the cell[504]. No data exists regarding the function of phosphatidylserine in the placenta or whether a broad increase in phosphatidylserine rather than specific localisation change to the cell membrane is linked to apoptosis. In chapter 4 we showed increased Bcl-2 and Bax levels in the male placentas exposed to metformin. One could thereby hypothesize that metformin treatment could affect apoptosis in the male placenta, but this needs further assessment.

5.4.2 Transcriptomic changes associated with metformin treatment

Very limited data exists on transcriptomic analyses of placentas exposed to metformin. Hosni et al. recently showed that a combined metformin and glyburide treatment in rats that were fed a high fat and sugar diet and were injected with streptozotocin led to only 8 differentially expressed genes compared to untreated obese and diabetic rats[349]. In the current study we identified only 7 genes significantly downregulated with metformin treatment (padj<0.05). Two of these genes were prolactins: Prl2c5 from the family of proliferins known to have angiogenic functions and Prl4a1 shown to suppress NK cells[505]. It is difficult to hypothesize based on this data and the little overall transcriptomic changes with metformin whether the reduction of the prolactins has functional consequences for the metformin-treated placenta and/or the fetus e.g. via alteration of angiogenesis. Interestingly metformin has been used in patients with hyperprolactinaemia due to its potential effects on pituitary hormone secretion[506,507]. However, an effect of metformin on prolactin gene expression in tissue has not been identified previously. Among the differentially expressed genes with a padj <0.05 was also one lncRNA. When applying a threshold of padj<0.1 more lncRNAs are significantly

downregulated with metformin treatment. A few studies have reported effects of metformin on regulation of lncRNAs[508]. Metformin could thereby potentially impact lncRNAs in the placenta, which could have functional consequences. This is only hypothetical but would be interesting to follow up further. The absence of major transcriptomic changes with metformin treatment matches our structural observations in which metformin treatment did not improve the obesity-induced reduction in placental efficiency and the labyrinthine zone or the increase in calcification. Additionally, our analyses showed no effects on AMPK or mTOR signalling in the placenta. In the future it will be helpful to perform proteomic analyses to complement the explorative approaches described in this chapter, this could help to characterize the effects of metformin on the placenta.

5.4.3 Sexual dimorphism

456 genes were significantly differentially expressed between male and female placentas. The importance of sexual dimorphism has become more and more evident and important in the field of developmental programming. Already a decade ago researchers suggested the male fetus was more vulnerable to a suboptimal *in utero* environment[59]. Male offspring exposed to maternal overnutrition are more likely to develop adiposity later in life[509], whereas female offspring have increased risks for adiposity development in response to maternal undernutrition[510]. The notion of increased vulnerability in the male offspring is therefore not clear-cut and a complex issue. However in fetal development and growth the male fetus is known to have an increased growth rate with a placenta supporting growth rather than keeping reserve functions to combat suboptimal environments[511]. A study feeding mice high and low calorie diets in pregnancy showed that the majority of gene expression changes was observed in the female placenta, highlighting the potential for better adaptation in the female placenta[512]. It needs to be noted that our identified sex differences likely are a sexually dimorphic response to the maternal obesogenic environment in our study.

Male fetuses are more likely to be delivered preterm and show increased perinatal mortality[513]. An increased association of gestational diabetes and late-onset preeclampsia in pregnancies with a male fetus has been shown in a recent meta-analysis[503]. Impaired uterine artery vascular adaptation to pregnancy which is increased in mothers carrying a male fetus could be the reason for the increased risk of late-onset preeclampsia[503]. In recent years sexual dimorphism in the placenta has therefore been of increasing interest as a potential key mediator of sexual dimorphism in fetal development, the occurrence of pregnancy complications and consequences for the offspring.

A human study comparing male and female placentas showed in line with our transcriptomic analysis 399 differentially regulated genes[514]. In their study they showed enrichment of pathways related to TGFβ and Wnt signalling in female placentas. Our study also highlighted Wnt signalling pathways enriched in the female placenta. As in our study most sexually dimorphic genes, except for sex chromosome linked genes, show a modest effect size of differential expression. This was shown in a

study looking at sexual dimorphism in the transcriptome of multiple somatic tissues (liver, adipose tissue, muscle, brain) where most differentially expressed genes showed only a fold change of below 1.2[515]. A recent human study showed that a large amount of sex differences was due to genes escaping X-inactivation in the female placentas, which the researchers linked to increased vulnerability of the male fetus when exposed to a suboptimal environment[516]. Many of these genes code for proteins involved in transcriptional and translation regulation and are thereby promising candidates to drive sex differences in the placenta. In our analysis X-linked genes were also among the differentially expressed ones and made up 5% of all differentially expressed genes (24 X-linked genes out of 456 differentially expressed genes overall). However, the majority of differentially regulated genes between the sexes were linked to autosomes.

Genes related to JAK-STAT signalling and immune regulation such as negative regulation of NK cell cytotoxicity were increased in the male placentas in our study. The male placenta has previously been shown to have a heightened acute immune response as shown by increased placental chemokine levels (including CXCL1) upon induction of maternal infection with injection of lipopolysaccharide[517]. Our results showed increased levels of Cxcl1 in the male placentas compared to the female placentas, indicative of an inflammatory state of the male placenta, here likely caused by maternal obesity per se. Sexual dimorphism in immune function in the placenta was also shown in a study by Cvitic et al. which showed increased inflammatory and immune genes in male placentas which they linked to the increased risk of male fetuses to be born preterm and show placental inflammation[518]. A recent study from 2020 investigated sexual dimorphism in the maternal-fetal crosstalk in early first trimester placentas and showed mainly immune genes being differentially expressed between males and females[519]. They highlight in their study the need to further understand the downstream implications of these differences. However, their study showed enrichment of cytokine signalling pathways in the female rather than the male placenta. Some of these differences could be explained by the fact that the human placentas used for transcriptomic analyses stem from healthy women and assess baseline sexual dimorphism, whereas our analysis assesses sexual dimorphism in a suboptimal pregnancy complicated by maternal obesity. These studies however might be crucial in identifying the underlying mechanism that lead to sex differences regarding adverse pregnancy outcomes.

It needs to be noted that in the male placenta immune pathways related to negative regulation of NK cell mediated cytotoxicity are increased, the negative regulation could reflect an attempt to compensate for a heightened inflammatory state in the male placenta. Similarly, it has been hypothesized that increased prolactin expression shown in the male placenta could be a mechanism to protect the male fetus from a maternal immune attack given the reduced regulation of the immune system in a male pregnancy[520]. As prolactins are known for their important role in mediating

immunomodulation in pregnancy allowing acceptance of the conceptus by the mother this is plausible and our data indeed shows higher prolactin expression in the male placentas.

5.4.4 Conclusions

This chapter highlighted no major transcriptomic changes upon metformin treatment; however it highlighted the importance of assessing sex differences in the placenta, especially in response to an adverse maternal environment. We also showed that metformin treatment affected lipid composition in the placenta in a sexually dimorphic manner. In both sexes, especially triglycerides with lower carbon atom number were reduced with metformin. This likely indicates a beneficial effect of metformin in reducing the increased lipid content in the placenta induced by the obese glucose-intolerant environment. However, the exact implications of these changes and potential metabolic effects in the placenta are not known and further follow-up of placental lipid changes with metformin treatment is needed. As highlighted in Table 5.1 no lipid metabolism analyses in response to metformin treatment have been reported in the placenta to date. Effects of metformin exposure on carnitine levels could contribute to the effects of metformin on fetal growth and preterm birth and require further follow up. Similarly, the sexually dimorphic response to metformin with regards to phosphatidylserine levels warrants further investigation. Increased apoptosis in the male placentas in response to metformin could be a mediating factor of long-term risks. A recent study from our lab showed increased adiposity at 8 weeks of age in offspring exposed to metformin *in utero*, this was specifically seen in male offspring[473].

We can thereby confirm direct effects of metformin on the placental lipidome which require further assessment as they can be linked to apoptosis, increased preterm birth risk and fetal growth.

Key findings

- Metformin treatment reduced triglycerides with lower carbon atom number and free carnitine in the placenta. In the female placenta lyso-PCs were reduced and in the male placenta sphingosine (18:0) increased. Placental phosphatidylserines were increased in male and decreased in female placentas with metformin treatment.
- The potential impact of metformin on apoptosis in male placentas and reduced carnitine levels in both sexes on fetal growth and preterm birth needs further investigation.
- Metformin treatment did not lead to major transcriptomic changes in the obese placenta.
- Clear sex differences were observed between the male and female placental transcriptome showing differences in immune regulation, JAK-STAT signalling and prolactin expression. This highlights the importance of taking sex differences into account in the field of developmental programming.

6 The role of placental extracellular vesicles and their miRNA content in programming

6.1 Introduction

6.1.1 Extracellular vesicles (EVs)

Extracellular vesicles are membranous vesicles that are loaded with proteins, lipids, mRNA and small RNA species and secreted by a variety of different cell types. First described in the 80s EVs, termed exosomes at the time, were thought to just be a waste product of the secreting cell. Experiments at the time showed that such vesicles were secreted upon maturation of reticulocytes to remove un-needed material during the maturation process[521]. However, over the past two decades the potential role of EVs has expanded to include multiple biological functions in many different physiological and pathological settings. In 2002 little was known about EVs, but a lot of research focussed on EVs from dendritic cells. They were shown to be involved in antigen presentation and could activate T helper cells[522]. This feature was harnessed to develop cancer immunotherapies with a study in 2002 showing that EVs from cancerous tissue pulsed onto dendritic cells leads to a beneficial expansion of tumour-specific T lymphocytes, a concept that has since been explored further[523,524]. The first evidence that EVs can transfer miRNAs and mRNAs between cells and therefore represent a novel route of interorgan communication was provided in 2007[525]. In the past decade EV research has increased exponentially[526] and it has been demonstrated that EVs play a crucial role in cancer metastasis, neurodegenerative disease as well as metabolic health[524,527,528]. In metabolic diseases it is thought that EVs play a role in communication between organs that could contribute to links between adiposity and insulin resistance[529]. EVs from adipose tissue macrophages were shown to regulate adipose tissue function and insulin sensitivity with macrophage EVs from obese mice leading to impaired glucose tolerance and insulin sensitivity in lean recipients[530]. Due to their high stability in various body fluids, EVs are also increasingly investigated as biomarkers of diseases such as cancer, renal dysfunction (via urinary EVs) and even male fertility (via EVs from seminal fluid)[531–533]. With the increasing amount of EV research a standardized nomenclature was introduced to avoid confusion between the terms exosomes, micro-vesicles and extracellular vesicles, that have all been in use since 2000. This was provided in a position statement from the International Society for Extracellular Vesicles (ISEV) in 2014[534]. Since then, the term extracellular vesicle includes three subtypes of vesicles: exosomes, micro-vesicles and apoptotic bodies. Exosomes (30 – 150 nm diameter) are formed via the endosomal route, which starts with an endosome with smaller intraluminal vesicles being formed by inward budding of the endosomal membrane. This subsequently forms a multivesicular body (MVB) that can then fuse with the plasma membrane to release its vesicle content (Figure 6.1). Recent research has shown that the endosomal sorting complex required for transport (ESCRT) is needed for the biogenesis of the multivesicular body itself. Before the inward budding of the endosomal membrane, lipids and membrane proteins such as

tetraspanins are clustered into microdomains from which cytoplasmic content is sorted towards the microdomains either without the involvement of ESCRT or with the help of ESCRT I and II[535]. Both pathways then use ESCRT III for the inward budding of the intraluminal vesicles itself. Another subtype of EVs are micro-vesicles (100 nm – 1µm) that form by budding off from the cell's plasma membrane (Figure 6.1). The micro-vesicle biogenesis is less well understood but includes sorting of lipids, membrane proteins and cytoplasmic content on the membrane via ESCRT I, the actual budding is then assisted by ESCRTIII and involves the cytoskeleton[535]. Apoptotic bodies (50 – 5000nm) are also a subtype of EVs but are often larger than the extracellular vesicles of biological interest and formed from the plasma membrane during apoptosis (Figure 6.1). As to date it is still very difficult to confirm the endosomal route for the exosome biogenesis the term EVs rather than exosomes is recommended by ISEV[534]. Throughout this chapter the term EV is therefore used.

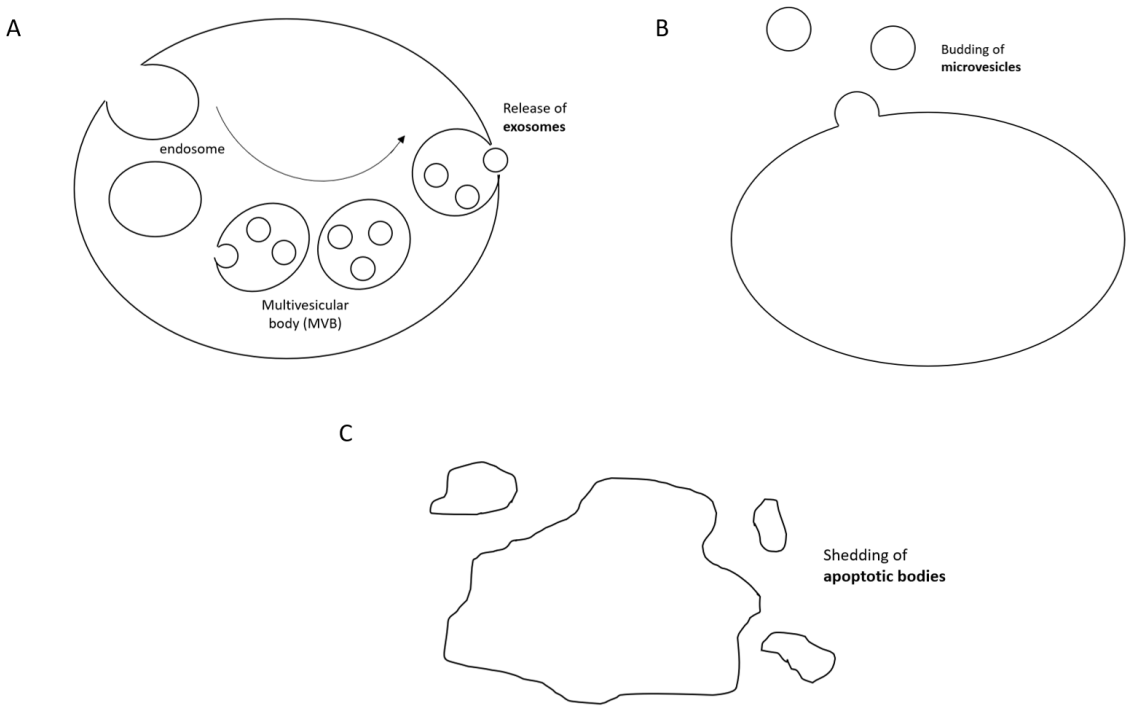

Figure 6.1: Different types of extracellular vesicles

Extracellular vesicles include three different subtypes: (A) exosomes, (B) micro-vesicles and (C) apoptotic bodies.

An important question in EV research is whether and how the sorting of EV cargo as well as the fate and target destination (cell or tissue type) of an EV is regulated. These basic mechanisms have been extensively investigated in recent years. Sorting of proteins into EVs is thought to be influenced by the fact that some proteins favourably associate with tetraspanins or the lipid microdomains that build the starting point of the exosome and micro-vesicle formation[536,537]. Interestingly it has been shown that

small RNAs are not just loaded randomly into the EVs. This is a relevant observation in the context of the potential biological function of inter-organ or intercell communication via small RNA species of EVs. In 2013 Villarroya-Beltri et al. [538] showed that activation of primary T lymphoblasts led to a different miRNA and mRNA content in the cell compared to the secreted EVs, pointing towards specific sorting of RNAs into EVs. In their study they showed that RNAs with the motif GGAG and CCCU were enriched in EVs. These motifs are recognized by the heterogeneous nuclear ribonucleoprotein A2B1 which sorts these RNAs into EVs. Since then other possible pathways for RNA sorting into EVs have been proposed such as sorting via components of the ESCRT complex or binding to other RNA-binding proteins[539]. One of these RNA-binding proteins is Argonaute 2 (Ago2), which is needed for miRNA maturation and has been shown to be involved in EV sorting. Sorting of Ago2 into exosomes is regulated via KRAS-dependent MEK-ERK signalling. An activating mutation in KRAS that inhibited the sorting of Ago2 and Ago2-associated miRNAs into EVs, highlighted mechanisms for regulation of EV cargo sorting and secretion via external stimuli[540]. However some studies don't report differences between the RNA content in the cell and the secreted EVs supporting the notion of random sorting of RNA into secreted EVs[541]. Given the increased data on the biological function of EVs in different diseases it is of current interest to disentangle the mechanisms that affect the composition of the EV content. Similarly, the fate of EVs within the cell and the body is of interest. Within the cell the MVB can be targeted towards degradation within the lysosome or be transported towards the membrane for secretion of exosomes. The presence of ESCRT components appears to play a crucial role in targeting MVBs to the plasma membrane rather than the lysosome[535]. Additionally the level of cholesterol in the membrane of the MVB influences its fate with cholesterol-enriched MVBs being targeted towards secretion[542].

Once secreted, EVs can either be taken up again by the secreting cell working in an autocrine fashion or be taken up and/or act on the cell surface of a distant cell type. Recent years have elucidated some patterns regarding the targeting of EVs with the first study demonstrating the involvement of EVs in organ-specific metastasis of cancer. It was shown that EVs from cancer cell lines are preferentially targeted to cells from the tissue type which is known to be the main metastasis location. The researchers showed that this was due to certain integrins on the exosomes secreted e.g. from breast and pancreatic cell lines[543]. These integrins interacted specifically with the extracellular cell matrix of lung and/or liver tissue dependent on the known organotropism of the cancer cell line. Another study has shown the contribution of the tetraspanin composition on EVs in targeting to specific cell types[544].

6.1.2 Isolation and characterisation of EVs

In the 2000s the most common method for isolation of EVs (at that time still termed exosomes) was differential ultracentrifugation shown in a paper from 1996 to isolate EVs from culture medium supernatant[545]. The idea is to first pellet cells (300 g, 10 minutes), then dead cells (2000 g, 10 minutes),

then cell debris (10000 g, 30 minutes) and eventually the EVs (10000 g, 1 hour). A few years later differential ultracentrifugation remained the main method highlighted in a method paper from 2006 by Théry et al. Their paper was the first paper that described the different techniques used for the isolation and characterisation of EVs[546]. Despite the development of novel methods for EV isolation ultracentrifugation remained by far the most popular isolation method in a survey performed by ISEV in 2016[547]. This is likely due to the low cost of the method, the ease of use and the ease of scaling the method up when using large amounts of starting material. However studies in recent years have identified challenges and disadvantages of differential ultracentrifugation: the EVs are exposed to harsh forces that might alter their integrity and consequently their biological function and contaminants like lipoproteins and even free RNA can co-isolate with the EV pellet[547]. Additionally differential ultracentrifugation might not be the best method when limited sample is available. In recent years size-exclusion chromatography (SEC) has gained popularity in the EV field with a survey in 2020 showing that most isolations are still performed with differential ultracentrifugation but that SEC is used significantly more compared to the survey in 2016[526]. SEC is thought to be a gentler approach compared to centrifugation leaving EVs more intact[548]. In SEC the sample is added onto a porous polymer column and eluted in buffer, small particles are eluted quickly early on whereas big particles and protein contaminants are retained in the column and only elute later. SEC is often preceded by centrifugation steps that remove cell debris prior to the SEC. Due to a similar size of lipoproteins compared to EVs, lipoprotein contamination can be a problem during EV isolation via SEC especially in serum samples[549]. Aside from SEC and ultracentrifugation multiple other methods have been established, including density-gradient centrifugation, commercial kits that isolate EVs via precipitation, ultrafiltration and immune-based methods e.g. isolating EVs via beads coated with antibodies against EV-enriched membrane proteins[550]. To date no gold standard method for EV isolation exists as the method of choice highly depends on the sample type and volume available, the downstream application as well as the funds and equipment available. Many studies however have assessed the differences between the isolation methods and Figure 6.2 gives an overview of the differences regarding yield and purity of EVs.

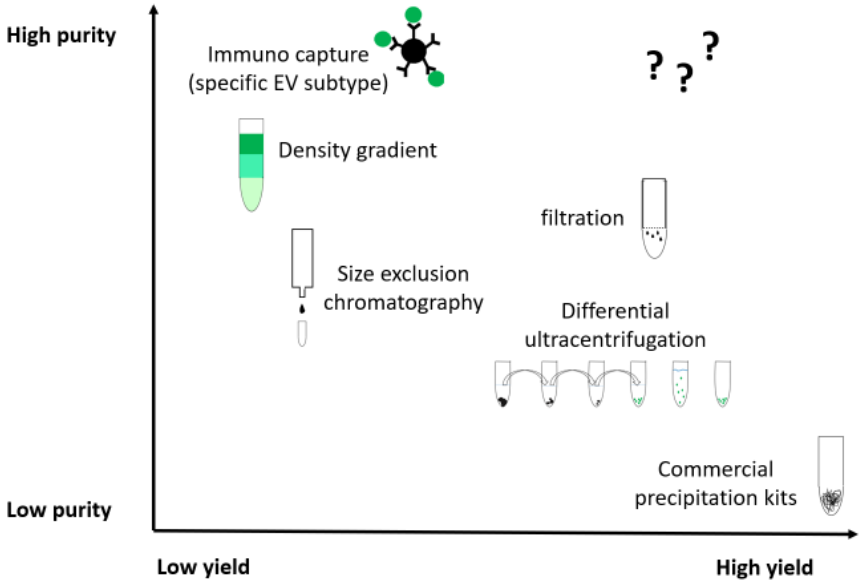

Figure 6.2: Methods for isolation of EVs and their yield and purity

The graphic summarizes different methods for isolation of EVs sorted by their yield and purity, a method that is shown to have a high purity and high yield has not yet been found. Figure drawn based on Théry et al. [551]

Depending on the downstream analysis it might not matter if EVs are fully intact whereas for other applications (e.g. functional assays or clinical use) it is crucial. The ultimate goal within the study presented in this chapter was to sequence the small RNA cargo of EVs isolated from placental explants. Given the increased use and recognition of SEC in the EV field we used SEC for isolation of our EVs. Other isolation techniques (differential ultracentrifugation and commercially available kits) were trialled, especially differential ultracentrifugation had a similar yield compared to the SEC and good quality of EVs. However, after consultations with an expert in the field, Dr. Sarah Stewart (La Trobe Institute for Molecular Science, Melbourne, Australia), we decided to use SEC, which is well-regarded in the field. A recent paper suggested that SEC is the best method for downstream RNA sequencing analysis compared to ultracentrifugation and commercial isolation kits[552]. In their study SEC EVs had the highest concentration of EV-specific miRNAs and the lowest level of unspecific miRNAs compared to the other isolation methods. In general, they also showed that EVs from SEC isolation were the purest EV population with the only note of caution being contamination with lipoproteins. As we are not isolating EVs from serum the disadvantage of SEC that lipoproteins are co-isolated is not a big issue for our purpose.

Given the high heterogeneity of isolation methods in EV research, consensus in the field is that a thorough characterisation of the EV population isolated needs to be carried out. This gives other

researchers the chance to understand and interpret the results carefully and allows comparison between studies. Rigor and standardization is thereby a particularly important aspect in the EV field[553]. Common methods for characterisation of EVs are western blotting, single particle tracking, electron microscopy and flow cytometry. Western blotting allows the general characterisation of the EVs with the Minimal Information for Studies of Extracellular Vesicles (MISEV) guidelines specifying the key markers that should be shown[551]. Ideally a transmembrane protein (e.g. a tetraspanin) should be shown to be present in the EVs to prove its lipid bilayer nature. Additionally, a protein involved in the biogenesis of EVs (e.g. component of the ESCRT complex like TSG101 or Alix) needs to be proven to be present. Negative markers that confirm no or only minor contamination by e.g. lipoproteins are encouraged as well. Additional characterisation can be obtained by including markers for other intracellular organelles in the western blotting analysis. This can establish that the vesicles are not derived from other secretory pathways such as the Golgi apparatus or the endoplasmic reticulum. Analysis of individual vesicles is additionally encouraged by at least two methods such as microscopy (electron microscopy being most used to visualise single EVs) and nanoparticle tracking analysis (NTA) to confirm biophysical properties. The NTA is a special microscope that can visualise the EVs as they scatter the light of a laser beam and measures their concentration. Based on Brownian motion and the Stokes-Einstein equation the diameter of the EVs can be calculated. Again, no gold standard exists regarding the characterisation of EVs but a combination of different methods is advised.

6.1.3 EVs in pregnancy

In 1893 Georg Schmorl observed placental cells and particles in the maternal circulation, mainly in women with preeclampsia[554]. Since then it has been proven that the placenta, more specifically trophoblasts, can secrete EVs[555]. One key role of placental EVs was identified around 15 years ago and is thought to contribute towards the establishment of the fetal immune privilege needed for a successful pregnancy. Fas-L was identified on placental EVs that were shown to suppress the maternal immune system by inducing apoptosis of maternal lymphocytes[556]. EVs in the uterus, termed uterosomes, are thought to be important for the fertilization and implantation of the embryo[557]. Thereby EVs are suggested to play a role in successful pregnancies.

It is now well-established that the EV concentration in serum is significantly increased in pregnant compared to non-pregnant women (50-fold) and that EVs in the serum of pregnant women increase with gestation[558]. In humans, the placental origin of EVs in the serum can be confirmed by the placental alkaline phosphatase (PLAP) being present in the human placenta and on placental EVs. Analysis of these PLAP-positive placental EVs showed lower levels of these EVs in the fetal and maternal circulation in situations of fetal growth restriction[559]. In addition to associations with fetal growth, placental EVs have also been linked to pregnancy complications such as preeclampsia and GDM. An early study from 1998 showed increased shedding of syncytiotrophoblasts into the maternal

circulation in preeclampisa[560]. These were likely particles we would today term EVs. More recent studies have indeed shown increased levels of EVs in the serum from women with preeclampsia[557]. These EVs secreted from the syncytiotrophoblast and isolated from placental perfusate bind VEGF, PLGF and TGF-β[561]. As these EVs are increased in preeclampsia they likely contribute to the endothelial dysfunction characteristic of the disease. Additionally reduced eNOS expression in EVs from preeclamptic women results in further vascular dysfunction[562]. Further evidence for the involvement of placental EVs in the development of preeclampsia comes from studies of mice that were infused with placental EVs from preeclamptic women. Both, pregnant and non-pregnant mice developed hypertension and proteinuria, hallmarks of preeclampsia in humans, when infused with placental EVs from women with preeclampsia[563]. Additionally, the EVs were shown to induce vasoconstriction, presenting a mechanism of action for the preeclamptic placental EVs.

A similar body of evidence exists for GDM pregnancies. Rice et al. detected increased EV secretion from primary trophoblast cultures when incubated with high levels of glucose[564]. The same group confirmed these findings *in vivo*, showing increased EV numbers in serum from women with GDM compared to healthy pregnant women[565]. Addition of these EVs onto Human Umbilical Vein Endothelial Cells (HUVECs) led to increased inflammatory cytokine release. A pro-inflammatory state is commonly observed in obese and GDM pregnancies[566]. Infusion of EVs from healthy pregnant women and women with GDM into non-pregnant mice showed that EVs from GDM women led to impaired glucose tolerance and impaired muscle insulin signalling[567]. The connection between GDM and placental EVs was recently proposed to allow the use of miRNA profiles of maternal serum EVs in early pregnancy to be a biomarker for the future development of GDM in later pregnancy[568].

Most of the data regarding placental EVs stems from human studies, however a study in 2019 highlighted that EV levels in serum of pregnant mice shows a similar trajectory compared to humans[569]. EV levels rose with advancing gestation and peaked at embryonic day E14.5. Only a few other studies of placental EVs have since emerged in rodents. Explant culture of the human placenta is regularly used to study the secretion of molecules, proteins and lately also EVs from the placenta[570]. In the mouse this method has not been commonly used for isolation of EVs so far with only one recent publication from 2021 that showed that isolated EVs from placental explants and showed that the EVs can target maternal immune cells directly[571]. Human and mouse placental EVs are both secreted from the syncytiotrophoblast of the placenta[572]. The use of mouse placental EVs is important in assessing potential mechanisms of actions of the EVs.

All examples described so far have focussed on the effects of EVs entering the maternal circulation, but with a Cre-reporter mouse model researchers showed that EVs could facilitate cross-talk between mother and fetus as EVs from the mother were found in the fetal circulation and vice versa[573]. It can

therefore be hypothesized that also placental EVs and their cargo could have programming effects on fetal development and consequently offspring health. The miRNA cargo of EVs could mediate these programming effects given the emerging evidence of the contribution of miRNAs in the DOHaD field[41]. However further research is needed in this area[555]. Additionally human data highlights the potential of EVs from maternal macrophages to affect the placenta, potentially to protect the fetus in the case of maternal infections[574]. This highlights the importance of EVs in pregnancy due to their mediating role in the crosstalk between mother, fetus and placenta. Many questions regarding placental EVs remain unanswered. For example, the exact biology of their biogenesis is not yet understood, it likely involves the mechanisms described under 6.1.1 but e.g. the uptake of placental EVs likely involves placenta-specific proteins such as syncytin-1 and -2 that are known to be required for the syncytialisation of the human trophoblast[575]. Additionally, it is relevant to determine the factors and composition markers of EVs that target EVs to different organs in the mother and/or the fetus. It is currently unclear how sorting of cargo into placental EVs occurs. In humans miRNAs from the chromosome 19 miRNA cluster (C19MC) are highly expressed in the placenta and also found in placental EVs, but it is not known whether a specific sorting mechanisms exists[555,576].

6.1.4 Aims

The aims of this chapter were therefore:

- To develop a pipeline for the isolation of EVs from murine placental explant supernatant.
- To thoroughly characterise isolated placental EVs to prove successful and pure EV isolation.
- To profile miRNA content of EVs isolated from placental cultures from male fetuses exposed to a maternal control or obesogenic diet *in utero* via small RNA sequencing.

6.2 Methods

Thanks to Dr. Karen Forbes, Dr. Rachel Quilang and Dr. Sarah Stewart for their help in setting up the EV isolation and characterisation in the lab. And thanks to Dr. Tim Williams, Dr. Jenni Karttunen and the Cambridge EV interest group (CEVSIG) for interesting and helpful EV discussions.

6.2.1 Placental explant culture

Placentas were obtained from the mouse model described under general methods (section 2.1). 6 male placentas per group (control and obese untreated) were cultured as explants for 24 hours. Upon dissection the placentas were placed in ice-cold PBS buffer and transferred to the lab. Placentas were then cut into three pieces of approximately equal size. The pieces were placed individually on netwells (costar 3477, 74 µm polyester mesh) in a 12-well plate filled with 3 ml medium per well (Dulbecco's Modified Eagle Medium/Nutrient Mixture F12, 2% FBS (EV-depleted, Thermo-Fisher Scientific, A2720801), 100 U/ml Penicillin and 100 µg/ml streptomycin). After incubation of the explants (37°C, 5% CO_2, 24 hours) the explant supernatant was taken and frozen on dry ice and stored at -80°C until processed further. The netwells were reused after washing in 2x Virkon solution (24 hours), rinsing in distilled water, washing in 1% Decon solution (24 hours), rinsing in distilled water and storage in 100% ethanol.

After the culture placentas were fixed in 10% formalin and embedded in paraffin by Tom Ashmore. Sections were cut at 5 µm thickness and stained for H&E as described in section 2.8 of the general methods. Scanning of the slides was performed with the Zeiss Axioscan microscopy slide scanner and visually inspected for necrotic areas.

6.2.2 Size exclusion chromatography (SEC)

For the SEC the supernatant was slowly thawn on ice and centrifuged to remove cell debris (1500 g, 10 minutes, 4°C). As the SEC columns used required an input of 500 µl, the supernatant was concentrated with Amicon Ultra-15 concentrator columns (UFC910024). Prior to use, the concentrator columns were rinsed with 15 ml PBS (4000 g, 2 minutes, 4°C), then the centrifuged supernatant was added and concentrated (4000 g, 30 minutes, 4 °C). The concentrate was collected after the first concentration and the column rinsed with PBS to collect any residuals (4000 g, 30 minutes, 4°C). The total concentrate was centrifuged again to remove large EVs (10000 g, 10 minutes, 4°C) and the sample then adjusted to a volume of 500 µL for the SEC. The SEC columns (Izon qEV original, 35 nm) were used according to the manufacturer's protocol. Briefly the columns were equilibrated to room temperature and flushed with 10 ml fresh PBS. The 500 µl sample was then loaded onto the loading frit and after a void volume of 2.5 ml (fractions 1-5) the fractions 6-15 (each 500 µl) were collected manually by flushing the column with PBS. The columns were used up to 6 times, between samples the column was washed with 20 ml of PBS. After proof of the pipeline, it was confirmed by silver staining (see 6.2.3) that fractions 6-11 consistently contained only EVs and no contamination. To avoid freeze-thaw cycles

these fractions were thereby pooled and concentrated from 3 ml to 100 µl via the Amicon Ultra-4 spin filter (UFC801024, Merck). The spin filter was rinsed with 2.5 ml PBS (4000 g, 5 minutes, 4°C). Then the samples were added and concentrated (4000 g, 10 minutes, 4°C). The filtrate was then briefly mixed via pipetting to be further concentrated (4000 g, 10 minutes, 4°C). For the actual final samples only 5 µl were taken out for analysis on the NTA and the rest was stored at -80°C until the RNA was extracted. Samples used for EV characterisation were also stored at -80°C for later Western blot and electron microscopy analysis.

6.2.3 Silver staining

8 µl of the SEC fraction was mixed on ice with 52 µl of RIPA buffer (ThermoFisher, addition of 1 PhosStopEasypack Roche tablet and 1 tablet complete Mini EDTA proteinase inhibitor Roche tablet for 10 ml of RIPA) and vortexed after 0, 10 and 20 minutes of incubation. 15 µl of 5x Laemmli buffer (5x: 20% glycerol, 2% SDS, 62.5 mM Tris-HCl (pH 6.8), 100 mM DTT, some Bromophenol blue) were added, the sample heated for 5 minutes at 95°C, before being loaded onto a 10% gel. The silver staining (Pierce, Silver Stain for Mass Spec (24600)) of the gel was performed according to the manufacturer's protocol, the only difference was that the gel was left for up to 10 minutes in the developing solution to clearly stain the bands.

6.2.4 Nanoparticle tracking analysis

All final samples used for RNA extraction were analysed on the NTA (Nanosight NS 300, NTA 3.2 Dev Build 3.2.16 Software). 5 µl of the concentrated EV samples (see 6.2.2) were mixed with 200 µl of PBS and then injected into the chamber. The camera level was kept at 15 throughout and particles captured for 60 seconds. The zoom was adjusted accordingly to focus on the particles, for processing of the video a particle detection threshold of 5 was used for all samples.

6.2.5 Western blotting

Protein content of the EV samples was determined with a BCA kit (Micro BCA™ Protein Assay kit, Thermo Scientific, 23235), which was used according to the manufacturer's instructions. Protein (2 µg) was taken from the EV sample (and the other samples: explant supernatant and non-EV fractions) and mixed with 1x Laemmli buffer without prior lysis to avoid further dilution of the small amount of sample available. For the placental lysate placental tissue was lysed in RIPA buffer prior to protein content determination and addition of 1x Laemmli buffer. Samples were incubated with Laemmli buffer (95°C, 5 minutes) and loaded onto a 10% gel as specified in section 2.4 of the general methods. Afterwards proteins were transferred onto a PDVF membrane (Thermo Scientific Pierce G2 Fast Blotter) according to manufacturer's instructions. Western blots were prepared as described in section 2.5 of the general methods and the following primary antibodies used for overnight incubation: αApoA1 (ab227455), αTSG1010 (ab125011) and αCalnexin (ab133615), all at 1:1000 in 5% BSA in 1xT-TBS. After washing the membrane with T-TBS the blot was incubated with Goat Anti-Rabbit IgG

(ab6721, at 1:2000) and imaged on the ChemiDoc MP Imaging System as explained in section 2.5 of the general methods. The gel was stained with Coomassie as described in section 2.5 of the general methods to check the loading of the gel[365].

6.2.6 Electron microscopy

Electron microscopy was performed in collaboration with Dr. Scott Dillon, Stem Cell Institute, Cambridge who provided the protocol below. Droplets of EVs in PBS were incubated for 10 minutes at room temperature on 200 mesh formvar-carbon coated copper grids (Sigma Aldrich, TEM-FCF200CU) which had been glow-discharged using a PELCO easiGlow glow discharging system (Ted Pella). Excess EV resuspension was removed using filter paper and grids stained by floating on a droplet of 1% aqueous uranyl acetate for 30 seconds. Excess solution was removed using filter paper and grids left to air dry. Grids were examined using a HT7800 transmission electron microscope (Hitachi High Technologies) with a LaB6 electron source operating at 100kV. Images were acquired using a bottom mounted Xarosa CMOS camera (EMSIS) with 5 frame averaging.

6.2.7 RNA extraction

RNA was extracted from the whole EV sample with the QIAGEN miRNeasy Micro kit (QIAGEN, 217084) and the Magnazol kit (Perkin Elmer, NOVA-3830-01) according to the manufacturer's protocol. The common QIAGEN kit was used as described in the general methods. In addition the Magnazol kit was tested due to previously reported improved recovery of small RNA[577]. For the Magnazol kit the EV sample was made up to 200 µl with clean PBS, 400 µl of the Magnazol reagent was added and the mixture vortexed. 40 µl of 1-bromo-3-chloropropane was then added, the sample vortexed again and then centrifuged (16000 g, 5 minutes, 4°C). This allowed the removal of the aqueous phase to which 2.5 volumes of 100% ethanol were added and mixed by pipetting up and down. The sample was then incubated with 50 µl of magnetic beads (55°C, 10 minutes). The beads were then collected on the side of the tube with a magnetic stand on which they were washed with 80% ethanol for a total of two washes. Beads were then dried thoroughly before resuspension in 15 µl RNase-free water and incubation (55°C, 3 minutes). The beads were attracted to the side of the tube on the magnetic stand and the bead-free liquid containing the RNA collected. All RNA was assessed on the 2100 Agilent Bioanalyzer with a Eukaryote Total RNA Pico chip.

6.2.8 miRNA assay

Reverse transcription was performed with the Taqman MicroRNA Reverse Transcription kit (Thermo Scientific, 4366596). The reaction mix was prepared according to the manufacturer's protocol (Figure 6.3 A), then 1 ng of RNA and the 5x primer for miR-16 and miR-183 were added as these miRNAs have been previously shown in EVs in general and placental EVs[539,572]. The whole 15 µl reaction mix was then incubated (16°C for 30 minutes, 42°C for 30 minutes, 85°C for 5 minutes). For the PCR the 20x small RNA assays for miR-16 and miR-183 were mixed with PCR master mix (TaqMan™ Universal Master Mix

II, with UNG, Thermo, 4440042) and water (Figure 6.3 B). 18.67 µl of this reaction mix were added into a 96-well plate together with 1.33 µl (0.11 ng) of the respective cDNA template and run on StepOnePlus Real-Time PCR system with the settings shown in Figure 6.3 C and raw CT values analysed. The samples were analysed in duplicates. As a control samples to assess whether the assay works RNA extracted from placental tissue was used.

A

	1x (ul)
100mM dNTPs	0.15
MultiScribe Reverse Transcriptase, 50 U/µl	1
10x Reverse Transcription Buffer	1.5
RNase Inhibitor, 20U/µl	0.19
Nuclease free water	4.16
Total	**7**

B

	1x (ul)
TaqMan Small RNA Assay (20x)	1
PCR Master Mix	10
Nuclease free water	7.67
Total	**18.67**

C

temp	time	
50°C	2 min	
95°C	10 min	
95°C	15 sec	40 x
60°C	60 sec	

Figure 6.3: miRNA assay protocol

(A) Taqman MicroRNA Reverse Transcription kit was used for the reverse transcription. (B) The Taqman small RNA assay was performed with the shown pipetting scheme and (C) according to the shown reaction conditions.

6.2.9 Library preparation and small RNA sequencing

Library preparation was performed by Dr. Marcella Ma in the Genomics / Transcriptomics Core Facility at the Institute of Metabolic Science (University of Cambridge). 1 ng of total RNA was used from each sample to make libraries with the QIAseq miRNA library Prep Kit (QIAGEN) following manufacturer's instructions. Briefly, RNA was ligated at both ends before reverse transcription. After a clean-up step indexed PCR was performed with QIAseq miRNA 96 Index IL to allow multiplex sequencing. Libraries were validated with a High Sensitivity DNA Bioanalyzer assay (Agilent). Sequencing was performed on the Illumina iSeq100 after equimolar pooling of the samples. Single reads (SE75) were obtained from the 12 samples with an average of 0.44 million reads sequences per sample.

6.2.10 Small RNASeq analysis

Small RNASeq analysis was performed by Dr. Lucas Pantaleão. SRNABench was used for sequence trimming and mapping to the mouse genome (GRCm38). Raw reads mapped to the miRNA mature sense strand were analysed using edgeR in RStudio via quasi-likelihood general linear models. MiRNA with no abundance in any one sample were excluded throughout.

Figure 6.4 summarizes the pipeline utilised in this chapter.

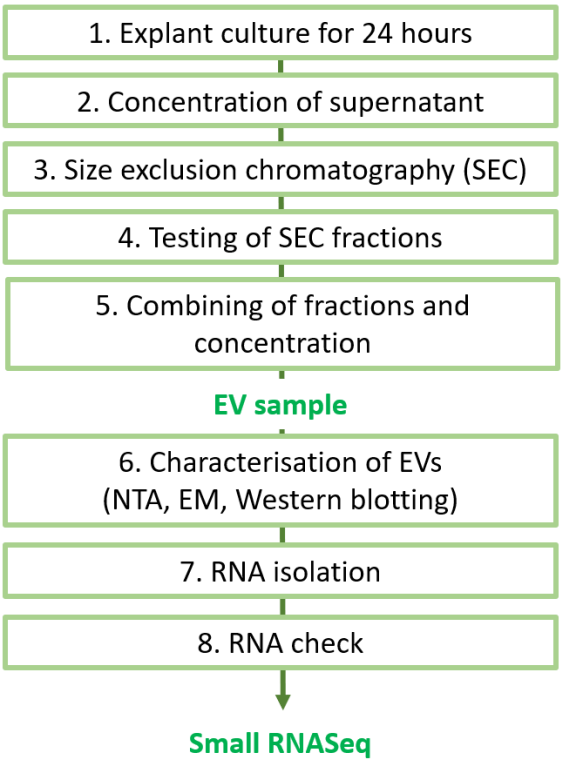

Figure 6.4: The established pipeline for EVs isolated from placental explants

6.3 Results

6.3.1 Placental culture

Assessment of placental tissue after 24h culture showed that there were no major necrotic areas highlighting good explant health (Figure 6.5).

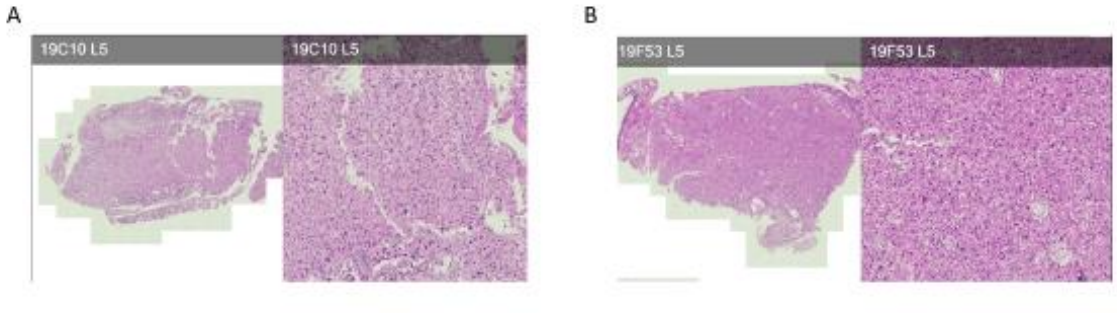

Figure 6.5: Placental explants did not show necrotic areas after 24 hours of culture

H&E stains of example placentas after explant culture from (A) control and (B) obese dams are shown.

6.3.2 Isolation of EVs

EVs were isolated via SEC according to the manufacturer's protocol to separate EVs from contaminating proteins (Figure 6.6A). After personal communication with Dr. Sarah Stewart (La Trobe Institute for Molecular Science, Melbourne, Australia) a slight modification of the manufacturer's protocol was performed. Fraction 6 is according to the manufacturer's protocol part of the void volume meant to not contain EVs. However, no contamination was seen in this fraction but EVs were detected via NTA so this fraction was included into the EV sample. Fractions 6 -11 did not show protein contamination as assessed by the silver-stained SDS-PAGE and were therefore pooled as the EV sample (Figure 6.6B).

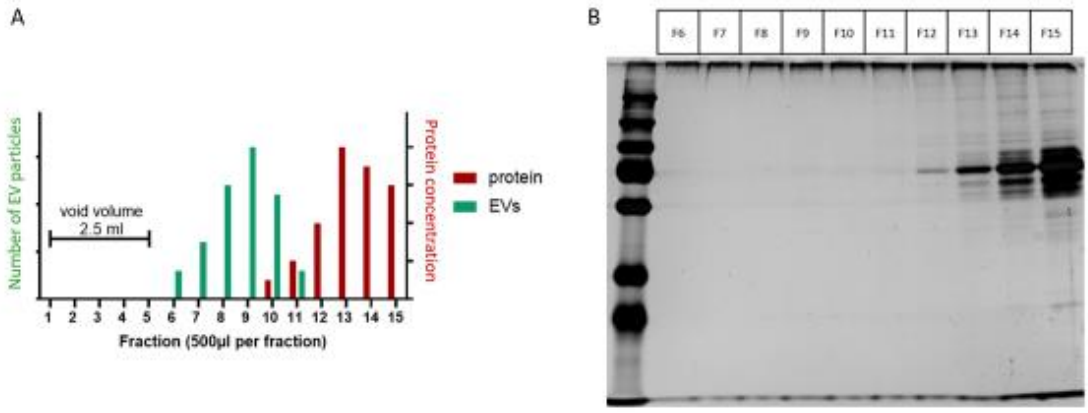

Figure 6.6: EV isolation was performed with size exclusion chromatography (SEC)

(A) EVs and contaminating proteins are separated via SEC in the different collected fractions and (B) the contamination of the fraction 6 to 15 tested on an SDS-PAGE via silver staining.

6.3.3 Characterisation of isolated EVs

Isolated EVs were analysed via the NTA to confirm a size of around 100 nm that was expected with this isolation technique (Figure 6.7A and B). Electron microscopy confirmed the presence of EVs as shown in Figure 6.7C with two EVs of around 100 nm diameter (arrows) and smaller EVs in the background.

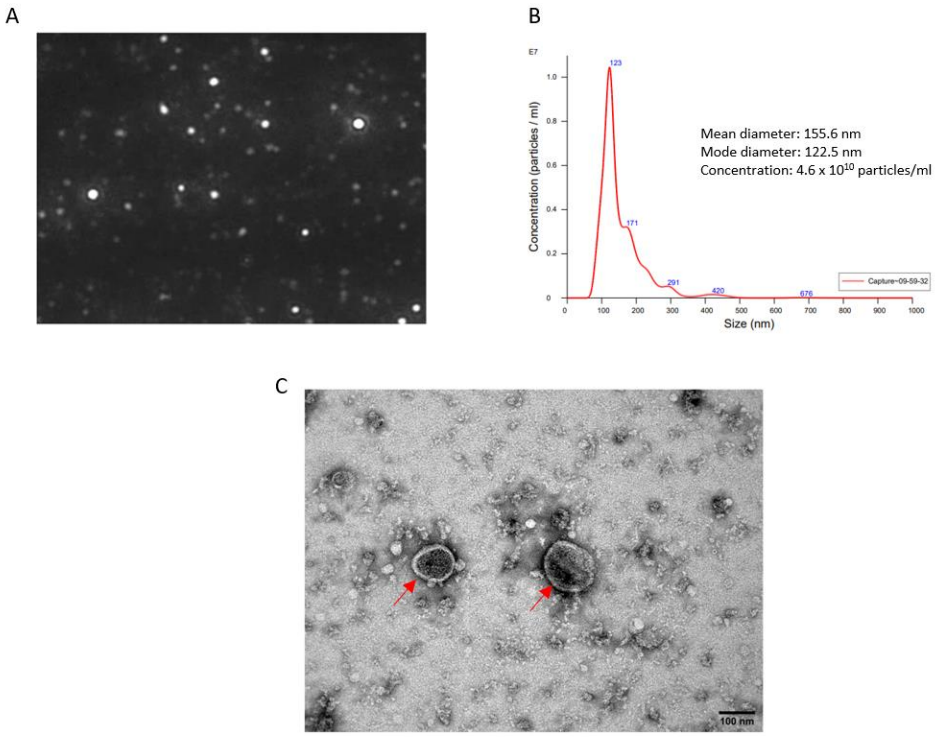

Figure 6.7: Nanoparticle tracking analysis (NTA) and electron microscopy confirmed the presence of EVs in the sample

(A) EVs were measured via the NTA to (B) obtain concentration and size of the EVs. (C) Individual EVs were additionally visualised via electron microscopy.

All samples were run on the NTA and no difference could be observed between control and obese placental EVs regarding EV diameter mean, mode or particle amount (Figure 6.8A-C).

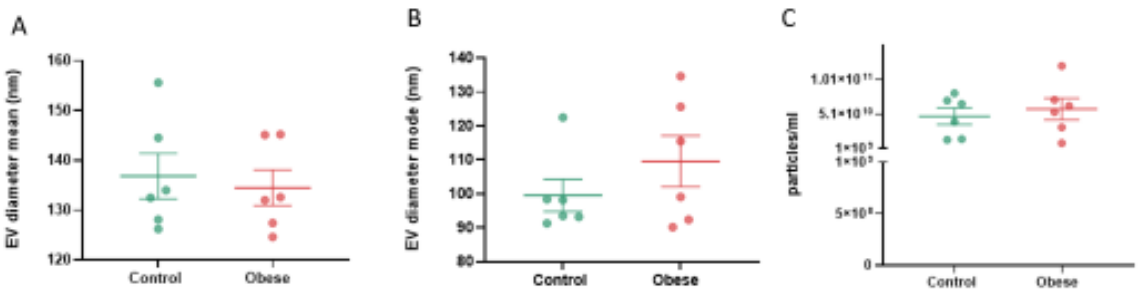

Figure 6.8: NTA analysis data did not differ between EVs from male control and obese placentas

Data from the NTA regarding (B) diameter mode, (C) diameter mean and (D) particle number is compared between the two different groups. Analysis was performed with an unpaired student's t-test.

EV samples were analysed via Western blotting for their presence of well-established EV- and non-EV markers. Four distinct samples (Placental explant lysate, explant supernatant without isolation of EVs, fraction 6-11 (EV fraction) and fraction 12-15 (protein contaminants), Figure 6.9A) were used. Enrichment of TSG101, a protein involved in EV biogenesis (Figure 6.9B), was specifically detected in the EV sample (Figure 6.9C). Lipoproteins detected via ApoA1 were only seen in the placental lysate but not in the EV sample (Figure 6.9C). Calnexin, a protein present in the endoplasmic reticulum (Figure 6.6B) was not seen in the EV sample but was present in all other samples (Figure 6.9C). Therefore, the western blot analysis together with the NTA and electron microscopy assessment confirmed the successful isolation of placental EVs.

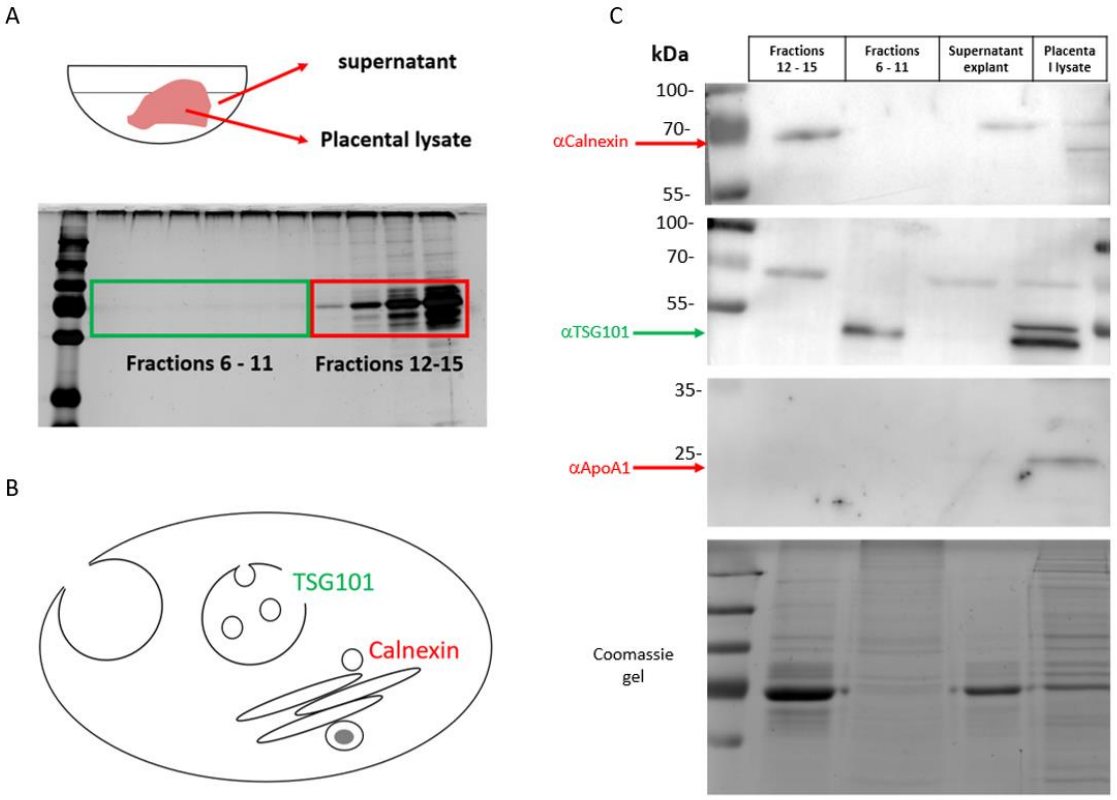

Figure 6.9**: **Western blot analysis confirmed presence of EV marker TSG101 and absence of non-EV markers

(A) Placental explant lysate, explant supernatant without isolation of EVs, fraction 6-11 (EV fraction) and fraction 12-15 (protein contaminants) were used for western blot assessment of (B) the EV marker TSG101 and non-EV marker Calnexin. (C) Blots were probed for Calnexin, TSG101, ApoA1 and the gel stained with Coomassie after the transfer to assess the loading of the SDS-PAGE.

6.3.4 RNA extraction

Extraction of RNA from EV samples showed improved yield when isolated with the Magnazol kit compared to the QIAGEN kit (Figure 6.10A and B). In a miRNA assay the presence of miR-16 and miR183, was assessed. MiR-183 has been shown in murine placental EVs[572] and miR-16 is a miRNA frequently detected in human EVs[539]. Lower CT values for both miRNAs were observed in samples extracted with the Magnazol kit (Figure 6.10C), highlighting increased abundances of the miRNA in these samples. The Magnazol kit was therefore used for all samples in the current study.

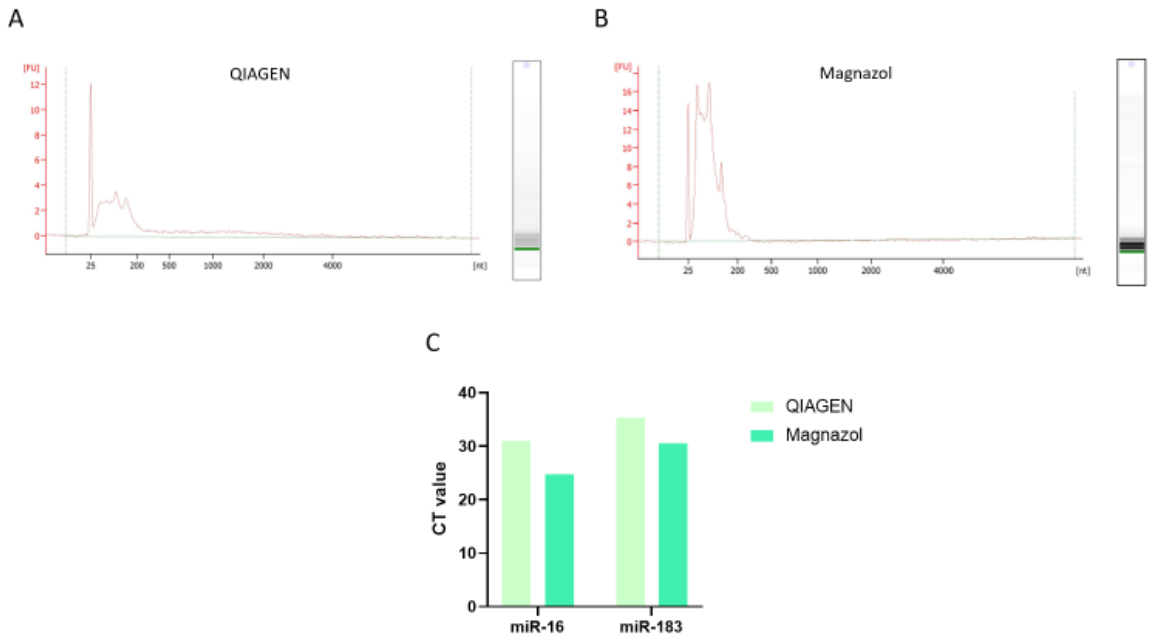

Figure 6.10: The Magnazol extraction kit was shown to have a high yield and a good isolation of small RNAs from the EV samples

RNA extracted via the (A) QIAGEN miRNeasy micro kit and via (B) the Magnazol kit was analysed on the Bioanalyser. (C) miRNA assay measured miR-16 and miR183 presence in RNA samples extracted via the QIAGEN and the Magnazol kit with the raw CT value shown in the graph.

6.3.5 Small RNASeq comparing EVs from control and obese untreated male placentas

As a pilot dataset, miRNA from EVs from 6 control placentas were compared to those from 6 obese placentas. 30-50% of reads from the dataset mapped to mature miRNAs with 440 miRNAs detected in the dataset, after trimming 175 miRNAs remained. PCA plot analysis showed that one sample (sample 4) did not cluster with any of the other samples (Figure 6.10 A). As this sample also had a small library size it was removed from the analysis. PCA analysis with removal of the outlier showed clustering of the obese and the control samples, with 2 obese samples (sample 11 and 12) clustering with the control samples (Figure 6.10 B). Overall, a high abundance of miRNAs from the let-7 family together with other miRNAs like miR-125a-5p, miR-669c-5p, miR-16-5p and miR-183-5p was seen in the samples as shown by the log of the counts per million (Figure 6.10C, Table with all miRNAs in the supplement in Supplement 9, p.238). Two miRNAs (miR370-3p and miR200-3p) were upregulated in obese placental EVs together with a low padj below 0.1 (Figure 6.10D).

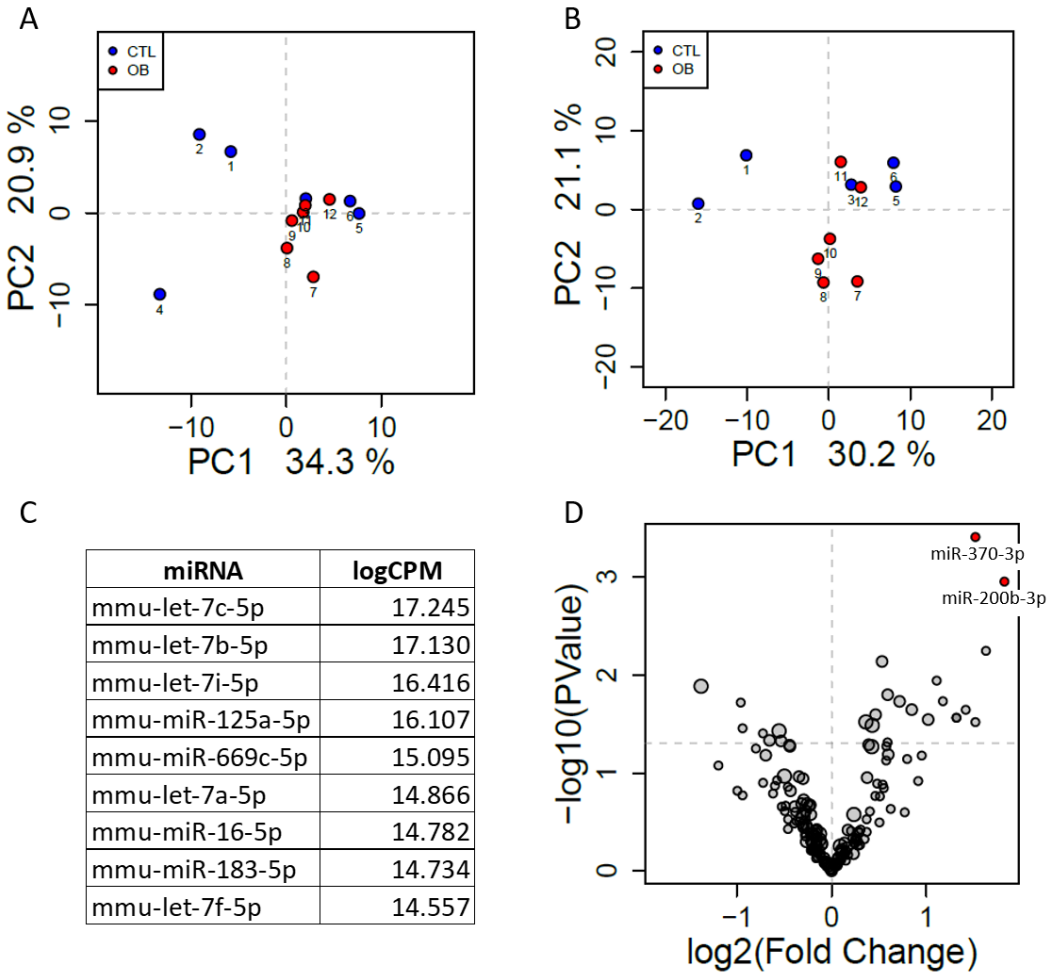

C

miRNA	logCPM
mmu-let-7c-5p	17.245
mmu-let-7b-5p	17.130
mmu-let-7i-5p	16.416
mmu-miR-125a-5p	16.107
mmu-miR-669c-5p	15.095
mmu-let-7a-5p	14.866
mmu-miR-16-5p	14.782
mmu-miR-183-5p	14.734
mmu-let-7f-5p	14.557

Figure 6.10: A small number of miRNAs is differentially expressed between EVS from obese compared to control placentas

(A) PCA plot showing control (CTL) and obese (OB) samples with (B) removal of sample number 4 that was an outlier in the shown analysis. (C) The 10 most highly expressed miRNAs in the dataset are shown here with their respective log counts per million (CPM). (D) Volcano plot plotting log10 of the p value against the log2 fold change comparing obese and control samples is shown.

No miRNAs had an adjusted p value below 0.05. However, overall 11 miRNAs showed a fold change of over 2 or below 0.5 and an unadjusted p value below 0.05. The following miRNAs fall under these categories: miR370-3p (see above, padj=0.1), miR200-3p (see above, padj=0.1), miR-429-3p, miR-485-5p, miR-483-5p, miR-200a-3p, miR-465a/b/c-3p, miR-485-3p and miR-741-3p (Table 6.1). Except for miR-483-5p all these miRNAs are upregulated in EVs from obese placentas.

miRNA	fold change	p value	padj	location
mmu-miR-200b-3p	3.54	1.1E-03	0.10	intergenic
mmu-miR-429-3p	3.09	0.01	0.29	intergenic
mmu-miR-370-3p	2.86	3.9E-04	0.07	intergenic
mmu-miR-741-3p	2.86	0.03	0.29	intergenic
mmu-miR-465a-3p	2.67	0.02	0.29	intergenic
mmu-miR-465b-3p	2.49	0.03	0.29	intergenic
mmu-miR-465c-3p	2.49	0.03	0.29	intergenic
mmu-miR-200a-3p	2.26	0.02	0.29	intergenic
mmu-miR-485-5p	2.16	0.01	0.29	intergenic
mmu-miR-485-3p	2.03	0.03	0.29	intergenic
mmu-miR-483-5p	0.38	0.01	0.29	intragenic (intron of Igf2)

up

down

Table 6.1: List of differential expression of miRNAs in obese placental EVs compared to control placental EVs

All miRNAs with a p value <0.1 and a fold change below 0.5 or above 2 are shown, miRNAs are sorted by fold change. The fold change, p value, adjusted p value and whether the miRNA is inter- or intragenic (+host gene) are indicated. A list of all 175 miRNAs and their fold change and p values can be found in the supplement (Supplement 9, p.238).

6.4 Discussion

The aim of this chapter was to establish a pipeline for EV isolation from mouse placental explants from which high-quality RNA could be extracted for small RNA sequencing analysis. Additionally, we aimed to compare miRNAs from male obese placental EVs with those from male control placental EVs. This chapter showed that this could be successfully done and highlights the differential regulation of a limited number of miRNAs in the EVs from male obese placentas.

6.4.1 The establishment of a pipeline

A pipeline for EV isolation was successfully established in line with the standards laid down within the MISEV guidelines published in 2018[551]. In line with a study from Wong et al. we showed that the Magnazol kit was best suited for the extraction of small RNAs in our sample[577].

6.4.2 Differential abundance of miRNAs in EVs from obese vs. control placentas

Highlighting the validity of this study highly abundant miRNAs in our placental EV samples have been previously shown in placental samples. MiRNAs of the let-7 family have previously been detected in human term placenta[578] and the miRNAs miR-669c-5p and miR-183-5p were among the most abundant miRNAs in EVs isolated from murine trophoblast stem cells differentiated into syncytial trophoblast[572]. Additionally other miRNAs, e.g. miR370-3p and miR-485-3p, found differently abundant between control and obese samples in our study, were shown to be unique to the serum of pregnant compared to non-pregnant mice[572].

Interestingly multiple of the miRNAs that are increased in the obese EV samples have been previously associated with preeclampsia. This is consistent with our model displaying a pre-eclamptic phenotype. In human placentas miR-200b-3p is increased in placentas from women with preeclampsia who delivered an SGA baby[579]. Similarly miR-429-3p was found to be increased in preeclamptic placentas and the researchers found that the miRNA could inhibit invasion, migration and angiogenesis in the trophoblast cell line HTR-8/SVneo[580]. Similar effects of the miR200b-3p have been found when studying hepatocellular carcinoma, where overexpression of miR200b-3p in EVs from hepatocytes reduced angiogenesis, making it a beneficial target for cancer therapy to limit cancer growth[581]. However, in the data presented in this chapter, these miRNAs in placental EVs could impair placental angiogenesis and/or could by reaching the maternal circulation play a role in the pathogenesis and development of preeclampsia given their previously found association to preeclampsia. Additionally, they could also be a representation of the state of the obese placenta, in which trophoblast invasion, development of the placenta and angiogenic potential are impaired.

The miR483-5p was decreased in the EVs from male obese placentas. This miRNA has been investigated in previous studies in the lab looking at the effects of maternal undernutrition. In adipose tissue from adults born with a low birth weight and in rat offspring exposed to a low-protein diet *in utero* miR483-5p was upregulated and involved in impaired adipocyte differentiation[582]. In the placenta this miRNA

has been shown previously to be reduced in cases of spontaneous preterm delivery[583]. This miRNA is an intronic miRNA located within the Igf2 gene and has been shown to be increased in placentas from macrosomic pregnancies and promotes cell proliferation in the trophoblast[584]. MiR-200a-3p binds to the 3'-UTR of the Igf2 gene and reduces its expression in the mouse placenta[585]. High levels of the miRNA in the obese placental EVs in the current study could therefore reduce placental Igf2 expression and therefore explain the reduction in miR483-5p. IGF2 is an important growth factor for fetal and placental development and placental specific knock-outs of Igf2 have reduced nutrient supply to the fetus and altered maternal metabolic and endocrine parameters[586]. This miRNA could thereby play an additional role in the observed fetal growth restriction in the obese group. As placental EVs have been detected in the fetal circulation, trafficking of this miRNA into the fetal circulation could also affect IGF2 signalling in the fetus. IGF2 is an important regulator of fetal growth and fetal IGF2 levels have been shown to be regulated by maternal nutrition[587]. MiR-200a-3p packaged into EVs could thereby be an important mediator between mother and fetus. If blood supply and placental efficiency is suboptimal as in our obese dams signalling of reduced growth to the fetus could be beneficial to match fetal demand and maternal supply. Follow-up of these findings could help in elucidating mechanisms of fetal growth restriction.

MiR-485-3p and -5p were both increased in obese placental EVs and have been linked to mitochondrial function in previous studies. MiR485-5p and MiR485-3p reduced cancer metastasis by inhibition of a key regulator of mitochondrial biogenesis (PGC1α) and thereby reduced mitochondrial respiration[588]. Other studies have highlighted the role of miR-485-5p in suppressing development of cardiac hypertrophy by inhibition of mitochondrial fission[589]. Mitochondrial dynamics have been shown to be altered in GDM placentas with insulin thought to promote increased mitochondrial fusion[590]. Fusion and fission of mitochondria are needed for balanced dynamics of mitochondria. Fission is used to fragment mitochondria so that damaged mitochondria can be eliminated via mitophagy, on the other hand fusion creates elongated mitochondria increasing their functional capacity. It is hypothesized that increased fusion in GDM placentas is a mechanism to respond to an increased demand of oxidative phosphorylation and to compensate for damaged mitochondria due to increased placental stress. There is growing interest in the effect of GDM on placental mitochondria with a recent paper showing mitochondrial dysfunction in placentas from GDM women[591]. Likely the miRNAs in the placental EVs could be reflective of the (mitochondrial) status of the placenta and could thereby help in explaining mechanisms of altered mitochondrial function in obese glucose-intolerant placentas.

6.4.3 Conclusion

This chapter highlighted the feasibility of isolating EVs from murine placental explants. We also considered the various requirements for optimising the protocol and assessing the best method for

isolation of high-quality small RNAs. This protocol can now be used further to not only address the effects of maternal obesity but also sexual dimorphism and effects of metformin. Many differentially regulated miRNAs did not reach statistical significance (<0.05) when using an adjusted p value to take into account the multiple comparisons, likely due to the low sample number. However, several miRNAs were differentially regulated with a fold change over 2 or below 0.5 and a significant unadjusted p value which warrants further investigation. These miRNAs had previously been linked to preeclampsia, placental and fetal growth and placental mitochondrial dysfunction. Further investigation could thereby determine their role in mechanism of placental pathologies of obese glucose-intolerant pregnancies and the use of placental EVs as biomarkers for placental dysfunction and preeclampsia.

Key points

- EVs were successfully isolated from murine placental explants and the process carefully optimized.
- RNA extraction from EVs with a Magnazol extraction kit allowed recovery of miRNAs which were subjected to small RNA sequencing.
- MiRNA content differed between EVs from control vs. obese male placentas with upregulation of miR-370-3p, miR-200b-3p, miR-429-3p, miR-485-5p, miR-485-3p, miR-200a-3p, miR-465a/b/c-3p, miR-741-3p and downregulation of miR-483-5p in the obese placental EVs.
- The differentially regulated miRNAs have been linked to preeclampsia, impairment of fetal growth and placental mitochondrial dysfunction.

7 General discussion

7.1 Metformin treatment in an obese glucose-intolerant pregnancy

The increased rates of obesity in women of reproductive age that has occurred in recent years has drastically increased the rate of obese pregnancies and thereby also pregnancies complicated by GDM. For a long time insulin was the first line treatment for GDM, however in recent years metformin has been used more and more in many countries worldwide and is now incorporated into many guidelines as first line treatment for GDM, such as the NICE guidelines. Therefore, an increasing number of pregnancies is and will in the future be subject to metformin treatment. At the time of the study conception of this thesis (2018), many human studies assessing metformin in pregnancy already existed. Many of these studies, especially the early ones, were related to PCOS pregnancies but multiple also assessed use of metformin in GDM[592,593]. However only a few of these studies assessed long-term health of the offspring and none of them systematically addressed effects of metformin on the fetus and/or the placenta[341]. Since then further studies have emerged extending the potential spectrum of metformin treatment to obese pregnancies without GDM and type 2 diabetes together with studies looking at long-term maternal health effects of metformin treatment[391,594]. However, despite the increasing interest into metformin treatment in pregnancy there is still little data regarding metformin's effects on the placenta and the fetus. Given the ability of metformin to cross the placenta this is crucial to investigate and many researchers have urged caution and the need for further research as early as 2006 and increasingly in the past decade [329,440,595]. The aim of this thesis was thereby to use our well-established mouse model to assess the impact of obesity and glucose-intolerance in pregnancy on maternal, fetal and placental health to then use the model to assess metformin treatment.

7.1.1 Effect of metformin on maternal health

Feeding a diet high in sugar and fat impaired maternal metabolic health as shown by increased fat mass, impaired glucose tolerance and liver steatosis. These parameters were improved with metformin treatment. This is in line with human data that shows improved maternal metabolic health in response to metformin. As highlighted in a meta-analysis from our lab from 2021 a consistently found benefit of metformin is the reduced gestational weight gain[596]. However, regarding glucose control the data is mixed. Studies in women with PCOS[330], with pregestational insulin resistance[597] or with obesity without GDM[342] showed no reduced GDM rate in women treated with metformin when compared to placebo treatment. The meta-analysis shows that in diabetic women glycaemic control is not different to other treatments such as insulin and glyburide[390]. However here it needs to be noted that the included studies were on an intention to treat basis so that women for whom metformin was not sufficient for glycaemic control were given additional insulin but were still included in the metformin study group. The meta-analysis reported that across the studies metformin could not

control glucose levels in 14-46 % of GDM pregnancies metformin is not sufficient[390]. It is therefore also important to dissect out which women are at increased risk of failure with metformin as in these patients it could be argued that these individuals should not be treated with metformin (avoiding any unnecessary exposure of the fetus to metformin and delaying the achievement of good maternal glycaemic control). In a study by McGrath et al. 53.9% of the women with GDM failed metformin treatment and needed insulin, failure on metformin treatment was more likely in those women that had elevated blood glucose levels at diagnosis and earlier initiation of treatment[598]. Interestingly 35% of the women completely stopped metformin treatment and switched to insulin due to a lack of benefit (66%) and gastrointestinal side effects (33%). Notably the dose of insulin was not different in the women ceasing metformin and only taking insulin compared to those continuing to take metformin with supplemental insulin. However other studies reported lower dose of insulin in women combining metformin and insulin and thereby reducing the cost of treatment[599]. Other studies also highlight that metformin failure is more likely in those women showing higher fasting glucose and HbA1c levels at diagnosis and additionally increased maternal age is also associated with increased risk of failure with metformin treatment[600,601]. A study by Tertii et al. suggests that specifically increased fructosamine levels at randomisation could be used as a predictor for failure of metformin treatment[601]. Interestingly a recent study on the Born in Bradford cohort, a large dataset with a high percentage of South Asian women, showed that women with GDM with increased obesity and with lower glucose levels were more likely to receive metformin[602]. Additionally, metformin was used more in women of South Asian ethnicity despite them having reduced adiposity but increased glucose – situations when insulin treatment would generally be expected. The authors suggest that social and cultural aspects could play a role - with South Asian women preferring metformin compared to insulin[602]. A similar recent study looking at treatment of GDM pregnancies showed that hispanic women without insurance and those managed by an obstetrician/gynaecologist rather than endocrinologist were treated more often with metformin than insulin[603]. These important studies highlight the complexity of treatment decision. As far back as 2001, studies considered what measures could be best used to inform the treatment decision, suggesting that assessing fetal growth in addition to glycaemic control reduced unnecessary use of insulin but did not increase negative outcomes in the fetus[604]. In the study they gave insulin only to women with impaired glycaemic control whose fetuses showed abdominal circumference (measured monthly) above the 70th percentile. This tight assessment of women and the fetus during pregnancy to finely adjust the treatment is likely not feasible in the clinic but it highlights the many considerations that can be considered for in deciding the most appropriate GDM treatment. In 2018 a Brazilian group suggested the use of a score to inform the treatment choice. The score included maternal glucose levels, fetal abdominal circumference percentile as well as, maternal BMI and gestational age at diagnosis. Interestingly their approach led to an increased use of metformin. A

recently published protocol for a new meta-analysis "Metformin in Pregnancy Study" (MiPS) will address the questions raised in this paragraph[605]. The meta-analysis aims to collate data from RCTs using metformin in the setting of obese, diabetic and PCOS pregnancies. However, in contrast to a usual meta-analysis the researchers aim to obtain individual patient data from all included RCTs. This allows them to link pregnancy outcomes to maternal characteristics and identify the subgroups that do and that don't benefit from metformin use.

In recent years metformin's potential to treat preeclampsia has emerged. A meta-analysis from our lab showed reduced preeclampsia incidence in obese (vs. placebo) and diabetic (vs. insulin and glyburide treated) pregnancies[596]. This has been implied previously in studies of explants from preeclamptic placentas where metformin reduced sFlt secretion[360]. Studies in a rat model of preeclampsia (induced by injection of lipopolysaccharide (LPS) in pregnant rats) also showed beneficial effects of metformin (300 mg/kg, gavage) - reducing the fetal growth restriction, placental injury and maternal hypertension and proteinuria[606]. Similarly a preeclampsia-like phenotype induced by high fat diet was shown to be ameliorated with metformin treatment (20mg/kg/day)[441]. In their study the placental labyrinthine zone was increased back to control levels with metformin along with improvement in fetal weight, maternal hypertension and maternal proteinuria. Our study adds to this evidence and highlights improved uterine artery function together with reduced sFlt secretion. Based on our findings, uterine artery function is likely linked to insulin levels in the dam presenting a possible mechanism of metformin action on preeclampsia via insulin reduction.

Metformin use in preeclampsia treatment could be especially relevant in developing countries where rates of preeclampsia are approximately seven times higher compared to developed countries (WHO data)[607]. Due to limited resources to diagnose and thereby treat preeclampsia at an early stage preeclampsia is associated with a high mortality rate in developing countries[608]. The easy storage and administration of metformin therefore makes it a particularly helpful drug for treatment of preeclampsia in these countries. A recent randomised placebo-controlled study in South Africa highlighted the benefits of metformin in prolonging gestation (i.e. delaying the need for early delivery) by 11.5 days compared to placebo in early-onset preeclampsia patients and thereby reducing the prematurity of the babies delivered[609]. However, metformin did not reduce maternal sFlt in their study. Overall, this study highlights the potential of metformin as a treatment for preeclampsia, which is in line with the mouse data presented in this thesis.

Open Questions

1. Is metformin treatment an effective means of preventing and/or treating preeclampsia?
   Method: Clinical studies
2. Can we tailor metformin use better to use it only in the treatment of women who will respond to it? Who fails glycaemic control with metformin treatment and who benefits from preeclampsia prevention?
   Method: Meta-analysis with individual patient data (MiPS) and then trials of implementation of guidelines for the treatment decision in the clinics.

7.1.2 Effect of metformin on fetoplacental health

In line with the impaired uterine artery function fetuses from obese and glucose-intolerant mothers showed symmetric fetal growth restriction. Additionally, reduced placental efficiency likely caused by a reduced labyrinthine zone and increased calcification was shown. However, despite beneficial effects of metformin on the mother, metformin did not improve fetal body weight or prevent placental pathologies (Figure 7.1). As we could detect high levels of metformin in the placenta, fetal tissues and the fetal circulation we hypothesized that direct effects of metformin affecting growth and development in the fetoplacental unit could explain the discrepancy between the improvements in maternal parameters and the lack of improvements in the fetus and the placenta. We focussed on the placenta as the key interface between mother and child. Systematic data in relation to the effects of metformin on the placenta is scarce and mainly looks at *in vitro* investigations using high metformin concentrations which likely do not give physiological results (see Table 1.1, p.52).

The existing studies show mostly beneficial effects of metformin on the placenta, with a few researchers also showing detrimental effects. Given that metformin is readily used in the clinic it is reassuring that no major transcriptomic differences were identified in our study, additionally reduction of placental triglycerides could be considered a beneficial effect of metformin on the placenta. It will be important to establish whether these lipid changes are also observed in human studies. However, despite the lack of major transcriptomic changes it can't be excluded that changes occur at a translational level. Further detailed analysis of the RNASeq data and validation of the findings is important to make a robust statement about the preliminary findings presented here. Proteomic analyses of the placentas from this study will be important in future studies to address the full spectrum of metformin's effects on the placenta. In the clinical situation pharmacological treatment is needed when diet and lifestyle interventions fail. Thereby metformin or insulin need to be used with no current alternative. It would be thereby beneficial to compare the use of insulin with the use of

metformin in our model to assess whether insulin or metformin is superior in not only improving maternal but potentially also fetal and placental parameters.

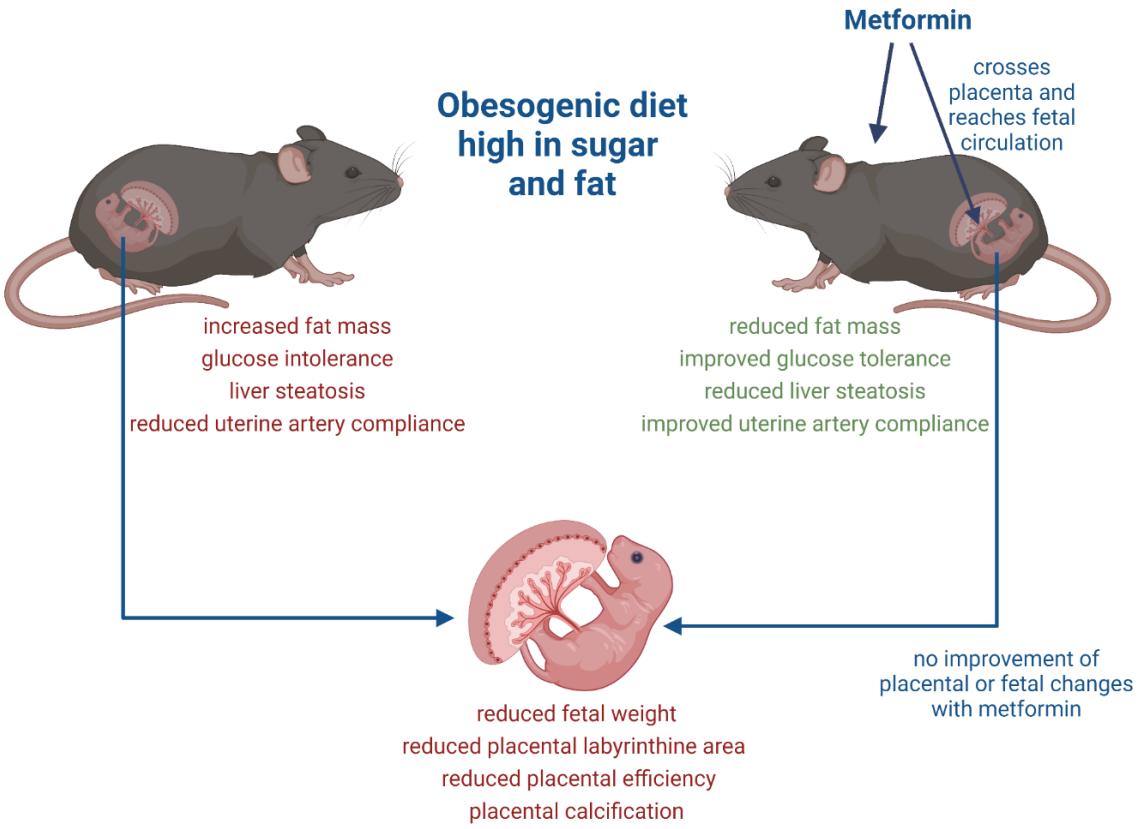

***Figure 7.1: Summary of some of the key findings in this thesis (from Hufnagel et al.*[364], figure used with permission (CC-BY licence))**

The effect of reduced free carnitine levels induced by metformin treatment will be important to follow up. As highlighted in chapter 5 carnitine levels have been linked to preterm birth. Some studies of metformin treatment in pregnant humans have suggested that it is associated with preterm birth. Therefore assessment of placental and fetal carnitine levels in human studies represent important future studies. The increased apoptosis identified in the male placenta in the current study needs further assessment. As highlighted by the sexually dimorphic gene expression in the placenta overall sex differences play an important role in developmental programming. Studies from our lab in offspring exposed to metformin *in utero* have shown that male and female offspring are affected differently by metformin with male, but not female, offspring showing increased adiposity at 8 weeks of age[473]. Increased adiposity was only observed in the female offspring at 6 months of age[610]. Thereby both sexual dimorphism and consideration of age are important factors to consider when assessing metformin effects. High levels of metformin were detected in the fetal circulation and fetal tissue, however the direct effects of this on fetal tissues was not explored in this thesis and is therefore an

important area to follow up and may give insight into mechanisms by which *in utero* metformin exposure leads to increased adiposity.

Currently there are only a limited number of animal studies that have addressed direct molecular effects of metformin treatment on fetal tissues. A study in mice fed a chow diet treated with 250 mg/kg/day metformin showed direct effects of metformin on the fetal liver leading to premature maturation and increased gluconeogenesis[611]. The authors hypothesized that this could lead to an increased risk for metabolic abnormalities in later life.

Given the increased adiposity shown in some human studies and in the offspring data from our lab assessment of the effects of metformin exposure on fetal adipogenesis is needed. Data from *in vitro* studies is mixed: treatment of 3T3-L1 preadipocytes with low (closer to physiological levels, 1.25 – 2.5 mM) metformin concentrations led to increased adipogenesis whereas high concentrations (5-10 mM) led to reduced adipogenesis[612]. In our studies we showed high metformin levels in the fetal kidney, therefore molecular analysis of the fetal kidneys is also needed which could start by addressing the typical mediators of metformin action such as AMPK, mTOR and markers of mitochondrial biogenesis. Oral treatment of pregnant mice fed a high fat diet with 380 mg/kg/day metformin showed that diet itself had a higher impact on the fetal renal proteome than metformin, however they showed that metformin changed some of the obesity-induced changes, but functional consequences of these changes are unknown[613]. Analysis of fetal tissue collected from the study presented in this PhD will help identify direct effects of metformin that could mediate effects on long-term outcome.

Open Questions

1. Does metformin affect human placental structure, transcriptome or lipidome?
   Methods: Systematic analyses of the placentas in clinical studies of metformin in pregnancy

2. Does insulin as a pharmacological alternative to metformin have beneficial effects on the fetus and/or the placenta?
   Methods: Same assessment of fetoplacental health as shown here in our mouse model with insulin treatment

3. What are direct effects of metformin on fetal metabolic tissues and fetal adipogenesis?
   Methods: Analysis of known metformin targets (AMPK, mTOR, mitochondrial biogenesis) in fetal tissues collected in this study (esp. kidney which had high metformin conc.)

4. What are direct effects of metformin on fetal adipogenesis that can explain the effects of metformin on increased adiposity later in life?
   Methods: Primary culture of adipocytes isolated from newborn mice exposed to metformin treatment

7.2 Novel effects of maternal obesity itself

Data presented in this thesis adds to the characterisation of the well-established mouse model of diet-induced maternal obesity used in the Ozanne lab. We showed that feeding a diet high in sugar and fat not only led to metabolic impairments such as glucose intolerance and liver steatosis, but also to vascular alterations. Heart rate of the dams was increased and importantly a preeclampsia-like phenotype with decreased uterine artery compliance and increased sFlt serum levels were observed. Increased risk for preeclampsia is observed in obese and diabetic human pregnancies highlighting that our model resembles the human situation[614]. Additionally, it provides a potential causal underlying mechanism for the observation of reduced fetal growth in the model. Interestingly in human obese and diabetic pregnancies both overgrowth and restricted growth of the fetus are observed with little understanding of which growth pattern will occur in a specific obese pregnancy[148]. A growth restriction phenotype could be related to mild or severe (such as preeclampsia) impairments in vascular adaptation of the mother as shown in this study.

Another resemblance to the human situation is the presence of calcium deposits in the obese placentas. These have been observed repeatedly in human placentas in pregnancies complicated by obesity, GDM and preeclampsia[458]. The underlying causes of this deposition are not known, hence our model could aid in dissecting the underlying mechanisms. Exact determination of the gestational age at which these deposits start to emerge and further assessment of their composition and development could elucidate the cause of placental calcification. As hypothesized in section 4.4.2 a mechanism similar to atherosclerosis could be the cause based on the data presented in this thesis. Further work should analyse immune cells like macrophages and neutrophils known to be involved in atherosclerotic plaque development just before the onset of calcification to see whether these are the starting point of calcification[615]. Another possible mechanism involved in placental calcification could be impaired phosphate transport as placental calcification is observed in a mouse with a knock-out of the phosphate transporter Slc20a2[616]. Evaluation of this transporter in the placenta could help to identify whether alterations in mineral transport play a role in placental calcification of the obese placenta. Slc20a2 (PIT-2) has been shown previously to be reduced in placentas from pregnancies complicated early-onset preeclampsia but this has not been followed-up further[617]. Thereby mineral transport together with atherosclerosis-like development could be causal for placental calcification. Interestingly staining and analyses performed for a colleague showed that placental calcification could be reduced with an exercise intervention in our mouse model. It is therefore of interest to see whether other interventions in obese glucose-intolerant pregnancies such as antioxidants or insulin can reduce placental calcification.

Open Questions

1. What causes placental calcification during obese pregnancy?
   Methods: Analyses of the obese placentas to determine exact onset of calcification and involvement of immune cells (atherosclerotic development) and assessment of placental Slc20a2 expression

2. Can placental calcification be reduced via pregnancy interventions?
   Methods: Assessment of placental calcification in studies with our mouse models assessing other interventions

7.3 The role of extracellular vesicles in developmental programming

In the past decade research on miRNAs has increased significantly with involvement of miRNAs identified in multiple diseases such as cancer and heart disease together with the potential of miRNAs as biomarkers[618,619]. A few studies from our lab have also highlighted the role of miRNAs in developmental programming with miR-126 targeting insulin signalling and miR-706 regulating adipose inflammation in offspring from obese mothers[41,620,621]. EVs can carry miRNAs and placental EVs have been shown to be involved in pregnancy complications such as GDM and preeclampsia[555]. As placental EVs can enter both the maternal and fetal circulation, they could represent an important communicator between mother and child. We aimed to establish methodology that would allow the determination of whether the miRNA content of placental EVs could contribute to the pregnancy complications and whether they could have the potential to exert programming effects on the fetus. In chapter 6 of this thesis the optimisation and successful isolation of EVs and the sequencing of the miRNA cargo was shown. The limitations of our optimisation experiments for the EV work are that only a small analysis of the different performance of two RNA extraction kits was performed by only looking at two miRNAs. A more systematic analysis of the use of potentially even more RNA extraction kits and analysis by small RNASeq to capture all differences could be important for the field in general and studies on placental EVs in the lab in the future.

Comparison between the miRNA content of placental EVs from obese compared to control placentas identified a few differentially regulated miRNAs. Many of these have been previously associated with preeclampsia or impaired mitochondrial respiration. These identified miRNA signatures could indicate the current state of placental health and be beneficial in detection of placental insufficiencies. Preeclampsia is a detrimental pregnancy complication which can be detected after 36 weeks by an abnormal sFlt/PlGF ratio[622]. However earlier detection could help to intervene even earlier and detect women at risk of preeclampsia development. Preeclampsia, especially early-onset preeclampsia, is thought to be a placental disease with impaired placental development, vascularisation and placental

stress[623]. EVs and their miRNA content have recently been suggested as additional biomarkers for preeclampsia. Li et al. showed a distinct miRNA signature in serum EVs from women with preeclampsia compared to healthy women[624]. Our data shows that it could potentially be beneficial to sort serum EVs via PLAP, which marks EVs of placental origin[625]. It would be helpful to assess the miRNA content of placental EVs specifically in serum from preeclamptic women to assess their potential as a biomarker, especially at earlier gestational ages. Enrichment of placental EVs from maternal serum and assessment of their miRNA content could allow detection of smaller placental impairments and therefore identify women who would benefit from increased monitoring and potentially earlier treatment.

We identified increased levels of miRNA 200a-3p in the obese placental EVs, which has been linked to IGF2 signalling. Placental EVs could therefore play an important role in communication to ensure balancing fetal demands to maternal supply. Further follow-up needs to assess IGF2 levels in the placenta and the fetus to confirm this relationship. Based on the sex differences between male and female placentas and fetuses described in this thesis it will be important to assess sexual dimorphism the miRNA content of placental EVs. Given the increased growth in male fetuses and an increased fetal growth response to IGF2 in male fetuses a difference in communication between maternal supply and fetal demands is likely[587]. The power of the findings from this EV study is limited by the low sample number, the study should be thereby further expanded to include more samples and also assess the effect of metformin treatment and sex on miRNAs derived from placental EVs (Figure 7.2).

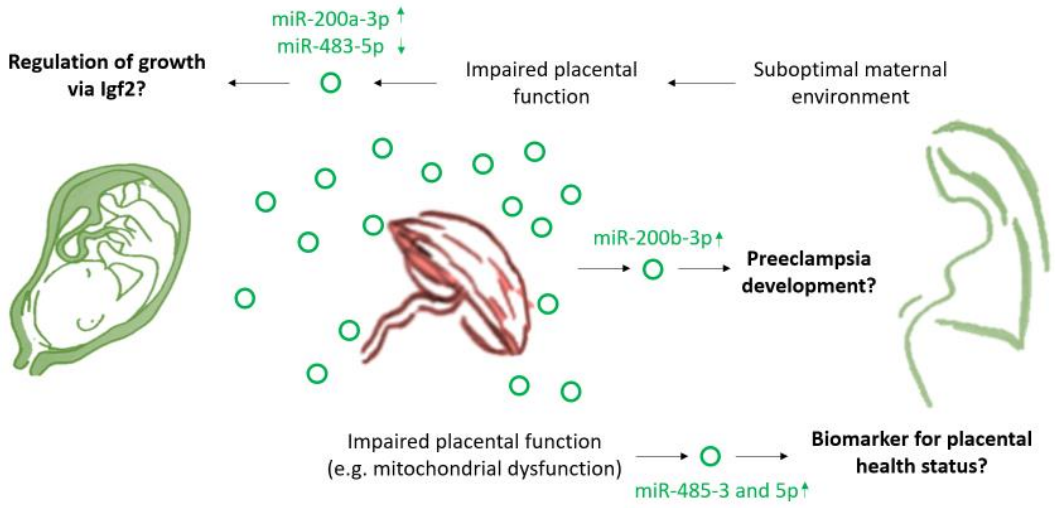

Figure 7.2: Summary of the potential effects and applications of miRNA content from obese placental EVs

Open Questions

1. How is the miRNA content in placental EVs affected by fetal sex and metformin treatment?
   Method: Expanding this pilot dataset with placental EVs from female placentas and obese metformin-treated placentas

2. Can PLAP-sorted (placental) EVs be a marker of placental health and aid the early detection of placental insufficiency and/or preeclampsia?
   Method: Assessing miRNAs from placental EVs rather than total blood EVs in clinical studies.

3. Is IGF2 signalling indeed reduced in the obese placentas and fetuses?
   Method: Measurement of IGF2 in the placentas and fetuses from this study

7.4 Concluding remarks

The prevalence of GDM is increasing worldwide with detrimental effects on the fetus, the offspring, the mother and subsequent generations. These include not only pregnancy complications but increased risk of cardiometabolic diseases in the offspring later in life. This creates a vicious cycle with both male and female offspring themselves being more likely to expose their offspring to suboptimal environments due to paternal and maternal programming effects. Mothers with GDM have an increased risk for long-term health effects themselves shown by increased risk of developing T2D and cardiovascular disease after the GDM-affected pregnancy[626]. Therefore good GDM treatment is crucial to reduce pregnancy complications and limit exposure of the fetus to hyperglycaemic episodes to reduce short- and long-term effects. In the past decade the use of metformin has been heavily debated[375]. This thesis has highlighted the growing interest in metformin for its use not only in GDM pregnancies but also obese pregnancies, PCOS and for the prevention of preeclampsia. In this thesis we confirm previous findings that metformin improves maternal metabolic parameters. Therefore combining animal and human data regarding metformin use in pregnancy it becomes evident that metformin has a myriad of beneficial effects for the mother, which are of immediate, practical and long-term nature (Figure 7.2). The novel findings presented, however, demonstrate that despite these beneficial effects on the mother, there was no improvement in fetal and placental parameters. Furthermore, metformin enters the fetal circulation with potential to have direct effects on the fetus and placenta which could mediate long-term risks in the offspring, such as increased obesity, as seen in our mouse model and reported in human studies (including a meta-analysis of randomised control trials comparing metformin versus insulin treatment of GDM[341]).

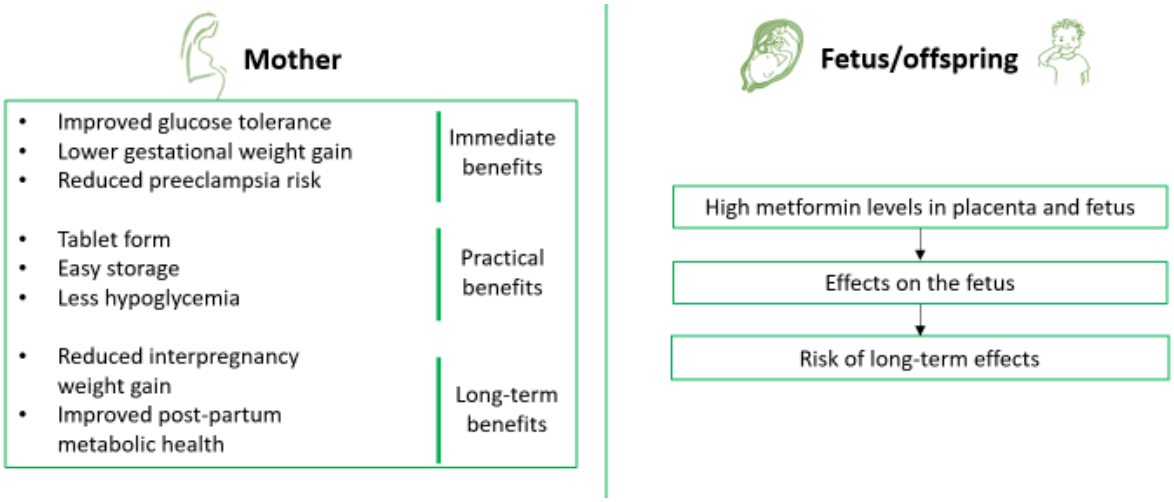

Figure 7.3: Summary of benefits of metformin for the mother and potential effects on the fetus

Assessing metformin treatment of GDM in pregnancy is complex given the balance between effects on the mother and the fetus but also given the fact that metformin might be clearly beneficial in some pregnancies and not in others. In developing countries metformin use might be hugely important despite uncertainties regarding long-term use. Here detrimental pregnancy complications like preeclampsia are highly prevalent, insulin treatment expensive[599] and glucose monitoring devices are rare[424]. Good monitoring is important in insulin treatment to avoid hypoglycaemic episodes and ensure good glycaemic control. This is not needed with metformin treatment which has been associated with a more stable glycaemic control[600]. Metformin use might thereby increase in developing countries. It is therefore even more important to be certain that no short- and long-term effects of metformin are at play. However, there are definitely situations especially in cases of increased risk of preeclampsia where the benefits of metformin to aid survival clearly outweigh the potential negative effects in the offspring. Further research and follow up of the model presented in this thesis and meta-analyses like the MiPS study will add to the ongoing debate regarding metformin use during pregnancy. Another approach that can harness the clear beneficial effects of metformin but reduce fetal exposure to metformin is the use of other formulations of metformin with different kinetics of release into the circulation. Extended release metformin formulations, which extend the time until metformin is absorbed in the gut, were used in the South African clinical study on preeclampsia treatment[609], but no studies have yet assessed the use of other formulations such as delayed release metformin. This formulation of metformin leads to absorption in the late gut[627] and importantly reduction of systemic exposure which in turn should reduce placental and fetal exposure. A Phase 2 study from 2018 in T2D patients showed improved glycaemic control and reduced gastrointestinal side effects with the delayed release formulation[628].

Open Questions

Could the use of different metformin formulations (e.g. delayed release) or different treatment regimens be beneficial for the use in pregnancy?
Method: Clinical studies

Our study adds to the knowledge and the debate about metformin use in pregnancy. However, the study is limited as it is a mouse model that can't be fully translated to the human situation. As highlighted in the introduction of this thesis, human and mouse pregnancy and placental biology differ from each other in quite a few different aspects. In our model the metformin treatment already starts one week prior to pregnancy. However, in treatment of women with GDM the metformin treatment usually starts at diagnosis around 24-28 weeks and after trialling lifestyle interventions first. Due to the short pregnancy in the mouse it is difficult to mirror this. Only T2D patients might be exposed to metformin already prior to pregnancy like in our mouse model. In future work it could be helpful to also add a group that only receives metformin at the beginning of pregnancy and compare this to mice treated with metformin already prior to pregnancy. In our study metformin is administered via feeding, thereby we can only estimate the amount of metformin received by the animal. The metformin measurements we have performed at E18.5 in the maternal and fetal circulation together with fetal tissues and the placenta is helpful in this regard, however it only gives a glimpse into the metformin levels achieved at the end of pregnancy. We have also measured metformin at E13.5 in the placenta and fetal tissue as shown in this thesis and in the maternal circulation (not shown in this thesis), where we could detect metformin levels similar to those detected at E18.5. This shows that the concentrations measured at E18.5 could be a good estimate of the overall metformin exposure in the animals. However, in future work it could be interesting to sample blood from a few metformin-treated dams at multiple times throughout the treatment period (prior to E13.5 in early pregnancy and in the first week of dosing before mating) to be able to assess metformin levels throughout the dosing period. Overall, the current study does not allow a statement on whether the long period in which the animals were fed a high-fat diet led to changes in the oocyte itself that just can't be reversed by a short metformin treatment and explain why fetuses are still growth-restricted and placentas still show pathologies despite metformin treatment and improvements in the mother. It would thereby be very important in a next study to assess insulin and metformin intervention in our model side-by-side to assess whether insulin can rescue some of the obesity-induced effects on the fetus and the placenta that metformin could not rescue in the presented study. The comparison between metformin and insulin would also make it easier to translate the study directly to the clinic as women with GDM always receive a form of treatment (insulin or metformin) once lifestyle interventions have failed. These next experiments together with the future work presented in the green boxes in this chapter will be helpful

in adding even more knowledge to the debate about metformin in pregnancy and will help to address some of the limitations of the study presented in this thesis.

References

1. Bray, G. A., Kim, K. K. & Wilding, J. P. H. Obesity: a chronic relapsing progressive disease process. A position statement of the World Obesity Federation. *Obes. Rev.* **18**, 715–723 (2017).

2. Blüher, M. Obesity: global epidemiology and pathogenesis. *Nat. Rev. Endocrinol.* **15**, 288–298 (2019).

3. Sumithran, P. *et al.* Long-Term Persistence of Hormonal Adaptations to Weight Loss. *N. Engl. J. Med.* **365**, 1597–1604 (2011).

4. Venditti, E. M., Bray, G. A. & Carrion-Petersen, M. L. First versus repeat treatment with a lifestyle intervention program: attendance and weight loss outcomes NIH Public Access. *Int J Obes* **32**, 1537–1544 (2008).

5. OECD. *OECD Obesity Update 2017*. www.oecd.org/health/obesity-update.htm (2017).

6. Fontaine, K. R., Redden, D. T., Wang, C., Westfall, A. O. & Allison, D. B. Years of life lost due to obesity. *J. Am. Med. Assoc.* **289**, 187–193 (2003).

7. WHO. *Noncommunicable diseases - Progress Monitor 2017*. https://apps.who.int/iris/bitstream/handle/10665/258940/9789241513029-eng.pdf?sequence=1 (2017).

8. World Health Organization and others. Global action plan for the prevention and control of noncommunicable diseases 2013-2020. *World Health Organization* (2013).

9. Obesity: Definition, Comorbidities, Causes, and Burden. https://www.ajmc.com/journals/supplement/2016/impact-obesity-interventions-managed-care/obesity-definition-comorbidities-causes-burden.

10. Abdullah, A. The Double Burden of Undernutrition and Overnutrition in Developing Countries: an Update. *Curr. Obes. Rep.* **4**, 337–349 (2015).

11. Antonopoulos, A. S. & Tousoulis, D. The molecular mechanisms of obesity paradox. *Cardiovasc. Res.* **113**, 1074–1086 (2017).

12. Huttunen, R. & Syrjänen, J. Obesity and the risk and outcome of infection. *Int. J. Obes.* **37**, 333–340 (2013).

13. Simonnet, A. *et al.* High Prevalence of Obesity in Severe Acute Respiratory Syndrome Coronavirus-2 (SARS-CoV-2) Requiring Invasive Mechanical Ventilation. *Obesity* **28**, 1195–1199 (2020).

14. Phelan, S. M. *et al.* Impact of weight bias and stigma on quality of care and outcomes for patients with obesity. *Obes. Rev.* **16**, 319–326 (2015).

15. Pont, S. J., Puhl, R., Cook, S. R. & Slusser, W. Stigma experienced by children and adolescents with obesity. *Pediatrics* **140**, e20173034 (2017).

16. Tomiyama, A. J. *et al.* How and why weight stigma drives the obesity 'epidemic' and harms health. *BMC Med.* **16**, (2018).

17. Geserick, M. *et al.* Acceleration of BMI in Early Childhood and Risk of Sustained

Obesity. *N. Engl. J. Med.* **379**, 1303–1312 (2018).

18. Vaamonde, J. G. & Álvarez-Món, M. A. Obesity and overweight. *Med.* **13**, 767–776 (2020).

19. Ford, N. D., Patel, S. A. & Narayan, K. M. V. Obesity in Low- and Middle-Income Countries: Burden, Drivers, and Emerging Challenges. *Annu. Rev. Public Health* **38**, 145–164 (2017).

20. Hannah Ritchie and Max Roser. Obesity - Our World in Data Published online at OurWorldInData.org. Retrieved from: 'https://ourworldindata.org/obesity'. https://ourworldindata.org/obesity#citation (2020).

21. Abarca-GÃ, L. *et al.* Worldwide trends in body-mass index, underweight, overweight, and obesity from 1975 to 2016: a pooled analysis of 2416 population-based measurement studies in 128·9 million children, adolescents, and adults NCD Risk Factor Collaboration (NCD-RisC)*. *Lancet* **390**, 2627–2642 (2017).

22. Alexandratos, N. & Bruinsma, J. *World agriculture towards 2030/2050*. www.fao.org/economic/esa (2012).

23. De Macedo, I. C., De Freitas, J. S. & Da Silva Torres, I. L. The influence of palatable diets in reward system activation: A mini review. *Adv. Pharmacol. Sci.* (2016) doi:10.1155/2016/7238679.

24. Monteiro, C. A., Moubarac, J. C., Cannon, G., Ng, S. W. & Popkin, B. Ultra-processed products are becoming dominant in the global food system. *Obes. Rev.* **14**, 21–28 (2013).

25. Peeters, A. Obesity and the future of food policies that promote healthy diets. *Nat. Rev. Endocrinol.* **14**, 430–437 (2018).

26. Smith, R., Kelly, B., Yeatman, H. & Boyland, E. Food marketing influences children's attitudes, preferences and consumption: A systematic critical review. *Nutrients* **11**, (2019).

27. Ludwig, J. *et al.* Neighborhoods, Obesity, and Diabetes — A Randomized Social Experiment. *N. Engl. J. Med.* **365**, 1509–1519 (2011).

28. Sarget, M. Why inequality is fatal. *Nature* 1109–1110 (2009).

29. Speakman, J. R. A Nonadaptive Scenario Explaining the Genetic Predisposition to Obesity: The 'Predation Release' Hypothesis. *Cell Metab.* **6**, 5–12 (2007).

30. Van Der Klaauw, A. A. & Sadaf Farooqi, I. The Hunger Genes: Pathways to Obesity. *Cell* **161**, 119–132 (2015).

31. Thaker, V. V. Genetic and epigenetic causes of obesity. *Adolesc. Med. State Art Rev.* **28**, 379–405 (2017).

32. Montague, C. T. *et al.* Congenital leptin deficiency is associated with severe early-onset obesity in humans. *Nature* **387**, 903–908 (1997).

33. Loos, R. J. F. & Yeo, G. S. H. The bigger picture of FTO - The first GWAS-identified obesity gene. *Nat. Rev. Endocrinol.* **10**, 51–61 (2014).

34. Tomar, A. S. ing. *et al.* Intrauterine Programming of Diabetes and Adiposity. *Curr. Obes. Rep.* **4**, 418–428 (2015).

35. Reilly, J. J. *et al.* Early life risk factors for obesity in childhood: Cohort study. *Br. Med. J.* **330**, 1357–1359 (2005).

36. Hu, Z. *et al.* Maternal metabolic factors during pregnancy predict early childhood growth trajectories and obesity risk: the CANDLE Study. *Int. J. Obes.* **43**, 1914–1922 (2019).

37. Godfrey, K. M. *et al.* Influence of maternal obesity on the long-term health of offspring. *Lancet Diabetes Endocrinol.* **5**, 53–64 (2017).

38. Fleming, T. P. *et al.* Origins of Lifetime Health Around the Time of Conception: Causes and Consequences. *Obstet. Gynecol. Surv.* **73**, 555–557 (2018).

39. Ong, K. K. L., Ahmed, M. L., Dunger, D. B., Emmett, P. M. & Preece, M. A. Association between postnatal catch-up growth and obesity in childhood: Prospective cohort study. *Br. Med. J.* **320**, 967–971 (2000).

40. Barclay, K. & Myrskylä, M. Maternal age and offspring health and health behaviours in late adolescence in Sweden. *SSM - Popul. Heal.* **2**, 68–76 (2016).

41. Fernandez-Twinn, D. S., Hjort, L., Novakovic, B., Ozanne, S. E. & Saffery, R. Intrauterine programming of obesity and type 2 diabetes. *Diabetologia* **62**, 1789–1801 (2019).

42. Barker, D. J. P. The origins of the developmental origins theory. *J. Intern. Med.* **261**, 412–417 (2007).

43. Rose, G. Familial patterns in ischaemic heart disease. *Br. J. Prev. Soc. Med.* **18**, 75–80 (1964).

44. Forsdahl, A. Are poor living conditions in childhood and adolescence an important risk factor for arteriosclerotic heart disease? *Br. J. Prev. Soc. Med.* **31**, 91–95 (1977).

45. Marmot, M. G., Shipley, M. J. & Rose, G. Inequalities in deatch - specific explanations of a general pattern. *Lancet* (1984).

46. Notkola, V., Punsar, S., Karvonen, M. J. & Haapakoski, J. Socio-economic conditions in childhood and mortality and morbidity caused by coronary heart disease in adulthood in rural Finland. *Soc. Sci. Med.* **21**, 517–523 (1985).

47. Cooper, C. David Barker (1938 - 2013). *Nature* **502**, 304 (2013).

48. Barker, D. J. P. & Osmond, C. INFANT MORTALITY, CHILDHOOD NUTRITION, AND ISCHAEMIC HEART DISEASE IN ENGLAND AND WALES. *Lancet* **327**, 1077–1081 (1986).

49. Barker, D. J. P., Winter, P. D., Osmond, C., Margetts, B. & Simmonds, S. J. Weight in infancy and death from ischeamic heart disease. *Lancet* **1**, 437–447 (1989).

50. Hales, C. N. *et al.* Fetal and infant growth and impaired glucose tolerance at age 64. *BMJ* **303**, 1019–1022 (1991).

51. Hales, C. N. & Barker, D. J. P. Type 2 (non-insulin-dependent) diabetes mellitus: the thrifty phenotype hypothesis. *Diabetologia* **35**, 595–601 (1992).

52. Bateson, P. *et al.* Developmental plasticity and human health. *Nature* **430**, 419–421 (2004).

53. Stein, C. E. *et al.* Fetal growth and coronary heart disease in South India. *Lancet* **348**, 1269–73 (1996).

54. Eriksson, J. G. *et al.* Catch-up growth in childhood and death from coronary heart disease: longitudinal study. *BMJ* **318**, (1999).

55. Barker, D. J. P. *et al.* Fetal nutrition and cardiovascular disease in adult life. *Lancet* **341**, 938–941 (1993).

56. Roseboom, T. J. *et al. Effects of prenatal exposure to the Dutch famine on adult disease in later life: an overview*. *Molecular and Cellular Endocrinology* vol. 185 www.elsevier.com/locate/mce (2001).

57. Gluckman, P. D., Hanson, M. A., Phil, D., Cooper, C. & Thornburg, K. L. Effect of In Utero and Early-Life Conditions on Adult Health and Disease. *N. Engl. J. Med.* **359**, 61–73 (2008).

58. Dearden, L., Bouret, S. G. & Ozanne, S. E. Sex and gender differences in developmental programming of metabolism. *Mol. Metab.* **15**, 8–19 (2018).

59. Eriksson, J. G., Kajantie, E., Osmond, C., Thornburg, K. & Barker, D. J. P. Boys Live Dangerously in the Womb. *Am J Hum Biol* **22**, 330–335 (2010).

60. Raad, G. *et al.* Paternal obesity: How bad is it for sperm quality and progeny health? *Basic Clin. Androl.* **27**, 20 (2017).

61. Watkins, A. J. *et al.* Paternal diet programs offspring health through sperm- and seminal plasma-specific pathways in mice. *Proc. Natl. Acad. Sci. U. S. A.* **115**, 10064–10069 (2018).

62. Mcpherson, N. O., Owens, J. A., Fullston, T. & Lane, M. Preconception diet or exercise intervention in obese fathers normalizes sperm microRNA profile and metabolic syndrome in female offspring. *Am J Physiol Endocrinol Metab* **308**, 805–821 (2015).

63. Zimmet, P., Shi, Z., El-Osta, A. & Ji, L. Epidemic T2DM, early development and epigenetics: implications of the Chinese Famine. *Nat. Rev. Endocrinol.* **14**, (2018).

64. Thurner, S. *et al.* Quantification of excess risk for diabetes for those born in times of hunger, in an entire population of a nation, across a century. *PNAS* **110**, 4703–4707 (2013).

65. Monrad, R. N. *et al.* Age-dependent nongenetic influences of birth weight and adult body fat on insulin sensitivity in twins. *J. Clin. Endocrinol. Metab.* **94**, 2394–2399 (2009).

66. Victora, C. G. *et al.* Maternal and child undernutrition: consequences for adult health and human capital. *Lancet* **371**, 340–357 (2008).

67. Chen, X. K. *et al.* Teenage pregnancy and adverse birth outcomes: A large population based retrospective cohort study. *Int. J. Epidemiol.* **36**, 368–373 (2007).

68. Ozanne, S. E. Metabolic programming in animals. *Br. Med. Bull.* **60**, 143–152 (2001).

69. Langley-Evans, S. C. Developmental programming of health and disease. *Proc. Nutr. Soc.* **65**, 97–105 (2006).

70. Winship, A., Gazzard, S., Cullen-McEwen, L., Bertram, J. & Hutt, K. Maternal low-protein diet programmes low ovarian reserve in offspring. *Reproduction* **156**, 1741–7899 (2018).

71. Begum, G. *et al.* Maternal undernutrition programs tissue-specific epigenetic changes in the glucocorticoid receptor in adult offspring. *Endocrinology* **154**, 4560–4569 (2013).

72. Darby, J. R. T., Mcmillen, I. C., Morrison, J. L., Barrett, K. & Ardell, J. Maternal undernutrition in late gestation increases IGF2 signalling molecules and collagen deposition in the right ventricle of the fetal sheep heart. *J. Physiol.* **596**, 2345–2358 (2018).

73. Correia-Branco, A., Keating, E. & Martel, F. Maternal undernutrition and fetal developmental programming of obesity: The glucocorticoid connection. *Reprod. Sci.* **22**, 138–145 (2015).

74. Fernandez-Twinn, D. S. *et al.* The maternal endocrine environment in the low-protein model of intra-uterine growth restriction. *Br. J. Nutr.* **90**, 815–822 (2003).

75. Khashan, A. *et al.* Reduced Infant Birthweight Consequent Upon Maternal Exposure to Severe Life Events. *Psychosom. Med.* **70**, 688–694 (2008).

76. Class, Q. A., Lichtenstein, P., Långström, N. & D'Onofrio, B. M. Timing of prenatal maternal exposure to severe life events and adverse pregnancy outcomes: A population study of 2.6 million pregnancies. *Psychosom. Med.* **73**, 234–241 (2011).

77. Dancause, K. N. *et al.* Prenatal exposure to a natural disaster increases risk for obesity in 5-year-old children. *Pediatr. Res.* **71**, 126–131 (2012).

78. Paxman, E. J. *et al.* Prenatal Maternal Stress from a Natural Disaster Alters Urinary Metabolomic Profiles in Project Ice Storm Participants OPEN. *Sci. Rep.* **8**, (2018).

79. Van den Bergh, B. R. H. *et al.* Prenatal developmental origins of behavior and mental health: The influence of maternal stress in pregnancy. *Neurosci. Biobehav. Rev.* **117**, 26–64 (2020).

80. Lesage, J. *et al.* Prenatal stress induces intrauterine growth restriction and programmes glucose intolerance and feeding behaviour disturbances in the aged rat. *J. Endocrinol.* **181**, 291–296 (2004).

81. Tamashiro, K. L. K., Terrillion, C. E., Hyun, J., Koenig, J. I. & Moran, T. H. Prenatal stress or high-fat diet increases susceptibility to diet-induced obesity in rat offspring. *Diabetes* **58**, 1116–1125 (2009).

82. Abraham, M. *et al.* A systematic review of maternal smoking during pregnancy and fetal measurements with meta-analysis. *PLoS One* **12**, (2017).

83. Weinberg, J., Sliwowska, J. H., Lan, N. & Hellemans, K. G. C. Prenatal Alcohol Exposure: Foetal Programming, the Hypothalamic-Pituitary-Adrenal Axis and Sex Differences in Outcome. *J. Neuroendocrinol.* **20**, 470–488 (2008).

84. Eustace, L. W., Kang, D. H. & Coombs, D. Fetal alcohol syndrome: a growing concern for health care professionals. *JOGNN* **32**, 215–221 (2003).

85. Segal, T. R. & Giudice, L. C. Before the beginning: environmental exposures and reproductive and obstetrical outcomes. *Fertil. Steril.* **112**, 613–621 (2019).

86. Vargesson, N. Thalidomide-induced teratogenesis: History and mechanisms. *Birth Defects Res. Part C - Embryo Today Rev.* **105**, 140–156 (2015).

87. Stillerman, K. P., Mattison, D. R., Giudice, L. C. & Woodruff, T. J. Environmental exposures and adverse pregnancy outcomes: A review of the science. *Reprod. Sci.* **15**, 631–650 (2008).

88. Bu¨s¸ra, B. *et al.* Parental smoking during pregnancy, early growth, and risk of obesity in preschool children: the Generation R Study 1-3. *Am J Clin Nutr* **94**, 164–71 (2011).

89. Harris, H. R., Willett, W. C. & Michels, K. B. Parental smoking during pregnancy and risk of overweight and obesity in the daughter. *Int. J. Obes.* **37**, 1356–1363 (2013).

90. Pringle, P. J. *et al.* The influence of cigarette smoking on antenatal growth, birth size, and the insulin-like growth factor axis. *J. Clin. Endocrinol. Metab.* **90**, 2556–2562 (2005).

91. Dutta, A. *et al.* Household air pollution and chronic hypoxia in the placenta of pregnant Nigerian women: A randomized controlled ethanol Cookstove intervention. *Sci. Total Environ.* **619**–**620**, 212–220 (2018).

92. Giussani, D. A. The fetal brain sparing response to hypoxia: physiological mechanisms. *J. Physiol.* **594**, 1215–30 (2016).

93. Barouki, R., Gluckman, P. D., Grandjean, P., Hanson, M. & Heindel, J. J. Developmental origins of non-communicable disease: Implications for research and public health. *Environ. Heal. A Glob. Access Sci. Source* **11**, 42 (2012).

94. Alonso-Magdalena, P. *et al.* Endocrine disruptors in the etiology of type 2 diabetes mellitus. *Nat. Rev. Endocrinol* **346**, 346–353 (2011).

95. Ritchie, H. E., Oakes, D. J., Kennedy, D. & Polson, J. W. Early Gestational Hypoxia and Adverse Developmental Outcomes. *Birth Defects Res.* **109**, 1358–1376 (2017).

96. Ducsay, C. A. *et al.* Gestational hypoxia and developmental plasticity. *Physiol. Rev.* **98**, 1241–1334 (2018).

97. Waldorf, K. M. A. & McAdams, R. M. Influence of Infection During Pregnancy on Fetal Development. *Reproduction* **146**, R151–R162 (2013).

98. Reyes, L. & Golos, T. G. Hofbauer cells: Their role in healthy and complicated pregnancy. *Front. Immunol.* **9**, 2628 (2018).

99. Knight, M. *et al.* Characteristics and outcomes of pregnant women admitted to hospital with confirmed SARS-CoV-2 infection in UK: National population based cohort study. *BMJ* **369**, (2020).

100. Shanes, E. D. *et al.* Placental Pathology in COVID-19. *Am J Clin Pathol* **154**, 23–32 (2020).

101. Karasek, D. *et al.* The association of COVID-19 infection in pregnancy with preterm birth: A retrospective cohort study in California. *Lancet Reg. Heal. - Am.* **2**, 100027 (2021).

102. McClure, E. M. & Goldenberg, R. L. Use of antibiotics to reduce preterm birth. *Lancet Glob. Heal.* **7**, e18–e19 (2019).

103. Locksmith, G. & Duff, P. Infection, Antibiotics, and Preterm Delivery. *Semin. Perinatol.* **25**, 295 (2001).

104. Nadeau-Vallée, M. *et al.* Sterile inflammation and pregnancy complications: a review. *Reproduction* **152**, 277–292 (2016).

105. Plows, J. F., Stanley, J. L., Baker, P. N., Reynolds, C. M. & Vickers, M. H. The pathophysiology of gestational diabetes mellitus. *Int. J. Mol. Sci.* **19**, 3342 (2018).

106. Grimes, S. B. & Wild, R. *Effect of Pregnancy on Lipid Metabolism and Lipoprotein Levels*. *Endotext* (MDText.com, Inc., 2018).

107. Ryckman, K. K., Spracklen, C. N., Smith, C. J., Robinson, J. G. & Saftlas, A. F. Maternal lipid levels during pregnancy and gestational diabetes: A systematic review and meta-analysis. *BJOG An Int. J. Obstet. Gynaecol.* **122**, 643–651 (2015).

108. Musial, B. *et al.* Proximity to delivery alters insulin sensitivity and glucose metabolism in pregnant mice. *Diabetes* **65**, 851–860 (2016).

109. Ramos, M. P., Crespo-Solans, M. D., Del Campo, S., Cacho, J. & Herrera, E. Fat accumulation in the rat during early pregnancy is modulated by enhanced insulin responsiveness. *Am. J. Physiol. - Endocrinol. Metab.* **285**, E318–E328 (2003).

110. Burke, S. D. Blood Pressure Regulation during Mouse Pregnancy. in *The Guide to Investigation of Mouse Pregnancy* 341–351 (Elsevier, 2014). doi:10.1016/b978-0-12-394445-0.00029-1.

111. Burke, S. D. *et al.* Spiral arterial remodeling is not essential for normal blood pressure regulation in pregnant mice. *Hypertension* **55**, 729–737 (2010).

112. Leonard, S., Lima, P. D. A., Croy, B. A. & Murrant, C. L. Gestational modification of murine spiral arteries does not reduce their drug-induced vasoconstrictive responses in vivo1. *Biol. Reprod.* **89**, 1–10 (2013).

113. James, J. L., Chamley, L. W. & Clark, A. R. Feeding Your Baby In Utero: How the Uteroplacental Circulation Impacts Pregnancy. *Physiology* **32**, 234–245 (2017).

114. Mecacci, F. *et al.* Fetal Growth Restriction : Does an Integrated Maternal Hemodynamic-Placental Model Fit Better ? *Reprod. Sci.* **28**, 2422–2435 (2020).

115. Soma-Pillay, P., Nelson-Piercy, C., Tolppanen, H. & Mebazaa, A. Physiological changes in pregnancy. *Cardiovasc. J. Afr.* **27**, 89–94 (2016).

116. Kulandavelu, S., Qu, D. & Adamson, S. L. Cardiovascular function in mice during normal pregnancy and in the absence of endothelial NO synthase. *Hypertension* **47**, 1175–1182 (2006).

117. Perry, H., Khalil, A. & Thilaganathan, B. Preeclampsia and the cardiovascular system:

An update. *Trends Cardiovasc. Med.* **0**, 1–9 (2018).

118. Sones, J. L. & Davisson, R. L. Preeclampsia, of mice and women. *Physiol. Genomics* **48**, 565–572 (2016).

119. Varas Enriquez, P. J., McKerracher, L. J. & Elliot, M. G. Pre-eclampsia and maternal–fetal conflict. *Evol. Med. Public Heal.* **2018**, 217–218 (2018).

120. WHO. WHO recommendations on antenatal Care for a Positive Pregnancy Experience. *World Heal. Organ.* **10**, 1–10 (2016).

121. Morgan, J. A. & Cooper, D. B. *Pregnancy Dating*. *StatPearls* (StatPearls Publishing, 2021).

122. Papageorghiou, A. T. *et al.* International standards for fetal growth based on serial ultrasound measurements: The Fetal Growth Longitudinal Study of the INTERGROWTH-21st Project. *Lancet* **384**, 869–879 (2014).

123. Stirnemann, J. *et al.* International estimated fetal weight standards of the INTERGROWTH-21st Project. *Ultrasound Obstet. Gynecol.* **49**, 478–486 (2017).

124. Meek, C. L. *et al.* Which growth standards should be used to identify large- and small-for-gestational age infants of mothers with type 1 diabetes? A pre-specified analysis of the CONCEPTT trial. *BMC Pregnancy Childbirth* **21**, 96 (2021).

125. Gardosi, J. & Francis, A. A customized standard to assess fetal growth in a US population. *Am. J. Obstet. Gynecol.* **201**, 25.e1–7 (2009).

126. Gardosi, J., Francis, A., Turner, S. & Williams, M. Customized growth charts: rationale, validation and clinical benefits. *Am. J. Obstet. Gynecol.* **218**, S609–S618 (2018).

127. Iliodromiti, S. & Smith, G. C. S. Aggregated data do not confer causality: there is a paucity of evidence supporting the Growth Assessment Protocol as the major cause of declining stillbirth rate in the UK. *Ultrasound Obstet. Gynecol.* **56**, 119–120 (2020).

128. Iliodromiti, S., Smith, G. C. S., Lawlor, D. A., Pell, J. P. & Nelson, S. M. UK stillbirth trends in over 11 million births provide no evidence to support effectiveness of Growth Assessment Protocol program. *Ultrasound Obstet. Gynecol.* **55**, 599–604 (2020).

129. Papageorghiou, A. T. *et al.* International standards for symphysis-fundal height based on serial measurements from the Fetal Growth Longitudinal Study of the INTERGROWTH-21(st) Project: Prospective cohort study in eight countries. *BMJ* **355**, i5662 (2016).

130. Hiersch, L. & Melamed, N. Fetal growth velocity and body proportion in the assessment of growth. *Am. J. Obstet. Gynecol.* **218**, S700–S711 (2018).

131. Dupak, J. D. L. & Trujillo, A. L. Ultrasound surveillance in pregnancy complicated by diabetes. *Diabetes Spectr.* **20**, 89–93 (2007).

132. Akolekar, R. *et al.* Fetal middle cerebral artery and umbilical artery pulsatility index: effects of maternal characteristics and medical history. *Ultrasound Obs. Gynecol* **45**, 402–408 (2015).

133. MacDonald, T. M. *et al.* Reduced growth velocity across the third trimester is associated with placental insufficiency in fetuses born at a normal birthweight: A prospective cohort study. *BMC Med.* **15**, 164 (2017).

134. Dilworth, M. R. *et al.* Defining fetal growth restriction in mice: A standardized and clinically relevant approach. *Placenta* **32**, 914–916 (2011).

135. Hayward, C. E. *et al.* Placental Adaptation: What Can We Learn from Birthweight:Placental Weight Ratio? *Front. Physiol.* **7**, 28 (2016).

136. Grantz, K. L. *et al.* Fetal growth velocity: the NICHD fetal growth studies. *Am. J. Obstet. Gynecol.* **219**, 285.e1-285.e36 (2018).

137. Desoye, G. The Human Placenta in Diabetes and Obesity: Friend or Foe? *Diabetes Care* **41**, 1362–1369 (2018).

138. Cline, J. M. *et al.* The Placenta in Toxicology. Part III:Pathologic Assessment of the Placenta. *Toxicol. Pathol.* **42**, 339–344 (2014).

139. Guariguata, L., Linnenkamp, U., Beagley, J., Whiting, D. R. & Cho, N. H. Global estimates of the prevalence of hyperglycaemia in pregnancy. *Diabetes Res. Clin. Pract.* **103**, 176–185 (2014).

140. Mcintyre, H. D. *et al.* Gestational diabetes mellitus. *Nat. Rev. Prim.* **5 (1)**, (2019).

141. Hillebrand, D. R. H. & B. The first recorded case of diabetic pregnancy (Bennewitz HG, 1824, University of Berlin). *Diabetologia* **32**, 625 (1989).

142. Brown, F. M. & Wyckoff, J. Application of One-Step IADPSG Versus Two-Step Diagnostic Criteria for Gestational Diabetes in the Real World: Impact on Health Services, Clinical Care, and Outcomes. *Curr. Diab. Rep.* **17**, (2017).

143. Kampmann, U., Knorr, S., Fuglsang, J. & Ovesen, P. Determinants of Maternal Insulin Resistance during Pregnancy: An Updated Overview. *J. Diabetes Res.* **2019**, (2019).

144. Di Cianni, G., Miccoli, R., Volpe, L., Lencioni, C. & Del Prato, S. Intermediate metabolism in normal pregnancy and in gestational diabetes. *Diabetes. Metab. Res. Rev.* **19**, 259–270 (2003).

145. Committee on Practice Bulletins - Obstetrics. ACOG Practice Bulletin Number 190: Gestational Diabetes Mellitus Interim Update. *Obstet. Gynecol.* **131**, e49–e64 (2018).

146. Gorgal, R. *et al.* Gestational diabetes mellitus: A risk factor for non-elective cesarean section. *J. Obstet. Gynaecol. Res.* **38**, 154–159 (2012).

147. Mitanchez, D. *et al.* The offspring of the diabetic mother e Short-and long-term implications. *Best Pract. Res. Clin. Obstet. Gynaecol.* **29**, 256–269 (2015).

148. Vambergue, A. & Fajardy, I. Consequences of gestational and pregestational diabetes on placental function and birth weight. *World J. Diabetes* **2**, 196 (2011).

149. Pasek, R. C. & Gannon, M. Advancements and challenges in generating accurate animal models of gestational diabetes mellitus. *Am. J. Physiol. - Endocrinol. Metab.* **305**, E1327 (2013).

150. Aasa, K. L., Kwong, K. K., Adams, M. A. & Croy, B. A. Analysis of maternal and fetal

cardiovascular systems during hyperglycemic pregnancy in the nonobese diabetic mouse. *Biol. Reprod.* **88**, 151 (2013).

151. Kahraman, S., Dirice, E., De Jesus, D. F., Hu, J. & Kulkarni, R. N. Maternal insulin resistance and transient hyperglycemia impact the metabolic and endocrine phenotypes of offspring. *Am. J. Physiol. - Endocrinol. Metab.* **307**, E906–E918 (2014).

152. Lapolla, A., Boyd, · & Metzger, E. The post-HAPO situation with gestational diabetes: the bright and dark sides. **55**, 885–892 (2018).

153. Mishra, S., Rao, C. R. & Shetty, A. Trends in the Diagnosis of Gestational Diabetes Mellitus. *Scientifica (Cairo).* **2016**, (2016).

154. Coustan, D. R., Lowe, L. P., Metzger, B. E. & Dyer, A. R. The Hyperglycemia and Adverse Pregnancy Outcome (HAPO) study: paving the way for new diagnostic criteria for gestational diabetes mellitus. *Am. J. Obstet. Gynecol.* **202**, 654.e1-654.e6 (2010).

155. Dickens, L. T. & Thomas, C. C. Updates in Gestational Diabetes Prevalence, Treatment, and Health Policy. *Curr. Diab. Rep.* **19**, (2019).

156. Landon, M. B. *et al.* A Multicenter, Randomized Trial of Treatment for Mild Gestational Diabetes. *N. Engl. J. Med.* **361**, 1339–1348 (2009).

157. Kim, W., Park, S. K. & Kim, Y. L. Gestational diabetes mellitus diagnosed at 24 to 28 weeks of gestation in older and obese women: Is it too late? *PLoS One* **14**, e0225955 (2019).

158. Gesellschaft, D. D. *Deutsche Diabetes Gesellschaft Deutsche Gesellschaft für Gynäkologie und Geburtshilfe Arbeitsgemeinschaft Diabetes und Schwangerschaft der DDG Arbeitsgemeinschaft Geburtshilfe und Pränatalmedizin in der DGGG*. (2018).

159. NICE (The National Institute for Health and Care Excellence). *Diabetes in pregnancy: management from preconception to the postnatal period*. https://www.nice.org.uk/guidance/ng3 (2015).

160. Rodrigo, N. & Glastras, S. The Emerging Role of Biomarkers in the Diagnosis of Gestational Diabetes Mellitus. *J. Clin. Med.* **7**, 120 (2018).

161. Jaskolka, D., Retnakaran, R., Zinman, B. & Kramer, C. K. Sex of the baby and risk of gestational diabetes mellitus in the mother: a systematic review and meta-analysis. *Diabetologia* **58**, 2469–2475 (2015).

162. Retnakaran, R. *et al.* Fetal sex and maternal risk of gestational diabetes mellitus: The impact of having a boy. *Diabetes Care* **38**, 844–851 (2015).

163. Anna, V., Van Der Ploeg, H. P., Cheung, N. W., Huxley, R. R. & Bauman, A. E. Sociodemographic correlates of the increasing trend in prevalence of gestational diabetes mellitus in a large population of women between 1995 and 2005. *Diabetes Care* **31**, 2288–2293 (2008).

164. Yuen, L., Wong, V. W. & Simmons, D. Ethnic Disparities in Gestational Diabetes. *Curr. Diab. Rep.* **18**, (2018).

165. Zhang, C. *et al.* Genetic variants and the risk of gestational diabetes mellitus: a systematic review. *Hum. Reprod. Update* **19**, 376–390 (2013).

166. Zhang, C. & Ning, Y. Effect of dietary and lifestyle factors on the risk of gestational diabetes: Review of epidemiologic evidence. *Am. J. Clin. Nutr.* **94**, 1975S–9S (2011).

167. Zhu, Y. & Zhang, C. Prevalence of Gestational Diabetes and Risk of Progression to Type 2 Diabetes: a Global Perspective. *Curr. Diab. Rep.* **16**, 1–11 (2016).

168. Hod, M. *et al.* The International Federation of Gynecology and Obstetrics (FIGO) Initiative on gestational diabetes mellitus: A pragmatic guide for diagnosis, management, and care. *Int. J. Gynecol. Obstet.* **131**, S173–S211 (2015).

169. Koyanagi, A. *et al.* Macrosomia in 23 developing countries: An analysis of a multicountry, facility-based, cross-sectional survey. *Lancet* **381**, 476–483 (2013).

170. Hill, B. *et al.* Health in Preconception, Pregnancy and Postpartum Global Alliance: International Network Preconception Research Priorities for the Prevention of Maternal Obesity and Related Pregnancy and Long-Term Complications. *J. Clin. Med.* **8**, 2119 (2019).

171. Kominiarek, M. A. & Peaceman, A. M. Gestational Weight Gain. *Am J Obs. Gynecol* **176**, 139–148 (2018).

172. Walter, J. R. *et al.* Associations of trimester-specific gestational weight gain with maternal adiposity and systolic blood pressure at 3 and 7 years postpartum HHS Public Access. *Am J Obs. Gynecol* **212**, 499–500 (2015).

173. Karachaliou, M. *et al.* Association of trimester-specific gestational weight gain with fetal growth, offspring obesity, and cardiometabolic traits in early childhood. *Am. J. Obstet. Gynecol.* **212**, 502.e1-502.e14 (2015).

174. Bodnar, L. M. *et al.* Maternal obesity and gestational weight gain are risk factors for infant death. *Obesity* **24**, 490–498 (2016).

175. Santos, S. *et al.* Impact of maternal body mass index and gestational weight gain on pregnancy complications: an individual participant data meta-analysis of European, North American and Australian cohorts. *BJOG An Int. J. Obstet. Gynaecol.* **126**, 984–995 (2019).

176. Voerman, E. *et al.* Association of Gestational Weight Gain With Adverse Maternal and Infant Outcomes. *JAMA* **321**, 1702–1715 (2019).

177. Health matters: reproductive health and pregnancy planning - GOV.UK. https://www.gov.uk/government/publications/health-matters-reproductive-health-and-pregnancy-planning/health-matters-reproductive-health-and-pregnancy-planning.

178. Poston, L. *et al.* Preconceptional and maternal obesity: epidemiology and health consequences. *Lancet Diabetes Endocrinol.* **4**, 1025–1036 (2016).

179. Bramham, K. *et al.* Chronic hypertension and pregnancy outcomes: Systematic review and meta-analysis. *BMJ* **348**, (2014).

180. Dashe, J. S., McIntire, D. D. & Twickler, D. M. Maternal obesity limits the ultrasound evaluation of fetal anatomy. *J. Ultrasound Med.* **28**, 1025–1030 (2009).

181. Marchi, J., Berg, M., Dencker, A., Olander, E. K. & Begley, C. Risks associated with

obesity in pregnancy, for the mother and baby: A systematic review of reviews. *Obes. Rev.* **16**, 621–638 (2015).

182. Metzger, B. E. Hyperglycaemia and adverse pregnancy outcome (HAPO) study: Associations with maternal body mass index. *BJOG An Int. J. Obstet. Gynaecol.* **117**, 575–584 (2010).

183. Zhang, L. *et al.* Maternal obesity in the ewe results in reduced fetal pancreatic β-cell numbers in late gestation, and decreased circulating insulin concentration at term. *Domest Anim Endocrinol* **40**, 30–39 (2011).

184. Frias, A. E. *et al.* Maternal high-fat diet disturbs uteroplacental hemodynamics and increases the frequency of stillbirth in a nonhuman primate model of excess nutrition. *Endocrinology* **152**, 2456–2464 (2011).

185. Hanssens, S. *et al.* Maternal obesity alters the apelinergic system at the feto-maternal interface. *Placenta* **39**, 41–44 (2016).

186. Chin, E. H. *et al.* A maternal high-fat, high-sucrose diet has sex-specific effects on fetal glucocorticoids with little consequence for offspring metabolism and voluntary locomotor activity in mice. *PLoS One* **12**, e0174030 (2017).

187. Huet, J., Beucher, G., Rod, A., Morello, R. & Dreyfus, M. Joint impact of gestational diabetes and obesity on perinatal outcomes. *J. Gynecol. Obstet. Hum. Reprod.* **47**, 469–476 (2018).

188. Wahabi, H. A., Fayed, A. A., Alzeidan, R. A. & Mandil, A. A. The independent effects of maternal obesity and gestational diabetes on the pregnancy outcomes. *BMC Endocr. Disord.* **14**, (2014).

189. Ijäs, H. *et al.* Independent and concomitant associations of gestational diabetes and maternal obesity to perinatal outcome: A register-based study. *PLoS One* **14**, e0221549 (2019).

190. Maltepe, E. & Fisher, S. J. Placenta: The Forgotten Organ. *Annu. Rev. Cell Dev. Biol* **31**, 523–52 (2015).

191. Mourier, E. *et al.* Non-invasive evaluation of placental blood flow: lessons from animal models. *Reproduction* **153**, R85–R96 (2017).

192. Mirbod, P. Analytical model of the feto-placental vascular system: consideration of placental oxygen transport. *R. Soc. open Sci.* **5**, 180219 (2018).

193. James-Allan, L. B., Arbet, J., Teal, S. B., Powell, T. L. & Jansson, T. Insulin Stimulates GLUT4 Trafficking to the Syncytiotrophoblast Basal Plasma Membrane in the Human Placenta. *J. Clin. Endocrinol. Metab.* **104**, 4225–4238 (2019).

194. Burton, G. J., Fowden, A. L. & Thornburg, K. L. Placental Origins of Chronic Disease. *Physiol. Rev.* **96**, 1509–1565 (2016).

195. Palmeira, P., Quinello, C., Ucia Silveira-Lessa, A. L. ´, Zago, C. A. & Carneiro-Sampaio, M. IgG Placental Transfer in Healthy and Pathological Pregnancies. *Clin. Dev. Immunol.* **2012**, 13 (2012).

196. Birn, H. & Christensen, E. Megalin and cubilin: multifunctional endocytic receptors.

Nat. Rev. **3**, 258–268 (2002).

197. Storm, T. *et al.* Megalin Is Predominantly Observed in Vesicular Structures in First and Third Trimester Cytotrophoblasts of the Human Placenta. *J. Histochem. Cytochem.* **64**, 769–784 (2016).

198. Cooke, L. D. F. *et al.* Endocytosis in the placenta: An undervalued mediator of placental transfer. *Placenta* **113**, 67–73 (2021).

199. Dally, A. Thalidomide: Was the tragedy preventable? *Lancet* **351**, 1197–1199 (1998).

200. Tetro, N., Moushaev, S., Rubinchik-Stern, M. & Eyal, S. The Placental Barrier: the Gate and the Fate in Drug Distribution. *Pharm Res* **35**, (2018).

201. Nair, S. & Salomon, C. Extracellular vesicles and their immunomodulatory functions in pregnancy. *Semin. Immunopathol.* **40**, 425–437 (2018).

202. Mitchell, M. D. *et al.* Placental exosomes in normal and complicated pregnancy. *Am. J. Obstet. Gynecol.* **213**, S173–S181 (2015).

203. Constância, M. *et al.* Adaptation of nutrient supply to fetal demand in the mouse involves interaction between the Igf2 gene and placental transporter systems. *Proc. Natl. Acad. Sci. U. S. A.* **102**, 19219–24 (2005).

204. Sandovici, I. *et al.* Fetus-derived IGF2 matches placental development to fetal demand. *In resubmission* doi:10.1101/520536.

205. Sferruzzi-Perri, A. N., López-Tello, J., Fowden, A. L. & Constancia, M. Maternal and fetal genomes interplay through phosphoinositol 3-kinase(PI3K)-p110α signaling to modify placental resource allocation. *Proc. Natl. Acad. Sci. U. S. A.* **113**, 11255–11260 (2016).

206. Croy, A., Yamada, A. T., DeMayo, F. J. & Adamson, S. L. *The Guide to Investigation of Mouse Pregnancy*. (2014).

207. Brett, K. E., Ferraro, Z. M., Yockell-Lelievre, J., Gruslin, A. & Adamo, K. B. Maternal–Fetal nutrient transport in pregnancy pathologies: The role of the placenta. *Int. J. Mol. Sci.* **15**, 16153–16185 (2014).

208. Rossant, J. & Cross, J. C. Placental development: Lessons from mouse mutants. *Nat. Rev. Genet.* **2**, 538–548 (2001).

209. Bedzhov, I. & Zernicka-Goetz, M. Self-organizing properties of mouse pluripotent cells initiate morphogenesis upon implantation. *Cell* **156**, 1032–1044 (2014).

210. Gumbiner, B. & Kim, N.-G. The Hippo-YAP signaling pathway and contact inhibition of growth. *J. Cell Sci.* **127**, 709–717 (2014).

211. Ander, S. E., Diamond, M. S. & Coyne, C. B. Immune responses at the maternal-fetal interface. *Sci. Immunol* **4**, 6114 (2019).

212. Leary, C., Leese, H. J. & Sturmey, R. G. Human embryos from overweight and obese women display phenotypic and metabolic abnormalities. *Hum. Reprod.* **30**, 122–132 (2015).

213. Eckert, J. J. *et al.* Metabolic Induction and Early Responses of Mouse Blastocyst

Developmental Programming following Maternal Low Protein Diet Affecting Life-Long Health. *PLoS One* **7**, e52791 (2012).

214. Ibáñez, L., Potau, N., Enriquez, G., Marcos, M. V. & De Zegher, F. Hypergonadotrophinaemia with reduced uterine and ovarian size in women born small-for-gestational-age. *Hum. Reprod.* **18**, 1565–1569 (2003).

215. Martyn, C. N., Barker, D. J. P. & Osmond, C. Mothers' pelvic size, fetal growth, and death from stroke and coronary heart disease in men in the UK. *Lancet* **348**, 1264–68 (1996).

216. Godfrey, K. M. The Role of the Placenta in Fetal Programming-A Review. *Placenta* **23**, 20–27 (2002).

217. Dwyer, C. M., Madgwick, A. J. A., Crook, A. R. & Stickland, N. C. The effect of maternal undernutrition on the growth and development of the guinea pig placenta. *J. Dev. Physiol.* **18**, 295–302 (1992).

218. Roberts, C. T. *et al.* Maternal Food Restriction Reduces the Exchange Surface Area and Increases the Barrier Thickness of the Placenta in the Guinea-pig. *Placenta* **22**, 177–185 (2001).

219. Thornburg, K. L. & Louey, S. Fetal roots of cardiac disease. *Heart* **91**, 867–868 (2005).

220. Camm, E. J., Botting, K. J. & Sferruzzi-Perri, A. N. Near to one's heart: The intimate relationship between the placenta and fetal heart. *Front. Physiol.* **9**, 629 (2018).

221. Uniacke, J. *et al.* An oxygen-regulated switch in the protein synthesis machinery. *Nature* **486**, 126–129 (2012).

222. Lea, R. G. *et al.* The expression of ovine placental lactogen, StaR and progesterone-associated steroidogenic enzymes in placentae of overnourished growing adolescent ewes. *Reproduction* **133**, 785–796 (2007).

223. Hastie, R. & Lappas, M. The effect of pre-existing maternal obesity and diabetes on placental mitochondrial content and electron transport chain activity. *Placenta* **35**, 673–683 (2014).

224. Mele, J., Muralimanoharan, S., Maloyan, A. & Myatt, L. Impaired mitochondrial function in human placenta with increased maternal adiposity. *Am J Physiol Endocrinol Metab* **307**, 419–425 (2014).

225. Buckberry, S., Bianco-Miotto, T., Bent, S. J., Dekker, G. A. & Roberts, C. T. Integrative transcriptome meta-analysis reveals widespread sex-biased gene expression at the human fetal–maternal interface. *Mol. Hum. Reprod.* **20**, 810 (2014).

226. Gohir, W. *et al.* High-fat diet intake modulates maternal intestinal adaptations to pregnancy and results in placental hypoxia, as well as altered fetal gut barrier proteins and immune markers. *J. Physiol.* **597**, 3029–3051 (2019).

227. Li, H.-P., Chen, X. & Li, M.-Q. Original Article Gestational diabetes induces chronic hypoxia stress and excessive inflammatory response in murine placenta. *Int J Clin Exp Pathol* **6**, 650–659 (2013).

228. Jack-Roberts, C. *et al.* Choline supplementation normalizes fetal adiposity and reduces

lipogenic gene expression in a mouse model of maternal obesity. *Nutrients* **9**, 899 (2017).

229. Fernandez-Twinn, D. S. *et al.* Exercise rescues obese mothers' insulin sensitivity, placental hypoxia and male offspring insulin sensitivity. *Sci. Rep.* **7**, 44650 (2017).

230. Musial, B. *et al.* Exercise alters the molecular pathways of insulin signaling and lipid handling in maternal tissues of obese pregnant mice. *Physiol. Rep.* **7**, e14202 (2019).

231. Alfaradhi, M. Z. *et al.* Oxidative stress and altered lipid homeostasis in the programming of offspring fatty liver by maternal obesity. *Am. J. Physiol. - Regul. Integr. Comp. Physiol.* **307**, R26–R34 (2014).

232. Wu, L. L. *et al.* Mitochondrial dysfunction in oocytes of obese mothers: Transmission to offspring and reversal by pharmacological endoplasmic reticulum stress inhibitors. *Development* **142**, 681–691 (2015).

233. Kim, D. W., Young, S. L., Grattan, D. R. & Jasoni, C. L. Obesity During Pregnancy Disrupts Placental Morphology, Cell Proliferation, and Inflammation in a Sex-Specific Manner Across Gestation in the Mouse 1. *Biol. Reprod.* **90**, 130–131 (2014).

234. Parker, V. J., Arck, P. C. & Douglas, A. J. Diet-induced obesity may affect the uterine immune environment in early–mid pregnancy, reducing NK-cell activity and potentially compromising uterine vascularization. *Int. J. Obes.* **38**, 766–774 (2014).

235. Bobadilla, R. A., Van Bree, R., Vercruysse, L., Pijnenborg, R. & Verhaeghe, J. Placental Effects of Systemic Tumour Necrosis Factor-α in an Animal Model of Gestational Diabetes Mellitus. *Placenta* **31**, 1057–1063 (2010).

236. Chen, Y. *et al.* Astaxanthin alleviates gestational diabetes mellitus in mice through suppression of oxidative stress. *Naunyn. Schmiedebergs. Arch. Pharmacol.* **393**, 2517–2527 (2020).

237. Stanley, J. L., Cheung, C. C., Sankaralingam, S., Baker, P. N. & Davidge, S. T. Effect of Gestational Diabetes on Maternal Artery Function. *Reprod. Sci.* **18**, 342–352 (2011).

238. Machado, A. F., Zimmerman, E. F., Hovland, D. N., Weiss, R. & Collins, M. D. Diabetic embryopathy in C57BL/6J mice: Altered fetal sex ratio and impact of the splotch allele. *Diabetes* **50**, 1193–1199 (2001).

239. Zabihi, S., Wentzel, P. & Eriksson, U. J. Maternal Blood Glucose Levels Determine the Severity of Diabetic Embryopathy in Mice with Different Expression of Copper-Zinc Superoxide Dismutase (CuZnSOD). *Toxicol. Sci.* **105**, 166–172 (2008).

240. Huang, L. *et al.* Combined intervention of swimming plus metformin ameliorates the insulin resistance and impaired lipid metabolism in murine gestational diabetes mellitus. *PLoS One* **13**, e0195609 (2018).

241. Lager, S. *et al.* Diet-induced obesity in mice reduces placental efficiency and inhibits placental mTOR signaling. *Physiol. Rep.* **2**, e00242 (2014).

242. Panchenko, P. E. *et al.* Expression of epigenetic machinery genes is sensitive to maternal obesity and weight loss in relation to fetal growth in mice. *Clin. Epigenetics* **8**, 22 (2016).

243. Son, J. S. *et al.* Exercise prevents the adverse effects of maternal obesity on placental vascularization and fetal growth. *J. Physiol.* **597**, 3333–3347 (2019).

244. Sha, H., Zeng, H., Zhao, J. & Jin, H. Mangiferin ameliorates gestational diabetes mellitus-induced placental oxidative stress, inflammation and endoplasmic reticulum stress and improves fetal outcomes in mice. *Eur. J. Pharmacol.* **859**, 172522 (2019).

245. De Barros Mucci, D. *et al.* Impact of maternal obesity on placental transcriptome and morphology associated with fetal growth restriction in mice. *Int. J. Obes.* **44**, 1087–1096 (2020).

246. Qiao, L. *et al.* Adiponectin enhances mouse fetal fat deposition. *Diabetes* **61**, 3199–3207 (2012).

247. Jungheim, E. S. *et al.* Preimplantation Exposure of Mouse Embryos to Palmitic Acid Results in Fetal Growth Restriction Followed by Catch-Up Growth in the Offspring. *Biol. Reprod.* **85**, 678–683 (2011).

248. Bae-Gartz, I. *et al.* Maternal Obesity Alters Neurotrophin-Associated MAPK Signaling in the Hypothalamus of Male Mouse Offspring. *Front. Neurosci.* **13**, (2019).

249. Qiao, L. *et al.* Maternal high-fat feeding increases placental lipoprotein lipase activity by reducing SIRT1 expression in mice. *Diabetes* **64**, 3111–3120 (2015).

250. Qiao, L. *et al.* Prolonged Prepregnant Maternal High-Fat Feeding Reduces Fetal and Neonatal Blood Glucose Concentrations by Enhancing Fetal β-Cell Development in C57BL/6 Mice. *Diabetes* **68**, 1604–1613 (2019).

251. Sugimura, Y. *et al.* Prevention of neural tube defects by loss of function of inducible nitric oxide synthase in fetuses of a mouse model of streptozotocin-induced diabetes. *Diabetologia* **52**, 962–971 (2009).

252. Moazzen, H. *et al.* N-Acetylcysteine prevents congenital heart defects induced by pregestational diabetes. *Cardiovasc. Diabetol.* **13**, 1–13 (2014).

253. Heerwagen, M. J. R., Stewart, M. S., de la Houssaye, B. A., Janssen, R. C. & Friedman, J. E. Transgenic Increase in N-3/N-6 Fatty Acid Ratio Reduces Maternal Obesity-Associated Inflammation and Limits Adverse Developmental Programming in Mice. *PLoS One* **8**, e67791. (2013).

254. Wang, H., Chen, Y., Mao, X. & Du, M. Maternal obesity impairs fetal mitochondriogenesis and brown adipose tissue development partially via upregulation of miR-204-5p. *Biochim. Biophys. Acta - Mol. Basis Dis.* **1865**, 2706–2715 (2019).

255. Jungheim, E. S. *et al.* Diet-induced obesity model: Abnormal oocytes and persistent growth abnormalities in the offspring. *Endocrinology* **151**, 4039–4046 (2010).

256. Cleal, J. K. *et al.* Maternal obesity during pregnancy alters daily activity and feeding cycles, and hypothalamic clock gene expression in adult male mouse offspring. *Int. J. Mol. Sci.* **20**, 1–19 (2019).

257. Samuelsson, A. M. *et al.* Diet-induced obesity in female mice leads to offspring hyperphagia, adiposity, hypertension, and insulin resistance: A novel murine model of

developmental programming. *Hypertension* **51**, 383–392 (2008).

258. Nicholas, L. M. *et al.* Exposure to maternal obesity programs sex differences in pancreatic islets of the offspring in mice. *Diabetologia* **63**, 324–337 (2020).

259. Dahlhoff, M. *et al.* Peri-conceptional obesogenic exposure induces sex-specific programming of disease susceptibilities in adult mouse offspring. *Biochim. Biophys. Acta - Mol. Basis Dis.* **1842**, 304–317 (2014).

260. Fernandez-Twinn, D. S. *et al.* The programming of cardiac hypertrophy in the offspring by maternal obesity is associated with hyperinsulinemia, AKT, ERK, and mTOR activation. *Endocrinology* **153**, 5961–5971 (2012).

261. Beeson, J. H. *et al.* Maternal exercise intervention in obese pregnancy improves the cardiovascular health of the adult male offspring. *Mol. Metab.* **16**, 35–44 (2018).

262. Loche, E. *et al.* Maternal diet-induced obesity programmes cardiac dysfunction in male mice independently of post-weaning diet. *Cardiovasc. Res.* **114**, 1372–1384 (2018).

263. Blackmore, H. L. *et al.* Maternal diet-induced obesity programs cardiovascular dysfunction in adult male mouse offspring independent of current body weight. *Endocrinology* **155**, 3970–3980 (2014).

264. Aiken, C. E., Tarry-Adkins, J. L., Penfold, N. C., Dearden, L. & Ozanne, S. E. Decreased ovarian reserve, dysregulation of mitochondrial biogenesis, and increased lipid peroxidation in female mouse offspring exposed to an obesogenic maternal diet. *FASEB J.* **30**, 1548–1556 (2016).

265. Mennitti, L. V. *et al.* Effects of maternal diet-induced obesity on metabolic disorders and age-associated miRNA expression in the liver of male mouse offspring. *Int. J. Obes.* 1–10 (2021) doi:10.1038/s41366-021-00985-1.

266. Zhu, C. *et al.* A mouse model of pre-pregnancy maternal obesity combined with offspring exposure to a high-fat diet resulted in cognitive impairment in male offspring. *Exp. Cell Res.* **368**, 159–166 (2018).

267. Chen, J. R., Lazarenko, O. P., Zhao, H., Alund, A. W. & Shankar, K. Maternal obesity impairs skeletal development in adult offspring. *J. Endocrinol.* **239**, 33–47 (2018).

268. Chang, E. *et al.* Programming effects of maternal and gestational obesity on offspring metabolism and metabolic inflammation. *Sci. Rep.* **9**, 16027 | (2019).

269. Wankhade, U. D. *et al.* Maternal High-Fat Diet Programs Offspring Liver Steatosis in a Sexually Dimorphic Manner in Association with Changes in Gut Microbial Ecology in Mice. *Sci. Rep.* **8**, 16502 (2018).

270. Yamashita, H., Shao, J., Qiao, L., Pagliassotti, M. & Friedman, J. E. Effect of Spontaneous Gestational Diabetes on Fetal and Postnatal Hepatic Insulin Resistance in Lepr db/ Mice. *Pediatr. Res.* **53**, 411–8 (2003).

271. Inoguchi, Y. *et al.* Poorly controlled diabetes during pregnancy and lactation activates the Foxo1 pathway and causes glucose intolerance in adult offspring. *Sci. Rep.* **9**, 10181 (2019).

272. Ge, Z.-J. *et al.* Maternal obesity and diabetes may cause DNA methylation alteration in the spermatozoa of offspring in mice. *Reprod. Biol. Endocrinol.* **12**, 1–8 (2014).

273. Hokke, S. N. *et al.* Maternal glucose intolerance reduces offspring nephron endowment and increases glomerular volume in adult offspring. *Diabetes. Metab. Res. Rev.* **32**, 13–23 (2016).

274. ACOG. Clinical Management Guidelines for Obstetrician – Gynecologists. *Obstet. Gynecol.* **133**, 168–186 (2019).

275. Vargas-Terrones, M., Nagpal, T. S. & Barakat, R. Impact of exercise during pregnancy on gestational weight gain and birth weight: an overview. *Brazilian J. Phys. Ther.* **23**, 164–169 (2019).

276. Brown, J. *et al.* Lifestyle interventions for the treatment of women with gestational diabetes. *Cochrane Database Syst. Rev.* **2017**, CD011970 (2017).

277. Yamamoto, J. M. *et al.* Gestational diabetes mellitus and diet: A systematic review and meta-analysis of randomized controlled trials examining the impact of modified dietary interventions on maternal glucose control and neonatal birth weight. *Diabetes Care* **41**, 1346–1361 (2018).

278. Han, S., Crowther, C. A., Middleton, P. & Heatley, E. Different types of dietary advice for women with gestational diabetes mellitus. *Cochrane Database Syst. Rev.* **2013**, CD009275 (2013).

279. Brown, J., Ceysens, G. & Boulvain, M. Exercise for pregnant women with gestational diabetes for improving maternal and fetal outcomes. *Cochrane Database Syst. Rev.* **2017**, CD012202 (2017).

280. Kusinski, L. C. *et al.* Dietary intervention in pregnant women with gestational diabetes; protocol for the digest randomised controlled trial. *Nutrients* **12**, 1165 (2020).

281. Jones, D. *et al.* Antenatal Determinants of Childhood Obesity in High-Risk Offspring: Protocol for the DiGest Follow-Up Study. (2021) doi:10.3390/nu13041156.

282. Aroda, V. R. *et al.* The effect of lifestyle intervention and metformin on preventing or delaying diabetes among women with and without gestational diabetes: The diabetes prevention program outcomes study 10-year follow-up. *J. Clin. Endocrinol. Metab.* **100**, 1646–1653 (2015).

283. Harreiter, J. *et al.* The Effects of Lifestyle and/or Vitamin D Supplementation Interventions on Pregnancy Outcomes: What Have We Learned from the DALI Studies? *Curr. Diab. Rep.* **19**, 162 (2019).

284. Poston, L. *et al.* Effect of a behavioural intervention in obese pregnant women (the UPBEAT study): a multicentre, randomised controlled trial. *Lancet Diabetes Endocrinol.* **3**, 767–777 (2015).

285. Mills, H. L. *et al.* The effect of a lifestyle intervention in obese pregnant women on gestational metabolic profiles: Findings from the UK Pregnancies Better Eating and Activity Trial (UPBEAT) randomised controlled trial. *BMC Med.* **17**, 15 (2019).

286. Renault, K. *et al.* Impact of lifestyle intervention for obese women during pregnancy

on maternal metabolic and inflammatory markers. *Int. J. Obes.* **41**, 598–605 (2017).

287. Garnæs, K. K., Mørkved, S., Salvesen, Ø. & Moholdt, T. Exercise Training and Weight Gain in Obese Pregnant Women: A Randomized Controlled Trial (ETIP Trial). *PLoS Med.* **13**, 1–18 (2016).

288. Simmons, D. Prevention of gestational diabetes mellitus: Where are we now? *Diabetes, Obes. Metab.* **17**, 824–834 (2015).

289. Fu, Q. *et al.* A short-term transition from a high-fat diet to a normal-fat diet before pregnancy exacerbates female mouse offspring obesity. *Int. J. Obes.* **40**, 564–572 (2016).

290. Janoschek, R. *et al.* Dietary intervention in obese dams protects male offspring from WAT induction of *TRPV4* , adiposity, and hyperinsulinemia. *Obesity* **24**, 1266–1273 (2016).

291. Platt, K. M., Charnigo, R. J., Kincer, J. F., Dickens, B. J. & Pearson, K. J. Controlled exercise is a safe pregnancy intervention in mice. *J. Am. Assoc. Lab. Anim. Sci.* **52**, 524–530 (2013).

292. Chung, E. *et al.* Maternal exercise upregulates mitochondrial gene expression and increases enzyme activity of fetal mouse hearts. *Physiol. Rep.* **5**, 1–11 (2017).

293. Son, J. S. *et al.* Maternal exercise via exerkine apelin enhances brown adipogenesis and prevents metabolic dysfunction in offspring mice. *Sci. Adv.* **6**, eaaz0359 (2020).

294. Xu, W. H. *et al.* Physical exercise before pregnancy helps the development of mouse embryos produced in vitro. (2016) doi:10.1016/j.mito.2016.12.004.

295. Falcao, S. *et al.* Exercise training can attenuate preeclampsia-like features in an animal model. *J. Hypertens.* **28**, 2446–2453 (2010).

296. Wasinski, F. *et al.* Maternal forced swimming reduces cell proliferation in the postnatal dentate gyrus of mouse offspring. *Front. Neurosci.* **10**, 1–6 (2016).

297. Bae-Gartz, I. *et al.* Running exercise in obese pregnancies prevents IL-6 trans-signaling in male offspring. *Med. Sci. Sports Exerc.* **48**, 829–838 (2016).

298. Stanford, K. I. *et al.* Exercise before and during pregnancy prevents the deleterious effects of maternal high-fat feeding on metabolic health of male offspring. *Diabetes* **64**, 427–433 (2015).

299. Carter, L. G., Tenlep, S. Y. N., Woollett, L. A. & Pearson, K. J. Exercise Improves Glucose Disposal and Insulin Signaling in Pregnant Mice Fed a High Fat Diet. *J. Diabetes Metab.* **6**, 634 (2015).

300. Ferrari, N. *et al.* Exercise during pregnancy and its impact on mothers and offspring in humans and mice. *J. Dev. Orig. Health Dis.* **9**, 63–76 (2018).

301. Finneran, M. M. & Landon, M. B. Oral Agents for the Treatment of Gestational Diabetes. *Curr. Diab. Rep.* **18**, 119 (2018).

302. Kalkhoff, R. K. Review. Therapeutic results of insulin therapy in gestational diabetes mellitus. *Diabetes* **34**, 97–100 (1985).

303. Berne, C., Wibell, L. & Lindmark, G. Ten-year experience of insulin treatment in gestational diabetes. *Acta Paediatr. Scand.* **74**, 85–93 (1985).

304. Moyer, V. A. & Force, U. P. S. T. Screening for Gestational Diabetes Mellitus: U.S. Preventive Services Task Force Recommendation Statement. *Ann. Intern. Med.* **160**, 414–420 (2014).

305. Zhu, H. *et al.* Insulin therapy for gestational diabetes mellitus does not fully protect offspring from diet-induced metabolic disorders. *Diabetes* **68**, 696–708 (2019).

306. Sadler, T. W. & Horton, W. E. Effects of maternal diabetes on early embryogenesis. The role of insulin and insulin therapy. *Diabetes* **32**, 1070–1074 (1983).

307. Jovanovic, L. Point: Oral hypoglycemic agents should not be used to treat diabetic pregnant women. *Diabetes Care* **30**, 2976–2979 (2007).

308. Camelo Castillo, W. *et al.* Trends in glyburide compared with insulin use for gestational diabetes treatment in the United States, 2000-2011. *Obstet. Gynecol.* **123**, 1177–1184 (2014).

309. Zhou, L., Zhang, Y., Hebert, M. F., Unadkat, J. D. & Mao, Q. Increased glyburide clearance in the pregnant mouse model. *Drug Metab. Dispos.* **38**, 1403–1406 (2010).

310. Shuster, D. L. *et al.* Maternal-Fetal Disposition of Glyburide in Pregnant Mice Is Dependent on Gestational Age. *J. Pharmacol. Exp. Ther.* **350**, 425–434 (2014).

311. Langer, O., Conway, D. L., Berkus, M. D., Xenakis, E. M.-J. & Gonzales, O. A comparison of glyburide and insulin in women with gestational diabetes mellitus. *N. Engl. J. Med.* **343**, 1134–8 (2000).

312. Hebert, M. F. *et al.* Are we optimizing gestational diabetes treatment with glyburide the pharmacologic basis for better clinical practice. *Clin. Pharmacol. Ther.* **85**, 607–614 (2009).

313. Bertini, A. M. *et al.* Perinatal outcomes and the use of oral hypoglycemic agents. *J. Perinat. Med.* **33**, 519–523 (2005).

314. Sénat, M. V. *et al.* Effect of Glyburide vs subcutaneous insulin on perinatal complications among women with gestational diabetes a randomized clinical trial. *JAMA* **319**, 1773–1780 (2018).

315. Nachum, Z. *et al.* Glyburide versus metformin and their combination for the treatment of gestational diabetes mellitus:arandomized controlled study. *Diabetes Care* **40**, 332–337 (2017).

316. Jacobson, G. F. *et al.* Comparison of glyburide and insulin for the management of gestational diabetes in a large managed care organization. *Am. J. Obstet. Gynecol.* **193**, 118–124 (2005).

317. Bailey, C. J. Metformin: historical overview. *Diabetologia* **60**, 1566–1576 (2017).

318. Lindsay, R. S. & Loeken, M. R. Metformin use in pregnancy: promises and uncertainties. *Diabetologia* **60**, 1612–1619 (2017).

319. Coetzee, E. J. & Jackson, W. P. U. Metformin in management of pregnant insulin-

independent diabetics. *Diabetologia* **16**, 241–245 (1979).

320. Nestler, J. E. & Jakubowicz, D. J. Lean women with polycystic ovary syndrome respond to insulin reduction with decreases in ovarian P450c17α activity and serum androgens. *J. Clin. Endocrinol. Metab.* **82**, 4075–4079 (1997).

321. Jakubowicz, D. J., Iuorno, M. J., Jakubowicz, S., Roberts, K. & Nestler, J. E. Effects of Metformin on Early Pregnancy Loss in the Polycystic Ovary Syndrome. *J. Clin. Endocrinol. Metab.* **87**, 524–529 (2002).

322. Glueck, C. J., Phillips, H., Cameron, D., Sieve-Smith, L. & Wang, P. Continuing metformin throughout pregnancy in women with polycystic ovary syndrome appears to safely reduce first-trimester spontaneous abortion: A pilot study. *Fertil. Steril.* **75**, 46–52 (2001).

323. Morin-Papunen, L. *et al.* Metformin improves pregnancy and live-birth rates in women with polycystic ovary syndrome (PCOS): A multicenter, double-blind, placebo-controlled randomized trial. *J. Clin. Endocrinol. Metab.* **97**, 1492–1500 (2012).

324. Roland, A. V. & Moenter, S. M. Prenatal androgenization of female mice programs an increase in firing activity of gonadotropin-releasing hormone (GnRH) neurons that is reversed by metformin treatment in adulthood. *Endocrinology* **152**, 618–628 (2011).

325. Sander, V. A., Facorro, G. B., Piehl, L., Rubín De Celis, E. & Motta, A. B. Effect of DHEA and metformin on corpus luteum in mice. *Reproduction* **138**, 571–579 (2009).

326. Luchetti, C. G., Mikó, E., Szekeres-Bartho, J., Paz, D. A. & Motta, A. B. Dehydroepiandrosterone and metformin modulate progesterone-induced blocking factor (PIBF), cyclooxygenase 2 (COX2) and cytokines in early pregnant mice. *J. Steroid Biochem. Mol. Biol.* **111**, 200–207 (2008).

327. Glueck, C. J., Goldenberg, N., Wang, P., Loftspring, M. & Sherman, A. Metformin during pregnancy reduces insulin, insulin resistance, insulin secretion, weight, testosterone and development of gestational diabetes: Prospective longitudinal assessment of women with polycystic ovary syndrome from preconception throughout preg. *Hum. Reprod.* **19**, 510–521 (2004).

328. Glueck, C. J. *et al.* Height, weight, and motor - Social development during the first 18 months of life in 126 infants born to 109 mothers with polycystic ovary syndrome who conceived on and continued metformin through pregnancy. *Hum. Reprod.* **19**, 1323–1330 (2004).

329. Brown, F. M. *et al.* Metformin in pregnancy - Its time has not come yet. *Diabetes Care* **29**, 485–486 (2006).

330. Vanky, E. *et al.* Metformin Versus placebo from first trimester to delivery in polycystic ovary syndrome: A randomized, controlled multicenter study. *J. Clin. Endocrinol. Metab.* **95**, 448–455 (2010).

331. Helseth, R., Vanky, E., Stridsklev, S., Vogt, C. & Carlsen, S. M. Maternal and fetal insulin levels at birth in women with polycystic ovary syndrome: Data from a randomized controlled study on metformin. *Eur. J. Endocrinol.* **170**, 769–775 (2014).

332. Guro, L. *et al.* Metformin use in PCOS pregnancies increases the risk of offspring

overweight at 4 years of age; follow-up of two RCTs. *J. Clin. Endocrinol. Metab.* **103**, 1612–1621 (2018).

333. Hanem, L. G. E. *et al.* Intrauterine metformin exposure and offspring cardiometabolic risk factors (PedMet study): a 5–10 year follow-up of the PregMet randomised controlled trial. *Lancet Child Adolesc. Heal.* **3**, 166–174 (2019).

334. Hjorth-Hansen, A. *et al.* Fetal Growth and Birth Anthropometrics in Metformin-Exposed Offspring Born to Mothers With PCOS. *J. Clin. Endocrinol. Metab.* **103**, 740–747 (2018).

335. Given, J. E. *et al.* Metformin exposure in first trimester of pregnancy and risk of all or specific congenital anomalies: exploratory case-control study. *BMJ* **361**, 2477 (2018).

336. Niromanesh, S. *et al.* Metformin compared with insulin in the management of gestational diabetes mellitus: A randomized clinical trial. *Diabetes Res. Clin. Pract.* **98**, 422–429 (2012).

337. Ainuddin, J., Karim, N., Hasan, A. A. & Naqvi, S. A. Metformin versus insulin treatment in gestational diabetes in pregnancy in a developing country. A randomized control trial. *Diabetes Res. Clin. Pract.* **107**, 290–299 (2015).

338. Mesdaghinia, E. *et al.* Comparison of newborn outcomes in women with gestational diabetes mellitus treated with metformin or insulin: A randomised blinded trial. *Int. J. Prev. Med.* **4**, 327–333 (2013).

339. Rowan, J. A., Hague, W. M., Gao, W., Battin, M. R. & Moore, M. P. Metformin versus insulin for the treatment of gestational diabetes. *Obstet. Gynecol. Surv.* **63**, 616–618 (2008).

340. Priya, G. & Kalra, S. Metformin in the management of diabetes during pregnancy and lactation. *Drugs Context* **7**, 212523 (2018).

341. Tarry-Adkins, J. L., Aiken, C. E. & Ozanne, S. E. Neonatal, infant, and childhood growth following metformin versus insulin treatment for gestational diabetes: A systematic review and meta-analysis. *PLoS Med.* **16**, e1002848 (2019).

342. Syngelaki, A. *et al.* Metformin versus Placebo in Obese Pregnant Women without Diabetes Mellitus. *N. Engl. J. Med.* **374**, 434–443 (2016).

343. Chiswick, C. *et al.* Effect of metformin on maternal and fetal outcomes in obese pregnant women (EMPOWaR): A randomised, double-blind, placebo-controlled trial. *Lancet Diabetes Endocrinol.* **3**, 778–786 (2015).

344. Arshad, R., Kanpurwala, M. A., Karim, N. & Hassan, J. A. Effects of diet and metformin on placental morphology in gestational diabetes mellitus. *Pakistan J. Med. Sci.* **32**, 1522–1527 (2016).

345. Vafaei, H., Karimi, Z., Akbarzadeh-Jahromi, M. & Asadian, F. Association of placental chorangiosis with pregnancy complication and prenatal outcome: a case-control study. *BMC Pregnancy Childbirth* **21**, 99 (2021).

346. Alzamendi, A. *et al.* Oral Metformin Treatment Prevents Enhanced Insulin Demand and Placental Dysfunction in the Pregnant Rat Fed a Fructose-Rich Diet. *ISRN*

Endocrinol. **2012**, 1–8 (2012).

347. Desai, N. *et al.* Maternal metformin treatment decreases fetal inflammation in a rat model of obesity and metabolic syndrome. *Am. J. Obstet. Gynecol.* **209**, 136.e1-136.e9 (2013).

348. Jiang, S., Teague, A. M., Tryggestad, J. B., Jensen, M. E. & Chernausek, S. D. Role of metformin in epigenetic regulation of placental mitochondrial biogenesis in maternal diabetes. *Sci. Rep.* **10**, 1–12 (2020).

349. Hosni, A. *et al.* Cinnamaldehyde mitigates placental vascular dysfunction of gestational diabetes and protects from the associated fetal hypoxia by modulating placental angiogenesis, metabolic activity and oxidative stress. *Pharmacol. Res.* **165**, 105426 (2021).

350. Deng, W. *et al.* P53 coordinates decidual sestrin 2/AMPK/mTORC1 signaling to govern parturition timing. *J. Clin. Invest.* **126**, 2941–2954 (2016).

351. Li, Y., Li, J. & Yang, D. ADAM7 promotes the proliferation and invasion in trophoblast cells. *Exp. Mol. Pathol.* **121**, 4–9 (2021).

352. Wang, Y. *et al.* The Globular Heads of the C1q Receptor Regulate Apoptosis in Human Extravillous Cytotrophoblast-derived Transformed Cells via a Mitochondria-dependent Pathway. *Am. J. Reprod. Immunol.* **71**, 73–85 (2014).

353. Vega, M., Mauro, M. & Williams, Z. Direct toxicity of insulin on the human placenta and protection by metformin. *Fertil. Steril.* **111**, 489-496.e5 (2019).

354. Sun, C. C. *et al.* Metformin Ameliorates Gestational Diabetes Mellitus-Induced Endothelial Dysfunction via Downregulation of p65 and Upregulation of Nrf2. *Front. Pharmacol.* **11**, 1–13 (2020).

355. Correia-Branco, A., Keating, E. & Martel, F. Involvement of mTOR, JNK and PI3K in the negative effect of ethanol and metformin on the human first-trimester extravillous trophoblast HTR-8/SVneo cell line. *Eur. J. Pharmacol.* **833**, 16–24 (2018).

356. Liao, M. Z. *et al.* Effects of Pregnancy on the Pharmacokinetics of Metformin. *Drug Metab. Dispos.* **48**, 264–271 (2020).

357. Dowling, R. J. O., Niraula, S., Stambolic, V. & Goodwin, P. J. Metformin in cancer: Translational challenges. *J. Mol. Endocrinol.* **48**, R31–R43 (2012).

358. Nishida, M. *et al.* Mitochondrial reactive oxygen species trigger metformin-dependent antitumor immunity via activation of Nrf2/mTORC1/p62 axis in tumor-infiltrating CD8T lymphocytes. *J. Immunother. Cancer* **9**, e002954 (2021).

359. Pettker, C. M., Flannery, C. A. & Abrahams, V. M. Associated Uteroplacental Insufficiency. *Am J Reprod Immunol* **73**, 362–371 (2016).

360. Hastie, R. *et al.* EGFR (Epidermal Growth Factor Receptor) signaling and the mitochondria regulate sFlt-1 (Soluble FMS-Like Tyrosine Kinase-1) secretion. *Hypertension* **73**, 659–670 (2019).

361. Zhang, L. *et al.* Gestational Diabetes Mellitus-Associated Hyperglycemia Impairs Glucose Transporter 3 Trafficking in Trophoblasts Through the Downregulation of

AMP-Activated Protein Kinase. *Front. Cell Dev. Biol.* **9**, 1–18 (2021).

362. Salomäki, H. *et al.* Prenatal Metformin Exposure in a Maternal High Fat Diet Mouse Model Alters the Transcriptome and Modifies the Metabolic Responses of the Offspring. *PLoS One* **9**, e115778 (2014).

363. Jenkins, B., Ronis, M. & Koulman, A. Lc–ms lipidomics: Exploiting a simple high-throughput method for the comprehensive extraction of lipids in a ruminant fat dose-response study. *Metabolites* **10**, 1–27 (2020).

364. Hufnagel, A. *et al.* Maternal but not fetoplacental health can be improved by metformin in a murine diet-induced model of maternal obesity and glucose intolerance. *J. Physiol.* **0**, 1–17 (2021).

365. Welinder, C. & Ekblad, L. Coomassie staining as loading control in Western blot analysis. *J. Proteome Res.* **10**, 1416–1419 (2010).

366. Narvaez-Sanchez, R., Calderón, J. C., Vega, G., Trillos, M. C. & Ospina, S. Skeletal muscle as a protagonist in the pregnancy metabolic syndrome. *Med. Hypotheses* **126**, 26–37 (2019).

367. Nathan, D. M. *et al.* Medical management of hyperglycemia in type 2 diabetes: A consensus algorithm for the initiation and adjustment of therapy. *Diabetes Care* **32**, 193–203 (2009).

368. Le, S. & Lee, G. C. Emerging Trends in Metformin Prescribing in the United States from 2000 to 2015. *Clin. Drug Investig.* **39**, 757–763 (2019).

369. Fontaine, E. Metformin-Induced Mitochondrial Complex I Inhibition: Facts, Uncertainties, and Consequences. *Front. Endocrinol. (Lausanne).* **9**, 753 (2018).

370. Tokubuchi, I. *et al.* Beneficial effects of metformin on energy metabolism and visceral fat volume through a possible mechanism of fatty acid oxidation in human subjects and rats. *PLoS One* **12**, (2017).

371. Rena, G., Hardie, D. G. & Pearson, E. R. The mechanisms of action of metformin. *Diabetologia* **60**, 1577–1585 (2017).

372. Minamii, T., Nogami, M. & Ogawa, W. Mechanisms of metformin action: In and out of the gut. *J. Diabetes Investig.* **9**, 701–703 (2018).

373. Duca, F. A. *et al.* Metformin activates a duodenal Ampk-dependent pathway to lower hepatic glucose production in rats. *Nat. Med.* **21**, 506–11 (2015).

374. Bahne, E. *et al.* Metformin-induced glucagon-like peptide-1 secretion contributes to the actions of metformin in type 2 diabetes. *JCI insight* **3**, e93936 (2018).

375. Nguyen, L., Chan, S. Y. & Teo, A. K. K. Metformin from mother to unborn child – Are there unwarranted effects? *EBioMedicine* **35**, 394–404 (2018).

376. Pernicova, I. & Korbonits, M. Metformin-Mode of action and clinical implications for diabetes and cancer. *Nat. Rev. Endocrinol.* **10**, 143–156 (2014).

377. Coll, A. P. *et al.* GDF15 mediates the effects of metformin on body weight and energy balance. *Nature* **578**, 444–448 (2020).

378. Wischhusen, J., Melero, I. & Fridman, W. H. Growth/Differentiation Factor-15 (GDF-15): From Biomarker to Novel Targetable Immune Checkpoint. *Front. Immunol.* **11**, (2020).

379. Feghali, M., Venkataramanan, R. & Caritis, S. Pharmacokinetics of drugs in pregnancy. *Semin. Perinatol.* **39**, 512–519 (2015).

380. Eyal, S. *et al.* Pharmacokinetics of metformin during pregnancy. *Drug Metab. Dispos.* **38**, 833–840 (2010).

381. Bake, T., Murphy, M., Morgan, D. G. A. & Mercer, J. G. Large, binge-type meals of high fat diet change feeding behaviour and entrain food anticipatory activity in mice. *Appetite* **77**, 60–71 (2014).

382. Andrikopoulos, S., Blair, A. R., Deluca, N., Fam, B. C. & Proietto, J. Evaluating the glucose tolerance test in mice. *Am. J. Physiol. Metab.* **295**, E1323–E1332 (2008).

383. Zhang, J. & Croy, A. Using Ultrasonography to Define Fetal-Maternal Relationships: Moving from Humans to Mice. *Comp. Med.* **59**, 527–553 (2009).

384. Ochi, H. *et al.* The Influence of the Maternal Heart Rate on the Uterine Artery Pulsatility Index in the Pregnant Ewe. *Gynecol. Obstet. Invest.* **47**, 73–75 (1999).

385. Ochi, H., Kusanagi, Y., Katayama, T., Matsubara, K. & Ito, M. Clinical significance of normalization of uterine artery pulsatility index with maternal heart rate for the evaluation of uterine circulation in pregnancy-induced hypertension. *Ultrasound Obstet. Gynecol.* **21**, 459–463 (2003).

386. Heo, M., Faith, M. S., Pietrobelli, A. & Heymsfield, S. B. Percentage of body fat cutoffs by sex, age, and race-ethnicity in the US adult population from NHANES 1999-2004 (American Journal of Clinical Nutrition (2012) 95, (594-602)). *Am. J. Clin. Nutr.* **96**, 448 (2012).

387. Neri, C. & Edlow, A. G. Effects of maternal obesity on fetal programming: Molecular approaches. *Cold Spring Harb. Perspect. Med.* **6**, a026591 (2016).

388. Sanders, T. R., Kim, D. W., Glendining, K. A. & Jasoni, C. L. Maternal Obesity and IL-6 Lead to Aberrant Developmental Gene Expression and Deregulated Neurite Growth in the Fetal Arcuate Nucleus. *endo.endojournals.org Endocrinol.* **155**, 2566–2577 (2014).

389. Appel, S. *et al.* A potential role for GSK3b in glucose-driven intrauterine catch-up growth in maternal obesity. *Endocrinology* **160**, 377–386 (2019).

390. Tarry-Adkins, J. L., Aiken, C. E. & Ozanne, S. E. Comparative impact of pharmacological treatments for gestational diabetes on neonatal anthropometry independent of maternal glycaemic control: A systematic review and meta-analysis. *PLoS Med.* **17**, e1003126 (2020).

391. Feig, D. S. *et al.* Articles Metformin in women with type 2 diabetes in pregnancy (MiTy): a multicentre, international, randomised, placebo-controlled trial. *Lancet Diabetes Endocrinol* **8**, 834–844 (2020).

392. Most, J., Dervis, S., Haman, F., Adamo, K. B. & Redman, L. M. Energy intake requirements in pregnancy. *Nutrients* **11**, 1812 (2019).

393. Most, J. *et al.* Evidence-based recommendations for energy intake in pregnant women with obesity. *J. Clin. Invest.* **129**, 4682–4690 (2019).

394. Patel, S. *et al.* GDF15 Provides an Endocrine Signal of Nutritional Stress in Mice and Humans. *Cell Metab.* **29**, 707–718 (2019).

395. Johnstone, L. E. & Higuchi, T. Food intake and leptin during pregnancy and lactation. *Prog. Brain Res.* **133**, 215–227 (2001).

396. Salomäki, H. *et al.* Prenatal Metformin Exposure in Mice Programs the Metabolic Phenotype of the Offspring during a High Fat Diet at Adulthood. *PLoS One* **8**, e56594 (2013).

397. Nair, A. & Jacob, S. A simple practice guide for dose conversion between animals and human. *J. Basic Clin. Pharm.* **7**, 27 (2016).

398. Vanky, E., Zahlsen, K., Spigset, O. & Carlsen, S. M. Placental passage of metformin in women with polycystic ovary syndrome. *Fertil. Steril.* **83**, 1575–1578 (2005).

399. Beeson, J. H. PhD thesis: An investigation into whether an exercise intervention during pregnancy can prevent the programming of cardiovascular disease in the offspring of obese mothers. (2018).

400. Steneberg, P. *et al.* Hyperinsulinemia enhances hepatic expression of the fatty acid transporter Cd36 and provokes hepatosteatosis and hepatic insulin resistance. *J. Biol. Chem.* **290**, 19034–19043 (2015).

401. Wu, Y. *et al.* Cellular stress, excessive apoptosis, and the effect of metformin in a mouse model of type 2 diabetic embryopathy. *Diabetes* **64**, 2526–2536 (2015).

402. Liu, Z., Yu, X., Tong, C. & Qi, H. Renal dysfunction in a mouse model of GDM is prevented by metformin through MAPKs. *Mol. Med. Rep.* **49**, 4491–4499 (2019).

403. Sales, W. B. *et al.* Effectiveness of Metformin in the Prevention of Gestational Diabetes Mellitus in Obese Pregnant Women Efetividade da metformina na prevenção do diabetes mellitus gestacional em gestantes obesas. *Rev Bras Ginecol Obs.* **40**, 180–187 (2018).

404. Helmreich, R. J., Hundley, V. & Varvel, P. The effect of obesity on heart rate (heart period) and physiologic parameters during pregnancy. *Biol. Res. Nurs.* **10**, 63–78 (2008).

405. Barazi, N. *et al.* Dissecting the Roles of the Autonomic Nervous System and Physical Activity on Circadian Heart Rate Fluctuations in Mice. *Front. Physiol.* **12**, 1787 (2021).

406. D'Souza, A. *et al.* A circadian clock in the sinus node mediates day-night rhythms in Hcn4 and heart rate. *Hear. Rhythm* **18**, 801–810 (2021).

407. Kurtz, T. W., Lujan, H. L. & DiCarlo, S. E. The 24 h pattern of arterial pressure in mice is determined mainly by heart Rate-Driven variation in cardiac output. *Physiol. Rep.* **2**, e12223 (2014).

408. Teulings, N. E. W. D. *et al.* Independent influences of maternal obesity and fetal sex on maternal cardiovascular adaptation to pregnancy: a prospective cohort study. *Int. J. Obes.* **44**, 2246–2255 (2020).

409. Kim, Y. H. *et al.* The predictive value of the uterine artery pulsatility index during the early third trimester for the occurrence of adverse pregnancy outcomes depending on the maternal obesity. *Obes. Res. Clin. Pract.* **9**, 374–381 (2015).

410. Morton, J. S., Care, A. S. & Davidge, S. T. Mechanisms of uterine artery dysfunction in pregnancy complications. *J. Cardiovasc. Pharmacol.* **69**, 343–359 (2017).

411. Chirayath, H. H., Wareing, M., Taggart, M. J. & Baker, P. N. Endothelial dysfunction in myometrial arteries of women with gestational diabetes. *Diabetes Res. Clin. Pract.* **89**, 134–140 (2010).

412. Knock, G. A., McCarthy, A. L., Lowy, C. & Poston, L. Association of gestational diabetes with abnormal maternal vascular endothelial function. *BJOG An Int. J. Obstet. Gynaecol.* **104**, 229–234 (1997).

413. Anastasiou, E. *et al.* Impaired endothelium-dependent vasodilatation in women with previous gestational diabetes. *Diabetes Care* **21**, 2111–2115 (1998).

414. Stanley, J. L., Ashton, N., Taggart, M. J., Davidge, S. T. & Baker, P. N. Uterine artery function in a mouse model of pregnancy complicated by diabetes. *Vascul. Pharmacol.* **50**, 8–13 (2009).

415. Tay, J. *et al.* Uterine and fetal placental Doppler indices are associated with maternal cardiovascular function. *Am. J. Obstet. Gynecol.* **220**, 96.e1–8 (2019).

416. Salvesen, K. ˚ A., Vanky, E. & Carlsen, S. M. Metformin treatment in pregnant women with polycystic ovary syndrome-is reduced complication rate mediated by changes in the uteroplacental circulation? *Ultrasound Obs. Gynecol* **29**, 433–437 (2007).

417. Jamal, A., Milani, F. & Al-Yasin, A. Evaluation of the effect of metformin and aspirin on utero placental circulation of pregnant women with PCOS. *Iran J Reprod Med* **10**, 265–270 (2012).

418. Stridsklev, S., Salvesen, Ø., Salvesen, K. Å., Carlsen, S. M. & Vanky, E. Uterine Artery Doppler in Pregnancy: Women with PCOS Compared to Healthy Controls. *Int. J. Endocrinol.* **2018**, 2604064 (2018).

419. Jakubowicz, D. J. *et al.* Insulin reduction with metformin increases luteal phase serum glycodelin and insulin-like growth factor-binding protein 1 concentrations and enhances uterine vascularity and blood flow in the polycystic ovary syndrome. *J. Clin. Endocrinol. Metab.* **86**, 1126–1133 (2001).

420. Baron, A. D. Insulin resistance and vascular function. *J. Diabetes Complications* **16**, 92–102 (2002).

421. Rosenfeld, C. R. & Roy, T. Prolonged uterine artery nitric oxide synthase inhibition modestly alters basal uteroplacental vasodilation in the last third of ovine pregnancy. *Am. J. Physiol. - Hear. Circ. Physiol.* **307**, H1196–H1203 (2014).

422. Boeldt, D. S., Yi, F. X. & Bird, I. M. eNOS activation and NO function: Pregnancy adaptive programming of capacitative entry responses alters nitric oxide (NO) output in vascular endothelium-new insights into eNOS regulation through adaptive cell signaling. *J. Endocrinol.* **210**, 243–258 (2011).

423. Kulandavelu, S. *et al.* Endothelial nitric oxide synthase deficiency reduces uterine blood flow, spiral artery elongation, and placental oxygenation in pregnant mice. *Hypertension* **60**, 231–238 (2012).

424. Ainuddin, J. A., Karim, N., Zaheer, S., Ali, S. S. & Hasan, A. A. Metformin treatment in type 2 diabetes in pregnancy: An active controlled, parallel-group, randomized, open label study in patients with type 2 diabetes in pregnancy. *J. Diabetes Res.* **2015**, 325851 (2015).

425. Brownfoot, F. C. *et al.* Metformin as a prevention and treatment for preeclampsia: effects on soluble fms-like tyrosine kinase 1 and soluble endoglin secretion and endothelial dysfunction. *Am. J. Obstet. Gynecol.* **214**, e1–e15 (2016).

426. Persson, M., Johansson, S. & Cnattingius, S. Inter-pregnancy Weight Change and Risks of Severe Birth-Asphyxia-Related Outcomes in Singleton Infants Born at Term: A Nationwide Swedish Cohort Study. *PLoS Med.* **13**, 1–14 (2016).

427. Ziauddeen, N. *et al.* Interpregnancy weight gain and childhood obesity: analysis of a UK population-based cohort. *Int. J. Obes.* 1–9 (2021) doi:10.1038/s41366-021-00979-z.

428. Guttmacher, A. E., Maddox, Y. T. & Spong, C. Y. The Human Placenta Project: Placental structure, development, and function in real time. *Placenta* **35**, 303–304 (2014).

429. Sadovsky, Y., Clifton, V. L. & Burton, G. J. Invigorating placental research through the 'human Placenta Project'. *Placenta* **35**, 527 (2014).

430. Schmidt, A., Morales-Prieto, D. M., Pastuschek, J., Fröhlich, K. & Markert, U. R. Only humans have human placentas: molecular differences between mice and humans. *J. Reprod. Immunol.* **108**, 65–71 (2015).

431. Burton, G. J., Watson, A. L., Hempstock, J., Skepper, J. N. & Jauniaux, E. Uterine glands provide histiotrophic nutrition for the human fetus during the first trimester of pregnancy. *J. Clin. Endocrinol. Metab.* **87**, 2954–2959 (2002).

432. Odland Karlsen, H. *et al.* The human yolk sac size reflects involvement in embryonic and fetal growth regulation. *Acta Obstet. Gynecol. Scand.* **98**, 176–182 (2019).

433. Freyer, C. & Renfree, M. B. The mammalian yolk sac placenta. *J. Exp. Zool. Part B Mol. Dev. Evol.* **312B**, 545–554 (2009).

434. Nanovskaya, T. N., Nekhayeva, I. A., Patrikeeva, S. L., Hankins, G. D. V. & Ahmed, M. S. Transfer of metformin across the dually perfused human placental lobule. *Am. J. Obstet. Gynecol.* **195**, 1081–1085 (2006).

435. Kovo, M., Haroutiunian, S., Feldman, N., Hoffman, A. & Glezerman, M. Determination of metformin transfer across the human placenta using a dually perfused ex vivo placental cotyledon model. *Eur. J. Obstet. Gynecol. Reprod. Biol.* **136**, 29–33 (2008).

436. Bertoldo, M. J., Faure, M., Dupont, J. & Froment, P. Impact of metformin on reproductive tissues: An overview from gametogenesis to gestation. *Ann. Transl. Med.* **2**, 1–13 (2014).

437. Luciano-Mateo, F. *et al.* Nutrients in energy and one-carbon metabolism: Learning

from metformin users. *Nutrients* **9**, 121 (2017).

438. Mallik, R. & Chowdhury, T. A. Metformin in cancer. *Diabetes Res. Clin. Pract.* **143**, 409–419 (2018).

439. Liang, X. *et al.* Effects of metformin on proliferation and apoptosis of human megakaryoblastic Dami and MEG-01 cells. *J. Pharmacol. Sci.* **135**, 14–21 (2017).

440. Barbour, L. A. *et al.* A cautionary response to SMFM statement: pharmacological treatment of gestational diabetes Abstract HHS Public Access. *Am J Obs. Gynecol* **219**, 367–368 (2018).

441. Wang, F. *et al.* Effect of Metformin on a Preeclampsia-Like Mouse Model Induced by High-Fat Diet. *Biomed Res. Int.* **2019**, 6547019 (2019).

442. Louden, E. D. *et al.* TallyHO obese female mice experience poor reproductive outcomes and abnormal blastocyst metabolism which is reversed by metformin HHS Public Access. *Reprod Fertil Dev* **27**, 31–39 (2014).

443. Vora, N. L. *et al.* Targeted Multiplex Gene Expression Profiling to Measure High-Fat Diet and Metformin Effects on Fetal Gene Expression in a Mouse Model. *Reprod. Sci.* **26**, 683–689 (2019).

444. Grace, M. R. *et al.* Effect of a High-Fat Diet and Metformin on Placental mTOR Signaling in Mice. *Am J Perinatol Rep* **9**, 138–143 (2019).

445. Hernandez-Andrade, E. *et al.* Evaluation of utero-placental and fetal hemodynamic parameters throughout gestation in pregnant mice using high-frequency ultrasound. *Ultrasound Med. Biol.* **40**, 351–60 (2014).

446. Cahill, L. S., Zhou, Y.-Q., Seed, M., Macgowan, C. K. & Sled, J. G. Brain sparing in fetal mice: BOLD MRI and Doppler ultrasound show blood redistribution during hypoxia. *J. Cereb. Blood Flow Metab.* **34**, 1082–8 (2014).

447. Deeney, S., Powers, K. N. & Crombleholme, T. M. A comparison of sexing methods in fetal mice. *Lab Anim* **45**, 380–4 (2016).

448. Mcfarlane, L. *et al.* Novel PCR Assay for Determining the Genetic Sex of Mice. *Sex. Dev.* **7**, 207–211 (2013).

449. Meller, M., Vadachkoira, S., Luthy, D. A. & Williams, M. A. Evaluation of housekeeping genes in placental comparative expression studies. *Placenta* **26**, 601–607 (2005).

450. Kamimae-Lanning, A. N. *et al.* Maternal high-fat diet and obesity compromise fetal hematopoiesis. *Mol. Metab.* **4**, 25–38 (2015).

451. Díaz, P., Harris, J., Rosario, F. J., Powell, T. L. & Jansson, T. Increased placental fatty acid transporter 6 and binding protein 3 expression and fetal liver lipid accumulation in a mouse model of obesity in pregnancy. *Am. J. Physiol. - Regul. Integr. Comp. Physiol.* **309**, R1569–R1577 (2015).

452. Albaghdadi, A. J. H. *et al.* Tacrolimus in the prevention of adverse pregnancy outcomes and diabetes-associated embryopathies in obese and diabetic mice. *J. Transl. Med.* **15**, 32 (2017).

453. Desoye, G. & Cervar-Zivkovic, M. Diabetes Mellitus, Obesity, and the Placenta. *Obstet. Gynecol. Clin. North Am.* **47**, 65–79 (2020).

454. Saben, J. *et al.* Maternal obesity is associated with a lipotoxic placental environment. *Placenta* **35**, 171–7 (2014).

455. Salge, A. K. M. *et al.* Macroscopic placental changes associated with fetal and maternal events in diabetes mellitus. *Clinics (Sao Paulo).* **67**, 1203–8 (2012).

456. Chen, K. H., Chen, L. R. & Lee, Y. H. The Role of Preterm Placental Calcification in High-Risk Pregnancy as a Predictor of Poor Uteroplacental Blood Flow and Adverse Pregnancy Outcome. *Ultrasound Med. Biol.* **38**, 1011–1018 (2012).

457. Chen, K.-H., Seow, K.-M. & Chen, L.-R. The role of preterm placental calcification on assessing risks of stillbirth. *Placenta* **36**, 1039–1044 (2015).

458. Wallingford, M. C., Benson, C., Chavkin, N. W., Chin, M. T. & Frasch, M. G. Placental Vascular Calcification and Cardiovascular Health: It Is Time to Determine How Much of Maternal and Offspring Health Is Written in Stone. *Front. Physiol.* **9**, 1–9 (2018).

459. Li, Y. *et al.* Role of Macrophages in the Progression and Regression of Vascular Calcification. *Front. Pharmacol.* **11**, 661 (2020).

460. Tertti, K. *et al.* The role of organic cation transporters (OCTs) in the transfer of metformin in the dually perfused human placenta. *Eur. J. Pharm. Sci.* **39**, 76–81 (2010).

461. Knox, K. & Baker, J. C. Genomic evolution of the placenta using co-option and duplication and divergence. *Genome Res.* **18**, 695–705 (2008).

462. Lee, N. *et al.* Taste of a Pill ORGANIC CATION TRANSPORTER-3 (OCT3) MEDIATES METFORMIN ACCUMULATION AND SECRETION IN SALIVARY GLANDS *. (2014) doi:10.1074/jbc.M114.570564.

463. Lee, N. *et al.* Effect of gestational age on mRNA and protein expression of polyspecific organic cation transporters during pregnancy. *Drug Metab. Dispos.* **41**, 2225–32 (2013).

464. Graham, G. G. *et al.* Clinical Pharmacokinetics of Metformin. **50**, 81–98 (2011).

465. Davies, J. Kidney Development. *eLS. John Wiley Sons* (2013) doi:10.1002/9780470015902.a0001152.pub3.

466. Underwood, M. A., Gilbert, W. M. & Sherman, M. P. State of the Art Amniotic Fluid: Not Just Fetal Urine Anymore. *J. Perinatol.* **25**, 341–348 (2005).

467. Paintner, A., Williams, A. D. & Burd, L. Fetal alcohol spectrum disorders-implications for child neurology, part 1: Prenatal exposure and dosimetry. *J. Child Neurol.* **27**, 258–263 (2012).

468. Díaz, P., Powell, T. L. & Jansson, T. The role of placental nutrient sensing in maternal-fetal resource allocation. *Biol. Reprod.* **91**, 1–10 (2014).

469. Jansson, N. *et al.* Activation of Placental mTOR Signaling and Amino Acid Transporters in Obese Women Giving Birth to Large Babies). *J Clin Endocrinol Metab* **98**, 105–113

(2013).

470. Sharma, P. & Kumar, S. Metformin inhibits human breast cancer cell growth by promoting apoptosis via a ROS-independent pathway involving mitochondrial dysfunction: pivotal role of superoxide dismutase (SOD). *Cell. Oncol.* **41**, 637–650 (2018).

471. Shinoura, N. *et al.* Expression level of Bcl-2 determines anti- or proapoptotic function. *Cancer Res.* **59**, 4119–4128 (1999).

472. Xiao, D. & Zhang, L. Upregulation of Bax and Bcl-2 following prenatal cocaine exposure induces apoptosis in fetal rat brain. *Int. J. Med. Sci.* **5**, 295–302 (2008).

473. Schoonejans, J. M. *et al.* Maternal Metformin Intervention during Obese Glucose-Intolerant Pregnancy Affects Adiposity in Young Adult Mouse Offspring in a Sex-Specific Manner. *Int. J. Mol. Sci.* **22**, 8104 (2021).

474. Foretz, M. *et al.* Metformin inhibits hepatic gluconeogenesis in mice independently of the LKB1/AMPK pathway via a decrease in hepatic energy state. *J. Clin. Invest.* **120**, 2355–69 (2010).

475. Hunter, R. W. *et al.* Metformin reduces liver glucose production by inhibition of fructose-1-6-bisphosphatase. *Nat. Med.* **24**, 1395 (2018).

476. Miller, R. A. *et al.* Biguanides suppress hepatic glucagon signaling by decreasing production of cyclic AMP. *Nature* **494**, 256 (2013).

477. Koffert, J. P. *et al.* Metformin treatment significantly enhances intestinal glucose uptake in patients with type 2 diabetes: Results from a randomized clinical trial. *Diabetes Res. Clin. Pract.* **131**, 208–216 (2017).

478. Gontier, E. *et al.* High and typical 18F-FDG bowel uptake in patients treated with metformin. *Eur. J. Nucl. Med. Mol. Imaging* **35**, 95–99 (2008).

479. Stepensky, D., Friedman, M., Raz, I. & Hoffman, A. Pharmacokinetic-Pharmacodynamic Analysis of the Glucose-Lowering Effect of Metformin in Diabetic Rats Reveals First-Pass Pharmacodynamic Effect. *Drug Metab. Dispos.* **30**, 861–868 (2002).

480. Yang, M. *et al.* Inhibition of mitochondrial function by metformin increases glucose uptake, glycolysis and GDF-15 release from intestinal cells. *Sci. Rep.* **11**, 2529 (2021).

481. Soukas, A. A., Hao, H. & Wu, L. Metformin as Anti-Aging Therapy: Is It for Everyone? *Trends Endocrinol. Metab.* **30**, 745 (2019).

482. Bharath, L. P. *et al.* Metformin Enhances Autophagy and Normalizes Mitochondrial Function to Alleviate Aging-Associated Inflammation. *Cell Metab.* **32**, 44 (2020).

483. Espada, L. *et al.* Loss of metabolic plasticity underlies metformin toxicity in aged Caenorhabditis elegans. *Nat. Metab.* **2**, 1316–1331 (2020).

484. Loubière, C. *et al.* Metformin-induced energy deficiency leads to the inhibition of lipogenesis in prostate cancer cells. *Oncotarget* **6**, 15652 (2015).

485. Bidault, G. *et al.* SREBP1-induced fatty acid synthesis depletes macrophages

antioxidant defences to promote their alternative activation. *Nat. Metab.* **3**, 1150–1162 (2021).

486. Stephens, M. False discovery rates: A new deal. *Biostatistics* **18**, 275–294 (2016).

487. Riken, T. *et al.* Functional annotation of a full-length mouse cDNA collection. *Nature* **13**, 685–690 (2001).

488. Desoye, G., Gauster, M. & Wadsack, C. Placental transport in pregnancy pathologies. *Am. J. Clin. Nutr.* **94**, 1896S-1902S (2011).

489. Herrera, E. & Desoye, G. Maternal and fetal lipid metabolism under normal and gestational diabetic conditions. *Horm. Mol. Biol. Clin. Investig.* **26**, 109–127 (2016).

490. Hirschmugl, B. *et al.* Maternal obesity modulates intracellular lipid turnover in the human term placenta. *Int. J. Obes.* **41**, 317–323 (2017).

491. Hulme, C. H. *et al.* The effect of high glucose on lipid metabolism in the human placenta. *Sci. Rep.* **9**, 14114 (2019).

492. Louwagie, E. J., Larsen, T. D., Wachal, A. L. & Baack, M. L. Placental lipid processing in response to a maternal high-fat diet and diabetes in rats. *Pediatr. Res.* **83**, 712 (2018).

493. Grube, M. *et al.* EXPRESSION, LOCALIZATION, AND FUNCTION OF THE CARNITINE TRANSPORTER OCTN2 (SLC22A5) IN HUMAN PLACENTA. *Drug Metab. Dispos.* **33**, 31–37 (2005).

494. Hu, C. *et al.* Inhibition of OCTN2-mediated transport of carnitine by etoposide. *Mol. Cancer Ther.* **11**, 921–929 (2012).

495. Manta-Vogli, P. D., Schulpis, K. H., Dotsikas, Y. & Loukas, Y. L. The significant role of carnitine and fatty acids during pregnancy, lactation and perinatal period. Nutritional support in specific groups of pregnant women. *Clin. Nutr.* **39**, 2337–2346 (2020).

496. Sánchez-Pintos, P. *et al.* The Journal of Maternal-Fetal & Neonatal Medicine Evaluation of carnitine deficit in very low birth weight preterm newborns small for their gestational age Evaluation of carnitine deficit in very low birth weight preterm newborns small for their gestational age. *J Matern Fetal Neonatal Med* **29**, 933–937 (2016).

497. Oey, N. A. *et al.* l-Carnitine is Synthesized in the Human Fetal-Placental Unit: Potential Roles in Placental and Fetal Metabolism. *Placenta* **27**, 841–846 (2006).

498. Vanlalhruaii *et al.* How safe is metformin when initiated in early pregnancy? A retrospective 5-year study of pregnant women with gestational diabetes mellitus from India. *Diabetes Res. Clin. Pract.* **137**, 47–55 (2018).

499. Cai, S., Huo, T., Li, N., Xiong, Z. & Li, F. Lysophosphatidylcholine - Biomarker of metformin action: Studied using UPLC/MS/MS. *Biomed. Chromatogr.* **23**, 782–786 (2009).

500. Wanninger, J. *et al.* Metformin reduces cellular lysophosphatidylcholine and thereby may lower apolipoprotein B secretion in primary human hepatocytes. *Biochim. Biophys. Acta - Mol. Cell Biol. Lipids* **1781**, 321–325 (2008).

501. Ferchaud-Roucher, V. *et al.* A potential role for lysophosphatidylcholine in the delivery of long chain polyunsaturated fatty acids to the fetal circulation. *Biochim. Biophys. Acta - Mol. Cell Biol. Lipids* **1864**, 394–402 (2019).

502. Del Gaudio, I., Sasset, L., Di Lorenzo, A. & Wadsack, C. Sphingolipid Signature of Human Feto-Placental Vasculature in Preeclampsia. *Int. J. Mol. Sci.* **21**, 1019 (2020).

503. Broere-Brown, Z. A. *et al.* Fetal sex and maternal pregnancy outcomes: a systematic review and meta-analysis. *Biol. Sex Differ.* **11**, 1–20 (2020).

504. Fadok, V. A., Bratton, D. L., Frasch, S. C., Warner, M. L. & Henson, P. M. The role of phosphatidylserine in recognition of apoptotic cells by phagocytes. *Cell Death Differ.* **5**, 551–562 (1998).

505. Simmons, D. G., Rawn, S., Davies, A., Hughes, M. & Cross, J. C. Spatial and temporal expression of the 23 murine Prolactin/Placental Lactogen-related genes is not associated with their position in the locus. *BMC Genomics* **9**, 1–20 (2008).

506. Krysiak, R., Okrzesik, J. & Okopien, B. The effect of short-term metformin treatment on plasma prolactin levels in bromocriptine-treated patients with hyperprolactinaemia and impaired glucose tolerance: a pilot study. *Endocrine* **49**, 242–249 (2015).

507. Krysiak, R., Kowalcze, K. & Okopień, B. The impact of metformin on prolactin levels in postmenopausal women. *J. Clin. Pharm. Ther.* **46**, 1433–1440 (2021).

508. Guo, J. *et al.* Metformin-Induced Changes of the Coding Transcriptome and Non-Coding RNAs in the Livers of Non-Alcoholic Fatty Liver Disease Mice. *Cell. Physiol. Biochem.* **45**, 1487–1505 (2018).

509. Andres, A. *et al.* Longitudinal body composition of children born to mothers with normal weight, overweight, and obesity. *Obesity* **23**, 1252–1258 (2015).

510. Stein, A. D. *et al.* Anthropometric measures in middle age after exposure to famine during gestation: evidence from the Dutch famine 14. *Am J Clin Nutr* **85**, 869–876 (2007).

511. Desoye, G. & Wells, J. C. K. Pregnancies in Diabetes and Obesity: The Capacity-Load Model of Placental Adaptation. *Diabetes* **70**, 823–830 (2021).

512. Mao, J. *et al.* Contrasting effects of different maternal diets on sexually dimorphic gene expression in the murine placenta. *PNAS* **107**, 5557–5562 (2010).

513. Vatten, L. J. & Skjærven, R. Offspring sex and pregnancy outcome by length of gestation. *Early Hum. Dev.* **76**, 47–54 (2004).

514. Sedlmeier, E. M. *et al.* Human placental transcriptome shows sexually dimorphic gene expression and responsiveness to maternal dietary n-3 long-chain polyunsaturated fatty acid intervention during pregnancy. *BMC Genomics* **15**, 941 (2014).

515. Yang, X. *et al.* Tissue-specific expression and regulation of sexually dimorphic genes in mice. *Genome Res.* **16**, 995 (2006).

516. Gong, S. *et al.* Placental polyamine metabolism differs by fetal sex, fetal growth restriction, and preeclampsia. *JCI insight* **3**, e120723 (2018).

517. Braun, A. E. *et al.* “Females Are Not Just ‘Protected’ Males”: Sex-Specific Vulnerabilities in Placenta and Brain after Prenatal Immune Disruption. *eNeuro* **6**, 1–25 (2019).

518. Cvitic, S. *et al.* The human placental sexome differs between trophoblast epithelium and villous vessel endothelium. *PLoS One* **8**, e79233. (2013).

519. Sun, T. *et al.* Sexually Dimorphic Crosstalk at the Maternal-Fetal Interface. *J. Clin. Endocrinol. Metab.* **105**, 4831–4847 (2020).

520. Rosenfeld, C. S. Sex-Specific Placental Responses in Fetal Development. *Endocrinology* **156**, 3422–3434 (2015).

521. Johnstone, R. M., Adam, M., Hammond, J. R., Orr, L. & Turbide, C. Vesicle formation during reticulocyte maturation. Association of plasma membrane activities with released vesicles (exosomes). *J. Biol. Chem.* **262**, 9412–9420 (1987).

522. Théry, C. *et al.* Indirect activation of naïve CD4+ T cells by dendritic cell-derived exosomes. *Nat. Immunol.* **3**, 1156–1162 (2002).

523. Andre, F. *et al.* Malignant effusions and immunogenic tumour-derived exosomes. *Lancet* **360**, 295–305 (2002).

524. Xu, R. *et al.* Extracellular vesicles in cancer — implications for future improvements in cancer care. *Nat. Rev. Clin. Oncol.* **15**, 617–638 (2018).

525. Valadi, H. *et al.* Exosome-mediated transfer of mRNAs and microRNAs is a novel mechanism of genetic exchange between cells. *Nat. Cell Biol.* **9**, 654–659 (2007).

526. Royo, F., Théry, C., Falcón-Pérez, J. M., Nieuwland, R. & Witwer, K. W. Methods for Separation and Characterization of Extracellular Vesicles: Results of a Worldwide Survey Performed by the ISEV Rigor and Standardization Subcommittee. *Cells* **9**, 1955 (2020).

527. Fowler, C. D. & Hill, A. F. NeuroEVs: Characterizing Extracellular Vesicles Generated in the Neural Domain, by Extracellular Vesicles and Neurodegenerative Diseases. *J. Neurosci.* **39**, 9269–9273 (2019).

528. Akbar, N., Azzimato, V., Choudhury, R. P. & Aouadi, M. Extracellular vesicles in metabolic disease. *Diabetologia* **62**, 2179–2187 (2019).

529. Samuelson, I. & Vidal-Puig, A. J. Fed-EXosome: extracellular vesicles and cell-cell communication in metabolic regulation. *Essays Biochem.* **62**, 165–175 (2018).

530. Ying, W. *et al.* Adipose Tissue Macrophage-Derived Exosomal miRNAs Can Modulate In Vivo and In Vitro Insulin Sensitivity. *Cell* **171**, 372-384.e12 (2017).

531. Urabe, F. *et al.* Extracellular vesicles as biomarkers and therapeutic targets for cancer. *Am. J. Physiol. - Cell Physiol.* **318**, C29–C39 (2020).

532. Merchant, M. L., Rood, I. M., Deegens, J. K. J. & Klein, J. B. Implications for Biomarker Discovery. *Nat Rev Nephrol* **13**, 731–749 (2018).

533. Foot, N. J. & Kumar, S. The Role of Extracellular Vesicles in Sperm Function and Male Fertility. *New Front. Extracell. Vesicles* **97**, 483–500 (2021).

534. Lötvall, J. *et al.* Minimal experimental requirements for definition of extracellular vesicles and their functions: A position statement from the International Society for Extracellular Vesicles. *J. Extracell. Vesicles* **3**, 1–6 (2014).

535. Van Niel, G., D'Angelo, G. & Raposo, G. Shedding light on the cell biology of extracellular vesicles. *Nat. Rev. Mol. Cell Biol.* **19**, 213–228 (2018).

536. Perez-Hernandez, D. *et al.* The Intracellular Interactome of Tetraspanin-enriched Microdomains Reveals Their Function as Sorting Machineries toward Exosomes. *J. Biol. Chem.* **288**, 11649 (2013).

537. De Gassart, A., Géminard, C., Février, B., Raposo, G. & Vidal, M. Lipid raft-associated protein sorting in exosomes. *Blood* **102**, 4336–4344 (2003).

538. Villarroya-Beltri, C. *et al.* Sumoylated hnRNPA2B1 controls the sorting of miRNAs into exosomes through binding to specific motifs. *Nat. Commun.* **4**, 2980 (2013).

539. Fabbiano, F. *et al.* RNA packaging into extracellular vesicles: An orchestra of RNA-binding proteins? *J. Extracell. Vesicles* **10**, e12043 (2020).

540. McKenzie, A. J. *et al.* KRAS-MEK Signaling Controls Ago2 Sorting into Exosomes. *Cell Rep.* **15**, 978 (2016).

541. Mateescu, B. *et al.* Obstacles and opportunities in the functional analysis of extracellular vesicle RNA-an ISEV position paper. *J. Extracell. VESICLES* **6**, 1286095 (2017).

542. Pfrieger, F. W. & Vitale, N. Cholesterol and the journey of extracellular vesicles. **59**, 2255–2261 (2018).

543. Hoshino, A., Costa-Silva, B., Shen, T.-L., Rodrigues, G. & Lyden, D. Tumour exosome integrins determine organotropic metastasis HHS Public Access. *Nature* **527**, 329–335 (2015).

544. Rana, S., Yue, S., Stadel, D. & Zöller, M. Toward tailored exosomes: The exosomal tetraspanin web contributes to target cell selection. *Int. J. Biochem. Cell Biol.* **44**, 1574–1584 (2012).

545. Raposo, G. *et al.* B Lymphocytes Secrete Antigen-presentingVesicles. *J. Exp. Med.* **183**, 1161–1172 (1996).

546. Théry, C., Amigorena, S., Raposo, G. & Clayton, A. Isolation and Characterization of Exosomes from Cell Culture Supernatants and Biological Fluids. *Curr. Protoc. Cell Biol.* **30**, 3.22.1-3.22.29 (2006).

547. Gardiner, C. *et al.* Techniques used for the isolation and characterization of extracellular vesicles: results of a worldwide survey. *J. Extracell. Vesicles* **5**, 32945 (2016).

548. Monguió-Tortajada, M., Gálvez-Montón, C., Bayes-Genis, A., Roura, S. & Borràs, F. E. Extracellular vesicle isolation methods: rising impact of size-exclusion chromatography. *Cell. Mol. Life Sci.* 2369–2382 (2019) doi:10.1007/s00018-019-03071-y.

549. Brennan, K. *et al.* A comparison of methods for the isolation and separation of

extracellular vesicles from protein and lipid particles in human serum. *Sci. Rep.* **10**, 1039 (2020).

550. Doyle, L. & Wang, M. Z. Isolation and Analysis. *Cells* **8**, 727 (2019).

551. Théry, C. *et al.* Minimal information for studies of extracellular vesicles 2018 (MISEV2018): a position statement of the International Society for Extracellular Vesicles and update of the MISEV2014 guidelines. *J. Extracell. Vesicles* **7**, 1535750 (2018).

552. Yang, Y. *et al.* Extracellular vesicles isolated by size-exclusion chromatography present suitability for RNomics analysis in plasma. *J. Transl. Med.* **19**, 1–12 (2021).

553. Nieuwland, R., Falcón-Pérez, J. M., Théry, C. & Witwer, K. W. Rigor and standardization of extracellular vesicle research: Paving the road towards robustness. *J. Extracell. Vesicles* **10**, e12037 (2020).

554. Lapaire, O., Holzgreve, W., Oosterwijk, J. C., Brinkhaus, R. & Bianchi, D. W. Georg Schmorl on Trophoblasts in the Maternal Circulation. *Placenta* **28**, 1–5 (2007).

555. Sadovsky, Y. *et al.* Placental small extracellular vesicles: Current questions and investigative opportunities. *Placenta* **102**, 34–38 (2020).

556. Frängsmyr, L. *et al.* Cytoplasmic microvesicular form of Fas ligand in human early placenta: Switching the tissue immune privilege hypothesis from cellular to vesicular level. *Mol. Hum. Reprod.* **11**, 35–41 (2005).

557. Chiarello, D. I. *et al.* Foetoplacental communication via extracellular vesicles in normal pregnancy and preeclampsia. *Mol. Aspects Med.* **60**, 69–80 (2018).

558. Salomon, C. *et al.* A Gestational Profile of Placental Exosomes in Maternal Plasma and Their Effects on Endothelial Cell Migration. *PLoS One* **9**, 98667 (2014).

559. Miranda, J. *et al.* Placental exosomes profile in maternal and fetal circulation in intrauterine growth restriction - Liquid biopsies to monitoring fetal growth. *Placenta* **64**, 34–43 (2018).

560. Knight, M., Fellow, C. R., Redman, C. W. G. & Linton, E. A. Shedding of syncytiotrophoblast microvilli into the maternal circulation in pre-eclamptic pregnancies. *Br. J. Obstet. Gynaecol.* **105**, 632–640 (1998).

561. Tannetta, D. S., Dragovic, R. A., Gardiner, C., Redman, C. W. & Sargent, I. L. Characterisation of Syncytiotrophoblast Vesicles in Normal Pregnancy and Pre-Eclampsia: Expression of Flt-1 and Endoglin. *PLoS One* **8**, e56754. (2013).

562. Motta-Mejia, C. *et al.* Placental Vesicles Carry Active Endothelial Nitric Oxide Synthase and Their Activity is Reduced in Preeclampsia. *Hypertension* **70**, 372–381 (2017).

563. Han, C. *et al.* Placenta-derived extracellular vesicles induce preeclampsia in mouse models. *Haematologica* **105**, 1686 (2020).

564. Rice, G. E. *et al.* The Effect of Glucose on the Release and Bioactivity of Exosomes From First Trimester Trophoblast Cells. *J. Clin. Endocrinol. Metab.* **100**, E1280–E1288 (2015).

565. Salomon, C. *et al.* Gestational Diabetes Mellitus Is Associated With Changes in the Concentration and Bioactivity of Placenta-Derived Exosomes in Maternal Circulation Across Gestation. *Diabetes* **65**, 598–609 (2016).

566. Pantham, P., Aye, I. L. M. H. & Powell, T. L. Inflammation in maternal obesity and gestational diabetes mellitus. *Placenta* **36**, 709–15 (2015).

567. James-Allan, L. B. *et al.* Regulation of glucose homeostasis by small extracellular vesicles in normal pregnancy and in gestational diabetes. *FASEB J.* **34**, 5724–5739 (2020).

568. Nair, S. *et al.* Extracellular vesicle-associated miRNAs are an adaptive response to gestational diabetes mellitus. *J. Transl. Med.* **19**, 360 (2021).

569. Nguyen, S. L. *et al.* Quantifying murine placental extracellular vesicles across gestation and in preterm birth data with tidyNano: A computational framework for analyzing and visualizing nanoparticle data in R. *PLoS One* **14**, 1–14 (2019).

570. Tong, M. & Chamley, L. W. Isolation and Characterization of Extracellular Vesicles from Ex Vivo Cultured Human Placental Explants. *Methods Mol. Biol.* **1710**, 117–129 (2018).

571. Nguyen, S. L. *et al.* Integrins mediate placental extracellular vesicle trafficking to lung and liver in vivo. *Sci. Rep.* **11**, 1–16 (2021).

572. Stefanski, A. L. *et al.* Murine trophoblast-derived and pregnancy-associated exosome-enriched extracellular vesicle microRNAs: Implications for placenta driven effects on maternal physiology. *PLoS One* **14**, 1–23 (2019).

573. Sheller-Miller, S., Choi, K., Choi, C. & Menon, R. Cre-Reporter Mouse Model to Determine Exosome Communication and Function during Pregnancy. *Am. J. Obstet. Gynecol.* **221**, 502.e1–12 (2019).

574. Holder, B. *et al.* Macrophage Exosomes Induce Placental Inflammatory Cytokines: A Novel Mode of Maternal–Placental Messaging. *Traffic* **17**, 168 (2016).

575. Vargas, A. *et al.* Syncytin proteins incorporated in placenta exosomes are important for cell uptake and show variation in abundance in serum exosomes from patients with preeclampsia. *FASEB J.* **28**, 3703–3719 (2014).

576. Donker, R. B. *et al.* The expression profile of C19MC microRNAs in primary human trophoblast cells and exosomes. *Mol. Hum. Reprod.* **18**, 417–424 (2012).

577. Wong, R. K. Y., MacMahon, M., Woodside, J. V & Simpson, D. A. A comparison of RNA extraction and sequencing protocols for detection of small RNAs in plasma. *BMC Genomics* **20**, 446 (2019).

578. Chan, H. W. *et al.* The expression of the let-7 miRNAs and Lin28 signalling pathway in human term gestational tissues. *Placenta* **34**, 443–448 (2013).

579. Pineles, B. L. *et al.* Distinct subsets of microRNAs are expressed differentially in the human placentas of patients with preeclampsia. *Am. J. Obstet. Gynecol.* **196**, 261.e1-261.e6 (2007).

580. Shi, M., Chen, X., Li, H. & Zheng, L. δ-tocotrienol suppresses the migration and

angiogenesis of trophoblasts in preeclampsia and promotes their apoptosis via miR-429/ ZEB1 axis. *Bioengineered* **12**, 1861–1873 (2021).

581. Moh-Moh-Aung, A. *et al.* Decreased miR-200b-3p in cancer cells leads to angiogenesis in HCC by enhancing endothelial ERG expression. *Sci. Rep.* **10**, 1–14 (2020).

582. Ferland-Mccollough, D. *et al.* Programming of adipose tissue miR-483-3p and GDF-3 expression by maternal diet in type 2 diabetes. *Cell Death Differ.* **19**, 1003–1012 (2012).

583. Mayor-Lynn, K., Toloubeydokhti, T., Cruz, A. C. & Chegini, N. Expression profile of microRNAs and mRNAs in human placentas from pregnancies complicated by preeclampsia and preterm labor. *Reprod. Sci.* **18**, 46–56 (2011).

584. Li, J. *et al.* IGF2-derived miR-483-3p contributes to macrosomia through regulating trophoblast proliferation by targeting RB1CC1. *Mol. Hum. Reprod.* **24**, 444–452 (2018).

585. Saha, S., Choudhury, J. & Ain, R. MicroRNA-141-3p and miR-200a-3p regulate insulin-like growth factor 2 during mouse placental development. *Mol. Cell. Endocrinol.* **414**, 186–193 (2015).

586. Sferruzzi-Perri, A. N. *et al.* Placental-specific Igf2 deficiency alters developmental adaptations to undernutrition in mice. *Endocrinology* **152**, 3202–3212 (2011).

587. White, V. *et al.* IGF2 stimulates fetal growth in a sex- and organ-dependent manner. *Pediatr. Res.* **83**, 183–189 (2018).

588. Lou, C. *et al.* MiR-485-3p and mir-485-5p suppress breast cancer cell metastasis by inhibiting PGC-1α expression. *Cell Death Dis.* **7**, 1–9 (2016).

589. Zhao, Y. *et al.* MiR-485-5p modulates mitochondrial fission through targeting mitochondrial anchored protein ligase in cardiac hypertrophy. *Biochim. Biophys. Acta - Mol. Basis Dis.* **1863**, 2871–2881 (2017).

590. Abbade, J. *et al.* Increased placental mitochondrial fusion in gestational diabetes mellitus: An adaptive mechanism to optimize feto-placental metabolic homeostasis? *BMJ Open Diabetes Res. Care* **8**, e000923 (2020).

591. Fisher, J. J. *et al.* Mitochondrial dysfunction in placental trophoblast cells experiencing gestational diabetes mellitus. *J. Physiol.* **599**, 1291–1305 (2021).

592. Lord, J. M., Flight, I. H. K. & Norman, R. J. Papers Metformin in polycystic ovary syndrome: systematic review and meta-analysis. *BMJ* **327**, 1–6 (2003).

593. Kitwitee, P. *et al.* Metformin for the treatment of gestational diabetes: An updated meta-analysis. *Diabetes Res. Clin. Pract.* **109**, 521–532 (2015).

594. Zhao, Y. *et al.* Metformin administration during pregnancy attenuated the long-term maternal metabolic and cognitive impairments in a mouse model of gestational diabetes. *Aging (Albany. NY).* **12**, 14019–14036 (2020).

595. Feig, D. S. & Moses, R. G. Metformin therapy during pregnancy: Good for the goose and good for the gosling too? *Diabetes Care* **34**, 2329–2330 (2011).

596. Tarry-Adkins, J. L., Ozanne, S. E. & Aiken, C. E. Impact of metformin treatment during

pregnancy on maternal outcomes: a systematic review/meta-analysis. *Sci. Rep.* **11**, 1–13 (2021).

597. Valdés, E. *et al.* Metformin as a prophylactic treatment of gestational diabetes in pregnant patients with pregestational insulin resistance: A randomized study. *J. Obstet. Gynaecol. Res.* **44**, 81–86 (2017).

598. McGrath, R. T., Glastras, S. J., Hocking, S. & Fulcher, G. R. Use of metformin earlier in pregnancy predicts supplemental insulin therapy in women with gestational diabetes. *Diabetes Res. Clin. Pract.* **116**, 96–99 (2016).

599. Ashoush, S., El-Said, M., Fathi, H. & Abdelnaby, M. Identification of metformin poor responders, requiring supplemental insulin, during randomization of metformin versus insulin for the control of gestational diabetes mellitus. *J. Obstet. Gynaecol. Res.* **42**, 640–647 (2016).

600. Khin, M. O., Gates, S. & Saravanan, P. Predictors of metformin failure in gestational diabetes mellitus (GDM). *Diabetes Metab. Syndr. Clin. Res. Rev.* **12**, 405–410 (2018).

601. Tertti, K., Ekblad, U., Koskinen, P. & Vahlberg, T. Metformin vs. insulin in gestational diabetes. A randomized study characterizing metformin patients needing additional insulin. *Diabetes, Obes. Metab.* **15**, 246–251 (2013).

602. Martine-Edith, G., Johnson, W., Hunsicker, E., Hamer, M. & Petherick, E. S. Associations between maternal characteristics and pharmaceutical treatment of gestational diabetes: an analysis of the UK Born in Bradford (BiB) cohort study. *BMJ Open* **11**, e053753 (2021).

603. Palatnik, A., Harrison, R. K., Thakkar, M. Y., Walker, R. J. & Egede, L. E. Correlates of Insulin Selection as a First-Line Pharmacological Treatment for Gestational Diabetes. *Am. J. Perinatol.* (2021) doi:10.1055/S-0041-1739266.

604. Kjos, S. L. *et al.* A Randomized Controlled Trial Using Glycemic Plus Fetal Ultrasound Parameters Versus Glycemic Parameters to Determine Insulin Therapy in Gestational Diabetes With Fasting Hyperglycemia. *Diabetes Care* **24**, 1904–1910 (2001).

605. Mousa, A. *et al.* Metformin in Pregnancy Study (MiPS): Protocol for a systematic review with individual patient data meta-analysis. *BMJ Open* **10**, 1–8 (2020).

606. Hu, J., Zhang, J. & Zhu, B. Protective effect of metformin on a rat model of lipopolysaccharide-induced preeclampsia. *Fundam. Clin. Pharmacol.* **33**, 649–658 (2019).

607. Osungbade, K. O. & Ige, O. K. Public Health Perspectives of Preeclampsia in Developing Countries: Implication for Health System Strengthening. *J. Pregnancy* **2011**, 481095 (2011).

608. Machano, M. M. & Joho, A. A. Prevalence and risk factors associated with severe pre-eclampsia among postpartum women in Zanzibar: A cross-sectional study. *BMC Public Health* **20**, 1–10 (2020).

609. Cluver, C. A. *et al.* Use of metformin to prolong gestation in preterm pre-eclampsia: randomised, double blind, placebo controlled trial. *BMJ* **374**, (2021).

610. Schoonejans, J. M. PhD thesis: The effect of metformin intervention on the programming of cardiometabolic health in offspring of obese pregnancy Josca Mariëtte Schoonejans. (2021).

611. Deng, J. *et al.* H19 lncRNA alters methylation and expression of Hnf4α in the liver of metformin-exposed fetuses. *Cell Death Dis.* **8**, e3175 (2017).

612. Chen, D., Wang, Y., Wu, K. & Wang, X. Dual effects of metformin on adipogenic differentiation of 3T3-L1 preadipocyte in AMPK-dependent and independent manners. *Int. J. Mol. Sci.* **19**, 1547 (2018).

613. Nüsken, E. *et al.* Maternal high fat diet and in-utero metformin exposure significantly impact upon the fetal renal proteome of male mice. *J. Clin. Med.* **8**, 663 (2019).

614. Lopez-Jaramillo, P., Barajas, J., Rueda-Quijano, S. M., Lopez-Lopez, C. & Felix, C. Obesity and Preeclampsia: Common Pathophysiological Mechanisms. *Front. Physiol.* **9**, 1838 (2018).

615. Pende, A., Artom, N., Bertolotto, M., Montecucco, F. & Dallegri, F. Role of neutrophils in atherogenesis: an update. *Eur. J. Clin. Invest.* **46**, 252–263 (2016).

616. Wallingford, M. C., Gammill, H. S. & Giachelli, C. M. Slc20a2 deficiency results in fetal growth restriction and placental calcification associated with thickened basement membranes and novel CD13 and lamininα1 expressing cells. *Reprod. Biol.* **16**, 13 (2016).

617. Yang, H., Kim, T. H., Lee, G. S., Hong, E. J. & Jeung, E. B. Comparing the expression patterns of placental magnesium/phosphorus-transporting channels between healthy and preeclamptic pregnancies. *Mol. Reprod. Dev.* **81**, 851–860 (2014).

618. Sayed, D. & Abdellatif, M. Micrornas in development and disease. *Physiol. Rev.* **91**, 827–887 (2011).

619. Condrat, C. E. *et al.* miRNAs as Biomarkers in Disease: Latest Findings Regarding Their Role in Diagnosis and Prognosis. *Cells* **9**, 276 (2020).

620. Alfaradhi, M. Z. *et al.* Maternal obesity in pregnancy developmentally programs adipose tissue inflammation in young, lean male mice offspring. *Endocrinology* **157**, 4246–4256 (2016).

621. Fernandez-Twinn, D. S. *et al.* Downregulation of IRS-1 in adipose tissue of offspring of obese mice is programmed cell-autonomously through post-transcriptional mechanisms. *Mol. Metab.* **3**, 325–333 (2014).

622. Sovio, U. *et al.* Prediction of Preeclampsia Using the Soluble fms-Like Tyrosine Kinase 1 to Placental Growth Factor Ratio: A Prospective Cohort Study of Unselected Nulliparous Women. *Hypertension* **69**, 731–738 (2017).

623. Mutter, W. P. & Karumanchi, S. A. Molecular mechanisms of preeclampsia. *Microvasc. Res.* **75**, 1–8 (2008).

624. Li, H. *et al.* Unique microRNA Signals in Plasma Exosomes from Pregnancies Complicated by Preeclampsia. *Hypertension* **75**, 762–771 (2020).

625. Sabapatha, A., Gercel-Taylor, C. & Taylor, D. D. Specific Isolation of Placenta-Derived

Exosomes from the Circulation of Pregnant Women and Their Immunoregulatory Consequences. *Am. J. Reprod. Immunol.* **56**, 345–355 (2006).

626. Shou, C., Wei, Y. M., Wang, C. & Yang, H. X. Updates in long-term maternal and fetal adverse effects of gestational diabetes mellitus. *Matern. Med.* **1**, 91–94 (2019).

627. Scheen, A. J. Will delayed release metformin provide better management of diabetes type 2? *https://doi.org/10.1517/14656566.2016.1149166* **17**, 627–630 (2016).

628. Henry, R. R. *et al.* Improved glycemic control with minimal systemic metformin exposure: Effects of Metformin Delayed-Release (Metformin DR) targeting the lower bowel over 16 weeks in a randomized trial in subjects with type 2 diabetes. *PLoS One* **13**, e0203946 (2018).

Supplement

Supplement 1: *References for Figure 1.13: Observations in mouse maternal obesity models (p.42)*

1. Gohir, W. *et al.* High-fat diet intake modulates maternal intestinal adaptations to pregnancy and results in placental hypoxia, as well as altered fetal gut barrier proteins and immune markers. *J. Physiol.* **597**, 3029–3051 (2019).

2. Hanssens, S. *et al.* Maternal obesity alters the apelinergic system at the feto-maternal interface. *Placenta* **39**, 41–44 (2016).

3. Jack-Roberts, C. *et al.* Choline supplementation normalizes fetal adiposity and reduces lipogenic gene expression in a mouse model of maternal obesity. *Nutrients* **9**, 899 (2017).

4. Qiao, L. *et al.* Maternal high-fat feeding increases placental lipoprotein lipase activity by reducing SIRT1 expression in mice. *Diabetes* **64**, 3111–3120 (2015).

5. Li, H. P., Chen, X. & Li, M. Q. Gestational diabetes induces chronic hypoxia stress and excessive inflammatory response in murine placenta. *Int. J. Clin. Exp. Pathol.* **6**, 650–659 (2013).

6. Wu, L. L. *et al.* Mitochondrial dysfunction in oocytes of obese mothers: Transmission to offspring and reversal by pharmacological endoplasmic reticulum stress inhibitors. *Development* **142**, 681–691 (2015).

7. Kim, D. W., Young, S. L., Grattan, D. R. & Jasoni, C. L. Obesity During Pregnancy Disrupts Placental Morphology, Cell Proliferation, and Inflammation in a Sex-Specific Manner Across Gestation in the Mouse 1. *Biol. Reprod.* **90**, 130–131 (2014).

8. Parker, V. J., Arck, P. C. & Douglas, A. J. Diet-induced obesity may affect the uterine immune environment in early–mid pregnancy, reducing NK-cell activity and potentially compromising uterine vascularization. *Int. J. Obes.* **38**, 766–774 (2014).

9. Fornes, R. *et al.* Mice exposed to maternal androgen excess and diet-induced obesity have altered phosphorylation of catechol-O-methyltransferase in the placenta and fetal liver. *Int. J. Obes.* **43**, 2176–2188 (2019).

10. Lager, S. *et al.* Diet-induced obesity in mice reduces placental efficiency and inhibits placental mTOR signaling. *Physiol Rep* **2**, 242 (2014).

11. Qiao, L. *et al.* Adiponectin enhances mouse fetal fat deposition. *Diabetes* **61**, 3199–3207 (2012).

12. Panchenko, P. E. *et al.* Expression of epigenetic machinery genes is sensitive to maternal obesity and weight loss in relation to fetal growth in mice. *Clin. Epigenetics* **8**, 22 (2016).

13. Son, J. S. *et al.* Exercise prevents the adverse effects of maternal obesity on placental vascularization and fetal growth. *J. Physiol.* **597**, 3333–3347 (2019).

14. Murabayashi, N. *et al.* Maternal high-fat diets cause insulin resistance through inflammatory changes in fetal adipose tissue. *Eur. J. Obstet. Gynecol. Reprod. Biol.* **169**, 39–44 (2013).

15. Qiao, L. *et al.* Prolonged Prepregnant Maternal High-Fat Feeding Reduces Fetal and Neonatal Blood Glucose Concentrations by Enhancing Fetal β-Cell Development in C57BL/6 Mice. *Diabetes* **68**, 1604–1613 (2019).

16. Musial, B. *et al.* A Western-style obesogenic diet alters maternal metabolic physiology with consequences for fetal nutrient acquisition in mice. *J. Physiol.* **595**, 4875–4892 (2017).

17. Appel, S. *et al.* A Potential Role for GSK3 *β* in Glucose-Driven Intrauterine Catch-Up Growth in

Maternal Obesity. *Endocrinology* **160**, 377–386 (2019).

18. Heerwagen, M. J. R., Stewart, M. S., de la Houssaye, B. A., Janssen, R. C. & Friedman, J. E. Transgenic Increase in N-3/N-6 Fatty Acid Ratio Reduces Maternal Obesity-Associated Inflammation and Limits Adverse Developmental Programming in Mice. *PLoS One* **8**, e67791. (2013).

19. Wang, H., Chen, Y., Mao, X. & Du, M. Maternal obesity impairs fetal mitochondriogenesis and brown adipose tissue development partially via upregulation of miR-204-5p. *Biochim. Biophys. Acta - Mol. Basis Dis.* **1865**, 2706–2715 (2019).

20. Joselit, Y. *et al.* Maternal betaine supplementation affects fetal growth and lipid metabolism of high-fat fed mice in a temporal-specific manner. *Nutr. Diabetes* **8**, 41 (2018).

21. Chen, J. R., Lazarenko, O. P., Zhao, H., Alund, A. W. & Shankar, K. Maternal obesity impairs skeletal development in adult offspring. *J. Endocrinol.* **239**, 33–47 (2018).

22. Kahraman, S., Dirice, E., De Jesus, D. F., Hu, J. & Kulkarni, R. N. Maternal insulin resistance and transient hyperglycemia impact the metabolic and endocrine phenotypes of offspring. *Am. J. Physiol. - Endocrinol. Metab.* **307**, E906–E918 (2014).

23. Jungheim, E. S. *et al.* Preimplantation Exposure of Mouse Embryos to Palmitic Acid Results in Fetal Growth Restriction Followed by Catch-Up Growth in the Offspring. *Biol. Reprod.* **85**, 678–683 (2011).

24. Bae-Gartz, I. *et al.* Maternal Obesity Alters Neurotrophin-Associated MAPK Signaling in the Hypothalamus of Male Mouse Offspring. *Front. Neurosci.* **13**, (2019).

25. Jungheim, E. S. *et al.* Diet-induced obesity model: Abnormal oocytes and persistent growth abnormalities in the offspring. *Endocrinology* **151**, 4039–4046 (2010).

26. Dahlhoff, M. *et al.* Peri-conceptional obesogenic exposure induces sex-specific programming of disease susceptibilities in adult mouse offspring. *Biochim. Biophys. Acta - Mol. Basis Dis.* **1842**, 304–317 (2014).

27. Ferey, J. L. A. *et al.* A maternal high-fat, high-sucrose diet induces transgenerational cardiac mitochondrial dysfunction independently of maternal mitochondrial inheritance. *Am. J. Physiol. - Hear. Circ. Physiol.* **316**, H1202–H1210 (2019).

28. Zhu, C. *et al.* A mouse model of pre-pregnancy maternal obesity combined with offspring exposure to a high-fat diet resulted in cognitive impairment in male offspring. *Exp. Cell Res.* **368**, 159–166 (2018).

29. Wankhade, U. D. *et al.* Maternal High-Fat Diet Programs Offspring Liver Steatosis in a Sexually Dimorphic Manner in Association with Changes in Gut Microbial Ecology in Mice. *Sci. Rep.* **8**, 16502 (2018).

Supplement 2: *References for Figure 1.14: Observations in mouse GDM models (page 42)*

1. Bobadilla, R. A., Van Bree, R., Vercruysse, L., Pijnenborg, R. & Verhaeghe, J. Placental Effects of Systemic Tumour Necrosis Factor-α in an Animal Model of Gestational Diabetes Mellitus. *Placenta* **31**, 1057–1063 (2010).

2. Stanley, J. L., Cheung, C. C., Sankaralingam, S., Baker, P. N. & Davidge, S. T. Effect of Gestational Diabetes on Maternal Artery Function. *Reprod. Sci.* **18**, 342–352 (2011).

3. Xing, B. heng, Yang, F. zhen & Wu, X. hua. Naringenin enhances the efficacy of human embryonic stem cell-derived pancreatic endoderm in treating gestational diabetes mellitus mice. *J. Pharmacol. Sci.* **131**, 93–100 (2016).

4. Chen, Y. *et al.* Astaxanthin alleviates gestational diabetes mellitus in mice through suppression of oxidative stress. *Naunyn. Schmiedebergs. Arch. Pharmacol.* **393**, 2517–2527 (2020).

5. Qiao, L. *et al.* Adiponectin Deficiency Impairs Maternal Metabolic Adaptation to Pregnancy in Mice. *Diabetes* **66**, 1121 (2017).

6. Huang, L. *et al.* Combined intervention of swimming plus metformin ameliorates the insulin resistance and impaired lipid metabolism in murine gestational diabetes mellitus. *PLoS One* **13**, e0195609 (2018).

7. Machado, A. F., Zimmerman, E. F., Hovland, D. N., Weiss, R. & Collins, M. D. Diabetic embryopathy in C57BL/6J mice: Altered fetal sex ratio and impact of the splotch allele. *Diabetes* **50**, 1193–1199 (2001).

8. Zabihi, S., Wentzel, P. & Eriksson, U. J. Maternal Blood Glucose Levels Determine the Severity of Diabetic Embryopathy in Mice with Different Expression of Copper-Zinc Superoxide Dismutase (CuZnSOD). *Toxicol. Sci.* **105**, 166–172 (2008).

9. Aasa, K. L., Kwong, K. K., Adams, M. A. & Croy, B. A. Analysis of maternal and fetal cardiovascular systems during hyperglycemic pregnancy in the nonobese diabetic mouse. *Biol. Reprod.* **88**, 151 (2013).

10. Kahraman, S., Dirice, E., De Jesus, D. F., Hu, J. & Kulkarni, R. N. Maternal insulin resistance and transient hyperglycemia impact the metabolic and endocrine phenotypes of offspring. *Am. J. Physiol. - Endocrinol. Metab.* **307**, E906–E918 (2014).

11. Sha, H., Zeng, H., Zhao, J. & Jin, H. Mangiferin ameliorates gestational diabetes mellitus-induced placental oxidative stress, inflammation and endoplasmic reticulum stress and improves fetal outcomes in mice. *Eur. J. Pharmacol.* **859**, 172522 (2019).

12. Yamashita, H. *et al.* Leptin administration prevents spontaneous gestational diabetes in heterozygous Leprdb/+ mice: Effects on placental leptin and fetal growth. *Endocrinology* **142**, 2888–2897 (2001).

13. Dowling, D. *et al.* Cardiomyopathy in offspring of pregestational diabetic mouse pregnancy. *J. Diabetes Res.* **2014**, 624939 (2014).

14. Sanders, T. R., Kim, D. W., Glendining, K. A. & Jasoni, C. L. Maternal Obesity and IL-6 Lead to Aberrant Developmental Gene Expression and Deregulated Neurite Growth in the Fetal Arcuate Nucleus. *endo.endojournals.org Endocrinol.* **155**, 2566–2577 (2014).

15. Hokke, S. N. *et al.* Maternal glucose intolerance reduces offspring nephron endowment and increases glomerular volume in adult offspring. *Diabetes. Metab. Res. Rev.* **32**, 13–23 (2016).

16. Moazzen, H. *et al.* N-Acetylcysteine prevents congenital heart defects induced by pregestational diabetes. *Cardiovasc. Diabetol.* **13**, 1–13 (2014).

17. Yamashita, H., Shao, J., Qiao, L., Pagliassotti, M. & Friedman, J. E. Effect of Spontaneous Gestational Diabetes on Fetal and Postnatal Hepatic Insulin Resistance in Lepr db/ Mice. *Pediatr. Res.* **53**, 411–8 (2003).

18. Ge, Z.-J. *et al.* Maternal obesity and diabetes may cause DNA methylation alteration in the spermatozoa of offspring in mice. *Reprod. Biol. Endocrinol.* **12**, 1–8 (2014).

19. Kagohashi, Y. *et al.* Maternal dietary n-6/n-3 fatty acid ratio affects type 1 diabetes development in the offspring of non-obese diabetic mice. *Congenit. Anom. (Kyoto).* **50**, 212–220 (2010).

Supplement 3: *References for Figure 3.1: Observations from our Ozanne lab mouse model (page 59)*

1. Samuelsson, A. M. *et al.* Diet-induced obesity in female mice leads to offspring hyperphagia, adiposity, hypertension, and insulin resistance: A novel murine model of developmental programming. *Hypertension* **51**, 383–392 (2008).

2. Fernandez-Twinn, D. S. *et al.* Downregulation of IRS-1 in adipose tissue of offspring of obese mice is programmed cell-autonomously through post-transcriptional mechanisms. *Mol. Metab.* **3**, 325–333 (2014).

3. Alfaradhi, M. Z. *et al.* Oxidative stress and altered lipid homeostasis in the programming of offspring fatty liver by maternal obesity. *Am. J. Physiol. - Regul. Integr. Comp. Physiol.* **307**, R26–R34 (2014).

4. Musial, B. *et al.* Exercise alters the molecular pathways of insulin signaling and lipid handling in maternal tissues of obese pregnant mice. *Physiol. Rep.* **7**, e14202 (2019).

5. Fernandez-Twinn, D. S. *et al.* Exercise rescues obese mothers' insulin sensitivity, placental hypoxia and male offspring insulin sensitivity. *Sci. Rep.* **7**, 44650 (2017).

6. Loche, E. *et al.* Maternal diet-induced obesity programmes cardiac dysfunction in male mice independently of post-weaning diet. *Cardiovasc. Res.* **114**, 1372–1384 (2018).

7. De Barros Mucci, D. *et al.* Impact of maternal obesity on placental transcriptome and morphology associated with fetal growth restriction in mice. *Int. J. Obes.* **44**, 1087–1096 (2020).

8. Fernandez-Twinn, D. S. *et al.* The programming of cardiac hypertrophy in the offspring by maternal obesity is associated with hyperinsulinemia, AKT, ERK, and mTOR activation. *Endocrinology* **153**, 5961–5971 (2012).

9. de Almeida Faria, J., Duque-Guimarães, D., Carpenter, A. A. M., Loche, E. & Ozanne, S. E. A post-weaning obesogenic diet exacerbates the detrimental effects of maternal obesity on offspring insulin signaling in adipose tissue. *Sci. Rep.* **7**, 44949 (2017).

10. Beeson, J. H. *et al.* Maternal exercise intervention in obese pregnancy improves the cardiovascular health of the adult male offspring. *Mol. Metab.* **16**, 35–44 (2018).

11. Nicholas, L. M. *et al.* Exposure to maternal obesity programs sex differences in pancreatic islets of the offspring in mice. *Diabetologia* **63**, 324–337 (2020).

12. Oben, J. A. *et al.* Maternal obesity during pregnancy and lactation programs the development of offspring non-alcoholic fatty liver disease in mice. *J. Hepatol.* **52**, 913–920 (2010).

13. Blackmore, H. L. *et al.* Maternal diet-induced obesity programs cardiovascular dysfunction in adult male mouse offspring independent of current body weight. *Endocrinology* **155**, 3970–

3980 (2014).

14. Aiken, C. E., Tarry-Adkins, J. L., Penfold, N. C., Dearden, L. & Ozanne, S. E. Decreased ovarian reserve, dysregulation of mitochondrial biogenesis, and increased lipid peroxidation in female mouse offspring exposed to an obesogenic maternal diet. *FASEB J.* **30**, 1548–1556 (2016).

15. Mennitti, L. V. *et al.* Effects of maternal diet-induced obesity on metabolic disorders and age-associated miRNA expression in the liver of male mouse offspring. *Int. J. Obes.* 1–10 (2021) doi:10.1038/s41366-021-00985-1.

Supplement 4: *Table of references and information for Figure 3.2: World map of metformin use in GDM treatment (p. 60)*

Country	Used in pregnancy?	Source and date	comment
Australia	Yes	Queensland Clinical Guidelines (2021)[1]	Alternative to insulin in GDM treatment
Brazil	No	Nicolosi et al. (2020)[2]	Brazilian Health Surveillance Agency does not recommend use of metformin in pregnancy
Canada	Yes	Feig et al. (2018)[3]	can be used in pregnancy (but women should be advised that it crosses the placenta)
China	Yes	Feng et al. (2020)[4]	Alternative to insulin in GDM treatment
Columbia	Yes	Ministerio de Salud Colombia (2016)[5]	Dependent on the preference of the patient insulin or metformin can be taken (google translate)
Denmark	No	Damm et al. (2009)[6], update online (https://www.sundhed.dk/sundhedsfaglig/laegehaandbogen/obstetrik/tilstande-og-sygdomme/risikofaktorer-i-svangerskabet/gestationel-diabetes-gdm/) the same (2021)	Oral antidiabetics are not used for pregnant women in Denmark.
Germany	No	Schäfer-Graf et al. (2018)[7]	Metformin not to be used in pregnancy, only if all other treatment options did not work metformin use can be evaluated
India	Yes	Mishra et al. (2018)[8]	Metformin and insulin accepted treatment for metformin
Iran	Yes	Valizadeh et al. (2020)[9]	Metformin use in mild GDM
Mexico	Yes	Dainelli et al. (2018)[10]	Can be used as second alternative to insulin, studies show high use of metformin
Netherlands	No	NVOG (2010)[11], Update online (https://www.isala.nl/patientenfolders/7188-diabetes-en-zwangerschap/) the same (2021)	Metformin not to be used in pregnancy
New Zealand	Yes	Ministry of Health (2014)	Alternative to insulin in GDM treatment
Norway	Yes	Helsedirektoratet (2020)[12]	Alternative to insulin in GDM treatment
Poland	No	Wender-Ozegowska et al. (2018)[13]	Metformin not to be used in pregnancy

Portugal	Yes	Almeida et al. (2017)[14]	Therapetuic options for GDM are insulin, metformin and glyburide
Russia	No	Sazanova et al. (2016)[15]	Metformin not allowed in pregnancy
South Africa	Yes	Dias et al. (2019)[16]	First-line treatment
Sweden	Yes	Fadl et al. (2019)[17]	Accepted for treatment of GDm by the Swedish National Board of Health
Turkey	No	SEMT (2019)[18]	Metformin contraindicated in pregnancy
UK	Yes	NICE guidelines (2015, updated 2020)[19]	Metformin is first-line treatment
United States	Yes	Adkins et al. (2021)[20] and ADA (2021)[21]	different recommendations by ADA and SFMF, can be used but not recommended
Venezuela	Yes	Brajkovich et al. (2016)[22]	Metformin can be considered first line treatment for GDM (google translate)

1. Queensland Clinical Guidelines. *Maternity and Neonatal Clinical Guideline Gestational diabetes mellitus (GDM)*. www.health.qld.gov.au/qcg (2021).

2. Nicolosi, B. F. *et al.* Maternal factors associated with hyperglycemia in pregnancy and perinatal outcomes: A Brazilian reference center cohort study. *Diabetol. Metab. Syndr.* **12**, 1–11 (2020).

3. Feig, D. S. *et al.* Diabetes and Pregnancy. *Can. J. Diabetes* **42**, S255–S282 (2018).

4. Feng, Y. & Yang, H. X. Metformin in Pregnancy with Diabetes-Opinions from Several Latest Guidelines. *Matern. Med.* **2**, 10–11 (2020).

5. Sistema General de Seguridad Social en Salud – Colombia. *Guía de práctica clínica para el diagnóstico, tratamiento y seguimiento de la diabetes Gestacional*. (2016).

6. Damm, P. *et al. Medlemmer af arbejdsgruppen: Repraesentanter for Dansk Selskab for Obstetrik og Gynaekologi Repraesentant for Dansk Oftalmologisk Selskab*. (2009).

7. Schäfer-Graf, U. M. *et al.* Gestational Diabetes Mellitus (GDM), Diagnosis, Treatment and Follow-Up. Guideline of the DDG and DGGG (S3 Level, AWMF Registry Number 057/088, February 2018). *Geburtshilfe Frauenheilkd.* **78**, 1219–1231 (2018).

8. Mishra, S., Bhadoria, A. S., Kishore, S. & Kumar, R. Gestational diabetes mellitus 2018 guidelines: An update. *J. Fam. Med. Prim. Care* **7**, 1169 (2018).

9. Valizadeh, M. *et al.* Iranian Endocrine Society Guidelines for Screening, Diagnosis, and Management of Gestational Diabetes Mellitus. *Int. J. Endocrinol. Metab.* **19**, (2021).

10. Dainelli, L. *et al.* Screening and management of gestational diabetes in Mexico: results from a survey of multilocation, multi-health care institution practitioners. *Diabetes, Metab. Syndr. Obes. Targets Ther.* **11**, 105 (2018).

11. Nederlandse Vereniging voor obstetrie and gynaecologie. *DIABETES MELLITUS EN ZWANGERSCHAP Methodiek Evidence based Discipline Monodisciplinair*. (2010).

12. Helsedirektoratet. *Svangerskapsdiabetes Kvinner med svangerskapsdiabetes bør få*

behandling med glukosesenkende legemidler når behandlingsmål ikke nås med livsstilsendringer Praktisk. (2020).

13. Wender-Ożegowska, E. *et al.* Standards of Polish Society of Gynecologists and Obstetricians in management of women with diabetes. *Recomm. Ginekol. Pol.* **89**, 341–350 (2018).

14. Almeida, M. do C. & Ruas, J. D. e L. Consenso " Diabetes Gestacional ": Atualização 2017. *Rev. Port. Diabetes* **12**, 24–38 (2017).

15. Sazanova, A. I., Esayan, R. M., Kolegaeva, O. I. & Gardanova, Z. R. Efficacy and safety of metformin for the treatment of gestational diabetes: a new approach to the problem. *Diabetes Mellit.* **19**, 164–170 (2016).

16. Dias, S., Adam, S., Rheeder, P. & Pheiffer, C. Prevalence of and risk factors for gestational diabetes mellitus in South Africa. *SAMJ South African Med. J.* **109**, 463–467 (2019).

17. Fadl, H. *et al.* Changing diagnostic criteria for gestational diabetes in Sweden - A stepped wedge national cluster randomised controlled trial - The CDC4G study protocol. *BMC Pregnancy Childbirth* **19**, 398 (2019).

18. SEMT (The Society of Endocrinology and Metabolism of Turkey). Clinical Practice Guideline for Diagnosis, Treatment and Follow-up of Diabetes Mellitus and Its Complications, 2019. 1–268 (2019).

19. NICE (The National Institute for Health and Care Excellence). *Diabetes in pregnancy: management from preconception to the postnatal period*. https://www.nice.org.uk/guidance/ng3 (2015).

20. Tarry-Adkins, J. L., Ozanne, S. E. & Aiken, C. E. Impact of metformin treatment during pregnancy on maternal outcomes: a systematic review/meta-analysis. *Sci. Rep.* **11**, 1–13 (2021).

21. American Diabetes Association. 14. Management of diabetes in pregnancy: Standards of Medical Care in Diabetes-2019. *Diabetes Care* **42**, S165–S172 (2019).

22. Brajkovich, I., Balestrini, F. F., Camejo, M. & Palacios, A. Manual Venezolano de diabetes gestacional. *Rev. Venez. Endocrinol. y Metab.* **14**, 56–90 (2016).

Supplement 5: *References for Figure 4.2: Observations in pregnancy mouse models with metformin treatment (p.88)*

1. Zhao, Y. *et al.* Metformin administration during pregnancy attenuated the long-term maternal metabolic and cognitive impairments in a mouse model of gestational diabetes. *Aging (Albany. NY).* **12**, 14019–14036 (2020).

2. Wang, F. *et al.* Effect of Metformin on a Preeclampsia-Like Mouse Model Induced by High-Fat Diet. *Biomed Res. Int.* **2019**, 6547019 (2019).

3. Liu, Z., Yu, X., Tong, C. & Qi, H. Renal dysfunction in a mouse model of GDM is prevented by metformin through MAPKs. *Mol. Med. Rep.* **49**, 4491–4499 (2019).

4. Roland, A. V. & Moenter, S. M. Prenatal androgenization of female mice programs an increase in firing activity of gonadotropin-releasing hormone (GnRH) neurons that is reversed by metformin treatment in adulthood. *Endocrinology* **152**, 618–628 (2011).

5. Sander, V. A., Facorro, G. B., Piehl, L., Rubín De Celis, E. & Motta, A. B. Effect of DHEA and metformin on corpus luteum in mice. *Reproduction* **138**, 571–579 (2009).

6. Huang, L. *et al.* Combined intervention of swimming plus metformin ameliorates the insulin resistance and impaired lipid metabolism in murine gestational diabetes mellitus. *PLoS One* **13**, e0195609 (2018).

7. Hastie, R. *et al.* EGFR (Epidermal Growth Factor Receptor) signaling and the mitochondria regulate sFlt-1 (Soluble FMS-Like Tyrosine Kinase-1) secretion. *Hypertension* **73**, 659–670 (2019).

8. Sun, X. *et al.* Metformin attenuates susceptibility to inflammation-induced preterm birth in mice with higher endocannabinoid levels. *Biol. Reprod.* **98**, 208–217 (2018).

9. Deng, W. *et al.* P53 coordinates decidual sestrin 2/AMPK/mTORC1 signaling to govern parturition timing. *J. Clin. Invest.* **126**, 2941–2954 (2016).

10. Grace, M. R. *et al.* Effect of a High-Fat Diet and Metformin on Placental mTOR Signaling in Mice. *Am J Perinatol Rep* **9**, 138–143 (2019).

11. Albaghdadi, A. J. H. *et al.* Tacrolimus in the prevention of adverse pregnancy outcomes and diabetes-associated embryopathies in obese and diabetic mice. *J. Transl. Med.* **15**, 32 (2017).

12. Louden, E. D. *et al.* TallyHO obese female mice experience poor reproductive outcomes and abnormal blastocyst metabolism which is reversed by metformin HHS Public Access. *Reprod Fertil Dev* **27**, 31–39 (2014).

13. Eng, G. S. *et al.* AMP kinase activation increases glucose uptake, decreases apoptosis, and improves pregnancy outcome in embryos exposed to high IGF-I concentrations. *Diabetes* **56**, 2228–2234 (2007).

14. Luchetti, C. G., Mikó, E., Szekeres-Bartho, J., Paz, D. A. & Motta, A. B. Dehydroepiandrosterone and metformin modulate progesterone-induced blocking factor (PIBF), cyclooxygenase 2 (COX2) and cytokines in early pregnant mice. *J. Steroid Biochem. Mol. Biol.* **111**, 200–207 (2008).

15. Jiang, S., Teague, A. M., Tryggestad, J. B., Jensen, M. E. & Chernausek, S. D. Role of metformin in epigenetic regulation of placental mitochondrial biogenesis in maternal diabetes. *Sci. Rep.* **10**, 1–12 (2020).

16. Ratchford, A. M., Chang, A. S., Chi, M. M. Y., Sheridan, R. & Moley, K. H. Maternal diabetes adversely affects AMP-activated protein kinase activity and cellular metabolism in murine oocytes. *Am. J. Physiol. - Endocrinol. Metab.* **293**, 1198–1206 (2007).

17. Wu, Y. *et al.* Cellular stress, excessive apoptosis, and the effect of metformin in a mouse model of type 2 diabetic embryopathy. *Diabetes* **64**, 2526–2536 (2015).

18. Vora, N. L. *et al.* Targeted Multiplex Gene Expression Profiling to Measure High-Fat Diet and Metformin Effects on Fetal Gene Expression in a Mouse Model. *Reprod. Sci.* **26**, 683–689 (2019).

19. Salomäki, H. *et al.* Prenatal Metformin Exposure in a Maternal High Fat Diet Mouse Model Alters the Transcriptome and Modifies the Metabolic Responses of the Offspring. *PLoS One* **9**, e115778 (2014).

20. Nüsken, E. *et al.* Maternal high fat diet and in-utero metformin exposure significantly impact upon the fetal renal proteome of male mice. *J. Clin. Med.* **8**, 663 (2019).

21. Deng, J. *et al.* H19 lncRNA alters methylation and expression of Hnf4α in the liver of metformin-exposed fetuses. *Nat. Publ. Gr.* **8**, 3175 (2017).

22. Gregg, B. *et al.* Exposure of mouse embryonic pancreas to metformin enhances the number of

pancreatic progenitors. *Diabetologia* **57**, 2566–75 (2014).

23. Tartarin, P. *et al.* Metformin exposure affects human and mouse fetal testicular cells. *Hum. Reprod.* **27**, 3304–3314 (2012).

24. Sainio, A. *et al.* Metformin decreases hyaluronan synthesis by vascular smooth muscle cells. *J. Investig. Med.* **68**, 383–391 (2020).

25. Gregg, B. E. *et al.* Gestational exposure to metformin programs improved glucose tolerance and insulin secretion in adult male mouse offspring. *Sci. Rep.* **8**, 5745 (2018).

26. Salomäki, H. *et al.* Prenatal Metformin Exposure in Mice Programs the Metabolic Phenotype of the Offspring during a High Fat Diet at Adulthood. *PLoS One* **8**, e56594 (2013).

Supplement 6: *Full table of differentially expressed genes comparing obese untreated and obese metformin-treated placentas (padj <0.1), sorted by fold change (see text in section 5.3.4, p. 125)*

Fold change	padj	gene_name
enriched with metformin		
2.49	0.09	Cntn2
2.08	0.14	Cnn1
1.94	0.14	Scn3b
1.67	0.14	Fam171a2
1.62	0.08	Tppp
1.61	0.07	Gldc
1.36	0.14	Adamtsl4
1.36	0.14	Bgn
1.33	0.14	Tril
1.25	0.12	Ank2
1.20	0.14	Armh4
1.17	0.14	Cpt1a
1.17	0.14	St3gal2
1.16	0.12	Ddr1
1.13	0.08	Zc3h4
1.11	0.07	Tmem184b
1.11	0.14	Ptpn1
reduced with metformin		
0.83	0.14	Rufy4
0.79	0.14	Plac8
0.78	0.14	Gm32885
0.78	0.14	A530058O07Rik
0.78	0.14	Pla2g4f
0.78	0.14	Serpinb9d
0.73	0.14	Clec12b
0.68	0.14	Gm26648
0.65	0.14	Gm15419
0.63	0.09	Gm14586

0.62	0.09	Gm10790
0.62	0.07	Clec1b
0.61	0.07	Srp54c
0.60	0.06	1810014B01Rik
0.56	0.05	Gm9
0.54	0.05	Gm27786
0.53	0.05	Syn3
0.52	0.05	Gm26899
0.47	0.01	Prl2c5
0.47	0.01	Rpp38
0.42	0.01	Prl4a1

Supplement 7: *Full table of differentially expressed genes comparing male and female placentas (padj<0.05), sorted by fold change (see text in section 5.3.5, p.1265.3.4)*

gene_name	**fold change**	***padj***	**chromsome**
enriched in females			
Xist	17.61	*1.1E-72*	X
Gm8488	2.23	*4.8E-03*	autosomal
Prkg2	2.19	*0.03*	autosomal
Igha	2.11	*1.0E-03*	autosomal
Cftr	2.08	*0.01*	autosomal
Arsj	2.07	*0.02*	autosomal
Cck	2.02	*0.01*	autosomal
Camk2a	2.01	*0.03*	autosomal
Zfp618	1.99	*0.01*	autosomal
Clic3	1.98	*0.05*	autosomal
2410004P03Rik	1.95	*0.03*	autosomal
Abcc8	1.90	*0.03*	autosomal
Paqr5	1.88	*8.4E-04*	autosomal
Ccdc160	1.87	*0.02*	X
Ptprr	1.86	*0.02*	autosomal
Aldh1l1	1.83	*3.3E-03*	autosomal
P4ha3	1.81	*0.02*	autosomal
Gm5122	1.81	*0.01*	autosomal
Syt15	1.81	*0.02*	autosomal
Col6a2	1.80	*0.05*	autosomal
Gm28875	1.79	*0.04*	autosomal
Tmem26	1.76	*0.02*	autosomal
Islr	1.75	*0.04*	autosomal
Gm8493	1.72	*7.6E-04*	autosomal
AI467606	1.71	*0.03*	autosomal
Zfp456	1.70	*0.05*	autosomal
Pcsk5	1.66	*0.02*	autosomal

Hmgb3	1.65	*0.01*	X
Tenm3	1.65	*0.05*	autosomal
Edn3	1.64	*0.05*	autosomal
Gm10638	1.63	*0.05*	autosomal
Susd2	1.61	*0.03*	autosomal
Maf	1.61	*0.05*	autosomal
Fam107a	1.61	*0.05*	autosomal
Itga8	1.59	*0.01*	autosomal
Hnf1b	1.59	*0.02*	autosomal
Col1a1	1.59	*0.05*	autosomal
S100g	1.58	*0.05*	X
A930024N18Rik	1.57	*0.01*	autosomal
Prkcb	1.56	*0.03*	autosomal
Cyp4b1	1.55	*0.05*	autosomal
P2ry6	1.55	*0.02*	autosomal
Hs6st2	1.55	*0.01*	X
Tbc1d2b	1.55	*0.04*	autosomal
Igfbp4	1.53	*0.02*	autosomal
Pin4	1.52	*8.3E-05*	X
Ttn	1.52	*0.02*	autosomal
Gja5	1.51	*1.3E-03*	autosomal
Gm11346	1.50	*0.03*	autosomal
Spink2	1.50	*0.05*	autosomal
Ndrg2	1.49	*0.01*	autosomal
Ccdc88c	1.49	*0.03*	autosomal
Erbb2	1.48	*0.05*	autosomal
Anxa8	1.48	*0.03*	autosomal
Col9a2	1.46	*0.03*	autosomal
Cyp11a1	1.46	*0.03*	autosomal
Sorl1	1.45	*0.04*	autosomal
Met	1.45	*0.01*	autosomal
Jade2	1.45	*3.1E-03*	autosomal
Jaml	1.43	*0.02*	autosomal
Npdc1	1.43	*0.05*	autosomal
Taf1	1.43	*3.0E-19*	X
Sh3bp5	1.43	*0.03*	autosomal
Col7a1	1.43	*0.04*	autosomal
Capn5	1.43	*0.05*	autosomal
Cchcr1	1.43	*0.05*	autosomal
Gm20559	1.42	*0.03*	autosomal
Myo7b	1.42	*0.01*	autosomal
Tmem176a	1.42	*1.3E-03*	autosomal
Cybrd1	1.42	*5.0E-03*	autosomal
Pcolce	1.42	*0.02*	autosomal
Deptor	1.41	*0.03*	autosomal
Bace2	1.41	*0.02*	autosomal
Bcorl1	1.41	*0.02*	X

P4htm	1.40	*0.02*	autosomal
Ogt	1.40	*5.7E-12*	X
Nr1h3	1.40	*0.03*	autosomal
Qsox2	1.40	*1.7E-03*	autosomal
Notch3	1.39	*0.04*	autosomal
Mfap2	1.39	*0.05*	autosomal
Itpr3	1.39	*0.03*	autosomal
Vwf	1.38	*0.03*	autosomal
Npnt	1.38	*0.05*	autosomal
Kcnj12	1.38	*2.0E-03*	autosomal
Prlr	1.37	*1.3E-03*	autosomal
Bgn	1.37	*0.01*	X
Trarg1	1.37	*0.03*	autosomal
Sp6	1.37	*0.05*	autosomal
Akr1b8	1.37	*1.3E-03*	autosomal
Cd248	1.36	*0.04*	autosomal
Rnasel	1.36	*0.03*	autosomal
Adgra2	1.35	*0.01*	autosomal
Ap1g2	1.35	*0.01*	autosomal
Ccdc8	1.35	*0.02*	autosomal
Tbx4	1.35	*0.04*	autosomal
Tspan17	1.35	*0.03*	autosomal
Tnfsf12	1.34	*0.04*	autosomal
Bicc1	1.34	*0.02*	autosomal
Map3k6	1.34	*3.6E-05*	autosomal
Atp2a3	1.34	*0.01*	autosomal
Col5a1	1.33	*0.04*	autosomal
Gtf2i	1.33	*0.02*	autosomal
Tmem176b	1.33	*0.01*	autosomal
Wscd2	1.33	*0.02*	autosomal
Bmf	1.33	*0.03*	autosomal
Nynrin	1.33	*0.05*	autosomal
Drp2	1.32	*0.01*	X
Zbtb8a	1.32	*2.5E-04*	autosomal
Iqce	1.32	*3.3E-03*	autosomal
Samd9l	1.32	*0.01*	autosomal
Tbx2	1.32	*0.02*	autosomal
Ehd3	1.31	*0.05*	autosomal
Eif2s3x	1.31	*2.7E-08*	X
Thra	1.31	*0.02*	autosomal
Cited4	1.30	*0.03*	autosomal
Kdm5c	1.30	*2.4E-04*	X
Trim16	1.30	*0.02*	autosomal
Zbtb4	1.30	*3.7E-03*	autosomal
Ptk7	1.29	*4.5E-03*	autosomal
Ifitm2	1.29	*0.05*	autosomal
Wipi1	1.29	*0.02*	autosomal

Ephx1	1.29	*0.03*	autosomal
Pdk2	1.29	*0.05*	autosomal
Axl	1.29	*0.02*	autosomal
Robo1	1.29	*0.05*	autosomal
Prag1	1.29	*2.4E-04*	autosomal
Etv5	1.28	*0.05*	autosomal
Sft2d2	1.28	*0.03*	autosomal
Igdcc4	1.28	*0.04*	autosomal
E2f1	1.27	*0.05*	autosomal
Sfxn3	1.27	*0.03*	autosomal
Rnf165	1.27	*0.03*	autosomal
Agrn	1.27	*0.04*	autosomal
Aes	1.27	*4.4E-04*	autosomal
Vim	1.27	*0.05*	autosomal
Coro2b	1.27	*0.04*	autosomal
Dhrs3	1.27	*3.3E-03*	autosomal
Ptprg	1.27	*0.02*	autosomal
Syk	1.27	*0.03*	autosomal
Anxa9	1.26	*0.02*	autosomal
Tgfb1i1	1.26	*1.3E-03*	autosomal
Glis2	1.26	*0.05*	autosomal
Ror1	1.26	*0.03*	autosomal
Rhoj	1.26	*3.3E-03*	autosomal
Notch4	1.26	*0.03*	autosomal
Asrgl1	1.26	*0.04*	autosomal
Mical1	1.25	*0.01*	autosomal
Tmtc1	1.25	*0.03*	autosomal
Tgfbr2	1.25	*2.5E-03*	autosomal
Aldh2	1.25	*0.04*	autosomal
Fzd4	1.25	*0.02*	autosomal
Nfatc1	1.25	*0.05*	autosomal
Adcy6	1.24	*0.05*	autosomal
Cotl1	1.24	*0.05*	autosomal
Ptpmt1	1.24	*0.02*	autosomal
Tmem198b	1.24	*0.05*	autosomal
Armc5	1.24	*0.01*	autosomal
Lix1l	1.24	*0.04*	autosomal
Ptprb	1.24	*0.04*	autosomal
Reck	1.23	*0.03*	autosomal
Chst2	1.23	*0.03*	autosomal
Dtx4	1.23	*0.05*	autosomal
Tob1	1.23	*0.05*	autosomal
2510009E07Rik	1.22	*0.05*	autosomal
Myo7a	1.22	*1.3E-03*	autosomal
Hpcal1	1.22	*0.03*	autosomal
Peg13	1.22	*0.03*	autosomal
Sox13	1.21	*4.3E-03*	autosomal

Abr	1.21	*0.05*	autosomal
Svil	1.20	*0.05*	autosomal
5730409E04Rik	1.20	*0.05*	autosomal
Nacc2	1.20	*0.05*	autosomal
Cd81	1.20	*5.9E-04*	autosomal
Tle4	1.20	*0.05*	autosomal
Corin	1.20	*0.05*	autosomal
Adck5	1.19	*0.01*	autosomal
Nkap	1.19	*3.3E-03*	X
Samhd1	1.18	*0.05*	autosomal
Glb1	1.18	*0.01*	autosomal
Oga	1.18	*0.04*	autosomal
Ermp1	1.18	*0.04*	autosomal
Phactr2	1.18	*0.05*	autosomal
Pnpla2	1.17	*0.01*	autosomal
Zbtb7a	1.17	*0.02*	autosomal
Ttyh3	1.17	*0.02*	autosomal
Slc43a3	1.17	*0.02*	autosomal
Fbxw5	1.17	*1.1E-03*	autosomal
Fadd	1.17	*0.04*	autosomal
Ttc30b	1.17	*0.05*	autosomal
Tmc6	1.16	*0.05*	autosomal
Fitm2	1.16	*0.05*	autosomal
Zfp398	1.16	*0.04*	autosomal
Wdtc1	1.16	*0.05*	autosomal
Arhgef10	1.16	*0.01*	autosomal
Rin2	1.15	*0.01*	autosomal
Tnks1bp1	1.15	*2.3E-03*	autosomal
Snx12	1.15	*0.01*	X
Fam214a	1.15	*0.01*	autosomal
Pofut1	1.14	*0.04*	autosomal
Tmem63a	1.14	*0.01*	autosomal
Rnf169	1.14	*0.04*	autosomal
Camta2	1.13	*0.05*	autosomal
Habp4	1.13	*0.03*	autosomal
Sgpl1	1.13	*0.02*	autosomal
Prxl2c	1.13	*0.02*	autosomal
Cnnm3	1.12	*0.04*	autosomal
Ucp2	1.12	*0.05*	autosomal
Kdm6a	1.12	*0.01*	X
Rhog	1.11	*0.02*	autosomal
Ino80d	1.11	*0.05*	autosomal
Ctdsp1	1.11	*0.02*	autosomal
Fam117b	1.10	*0.03*	autosomal
Pef1	1.10	*0.04*	autosomal
Rnf187	1.10	*0.03*	autosomal
Map2k3	1.10	*4.8E-03*	autosomal

Pitpna	1.09	*0.01*	autosomal
Ssbp3	1.09	*0.02*	autosomal
Tmem184b	1.09	*0.04*	autosomal
Crtap	1.09	*0.05*	autosomal
Maf1	1.08	*0.03*	autosomal
Dazap2	1.07	*1.3E-03*	autosomal
Mxd4	1.07	*0.02*	autosomal
reduced in females			
Ptp4a2	0.94	*0.05*	autosomal
Nipa2	0.94	*0.04*	autosomal
Eif1	0.94	*0.01*	autosomal
Ergic2	0.93	*0.03*	autosomal
Golga7	0.93	*0.01*	autosomal
Usp8	0.93	*0.03*	autosomal
Tpm4	0.93	*0.03*	autosomal
Golga5	0.93	*0.02*	autosomal
Eef1g	0.93	*0.05*	autosomal
Gskip	0.92	*0.05*	autosomal
Arcn1	0.92	*0.03*	autosomal
Amz2	0.92	*0.03*	autosomal
Ist1	0.92	*0.03*	autosomal
Copb1	0.92	*0.05*	autosomal
Trap1a	0.92	*0.04*	X
Actr2	0.92	*4.0E-03*	autosomal
Nap1l4	0.92	*0.01*	autosomal
Eif4a2	0.92	*0.05*	autosomal
Prpf18	0.92	*0.01*	autosomal
Zc3h15	0.92	*1.3E-03*	autosomal
Gmps	0.92	*0.04*	autosomal
Gtf3c3	0.92	*0.05*	autosomal
Eif3a	0.92	*3.1E-03*	autosomal
Fyttd1	0.92	*0.05*	autosomal
Gtf2e2	0.91	*0.03*	autosomal
Tapt1	0.91	*0.05*	autosomal
Lrrc59	0.91	*0.05*	autosomal
Gpat4	0.91	*0.04*	autosomal
Utp6	0.91	*0.04*	autosomal
Usp32	0.91	*0.05*	autosomal
Trnt1	0.91	*0.05*	autosomal
Rars	0.91	*0.04*	autosomal
Gtpbp4	0.91	*0.05*	autosomal
Nsun2	0.91	*0.02*	autosomal
Ran	0.91	*0.01*	autosomal
Fam49b	0.91	*4.8E-03*	autosomal
Ppp1r8	0.91	*0.05*	autosomal
Cyb561a3	0.91	*0.03*	autosomal
Fermt2	0.91	*0.05*	autosomal

Pdhb	0.91	*0.04*	autosomal
Gpr180	0.91	*0.05*	autosomal
Eif3l	0.90	*0.02*	autosomal
Tomm70a	0.90	*0.05*	autosomal
Sars	0.90	*0.02*	autosomal
Yme1l1	0.90	*4.3E-03*	autosomal
Fam129a	0.90	*0.02*	autosomal
Atad1	0.90	*0.05*	autosomal
Ddx50	0.90	*0.02*	autosomal
Trappc4	0.90	*0.02*	autosomal
Zranb2	0.90	*0.01*	autosomal
Krt19	0.90	*0.04*	autosomal
Prmt2	0.90	*0.02*	autosomal
Cdk4	0.90	*0.01*	autosomal
Sp3	0.90	*0.01*	autosomal
Braf	0.89	*0.04*	autosomal
Basp1	0.89	*0.01*	autosomal
Cct2	0.89	*2.6E-03*	autosomal
Ncbp1	0.89	*0.05*	autosomal
Crebzf	0.89	*0.03*	autosomal
Entpd1	0.89	*0.02*	autosomal
Vezt	0.89	*0.04*	autosomal
Usp15	0.89	*0.02*	autosomal
Wdr47	0.89	*0.04*	autosomal
Fam171a1	0.89	*0.03*	autosomal
Cct4	0.89	*1.3E-03*	autosomal
Gnai3	0.89	*0.02*	autosomal
Tmem209	0.89	*0.01*	autosomal
Caprin1	0.89	*1.4E-05*	autosomal
Eef1b2	0.89	*0.02*	autosomal
Blzf1	0.89	*0.01*	autosomal
Erlin1	0.89	*0.01*	autosomal
Usp37	0.89	*0.02*	autosomal
Tgs1	0.89	*0.01*	autosomal
Nup107	0.88	*0.01*	autosomal
Gramd4	0.88	*0.01*	autosomal
Zdhhc13	0.88	*0.01*	autosomal
Prkci	0.88	*0.02*	autosomal
Ptp4a3	0.88	*0.05*	autosomal
Fxr1	0.88	*0.03*	autosomal
Serpinb6b	0.88	*0.03*	autosomal
Hspa9	0.88	*2.3E-04*	autosomal
March5	0.88	*0.02*	autosomal
Pkp2	0.88	*0.01*	autosomal
Crlf2	0.88	*0.03*	autosomal
Phf10	0.88	*0.01*	autosomal
Ttll12	0.88	*4.0E-03*	autosomal

2810013P06Rik	0.88	*0.05*	autosomal
Mrpl35	0.88	*0.04*	autosomal
Fkbp9	0.88	*3.2E-03*	autosomal
Zfyve16	0.87	*1.0E-03*	autosomal
Pik3cb	0.87	*0.03*	autosomal
Slc35a1	0.87	*4.8E-03*	autosomal
Krt8	0.87	*0.02*	autosomal
Asb3	0.87	*0.04*	autosomal
Ncbp2	0.87	*0.05*	autosomal
Eif4e3	0.87	*0.05*	autosomal
Adcy7	0.87	*0.01*	autosomal
Tex10	0.87	*0.04*	autosomal
Tnfaip8	0.87	*0.03*	autosomal
Plekha8	0.87	*0.02*	autosomal
Psip1	0.87	*0.03*	autosomal
Dsc2	0.87	*0.01*	autosomal
Krtcap3	0.87	*0.05*	autosomal
Pcnx4	0.86	*0.03*	autosomal
Gnl3	0.86	*2.2E-04*	autosomal
Nt5e	0.86	*0.03*	autosomal
Arl5b	0.86	*0.04*	autosomal
Abhd6	0.86	*0.01*	autosomal
Ctnnbip1	0.86	*0.01*	autosomal
Stx2	0.86	*0.03*	autosomal
Jdp2	0.86	*0.01*	autosomal
Mettl16	0.86	*0.05*	autosomal
Wsb1	0.86	*9.3E-04*	autosomal
Rap2a	0.86	*0.02*	autosomal
Tnfaip8l1	0.86	*0.05*	autosomal
1700025G04Rik	0.86	*0.01*	autosomal
Cers5	0.86	*0.05*	autosomal
Cse1l	0.86	*0.01*	autosomal
Cep170	0.86	*0.03*	autosomal
Myo1b	0.86	*0.02*	autosomal
Tmem39a	0.86	*2.6E-03*	autosomal
Hand1	0.86	*0.05*	autosomal
Ddit3	0.86	*0.04*	autosomal
Uros	0.86	*0.02*	autosomal
Stk31	0.86	*0.01*	autosomal
Sfmbt2	0.85	*2.6E-03*	autosomal
Zfp868	0.85	*0.02*	autosomal
Upp1	0.85	*0.04*	autosomal
Vstm4	0.85	*4.0E-03*	autosomal
Mpzl3	0.85	*0.03*	autosomal
Hrct1	0.85	*0.04*	autosomal
Sh3kbp1	0.85	*0.03*	X
Eva1a	0.85	*0.04*	autosomal

Il2rg	0.85	*0.02*	X
Ctsj	0.85	*0.02*	autosomal
Jmjd6	0.85	*0.05*	autosomal
Serpinb9	0.84	*0.02*	autosomal
Mfsd2a	0.84	*0.05*	autosomal
Map9	0.84	*0.02*	autosomal
Gpat3	0.84	*1.1E-03*	autosomal
Naa16	0.84	*0.02*	autosomal
Man1a	0.84	*0.05*	autosomal
1700066M21Rik	0.84	*0.05*	autosomal
Rdh12	0.83	*0.02*	autosomal
Pde10a	0.83	*4.0E-03*	autosomal
Stk39	0.83	*4.7E-04*	autosomal
2610021A01Rik	0.83	*0.03*	autosomal
Rpp40	0.83	*0.04*	autosomal
Rpp38	0.83	*0.02*	autosomal
Coq3	0.83	*1.3E-03*	autosomal
Cdc42se2	0.83	*3.6E-05*	autosomal
Zmat1	0.83	*0.03*	X
Rdh13	0.82	*0.01*	autosomal
Syce2	0.82	*1.0E-03*	autosomal
Nostrin	0.82	*0.01*	autosomal
Tmem41b	0.82	*9.4E-04*	autosomal
Trpv2	0.82	*3.3E-03*	autosomal
Desi2	0.82	*0.04*	autosomal
Cd24a	0.82	*0.04*	autosomal
Fbxo27	0.81	*7.9E-04*	autosomal
Slco3a1	0.81	*3.3E-03*	autosomal
Sct	0.81	*2.6E-09*	autosomal
Nmt2	0.81	*3.7E-05*	autosomal
Ednrb	0.81	*0.01*	autosomal
Mypop	0.80	*0.03*	autosomal
Pitrm1	0.80	*0.01*	autosomal
Fndc4	0.80	*0.05*	autosomal
Tfpi	0.80	*0.02*	autosomal
3632454L22Rik	0.80	*0.03*	autosomal
Prom1	0.80	*0.05*	autosomal
Gm10557	0.79	*0.03*	autosomal
Slc19a3	0.79	*0.03*	autosomal
Adgrg3	0.79	*0.01*	autosomal
Fry	0.78	*0.05*	autosomal
Serpinb9c	0.78	*4.9E-03*	autosomal
Mllt11	0.78	*0.01*	autosomal
Star	0.78	*0.01*	autosomal
Serpinb9g	0.78	*0.03*	autosomal
Hrk	0.78	*0.04*	autosomal
Ghrh	0.78	*0.04*	autosomal

Serpinb9f	0.77	*4.1E-03*	autosomal
Rgs16	0.77	*0.03*	autosomal
Serpinb9e	0.77	*3.7E-04*	autosomal
Gramd2	0.76	*0.01*	autosomal
Snhg14	0.76	*0.04*	autosomal
Prl2a1	0.76	*4.3E-03*	autosomal
Ccr1l1	0.76	*0.05*	autosomal
Gm26542	0.75	*0.04*	autosomal
Rasal1	0.75	*3.9E-04*	autosomal
Nrg4	0.75	*0.05*	autosomal
Kiss1r	0.75	*0.02*	autosomal
Gm12715	0.75	*0.04*	autosomal
Snrpn	0.74	*4.1E-04*	autosomal
Plac8	0.74	*0.03*	autosomal
Serpinb9d	0.74	*1.3E-03*	autosomal
Hunk	0.74	*7.5E-06*	autosomal
Hmox1	0.74	*0.04*	autosomal
Prl8a1	0.73	*0.05*	autosomal
Ccl27a	0.73	*0.03*	autosomal
1500009L16Rik	0.73	*0.03*	autosomal
Tmem267	0.73	*0.03*	autosomal
Scrn1	0.72	*1.3E-03*	autosomal
Prl2c5	0.72	*2.8E-08*	autosomal
2810032G03Rik	0.71	*0.03*	autosomal
Prl7d1	0.70	*3.1E-09*	autosomal
Scn9a	0.70	*0.02*	autosomal
Spn	0.70	*7.5E-04*	autosomal
Gm10433	0.70	*0.05*	autosomal
Cyp39a1	0.69	*2.4E-03*	autosomal
Syt13	0.69	*3.3E-03*	autosomal
Unc5a	0.69	*8.9E-04*	autosomal
Prl3c1	0.68	*0.01*	autosomal
Gm2792	0.68	*0.02*	autosomal
Dctd	0.66	*0.02*	autosomal
Brsk1	0.66	*0.04*	autosomal
Efcab8	0.65	*0.05*	autosomal
Tvp23a	0.64	*2.1E-04*	autosomal
Prl2c2	0.63	*5.7E-08*	autosomal
Clec12b	0.63	*0.02*	autosomal
Il1a	0.63	*3.2E-03*	autosomal
Myo16	0.63	*0.02*	autosomal
Prl2c3	0.62	*7.5E-06*	autosomal
Prl4a1	0.62	*1.6E-04*	autosomal
Gm38393	0.62	*2.0E-03*	autosomal
Gm20541	0.61	*0.03*	autosomal
Zcchc18	0.57	*0.02*	X
Pcdhgc4	0.54	*0.05*	autosomal

Prl7a1	0.54	*1.2E-05*	autosomal
Gm11427	0.51	*0.03*	autosomal
Hoxd13	0.50	*3.1E-03*	autosomal
Otoa	0.50	*0.01*	autosomal
Cxcl1	0.49	*4.3E-03*	autosomal
Tmem114	0.44	*0.01*	autosomal
Sohlh2	0.39	*5.1E-04*	autosomal

Supplement 8: *All results of the GO-term analysis comparing male and female placentas, fold enrichment and FDR shown (see text in section 5.3.5, p. 126)*

enriched in the female placenta		
GO biological process complete	**fold enrichment**	**FDR**
cardiac septum morphogenesis (GO:0060411)	7.78	3.4E-02
regulation of Notch signaling pathway (GO:0008593)	7.07	4.7E-02
Notch signaling pathway (GO:0007219)	6.91	1.1E-02
cardiac septum development (GO:0003279)	6.75	1.1E-02
cell-cell signaling by wnt (GO:0198738)	4.29	3.3E-02
Wnt signaling pathway (GO:0016055)	4.29	3.3E-02
regulation of canonical Wnt signaling pathway (GO:0060828)	4.2	3.6E-02
regulation of leukocyte differentiation (GO:1902105)	3.95	1.8E-02
angiogenesis (GO:0001525)	3.89	2.1E-02
cell surface receptor signaling pathway involved in cell-cell signaling (GO:1905114)	3.87	3.5E-02
blood vessel development (GO:0001568)	3.86	3.7E-04
regulation of cellular response to growth factor stimulus (GO:0090287)	3.83	3.6E-02
vasculature development (GO:0001944)	3.83	3.1E-04
blood vessel morphogenesis (GO:0048514)	3.81	3.7E-03
regulation of hemopoiesis (GO:1903706)	3.45	3.1E-02
positive regulation of kinase activity (GO:0033674)	3.36	2.4E-02
circulatory system development (GO:0072359)	3.14	1.9E-04
tube morphogenesis (GO:0035239)	3.12	2.0E-03
anatomical structure formation involved in morphogenesis (GO:0048646)	3.05	3.0E-04
positive regulation of transferase activity (GO:0051347)	3.01	3.5E-02
cell morphogenesis involved in differentiation (GO:0000904)	3.01	1.8E-02
tube development (GO:0035295)	2.94	5.4E-04
heart development (GO:0007507)	2.91	3.5E-02
regulation of kinase activity (GO:0043549)	2.81	1.6E-02
regulation of cell migration (GO:0030334)	2.71	3.8E-03

regulation of cell motility (GO:2000145)	2.66	3.5E-03
regulation of cellular component movement (GO:0051270)	2.65	2.0E-03
regulation of locomotion (GO:0040012)	2.64	2.9E-03
anatomical structure morphogenesis (GO:0009653)	2.46	7.8E-06
regulation of cell differentiation (GO:0045595)	2.44	3.8E-04
negative regulation of transcription by RNA polymerase II (GO:0000122)	2.41	3.9E-02
animal organ morphogenesis (GO:0009887)	2.4	2.5E-02
positive regulation of catalytic activity (GO:0043085)	2.36	2.8E-02
regulation of multicellular organismal development (GO:2000026)	2.32	3.5E-03
positive regulation of molecular function (GO:0044093)	2.29	7.2E-03
regulation of phosphorylation (GO:0042325)	2.2	3.2E-02
regulation of phosphate metabolic process (GO:0019220)	2.2	1.5E-02
regulation of phosphorus metabolic process (GO:0051174)	2.2	1.5E-02
regulation of multicellular organismal process (GO:0051239)	2.18	3.4E-05
positive regulation of signal transduction (GO:0009967)	2.18	1.1E-02
positive regulation of cell communication (GO:0010647)	2.16	6.4E-03
regulation of developmental process (GO:0050793)	2.14	1.4E-04
tissue development (GO:0009888)	2.1	1.3E-02
positive regulation of signaling (GO:0023056)	2.09	1.1E-02
cell surface receptor signaling pathway (GO:0007166)	2.03	9.7E-03
positive regulation of nucleic acid-templated transcription (GO:1903508)	2.03	3.9E-02
positive regulation of transcription, DNA-templated (GO:0045893)	2.03	3.9E-02
positive regulation of macromolecule biosynthetic process (GO:0010557)	1.99	2.6E-02
positive regulation of RNA metabolic process (GO:0051254)	1.98	3.9E-02
regulation of localization (GO:0032879)	1.96	7.6E-04
regulation of catalytic activity (GO:0050790)	1.95	3.9E-02
regulation of signaling (GO:0023051)	1.93	3.5E-04
positive regulation of cellular biosynthetic process (GO:0031328)	1.93	3.6E-02

positive regulation of nucleobase-containing compound metabolic process (GO:0045935)	1.92	4.3E-02
nervous system development (GO:0007399)	1.91	2.1E-02
regulation of cell communication (GO:0010646)	1.9	4.2E-04
regulation of signal transduction (GO:0009966)	1.89	2.7E-03
system development (GO:0048731)	1.89	3.8E-05
animal organ development (GO:0048513)	1.89	7.8E-04
cell differentiation (GO:0030154)	1.86	3.8E-04
regulation of molecular function (GO:0065009)	1.85	1.4E-02
cellular developmental process (GO:0048869)	1.83	5.1E-04
multicellular organism development (GO:0007275)	1.78	7.9E-05
regulation of protein metabolic process (GO:0051246)	1.77	3.7E-02
positive regulation of nitrogen compound metabolic process (GO:0051173)	1.73	3.2E-02
regulation of transcription, DNA-templated (GO:0006355)	1.72	1.5E-02
regulation of nucleic acid-templated transcription (GO:1903506)	1.72	1.5E-02
regulation of RNA biosynthetic process (GO:2001141)	1.72	1.5E-02
regulation of primary metabolic process (GO:0080090)	1.71	5.1E-05
negative regulation of cellular process (GO:0048523)	1.7	3.5E-04
regulation of response to stimulus (GO:0048583)	1.7	3.9E-03
negative regulation of biological process (GO:0048519)	1.7	1.1E-04
regulation of nitrogen compound metabolic process (GO:0051171)	1.68	1.6E-04
regulation of cellular macromolecule biosynthetic process (GO:2000112)	1.67	1.3E-02
regulation of nucleobase-containing compound metabolic process (GO:0019219)	1.67	1.1E-02
regulation of RNA metabolic process (GO:0051252)	1.67	1.8E-02
anatomical structure development (GO:0048856)	1.66	3.6E-04
positive regulation of cellular metabolic process (GO:0031325)	1.66	4.2E-02
regulation of cellular metabolic process (GO:0031323)	1.66	1.1E-04
regulation of biological quality (GO:0065008)	1.66	1.2E-02
regulation of cellular biosynthetic process (GO:0031326)	1.66	1.0E-02
regulation of macromolecule biosynthetic process (GO:0010556)	1.65	1.4E-02
regulation of biosynthetic process (GO:0009889)	1.65	1.1E-02

positive regulation of metabolic process (GO:0009893)	1.62	3.0E-02
developmental process (GO:0032502)	1.62	4.0E-04
regulation of metabolic process (GO:0019222)	1.62	6.6E-05
regulation of macromolecule metabolic process (GO:0060255)	1.56	1.2E-03
localization (GO:0051179)	1.56	9.3E-03
positive regulation of cellular process (GO:0048522)	1.53	4.3E-03
regulation of gene expression (GO:0010468)	1.53	3.5E-02
positive regulation of biological process (GO:0048518)	1.5	3.8E-03
regulation of cellular process (GO:0050794)	1.28	6.4E-03
regulation of biological process (GO:0050789)	1.28	3.6E-03
biological regulation (GO:0065007)	1.25	8.8E-03
cellular process (GO:0009987)	1.19	8.6E-03
sensory perception of chemical stimulus (GO:0007606)	0.08	3.6E-02
enriched in the male placenta		
protection from natural killer cell mediated cytotoxicity (GO:0042270)	55.02	3.7E-05
positive regulation of lactation (GO:1903489)	33.62	8.5E-07
regulation of lactation (GO:1903487)	32.42	5.5E-07
negative regulation of natural killer cell mediated cytotoxicity (GO:0045953)	29.42	4.5E-05
negative regulation of natural killer cell mediated immunity (GO:0002716)	28.24	4.9E-05
glomerular epithelial cell differentiation (GO:0072311)	23.73	1.8E-02
glomerular visceral epithelial cell differentiation (GO:0072112)	23.73	1.8E-02
renal filtration cell differentiation (GO:0061318)	23.73	1.7E-02
negative regulation of leukocyte mediated cytotoxicity (GO:0001911)	23.53	1.3E-04
glomerular epithelium development (GO:0072010)	21.23	2.2E-02
negative regulation of cell killing (GO:0031342)	20.17	2.1E-04
positive regulation of receptor signaling pathway via STAT (GO:1904894)	16.53	9.7E-06
positive regulation of receptor signaling pathway via JAK-STAT (GO:0046427)	16.5	3.9E-05
positive regulation of pri-miRNA transcription by RNA polymerase II (GO:1902895)	13.16	1.3E-04
negative regulation of lymphocyte mediated immunity (GO:0002707)	13.01	4.2E-04
regulation of natural killer cell mediated cytotoxicity (GO:0042269)	12.84	1.6E-03

regulation of natural killer cell mediated immunity (GO:0002715)	12.17	2.0E-03
negative regulation of leukocyte mediated immunity (GO:0002704)	12.1	2.0E-04
negative regulation of endothelial cell proliferation (GO:0001937)	11.69	6.7E-04
negative regulation of innate immune response (GO:0045824)	11.21	3.1E-04
regulation of pri-miRNA transcription by RNA polymerase II (GO:1902893)	10.94	3.2E-04
regulation of receptor signaling pathway via STAT (GO:1904892)	10.29	1.8E-04
regulation of receptor signaling pathway via JAK-STAT (GO:0046425)	10.09	5.1E-04
negative regulation of response to biotic stimulus (GO:0002832)	7.96	2.0E-03
female pregnancy (GO:0007565)	7.65	3.9E-04
regulation of leukocyte mediated cytotoxicity (GO:0001910)	7.56	2.8E-03
negative regulation of immune effector process (GO:0002698)	7.04	4.5E-03
mammary gland development (GO:0030879)	6.68	2.5E-03
regulation of cell killing (GO:0031341)	6.48	7.7E-03
multi-multicellular organism process (GO:0044706)	6.3	1.5E-03
negative regulation of defense response (GO:0031348)	5.6	7.8E-04
regulation of endothelial cell proliferation (GO:0001936)	5.5	1.9E-02
negative regulation of immune response (GO:0050777)	5.41	4.8E-03
response to nutrient levels (GO:0031667)	4.69	4.9E-04
regulation of body fluid levels (GO:0050878)	4.66	5.1E-04
regulation of innate immune response (GO:0045088)	4.65	2.7E-02
regulation of lymphocyte mediated immunity (GO:0002706)	4.61	2.8E-02
response to extracellular stimulus (GO:0009991)	4.28	1.2E-03
regulation of leukocyte mediated immunity (GO:0002703)	4.16	1.7E-02
regulation of response to biotic stimulus (GO:0002831)	3.9	1.8E-02
negative regulation of response to external stimulus (GO:0032102)	3.57	1.9E-02
gland development (GO:0048732)	3.49	1.6E-02
positive regulation of secretion (GO:0051047)	3.41	2.8E-02
regulation of defense response (GO:0031347)	2.88	3.6E-02

gene expression (GO:0010467)	1.96	1.9E-02
regulation of developmental process (GO:0050793)	1.85	1.3E-02
regulation of biological quality (GO:0065008)	1.69	5.0E-03
negative regulation of cellular process (GO:0048523)	1.66	8.0E-04
negative regulation of biological process (GO:0048519)	1.65	3.5E-04
positive regulation of metabolic process (GO:0009893)	1.63	2.7E-02
regulation of cellular metabolic process (GO:0031323)	1.47	2.0E-02
regulation of primary metabolic process (GO:0080090)	1.47	3.5E-02
regulation of metabolic process (GO:0019222)	1.47	8.6E-03

Supplement 9: *Table of all 175 miRNAs, fold enrichment, p value and padj shown, miRNAs are sorted by fold enrichment (see text in section 6.3.5, p.154)*

miRNA	fold change	logCPM	p value	padj
fold change below 1				
mmu-miR-483-5p	0.38	14.09	0.01	0.29
mmu-miR-195a-5p	0.44	7.56	0.08	0.40
mmu-miR-29b-3p	0.50	9.08	0.15	0.52
mmu-miR-101a-3p	0.51	8.94	0.02	0.29
mmu-miR-122-5p	0.52	9.53	0.17	0.55
mmu-miR-451a	0.52	7.74	0.03	0.31
mmu-miR-1839-5p	0.57	7.55	0.06	0.32
mmu-miR-29c-3p	0.61	8.73	0.04	0.31
mmu-miR-877-5p	0.61	7.61	0.13	0.50
mmu-miR-191-5p	0.62	11.53	0.07	0.34
mmu-miR-141-3p	0.63	11.50	0.05	0.31
mmu-miR-140-3p	0.65	8.17	0.16	0.55
mmu-miR-125a-3p	0.66	7.36	0.14	0.50
mmu-miR-450b-5p	0.67	8.51	0.12	0.49
mmu-miR-148a-3p	0.68	14.13	0.04	0.31
mmu-miR-342-3p	0.69	10.77	0.05	0.31
mmu-miR-106b-3p	0.69	8.37	0.22	0.61
mmu-miR-322-5p	0.71	14.25	0.11	0.49
mmu-miR-147-3p	0.71	7.40	0.24	0.64
mmu-miR-542-3p	0.71	8.69	0.22	0.61
mmu-miR-872-5p	0.73	8.96	0.14	0.51
mmu-miR-107-3p	0.73	7.47	0.37	0.75
mmu-miR-5126	0.73	9.13	0.30	0.69
mmu-miR-486a-5p	0.73	12.28	0.05	0.31
mmu-miR-486b-5p	0.74	12.28	0.05	0.31

mmu-miR-296-3p	0.74	10.89	0.15	0.52
mmu-miR-30e-5p	0.76	8.34	0.33	0.73
mmu-miR-22-3p	0.76	11.03	0.22	0.61
mmu-miR-671-5p	0.77	8.14	0.25	0.64
mmu-miR-326-3p	0.77	8.13	0.31	0.70
mmu-miR-27b-3p	0.79	10.23	0.11	0.49
mmu-miR-199a-5p	0.79	8.62	0.31	0.70
mmu-miR-503-5p	0.80	11.49	0.21	0.61
mmu-miR-16-5p	0.81	14.78	0.28	0.68
mmu-miR-23a-3p	0.81	11.78	0.11	0.49
mmu-miR-29a-3p	0.81	12.13	0.34	0.73
mmu-miR-101b-3p	0.81	9.32	0.35	0.74
mmu-miR-425-5p	0.81	10.55	0.19	0.59
mmu-miR-24-3p	0.81	11.81	0.36	0.75
mmu-miR-99a-5p	0.82	7.68	0.42	0.75
mmu-miR-186-5p	0.82	9.01	0.44	0.78
mmu-miR-224-5p	0.83	9.82	0.26	0.65
mmu-miR-196b-5p	0.83	13.46	0.24	0.64
mmu-miR-292a-5p	0.83	13.11	0.50	0.79
mmu-miR-151-3p	0.83	11.11	0.34	0.74
mmu-miR-542-5p	0.84	11.93	0.20	0.61
mmu-miR-503-3p	0.84	12.51	0.37	0.75
mmu-miR-423-5p	0.85	12.85	0.22	0.61
mmu-miR-295-3p	0.85	9.18	0.50	0.79
mmu-miR-126a-3p	0.86	12.03	0.21	0.61
mmu-miR-484	0.86	8.70	0.51	0.79
mmu-miR-181b-5p	0.86	8.00	0.61	0.80
mmu-miR-143-3p	0.86	12.16	0.27	0.65
mmu-miR-25-3p	0.86	10.67	0.41	0.75
mmu-miR-205-5p	0.86	9.00	0.53	0.79
mmu-miR-6538	0.86	8.62	0.60	0.80
mmu-miR-128-3p	0.87	7.91	0.63	0.80
mmu-miR-182-5p	0.87	13.09	0.41	0.75
mmu-miR-20a-5p	0.87	7.49	0.61	0.80
mmu-miR-185-5p	0.87	7.87	0.62	0.80
mmu-miR-203-3p	0.88	9.83	0.58	0.80
mmu-miR-10b-5p	0.88	11.62	0.43	0.77
mmu-miR-450b-3p	0.88	8.36	0.59	0.80
mmu-miR-361-3p	0.88	7.74	0.62	0.80
mmu-miR-148b-3p	0.89	9.31	0.63	0.80
mmu-miR-92a-3p	0.89	13.42	0.55	0.79
mmu-miR-320-3p	0.89	12.09	0.42	0.75
mmu-miR-26a-5p	0.89	13.27	0.45	0.78
mmu-miR-99b-3p	0.89	8.00	0.74	0.85
mmu-miR-152-3p	0.89	11.73	0.55	0.79
mmu-miR-21a-5p	0.90	13.04	0.48	0.79
mmu-miR-199b-3p	0.90	11.99	0.39	0.75

mmu-miR-199a-3p	0.90	12.98	0.38	0.75
mmu-miR-378a-3p	0.90	9.44	0.59	0.80
mmu-miR-351-3p	0.90	9.99	0.65	0.81
mmu-miR-381-3p	0.90	7.42	0.72	0.84
mmu-miR-187-3p	0.90	8.28	0.65	0.81
mmu-miR-328-3p	0.91	11.92	0.61	0.80
mmu-miR-365-2-5p	0.91	9.46	0.64	0.80
mmu-miR-183-5p	0.91	14.73	0.48	0.79
mmu-miR-669c-5p	0.91	15.09	0.42	0.75
mmu-miR-23b-3p	0.92	9.25	0.71	0.84
mmu-let-7c-5p	0.92	17.25	0.53	0.79
mmu-miR-96-5p	0.92	9.97	0.67	0.81
mmu-miR-99b-5p	0.93	12.17	0.54	0.79
mmu-miR-126a-5p	0.94	8.46	0.78	0.87
mmu-let-7d-3p	0.95	9.48	0.81	0.89
mmu-miR-30d-5p	0.95	13.43	0.74	0.85
mmu-miR-760-3p	0.95	9.41	0.77	0.87
mmu-miR-501-3p	0.95	10.15	0.82	0.89
mmu-miR-2137	0.96	8.49	0.86	0.91
mmu-miR-196a-5p	0.96	10.11	0.82	0.89
mmu-miR-294-3p	0.97	8.48	0.89	0.91
mmu-let-7b-5p	0.98	17.13	0.87	0.91
mmu-miR-744-5p	0.99	10.37	0.95	0.97
mmu-miR-361-5p	0.99	9.17	0.97	0.98
fold change above 1				
mmu-miR-93-5p	1.00	10.05	1.00	1.00
mmu-miR-100-5p	1.00	7.67	0.99	1.00
mmu-miR-200c-3p	1.02	13.70	0.88	0.91
mmu-miR-434-3p	1.03	11.51	0.86	0.91
mmu-miR-30a-5p	1.03	10.11	0.84	0.89
mmu-miR-218-5p	1.04	7.80	0.90	0.92
mmu-miR-3099-3p	1.04	11.26	0.77	0.87
mmu-miR-184-3p	1.04	8.06	0.83	0.89
mmu-miR-339-5p	1.05	6.58	0.88	0.91
mmu-miR-298-5p	1.05	11.84	0.74	0.85
mmu-miR-324-5p	1.05	8.08	0.82	0.89
mmu-let-7i-5p	1.07	16.42	0.56	0.79
mmu-miR-369-5p	1.07	8.25	0.78	0.87
mmu-miR-125b-5p	1.07	13.60	0.66	0.81
mmu-let-7d-5p	1.07	12.40	0.60	0.80
mmu-miR-10a-5p	1.08	10.60	0.63	0.80
mmu-miR-1198-5p	1.08	8.10	0.72	0.84
mmu-miR-193a-5p	1.10	9.63	0.67	0.81
mmu-miR-26b-5p	1.10	12.19	0.52	0.79
mmu-miR-146a-5p	1.10	9.72	0.65	0.81
mmu-miR-6240	1.11	7.59	0.79	0.87

mmu-miR-345-3p	1.12	8.87	0.63	0.80
mmu-miR-103-3p	1.12	10.87	0.58	0.80
mmu-let-7g-5p	1.13	10.60	0.38	0.75
mmu-miR-574-3p	1.13	7.58	0.69	0.82
mmu-miR-155-5p	1.15	9.83	0.39	0.75
mmu-miR-28a-3p	1.16	8.83	0.47	0.79
mmu-miR-379-5p	1.17	12.06	0.67	0.81
mmu-miR-351-5p	1.18	14.18	0.27	0.65
mmu-miR-770-3p	1.18	8.65	0.52	0.79
mmu-miR-210-3p	1.18	8.73	0.48	0.79
mmu-miR-673-5p	1.19	8.63	0.52	0.79
mmu-miR-296-5p	1.19	9.21	0.46	0.79
mmu-miR-676-3p	1.19	8.61	0.49	0.79
mmu-miR-139-3p	1.21	7.16	0.50	0.79
mmu-miR-411-5p	1.21	8.92	0.55	0.79
mmu-miR-433-3p	1.22	9.10	0.39	0.75
mmu-miR-423-3p	1.23	8.37	0.41	0.75
mmu-miR-532-5p	1.23	8.43	0.54	0.79
mmu-miR-146b-5p	1.24	8.23	0.38	0.75
mmu-miR-127-5p	1.27	7.15	0.47	0.79
mmu-let-7a-5p	1.28	14.87	0.03	0.29
mmu-miR-181a-5p	1.29	9.21	0.30	0.69
mmu-miR-674-5p	1.29	7.34	0.40	0.75
mmu-miR-431-5p	1.30	12.50	0.11	0.49
mmu-miR-382-5p	1.31	13.53	0.05	0.31
mmu-miR-34a-5p	1.32	9.96	0.25	0.64
mmu-miR-125a-5p	1.34	16.11	0.05	0.31
mmu-let-7f-5p	1.35	14.56	0.03	0.30
mmu-miR-141-5p	1.38	8.57	0.17	0.55
mmu-miR-1981-5p	1.38	11.43	0.03	0.29
mmu-miR-221-3p	1.40	9.82	0.13	0.50
mmu-miR-668-3p	1.42	7.28	0.32	0.72
mmu-miR-300-3p	1.42	8.18	0.17	0.55
mmu-let-7e-5p	1.45	12.90	0.01	0.29
mmu-miR-540-3p	1.45	9.39	0.13	0.50
mmu-miR-98-5p	1.46	7.79	0.14	0.51
mmu-miR-7a-5p	1.49	9.68	0.07	0.36
mmu-miR-434-5p	1.49	9.63	0.05	0.31
mmu-miR-134-5p	1.50	9.76	0.05	0.31
mmu-miR-541-5p	1.51	13.37	0.02	0.29
mmu-miR-483-3p	1.51	11.64	0.06	0.34
mmu-miR-467d-5p	1.54	7.52	0.23	0.64
mmu-miR-127-3p	1.64	13.77	0.02	0.29
mmu-miR-194-5p	1.71	8.06	0.25	0.64
mmu-miR-27a-3p	1.74	7.59	0.07	0.36
mmu-miR-409-3p	1.80	10.58	0.02	0.29
mmu-miR-192-5p	1.88	9.28	0.12	0.49

mmu-miR-341-3p	1.93	8.37	0.07	0.34
mmu-miR-485-3p	2.03	10.44	0.03	0.29
mmu-miR-485-5p	2.16	9.16	0.01	0.29
mmu-miR-200a-3p	2.26	8.42	0.02	0.29
mmu-miR-465b-3p	2.49	8.16	0.03	0.29
mmu-miR-465c-3p	2.49	8.16	0.03	0.29
mmu-miR-465a-3p	2.67	6.58	0.02	0.29
mmu-miR-741-3p	2.86	9.00	0.03	0.29
mmu-miR-370-3p	2.86	9.50	3.9E-04	0.07
mmu-miR-429-3p	3.09	9.18	0.01	0.29
mmu-miR-200b-3p	3.54	8.22	1.1E-03	0.10